(NASA-CR-135242) NASA/NAVY LIFT/CRUISE FAN. PHASE 1: DESIGN SUMMARY (General Electric Co.) 276 p HC A11/MF A01 CSCL 21E

N77-31149

Unclas
G3/07 46277

NASA CR-135242
R77AEG180

NASA/Navy Lift/Cruise Fan
Phase I Design Summary

by

Advanced Engineering & Technology Programs Department
Group Engineering Division
Aircraft Engine Group

GENERAL ELECTRIC COMPANY

Prepared For

National Aeronautics and Space Administration

NASA Lewis Research Center

NAS3-20046

1. Report No.	2. Government Accession No.	3. Recipient's Catalog No.
NASA CR-135242	--	--

4. Title and Subtitle	5. Report Date
NASA/Navy Lift/Cruise Fan Phase I Design Summary	September, 1977
	6. Performing Organization Code --
7. Author(s) Advanced Engineering & Technology Programs Department Group Engineering Division	8. Performing Organization Report No. R77AEG180
	10. Work Unit No. --
9. Performing Organization Name and Address General Electric Company Aircraft Engine Group Cincinnati, Ohio 45215	11. Contract or Grant No. NAS3-20046
	13. Type of Report and Period Covered Contractor Report
12. Sponsoring Agency Name and Address National Aeronautics and Space Administration Washington, DC 20546	14. Sponsoring Agency Code --

15. Supplementary Notes

Project Manager, Laurence Gertsma
Fluid Systems Components Division
NASA Lewis Research Center, Cleveland, Ohio

16. Abstract

This report documents the initial design, phase I, of the LCF459 lift/cruise fan system. The LCF459 is a 1.5 meter (59 inch) diameter turbotip lift/cruise fan designed for the NASA/Navy research and technology aircraft. The fan has a design point pressure ratio of 1.32 at a tip speed of 353 meters per second (1125 feet per second). The gas source for the tip turbine is the YJ97-GE-100 engine.

17. Key Words (Suggested by Author(s))	18. Distribution Statement
Fan V/STOL Propulsion Turbotip	Unclassified - Unlimited

19. Security Classif. (of this report)	20. Security Classif. (of this page)	21. No. of Pages	22. Price*
Unclassified	Unclassified	212	--

* For sale by the National Technical Information Service, Springfield, Virginia 22151

TABLE OF CONTENTS

TABLE OF CONTENTS (Continued)

TABLE OF CONTENTS (Concluded)

LIST OF ILLUSTRATIONS

LIST OF ILLUSTRATIONS (Continued)

LIST OF ILLUSTRATIONS (Continued)

LIST OF ILLUSTRATIONS (Concluded)

LIST OF TABLES

LIST OF TABLES (Concluded)

1.0 SUMMARY

The LCF459 is a turbotip, lift/cruise fan designed to meet the requirements of a NASA/Navy research and technology aircraft (RTA). This report documents the results of the initial detail design of the fan system. Low cost and reduced risk design features were weighted heavily during the selection of materials and fabrication methods.

The LCF459 is a 1.5-meter (59 inch) tip-diameter, lift/cruise fan with a design pressure ratio of 1.32 and a tip speed of 343 meters per second (1125 feet per second). The fan is designed to operate with the YJ97-GE-100 engine as the hot gas source. Interconnect gas ducting is used to provide thrust modulation by gas power transfer and to provide balanced thrust for the one-engine-inoperative (OEI) condition.

The sketch of the fan, shown below, depicts the design features which represent a blend of low cost, long life, low risk, and maintainability.

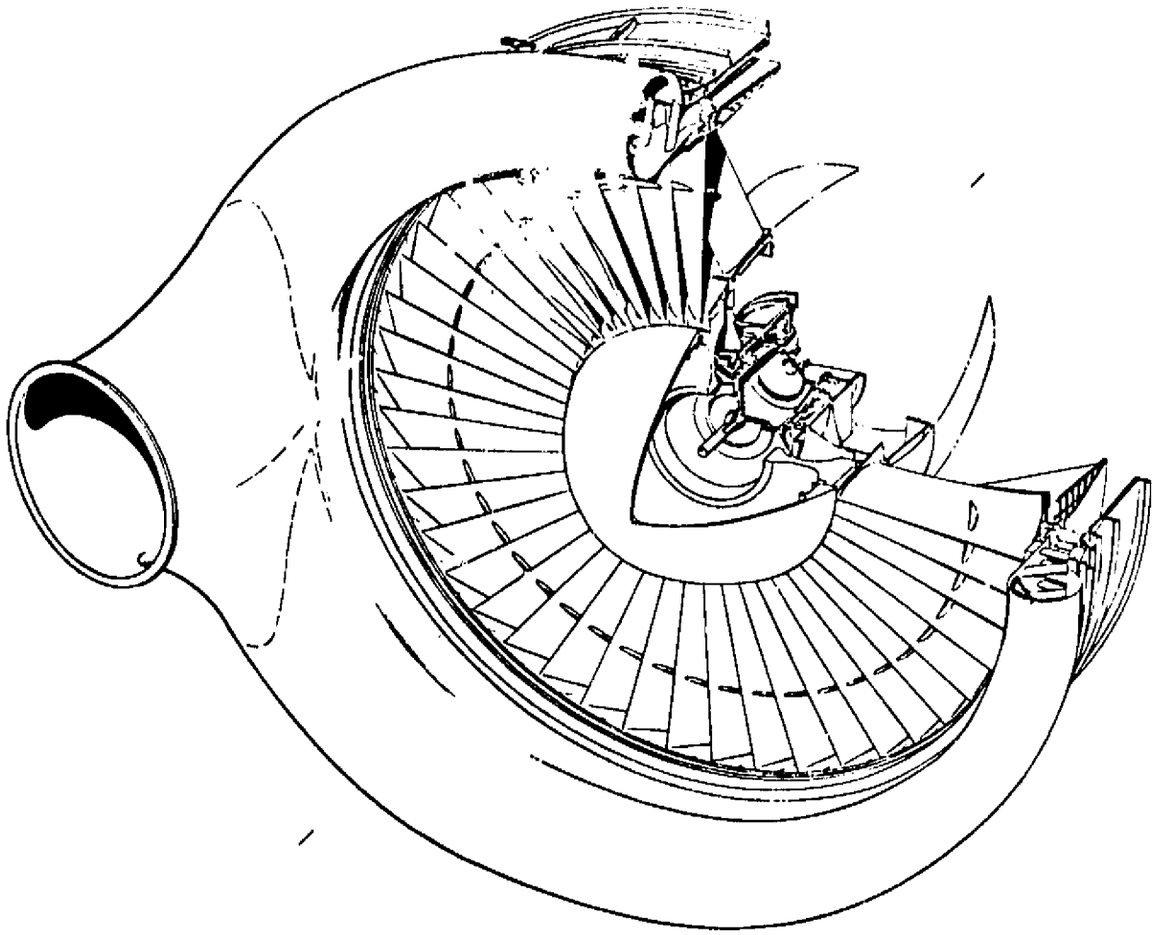

The fan design includes the following mechanical features:

- A 52-bladed titanium rotor with midspan and tip shrouds.
- A cast turbine carrier with one carrier per fan blade.
- A structural rear frame for supporting the rotor in addition to serving as the fan outlet guide vane row.
- A self-contained lubrication system integrated in the bearing housing.
- A single-bubble, HS188 material scroll with shutoff valve for one-engine-inoperative conditions.
- A carrier pumping system for fan inlet air seal pressurization.
- Impingement cooling of outer casings for turbine and fan tip clearance control.
- A power takeoff attachment on the fan shaft for aircraft accessories.

The estimated weight of the fan unit is 416 kg (917 lbm), and the YJ97-GE-100 weight is 326 kg (719 lbm). Installed V/STOL thrust on a 32° C (90° F) day is 57.96 kN (13,030 lbf). This gives a fan thrust-to-weight ratio of 14.2 and a system thrust-to-weight ratio of 8.0.

2.0 INTRODUCTION

The General Electric Company, in a joint effort with NASA, has been engaged in a continuing program to define the advancements in component and system technology which will lead to advanced lift fan systems applicable to vertical and short takeoff and landing (V/STOL) aircraft. The turbotip lift fan concept has been shown consistently to be an attractive system for propulsion in V/STOL aircraft.

Recently, an application was identified using V/STOL aircraft to meet the Navy applications in the late 1980 period. Integrated, NASA-sponsored, aircraft and propulsion studies were conducted and succeeded in defining the specific requirements of the turbotip fan system for this Navy multimission aircraft. Subsequent preliminary design studies were completed and are summarized in Reference 1. The specfic turbotip fan system selected was a 1.5-meter (59 inch) diameter fan driven by a growth version of the J97 engine. The propulsion system consists of three gas-coupled fan systems and either two or three engines. The fan system was identified as the LCF459.

In coincidence with these activities, NASA initiated studies to define a research and technology aircraft (RTA). The intent of this aircraft program is to provide a technology base directly applicable to the needs for the operational aircraft system. The aircraft is to be a modification of an existing aircraft in a gross weight category comparable with the operational aircraft. In addition, the propulsion system will be representative of the operational system, with design changes and modifications consistent with a low cost, low risk approach. The gas generator for the RTA was identified as the YJ97-GE-100. This engine is a close derivative, with only minor changes, of the available YJ97-GE-3 engine used in a different aircraft program.

Detailed design of the LCF459 turbotip fan was initiated in mid-1976. The results of Phase I of this detailed design activity are summarized in this report. The scope of this detailed design is to define the fan configuration and components to the point where the Phase II of detail design could be initiated. Phase II would include additional detail design and generation of component drawings as required for initiation of hardware fabrication.

3.0 REQUIREMENTS

The LCF459 is designed to meet the requirements of a typical V/STOL research and technology aircraft (RTA) planned by NASA as a development vehicle to provide technology for aircraft in the 11,300 to 13,600 kg (25,000 to 30,000 lbm) gross weight catagory. The design requirements established for the turbotip fan are based on presently available V/STOL aircraft and propulsion experience, applicable engine design requirements, General Electric experience, and results of previous and concurrent aircraft study programs.

At the initiation of the preliminary design of the LCF459, Reference 1, design requirements were defined. Minor revisions were later made to the requirements at the initiation of the detailed design phase. The basic sources for the design criteria were as follows:

- MIL-E-5007D, engine design specification, Reference 4.
- General Electric experience in military and commercial engines.
- Design requirements and goals as pr ied by NASA.
- Aircraft design studies and related programs, References 5 through 12.

The following is a description of the more significant requirements which have a direct influence on the fan design.

3.1 GENERAL REQUIREMENTS

The lift/cruise turbofan shall be designed to operate with the YJ97-GE-100 engine as the gas source. The following are some of the general requirements considered in the design of the LCF459 fan system.

- The fan tip shall have a 1.5-meter (59 inch) diameter.
- The number of fans and engines shall be interconnected using the energy transfer control system described in Reference 7.
- The fan shall be capable of operation with the thrust axis either horizontal or vertical.
- Installation flexibility shall be maintained for use as a lift/cruise fan or a lift-only (nose) fan.
- All services, cooling, and lubrication shall be integral with the fan assembly.

- Low cost maintenance features shall be considered, such as on-wing fan blade and turbine carrier removal, sump and disk removal, and field balance provisions.

- The fan thrust time constant shall be less then 0.3 seconds at a nominal 90-percent thrust level.

- The fan shall be capable of operating in the anticipated distortion environment of a research aircraft as described in Section 8.0.

- The fan shall include provision for accessory mounting and power extraction.

- The weight objective of the fan assembly, less scroll insulation, is 386 kg (850 lbm).

- The objective performance is shown in Table I at takeoff, loiter, cruise, and climb conditions.

- The fan shall produce a minimum control thrust change of 20 percent at a nominal thrust level of 41.26 kN (9275 lbm), hot day, installed.

- The fan system shall be capable of operating with one gas generator inoperative for a minimum of 100 cycles of 30-seconds duration each.

- With one engine inoperative (OEI), the minimum control thrust shall be eight percent at a nominal thrust level of 41.26 kN (9275 lbf).

3.2 MISSION AND DUTY CYCLE

The LCF459 shall be designed to meet the mission requirements of a typical research aircraft for the design life as specified in Section 3.3. The one-hour mission, as shown in Figure 1, consists of a cruise leg, three short takeoff and landing (STOL) circuits, and two vertical takeoff and landing (VTOL) circuits. The propulsion duty cycle based on this mission is shown in Table II. For a representative aircraft gross weight of 12,000 kg (26,500 lbm) the design takeoff thrust per fan is 41.26 kN (9275 lbf) at an aircraft thrust-to-weight ratio of 1.05. Table II identifies the fan nominal thrust associated with this duty cycle and aircraft weight.

Since V/STOL aircraft require reaction control for stability, the propulsion duty cycle must also include a design requirement to cover these thrust variations. In the turbotip fan system, thrust modulation is achieved by variations of fan thrust. The fan design requirements establish a minimum control level of 20 percent.

Table I. Performance Goals.

Power Setting	Altitude m	Altitude ft	Amb. Temp. K	Amb. Temp. °R	Mach Number	Turbine Flow kg/sec	Turbine Flow lbm/sec	Fuel Flow kg/hr	Fuel Flow lbm/hr	Pressure kN/m^2	Pressure $lbm/in.^2$	Temperature K	Temperature °R	Thrust per Fan N	Thrust per Fan lbf
Takeoff	0	0	288.1	518.7	0	34.16	75.32	2807	6190	404.6	58.69	1144	2060	74,685	16,790
(360° scroll)	0	0	305.3	549.7	0	32.81	72.23	2624	5786	385.2	55.87	1144	2060	69,881	15,710
Takeoff	0	0	288.1	518.7	0	21.62	47.66	1763	3887	381.3	55.31	1144	2060	52,000	11,690
(240° scroll)	0	0	305.3	549.7	0	20.96	46.20	1678	3699	369.6	53.61	1144	2060	49,509	
Loiter	3,048	10,000	268.3	483.0	0.4	18.12	39.94	639	1409	141.7	20.55	702	1264	8,896	2,000
Cruise	12,192	40,000	216.6	390.0	0.7	9.06	19.97	527	1162	92.8	13.45	873	1572	7,562	1,700
Climb	3,048	10,000	268.3	483.0	0.6	28.06	61.87	1920	4232	310.7	45.07	1019	1835	26,992	6,068
Climb	12,192	40,000	216.6	390.0	0.6	8.62	19.01	583	1286	92.80	13.46	966	1738	8,932	2,008

Notes:
(1) Based on JP-5 fuel
(2) YJ97-GE-100 and fan are uninstalled
(3) Duct total pressure loss (less scroll) = 3 percent
(4) Takeoff is maximum control conditions with power transfer from second engine

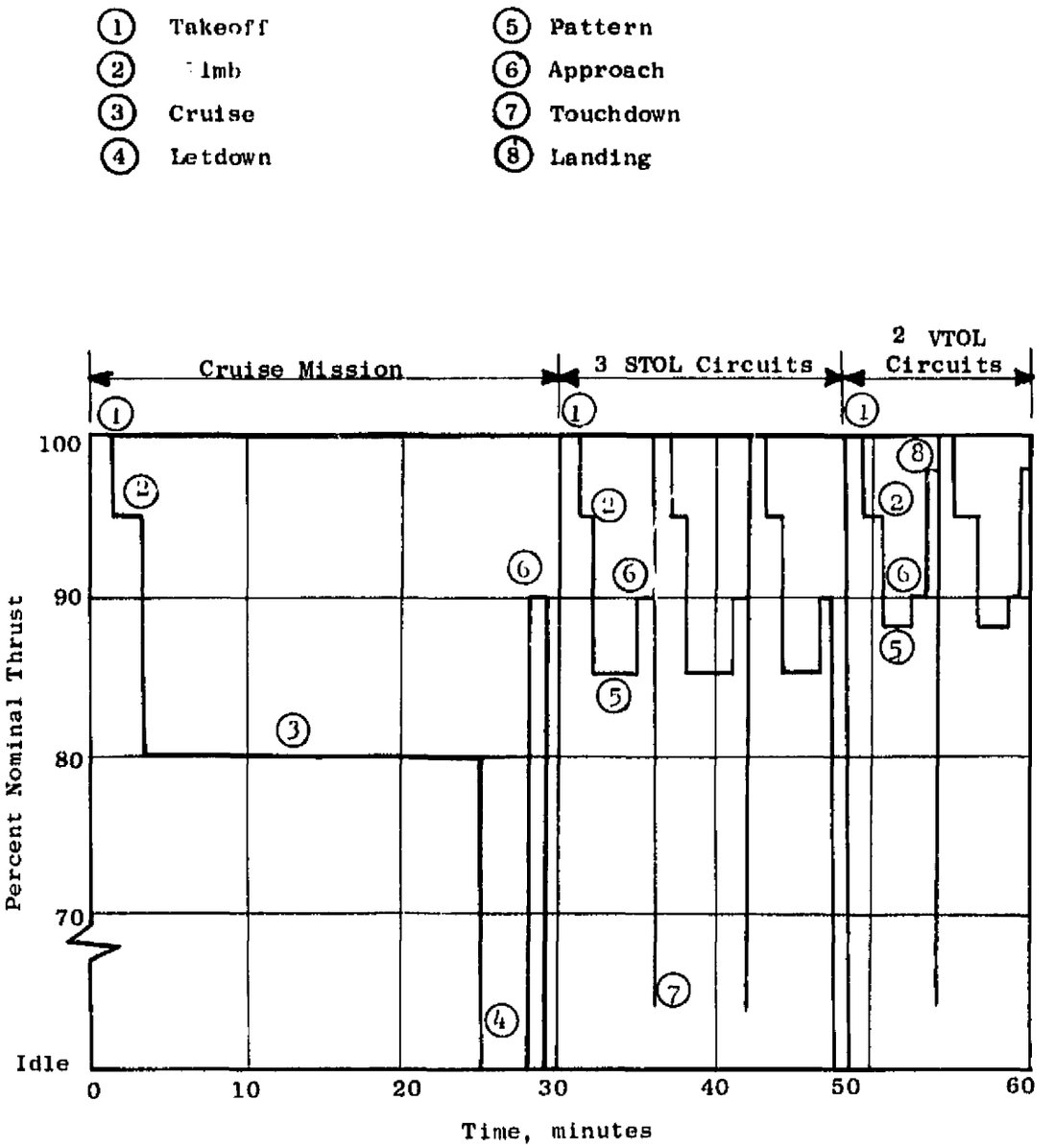

Figure 1. Mission Duty Cycle.

Table II. Propulsion Duty Cycle.

Percent Life	Percent Nominal Thrust*
10.0	100
5.0	98
13.3	95
13.3	90
15.0	85
36.7	80
6.7	Idle

*100% nominal thrust = 41,260 N (9,275 lbf) on a 305.3 K (549.7° R) day

Based on the evaluation of control utilization for existing V/STOL aircraft and numerous simulator studies, typical duty cycle requirements as shown in Figure 2 were established as criteria for designing the LCF459. The control levels are also time dependent. The maximum duration per control input event to be used for design purposes is also shown in Figure 2. This time duration is at least twice as long as that anticipated for normal control application.

For evaluation of the cyclic effects of control applications, the average rate based on flight and simulator experience appears to be about one event per second. This cyclic rate shall be applied as a design criterion.

3.3 MECHANICAL DESIGN CRITERIA

The significant criteria applied during the design of the LCF459 are as follows. Other significant criteria of Reference 4 were also considered.

- The fan shall be designed to the research duty cycle for the minimum life of 600 hours for hot parts and 1200 hours for cold parts.
- The fan shall be capable of operating within the envelope as defined in Figure 3.
- The fan and mounting system shall withstand, without permanent deformation, the conditions given in Figure 4.
- Bird-ingestion objectives shall include safe shutdown following ingestion of a 1-kg (2.2 lbm) bird.
- Fan blade containment will not be considered in the design. A failed turbine airfoil at the root shall be contained within the fan frame.

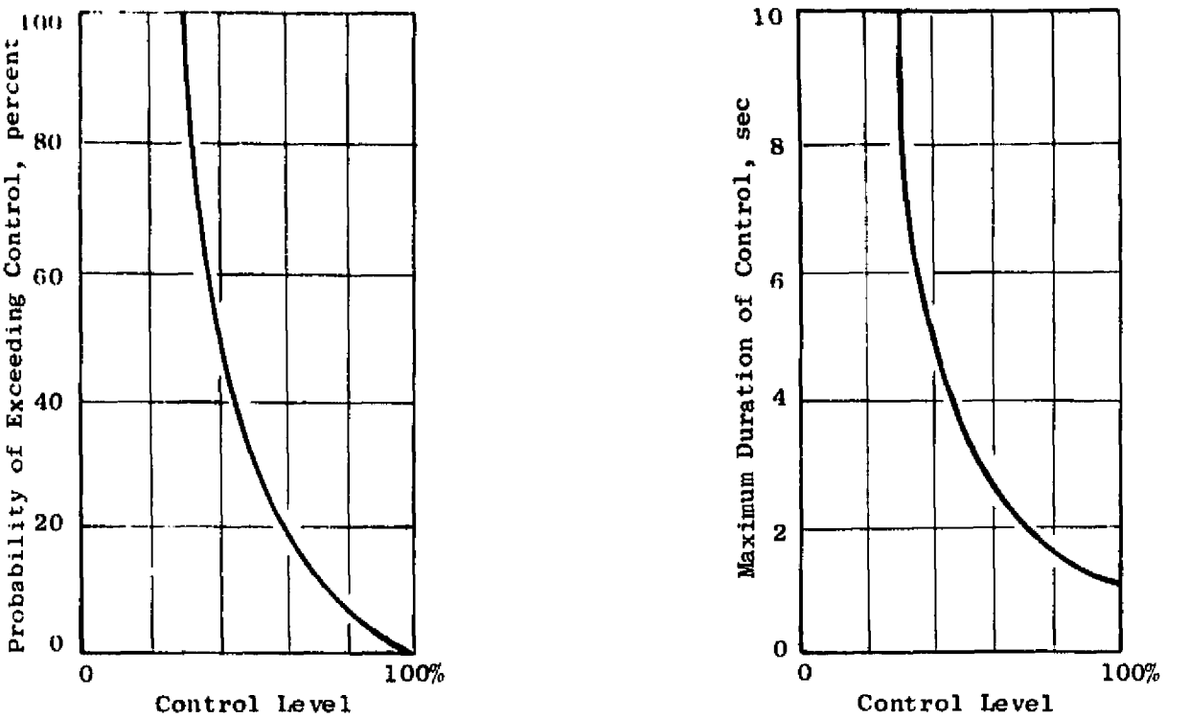

Figure 2. Control Duty Cycle.

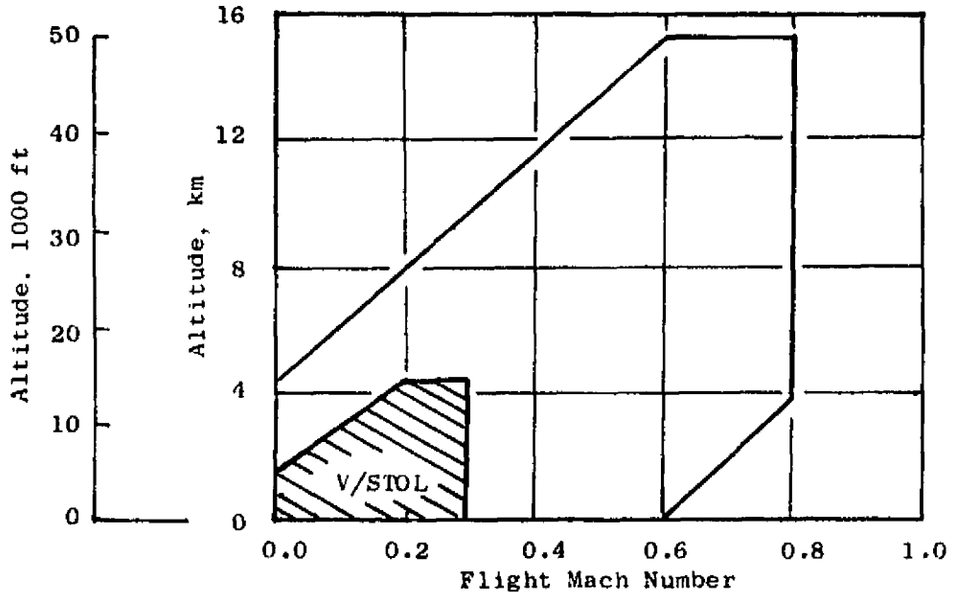

Figure 3. Flight Envelope.

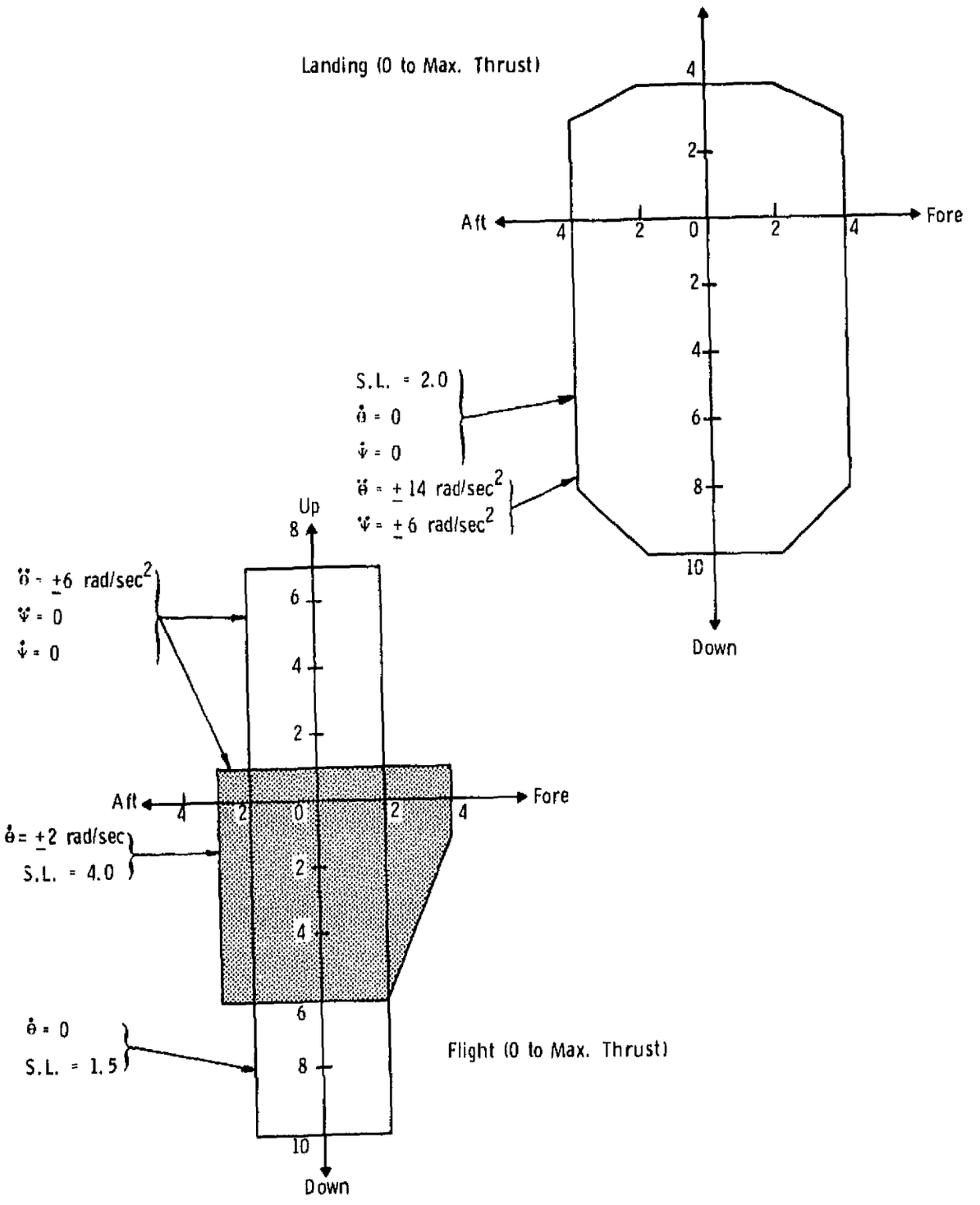

Figure 4. Load Diagrams.

- The fan assembly shall be capable of safe shutdown following failure of a fan blade. The frame and bearings shall be capable ot withstanding the loads due to this unbalance for 30 seconds.

3.4 AERODYNAMIC DESIGN POINT

Coordinated aircraft and propulsion studies during the preliminary design phase produced the LCF459 fan. This fan was driven by two growth versions of the J97 engine. The fan design point was selected to have a pressure ratio of 1.32 at a corrected flow rate of 293 kg/sec (646 lbm/sec). The fan tip diameter was 1.5 meters (59 inches).

This fan aerodynamic design was used for the detail design with the YJ97-GE-100 substituted as the gas generator. A new turbine design point was defined for this match of the LCF459 and the YJ97-GE-100 engine. Matching of the fan and turbine was made at the maximum power level of the engine: the VTO rating, with flow or power transfer, with an engine discharge temperature of 1144 K (2060° R). Table III gives the engine discharge conditions at this maximum power level along with the nominal or no-power-transfer condition.

The fan and turbine design points established for this configuration are given in Table IV.

Table III. YJ97-GE-100 Discharge Conditions.

Sea Level Static; 305.3 K (549.7° R) Day, Installed*

	Intermediate		Takeoff		Maximum Control	
Engine Speed, percent	101.5		102.7		102.7	
Flow, kg/sec (lbm/sec)	29.73	(65.54)	30.15	(66.48)	30.31	(66.82)
Pressure, kN/m^2 ($lbf/in.^2$)	343.3	(49.79)	351.1	(50.93)	288.31	(56.36)
Temperature, K (° R)	1043.0	(1878)	1060.0	(1909)	1144.0	(2060)
Fuel Flow, kg/hr (lbm/hr)	2069.0	(4561)	2154.0	(4749)	2433.0	(5366)
Flow Transfer, percent	0		0		6.3	
Total Fan Scroll Flow kg/sec (lbm/sec)	29.73	(65.59)	30.15	(66.48)	32.05	(70.66)

*Installation Factors

Recovery = 0.985
Compressor Bleed = 0.5%
Power Extraction = 18.6 kW (25 horsepower)

Table IV. LCF459 Fan and Turbine Design Point.

Gas Conditions		
Engine Discharge Flow, kg/sec (lbm/sec)	30.31	(66.82)
Engine Discharge Temperature, K (° R)	1144	(2060)
Engine Discharge Pressure kN/m^2 (lbf/in.^{2})	388.6	(56.36)
Engine Fuel Flow, kg/hr (lbm/hr)	2433	(5366)
Scroll Inlet Pressure, kN/m^2 (lbf/in.^{2})	372.3	(53.99)
Scroll Inlet Flow, kg/sec (lbm/sec)	32.05	(70.66)
Turbine and Scroll		
Duct Diameter, m (in.)	0.445	(17.50)
Turbine Inlet Pressure, kN/m^2 (lbf/in.^{2})	357.5	(51.85)
Pitch Line Reaction, percent	15	(15)
Corrected Speed, rpm/$\sqrt{K}$ (rpm/$\sqrt{°\ R}$)	133.0	(99.12)
Energy, kW/g K (Btu/lbm ° R)	0.2277	(0.05441)
Efficiency, percent	0.86	(0.86)
Exit Mach Number	0.55	(0.55)
Exit Total Pressure, kN/m^2 (lbf/in.^{2})	126.1	(18.29)
Exit Total Temperature, K (° R)	926	(1666)
Effective Annulus Area, m^2 (in.^{2})	34.80	(374.6)
Diffuser		
Inlet Mach Number	0.55	(0.55)
Inlet Static Pressure, kN/m^2 (lbf/in.^{2})	103.7	(15.04)
Loss Coefficient	0.15	(0.15)
Exit Total Pressure, kN/m^2 (lbf/in.^{2})	123.0	(17.84)
Exit Mach Number	0.414	(0.414)
Exit Effective Area, m^2 (in.^{2})	42.98	(462.6)
Fan		
Pressure Ratio	1.319	(1.319)
Corrected Flow, kg/sec (lbm/sec)	293	(646)
Radius Ratio	0.407	(0.407)
Speed, rpm	4499	(4499)
Efficiency	0.86	(0.86)
Corrected Specific Flow, kg/sec-m^2 (lbm/sec-ft^2)	199.2	(40.8)
Corrected Tip Speed, m/sec (ft/sec)	342.9	(1125)
Tip Diameter, m (in.)	1.50	(59.0)
Ideal Thrust (1.00 Thrust Coefficient)		
Fan Stream, kN (lbf)	60.411	(13581)
Turbine Stream, kN (lbf)	9.857	(2216)
Total, kN (lbf)	72.268	(15797)

4.0 FAN DESIGN DESCRIPTION

4.1 FAN SYSTEM

The LCF459 fan is the thrust component of a complete propulsion system that also includes the following components:

- gas generators
- Interconnect ducting
- Thrust vectoring devices
- Control valves for power transfer

Figure 5 shows a schematic of a typical propulsion system consisting of three engines and fans which will be provided by the engine manufacturer. The ducting, valves, and thrust-vectoring systems are assumed to be aircraft-furnished components because of the unique integration requirements of the aircraft structure.

The propulsion system for the RTA uses YJ97-GE-100 engines as the gas generators. These engines are derivatives of the YJ97-GE-3 engine which are existing and readily available in adequate quantities for a research aircraft program. The required engine modifications for conversion to the -100 engine are described in Section 5.3.

The LCF459, which is described in this report, is shown in Figure 6. The fan assembly consists of the following major components as identified in the figure.

- Fan and tip-turbine rotor assembly
- Turbine scroll
- Structural rear frame
- Bearings and sump

The following discussions describe the features and design details of each of the major fan components.

4.2 AERODYNAMIC DESIGN

The LCF459 is a single-stage turbotip fan with a design-point pressure ratio of 1.319 and a fan tip diameter of 1.50 m (59 inches). The fan rotor is a conventional, single-stage, high bypass fan with both a tip and a part-

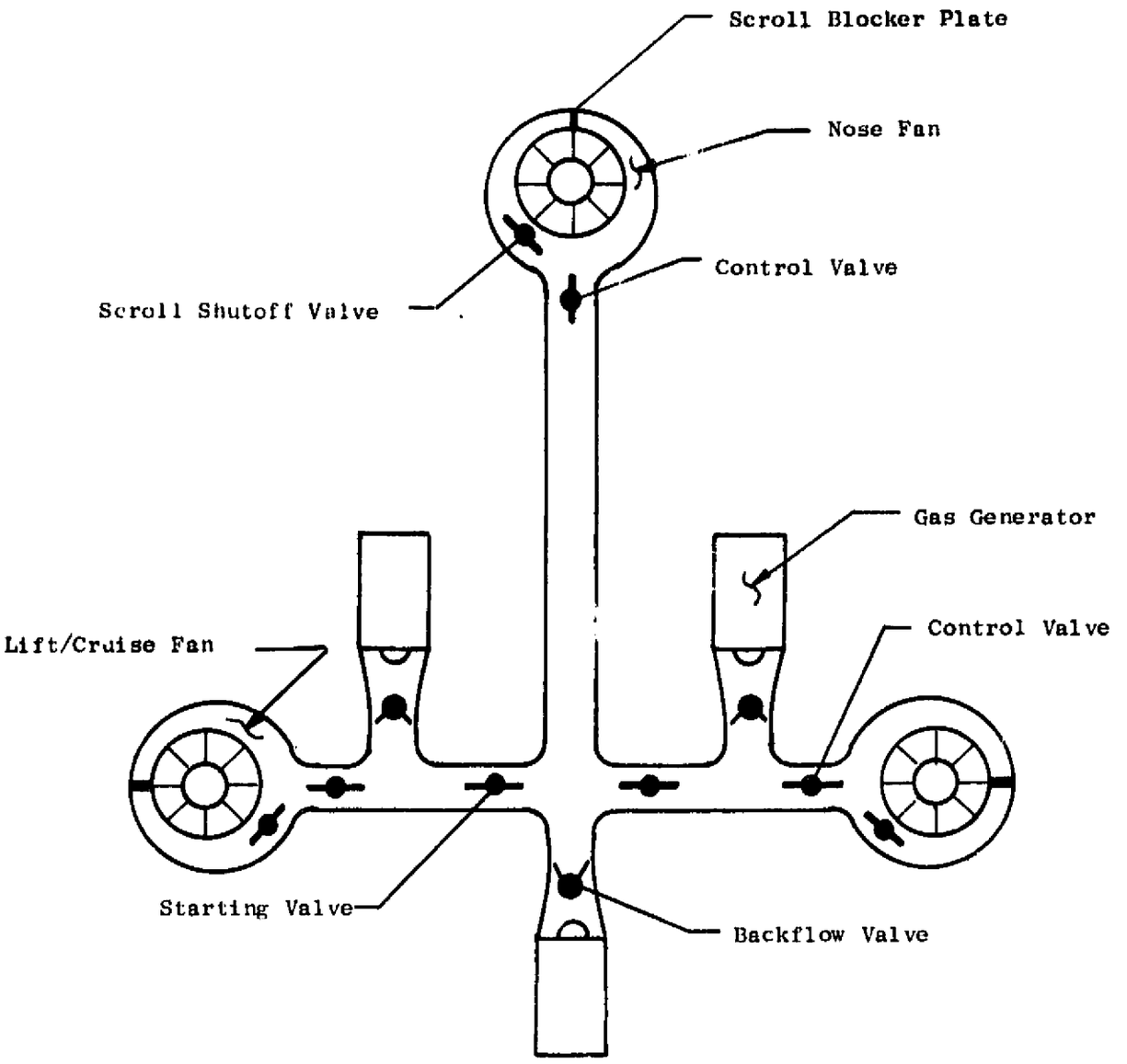

Figure 5. Turbotip Propulsion System Schematic.

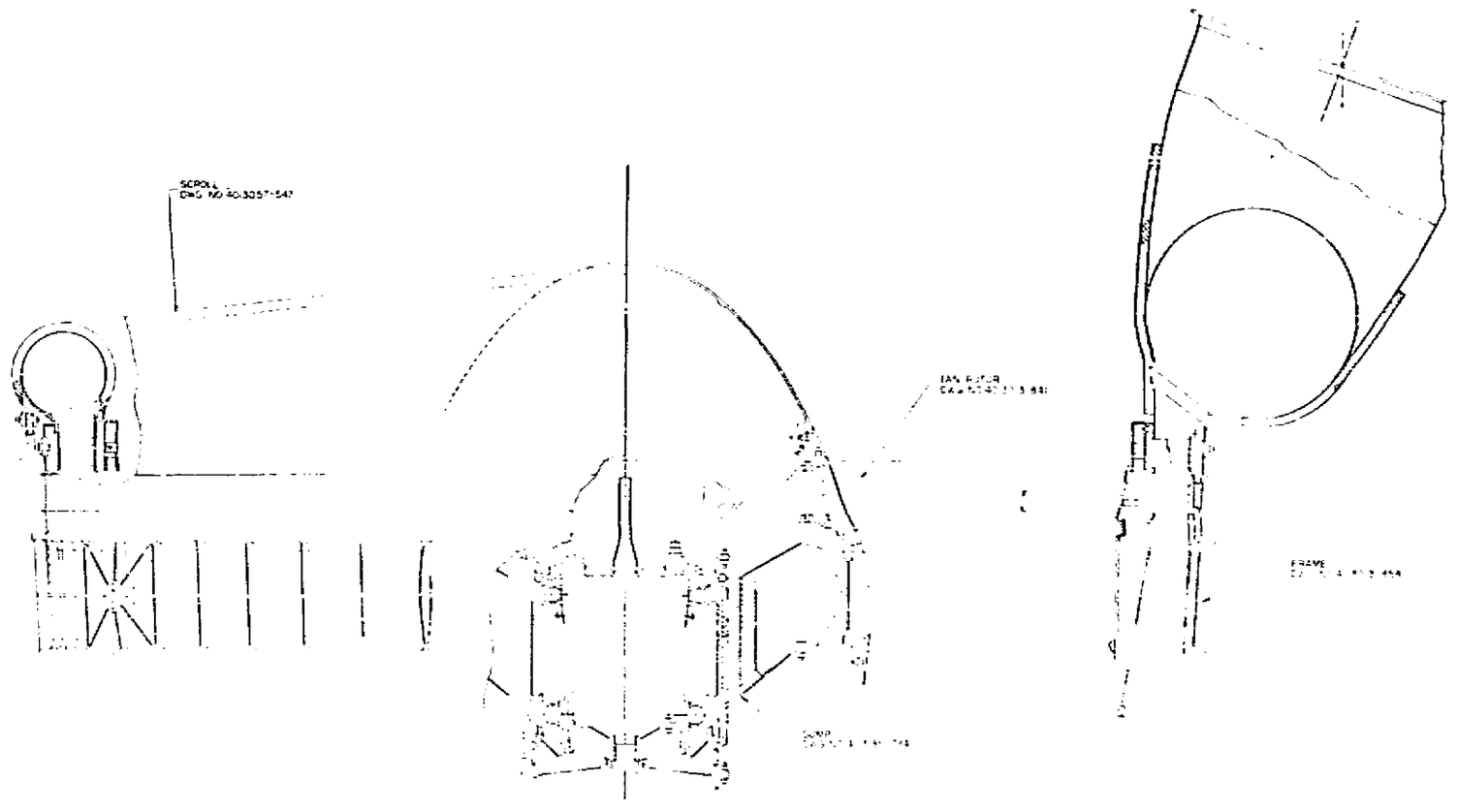

Figure 6. LCF459 Fan Cross Section.

span shroud; the rotor contains 52 blades. The blade geometry was established for minimum stage weight, consistent with General Electric standards of rotor strength and life, aeromechanical stability, aerodynamic stall margin, and bird-strike resistance. A fan vane-frame provides the dual function of an outlet guide vane row for the fan flow and the support for the fan rotor bearing system.

A tip turbine is attached to the outer shroud of the fan rotor. The inlet stators or nozzles of the turbine are contained in the scroll. The turbine has a low level of positive reaction to minimize exit swirl. The turbine stage does not require exit stators because of this low exit swirl. The turbine stage discharges into a low area-ratio diffuser which serves to increase the static pressure to a level compatible with the fan exit flow at the mixing plane. The mixing plane conditions were established by optimization of fan static thrust while providing adequate fan stall margins. The diffuser flow path is penetrated by nine, long-chord vanes which are structural components of the rear frame and not exit deswirl vanes.

Fan and turbine leakage is controlled by seals at both the fan inlet and the fan exit. Multitooth, double seals are used at each location. An air pump is provided in the space between the fan and turbine for delivery of seal buffer or pressurization air into the forward seal cavity. This system prevents hot turbine gas from leaking into the fan inlet, which would yield significant performance penalties. Two seal teeth are also provided on the tip of the shrouded turbine blades for leakage control.

4.2.1 Fan

The primary aerodynamic parameters which describe the fan stage aerodynamic design are presented in Table V. Except for the hub work coefficient, these parameters are identical to those defined at the conclusion of the preliminary design phase, Reference 1. The small rise in hub work coefficient is the result of designing to a less skewed fan exit radial total pressure profile. These parameters are all well within past General Electric experience on either tip-turbine-driven fans or high bypass engine fans. In general, the aerodynamic design of this fan stage can be said to be well within the "state of the art."

Table VI gives the fan flow-path coordinates, and Figure 7 shows the aerodynamic flow path with calculated flow streamlines. For purposes of this design, the flow path has been defined for some distance upstream and downstream of the fan blading in order to establish reasonable boundary conditions. The inlet flow path as shown represents an axisymmetric inlet with a throat located 8.99 cm (35 inches) ahead of the rotor face and a 0.6 Mach number at design corrected flow. It is recognized that different inlet geometries might be more suitable for particular installations, and these can be faired into the design flow path. This is an interface problem which must be defined on each particular installation. Similarly, the tail cone at the fan exit can also be modified somewhat, to suit particular installations, with only small effects on the fan performance.

Table V. Fan Aerodynamic Design Parameters.

Total Pressure Ratio	1.319
Static Pressure Ratio	1.074
Corrected Airflow, kg/sec (lbm/sec)	293 (646)
Adiabatic Efficiency	0.86
Corrected Tip Speed, m/sec (ft/sec)	342.9 (1125)
Tip Diameter, m (in.)	1.499 (59.0)
Radius Ratio	0.407
Specific Flow, kg/sec m^2 (lbm/sec ft^2)	199.2 (40.8)
Rotor Tip Relative Mach Number	1.19
Hub Work Coefficient, $2gJ\Delta H/u_h^2$	2.05
Number of Blades	52
Number of Vanes	27
Blade Aspect Ratio	3.77
Vane Aspect Ratio	2.33
Exit Mach Number	0.55

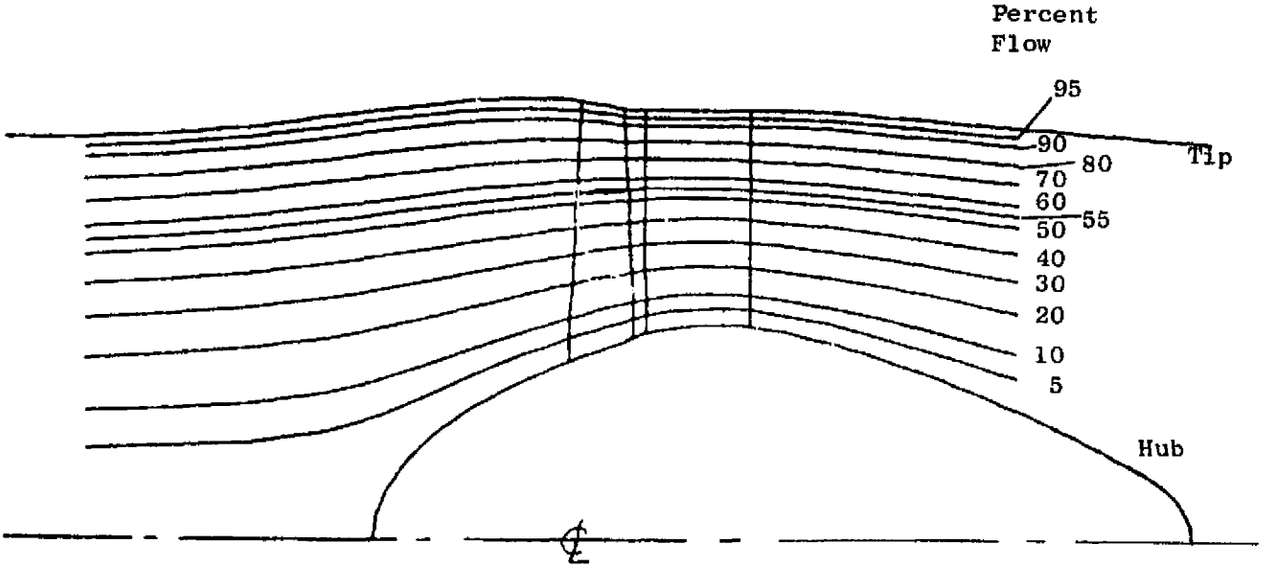

Figure 7. Fan Aerodynamic Flow Path.

Table VI. Fan Flow-Path Coordinates.

Tip:

Axial Station (cm)	Axial Station (in.)	Radius (cm)	Radius (in.)	
-88.90	-35.00	68.45	26.95	inlet
-76.20	-30.00	68.58	27.00	
-63.50	-25.00	69.14	27.22	
-50.80	-20.00	70.31	27.68	
-38.10	-15.00	71.86	28.29	
-25.40	-10.00	73.66	29.00	
-12.70	- 5.00	74.98	29.52	
+ 1.37	+ 0.54	74.93	29.50	conical rotor tip
+ 8.31	+ 3.27	73.71	29.02	
+12.70	+ 5.00	73.41	28.90	cylindrical
+35.56	+14.00	73.41	28.90	stator tip

Hub:

Axial Station (cm)	Axial Station (in.)	Radius (cm)	Radius (in.)	
-30.48	-12.00	0.00	0.00	ellipsoidal spinner
-24.48	- 9.64	14.32	5.64	
-19.17	- 7.55	19.42	7.65	
-15.43	- 6.08	22.22	8.75	
-10.88	- 4.28	25.10	9.88	
- 6.25	- 2.50	27.54	10.84	
- 2.50	- 0.99	29.38	11.57	
+ 0.00	+ 0.00	30.48	12.00	rotor leading edge
+ 5.08	2.00	32.23	12.69	
+ 7.62	3.00	33.27	13.10	
+10.16	4.00	34.59	13.62	
+10.28	+ 4.05	34.65	13.64	rotor trailing edge
+12.13	+ 4.78	35.37	13.92	stator leading edge
+12.70	5.00	35.53	13.99	
+15.24	6.00	36.07	14.20	
+20.30	8.00	36.65	14.43	
+25.40	10.00	36.75	14.43	
+28.51	+11.22	36.56	14.39	stator trailing edge
+30.48	12.00	36.32	14.30	tail cone
+34.39	13.50	35.64	14.03	
+38.10	15.00	33.25	13.09	
+50.80	20.00	30.71	12.09	
+63.50	25.00	25.65	10.10	
+76.20	30.00	17.99	7.79	
+88.90	35.00	12.90	5.08	
+99.06	39.00	0	0.00	

The fan rotor incorporates 52 blades which feature both a tip shroud and a part-span shroud. The tip shroud also serves as part of the rotating seal system separating the fan and turbine flow paths.

The fan rear frame operates functionally as the stage exit stators and also provides the mechanical support for the rotor and scroll. The mechanical requirements established the need for nine structural vanes with a chord of 16.9 cm (6.67 inches) and a thickness-to-chord ratio of eight percent. The aerodynamic configuration is completed by inserting two nonstructural vanes between each pair of structural vanes, giving a total vane number of 27. The vane thickness-to-chord ratio of the nonstructural vanes is four percent. The stacking axes of all vanes are leaned 20° at the hub to benefit both the mechanical and the aerodynamic design.

The rotor blade airfoil sections are defined by a quarter sine-wave thickness distribution on an arbitrarily defined mean line. The thickness distribution is modified to give leading and trailing edge thickness-to-chord ratios of 0.0075. The location of the maximum section thickness point is at 55 percent of the chord from the leading edge for all rotor blade sections, except for the tip section which is at 57 percent.

Figures 8 and 9 show the spanwise variation of chord and maximum thickness-to-chord ratio respectively. The rotor blade chord is seen to vary linearly from 10.5 cm (4.15 inches) at the hub to 11.3 cm (4.46 inches) at the tip. The maximum thickness-to-chord ratio is seen to vary from nine percent at the hub to four percent at the tip. The variation from hub to tip is not entirely smooth but shows a thickening of the blade just below the midspan shroud and a rather rapid decrease in thickness just outboard of the midspan.

Arbitrary mean-line shapes are specified for the rotor blade sections, rather than circular arc or multiple circular arc shapes, since they allow more flexibility in defining blade throat and passage area distributions while maintaining desired incidence and deviation angles. This is particularly important in the vicinity of the midspan shroud. Use of the arbitrary mean-line shape for rotor blades is a standard General Electric Company practice. Figure 10 shows the rotor blade incidence and deviation angles. Deviation angles are calculated from "Carter's Rule" plus an empirical "X factor" correction. The empirical "X factor" is also shown in Figure 10.

Stator vane airfoil sections are defined by NACA 65 series thickness distributions on circular-arc mean lines. These sections have been found to work well at the lower Mach number levels at which the stator vanes are required to operate. Figure 11 shows the incidence and deviation angles used for the stator vanes. Past experience has shown that no "X factor" correction has been necessary for fan stator vanes; so, "Carter's Rule" has been used directly to calculate stator deviation angles. Stator incidence angle selections have been based largely on NACA cascade data with checks being made to assure adequate throat margin. Stator vane incidence and deviation angles were selected under the assumption that all vanes had a maximum

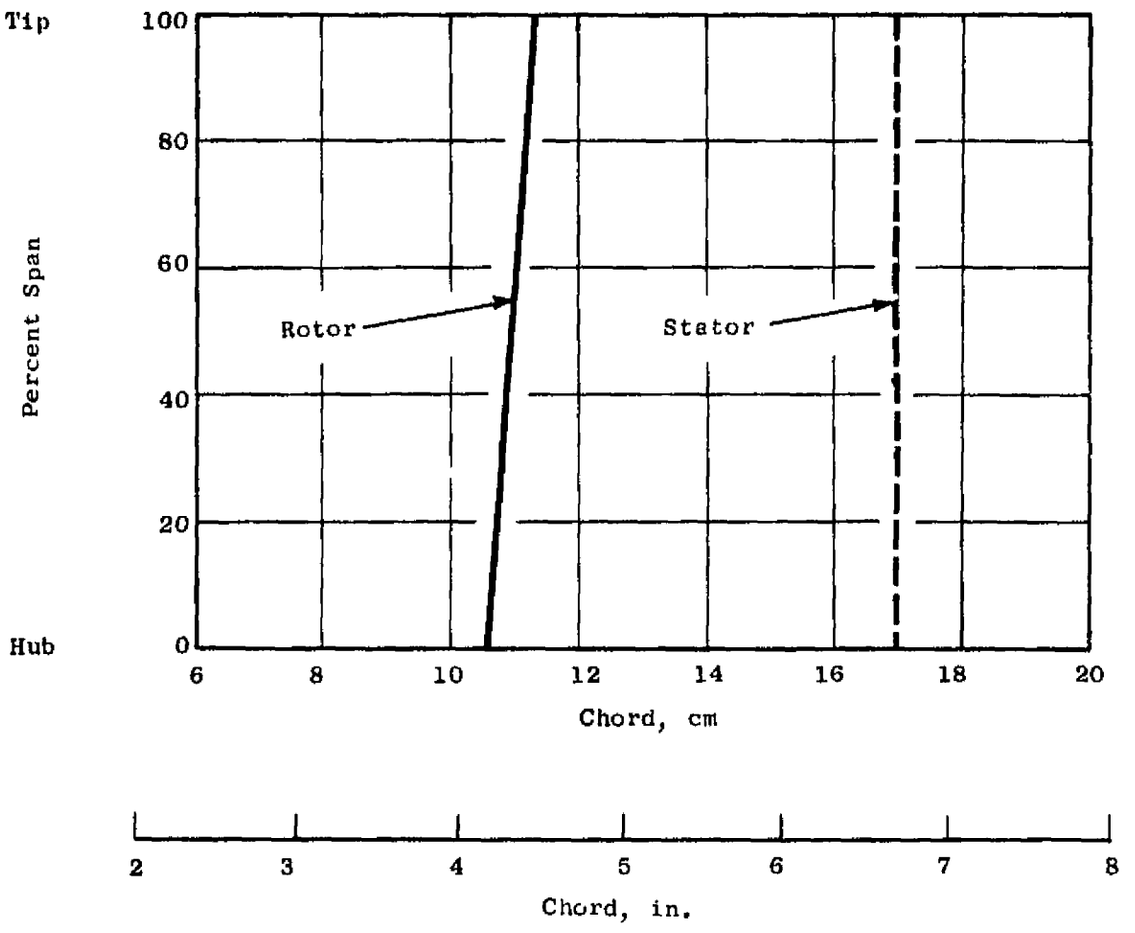

Figure 8. Blade and Vane Chords.

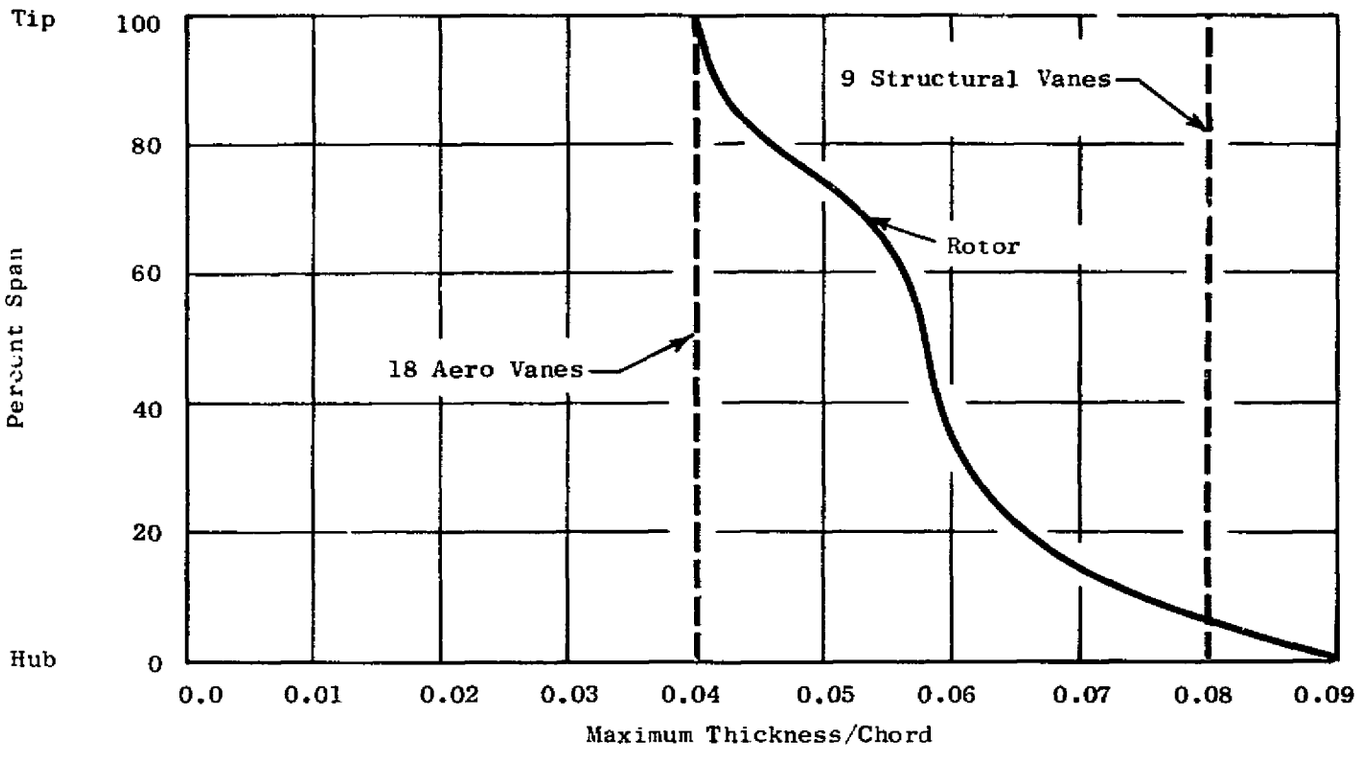

Figure 9. Blade and Vane Thickness.

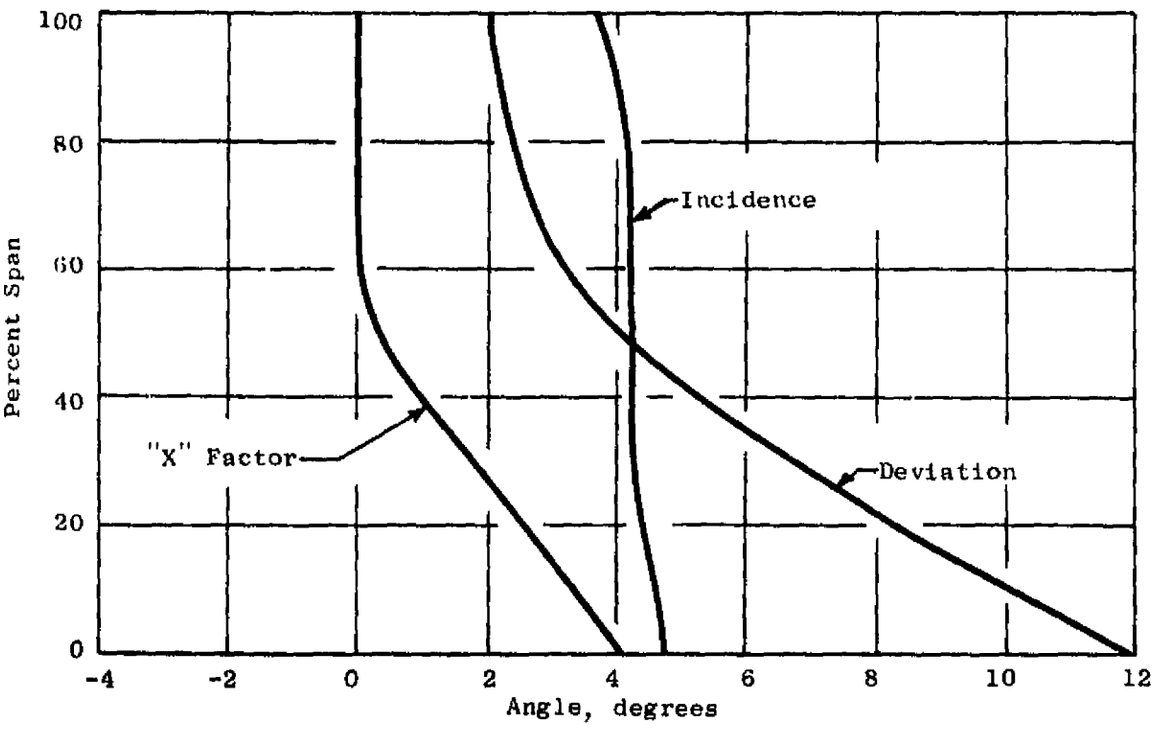

Figure 10. Rotor Incidence and Deviation Angles.

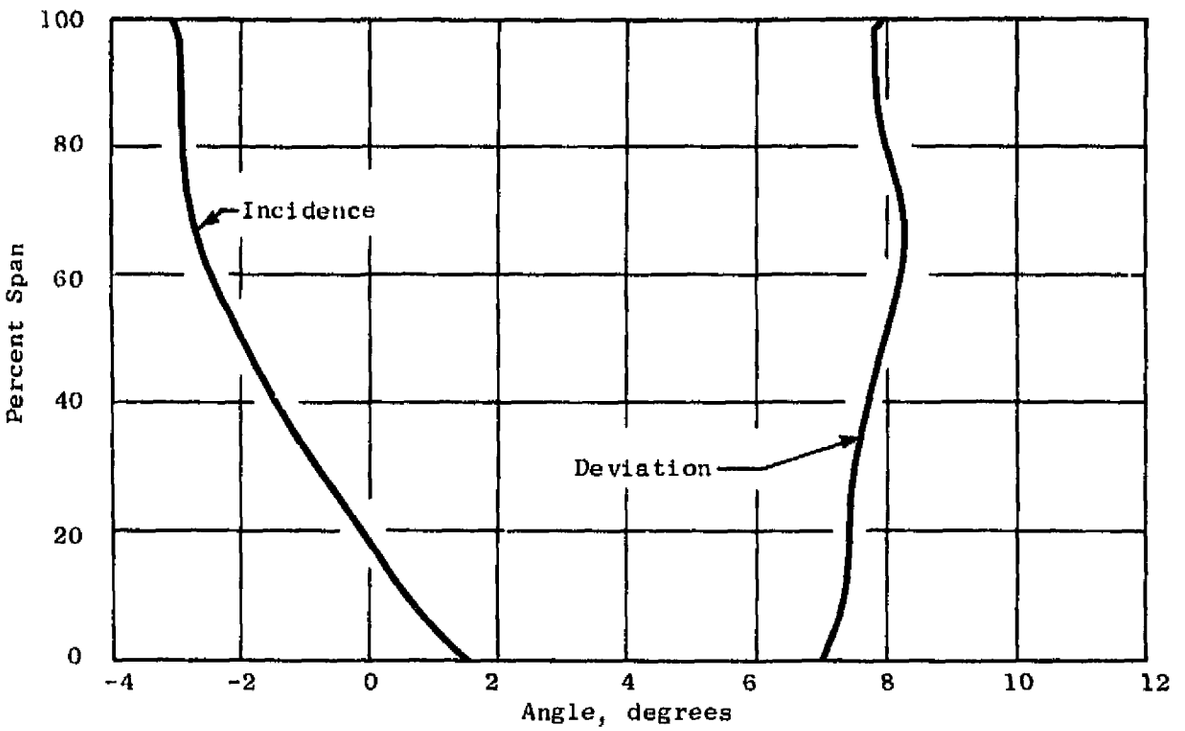

Figure 11. Stator Incidence and Deviation Angles.

thickness-to-chord ratio equal to the weighted average of the values for the structural vanes and the nonstructural vanes.

Figures 12 through 19 show additional aerodynamic design parameters for both the rotor and the stator. Figures 12 through 14 give blade geometric parameters such as solidities, camber, and stage angles. Figure 15 shows the blade air angles consistent with the estimated deviation angles as shown in Figures 10 and 11. Blade relative Mach number distributions are shown in Figure 16. Radial distributions of diffusion factors are shown in Figure 17 for the defined fan design. The factors for both the stator and the rotor are low relative to maximum criteria.

Figure 18 shows the radial distribution of efficiency selected for this design. The assumption of efficiency, rather than pressure loss coefficient, is a General Electric design practice for fans of this type. This distribution was based on measured results, from similar configurations, with adjustments to account for recognized differences. Average adiabatic efficiency is 0.89 at the rotor exit and 0.86 at the stator exit. For design purposes, local losses due to the midspan shroud have been assumed to be spread uniformly over the fan annulus.

Figure 19 shows the fan total pressure ratio profile at the rotor exit and at the stator exit. The profile at the rotor exit plane is intended to have a linear variation with stream function from 1.296 at the hub to 1.365 at the tip. The slightly higher loading at the tip is intended to take advantage of the higher blade speed in this area. Average total pressure ratio at the rotor exit is 1.331. Stator vane losses reduce this to an average value of 1.319 at the stator exit. Higher losses in the stator vane end regions also cause the pressure ratio profile to become nonlinear.

4.2.2 Turbine

The LCF459 tip turbine is a full-admission, single-stage, axial-flow configuration with tip-shrouded blades and is fed by a single-entry scroll designed to efficiently distribute the engine discharge gas to the turbine nozzle ring. The aerodynamic design of the scroll is discussed in Section 4.2.3. The turbine stage discharges into a diffuser section which serves to increase the exit static pressure to a level compatible with that of the fan exit flow at the mixing plane.

A number of turbine aerodynamic design parameters are presented in Table VII. The 1144 K (2060° R) design point corresponds to the fan maximum control point at which the tip turbine receives 5.4 percent of its flow from a second, interconnected, gas generator. The 0.55 exit Mach number represents a compromise between the mechanical impetus to minimize blade length and to provide adequate choking margin at the turbine exit.

At design point, the turbine was selected to have reactions of 10 percent at the hub and 20 percent at the tip. With this amount of reaction, the exit swirl angle is about three degrees forward running, and turbine outlet

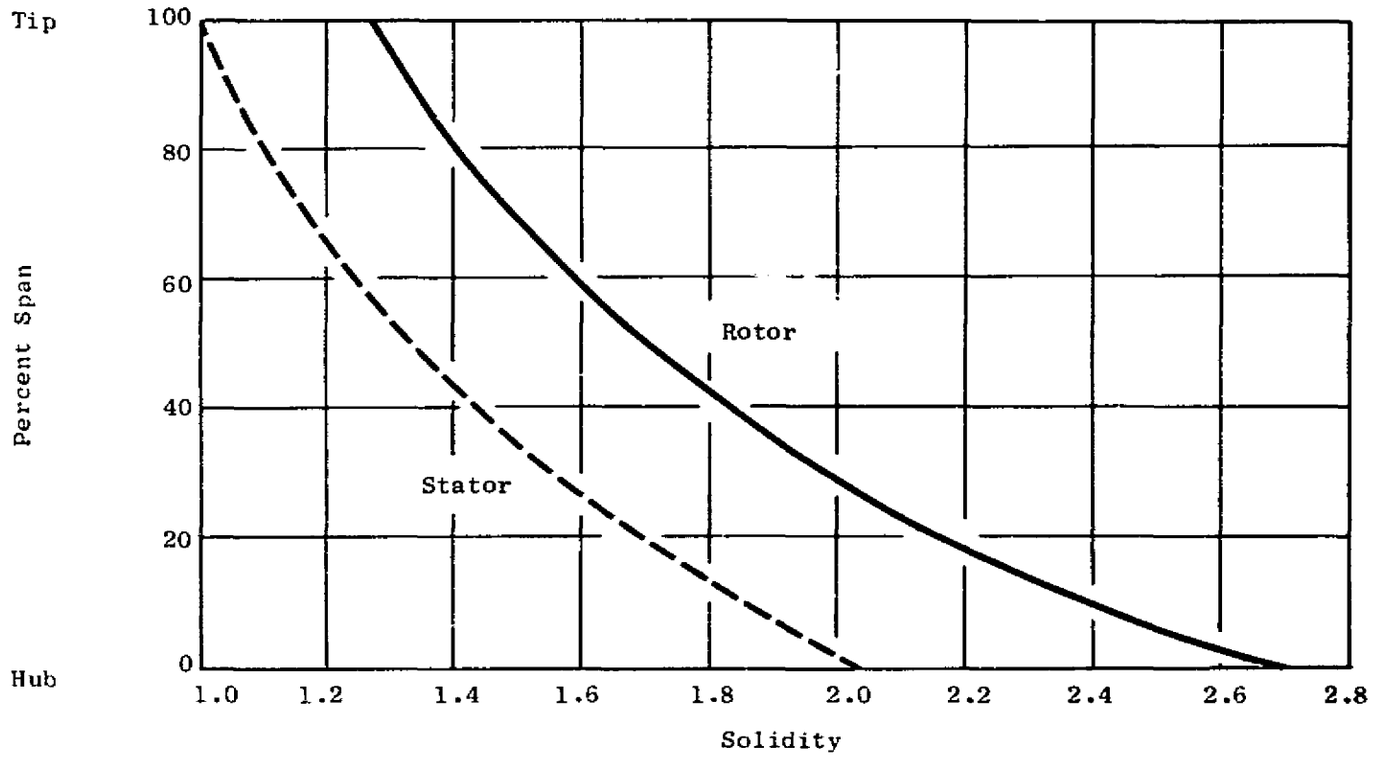

Figure 12. Blade and Vane Solidities.

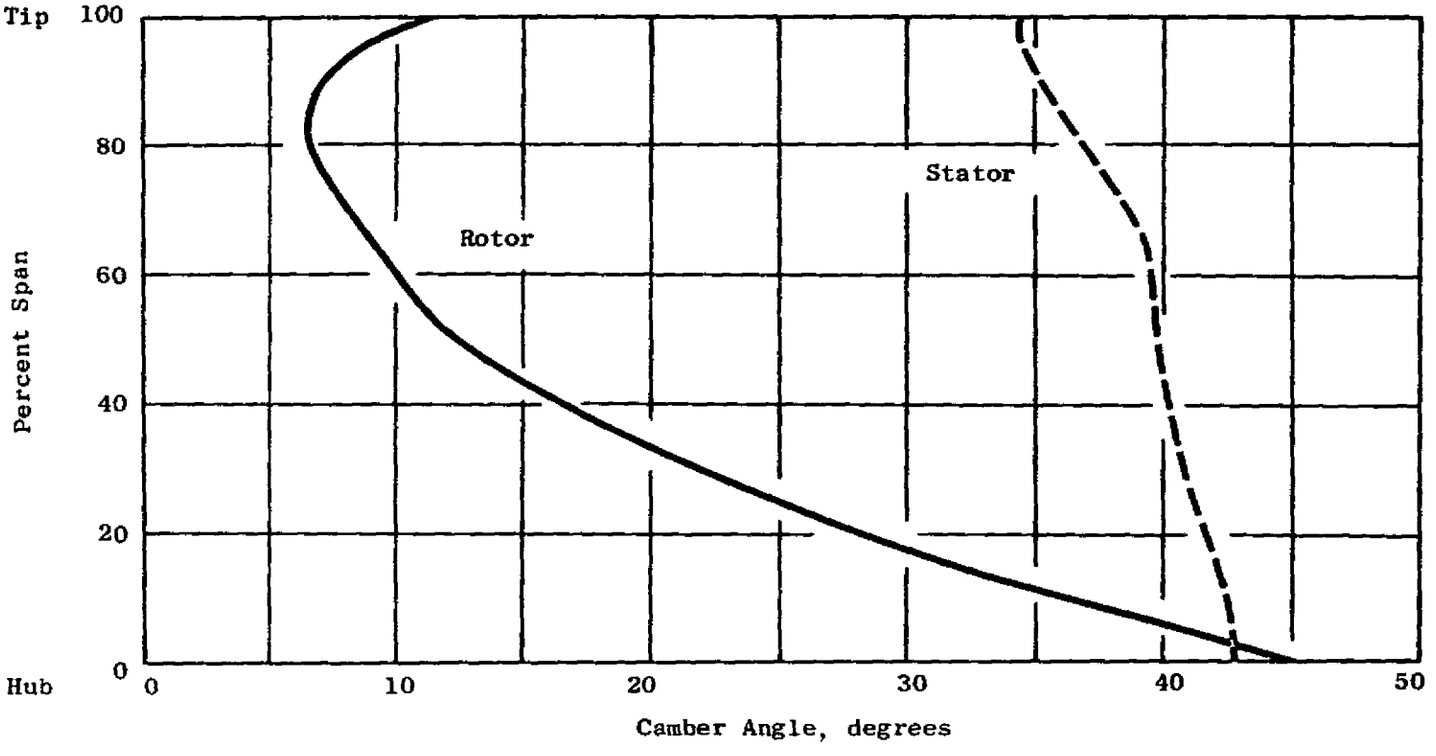

Figure 13. Blade and Vane Camber Angles.

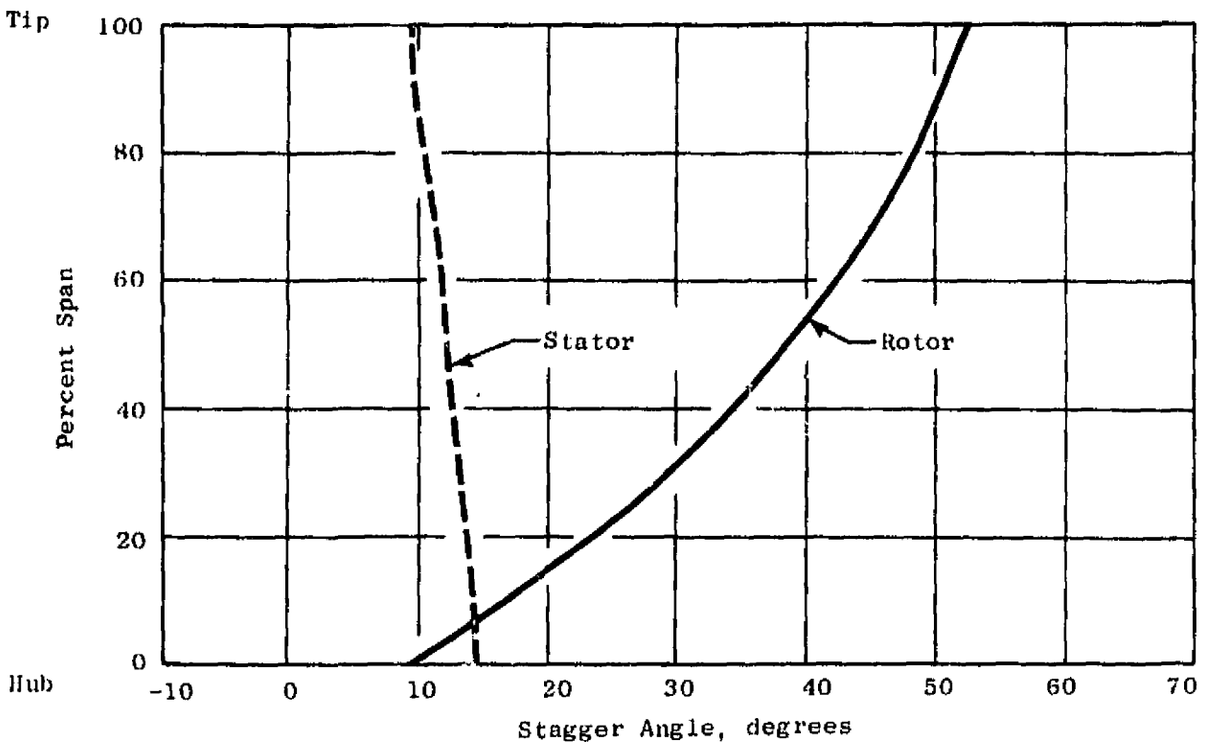

Figure 14. Blade and Vane Stagger Angles.

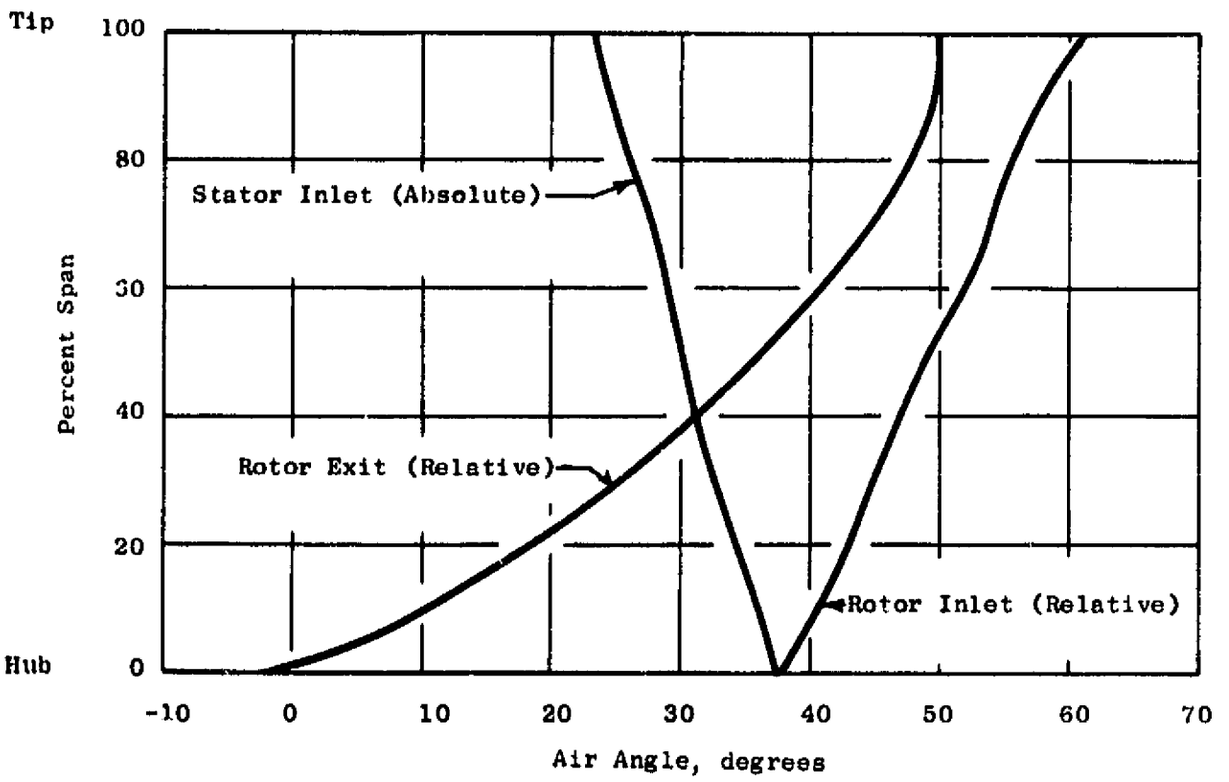

Figure 15. Blade and Vane Air Angles.

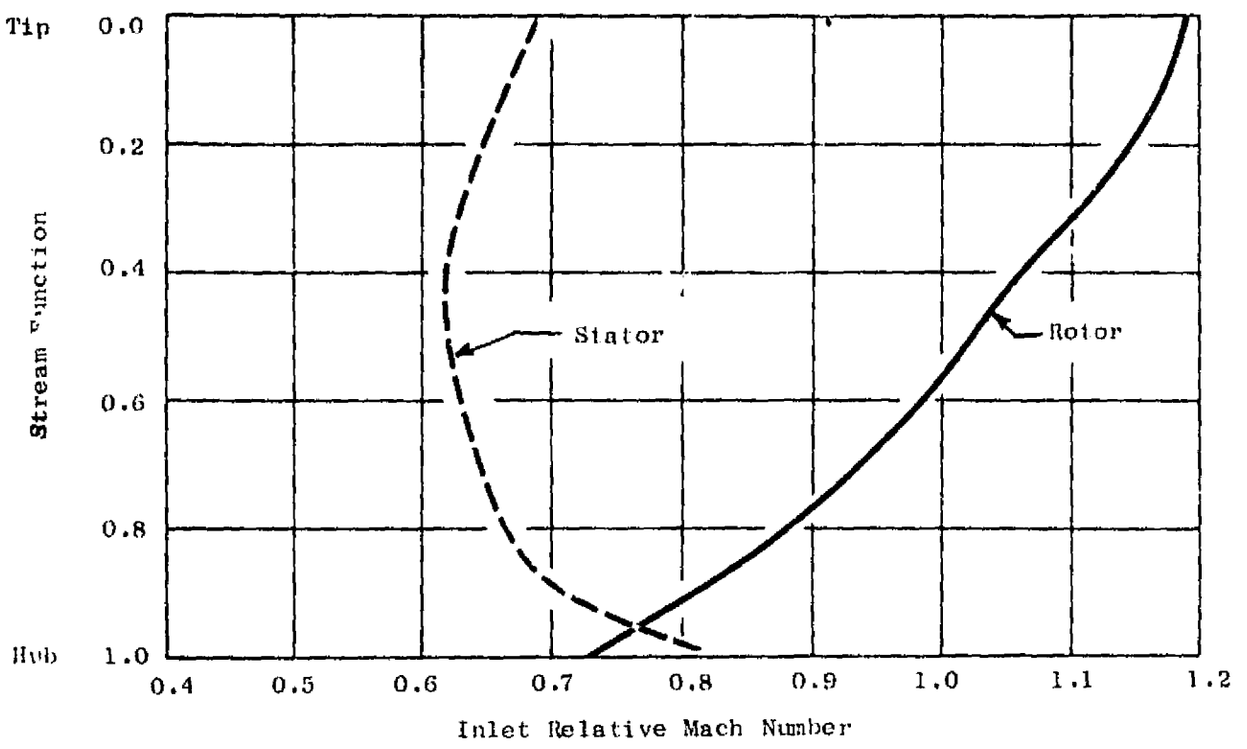

Figure 16. Relative Mach Number Profiles.

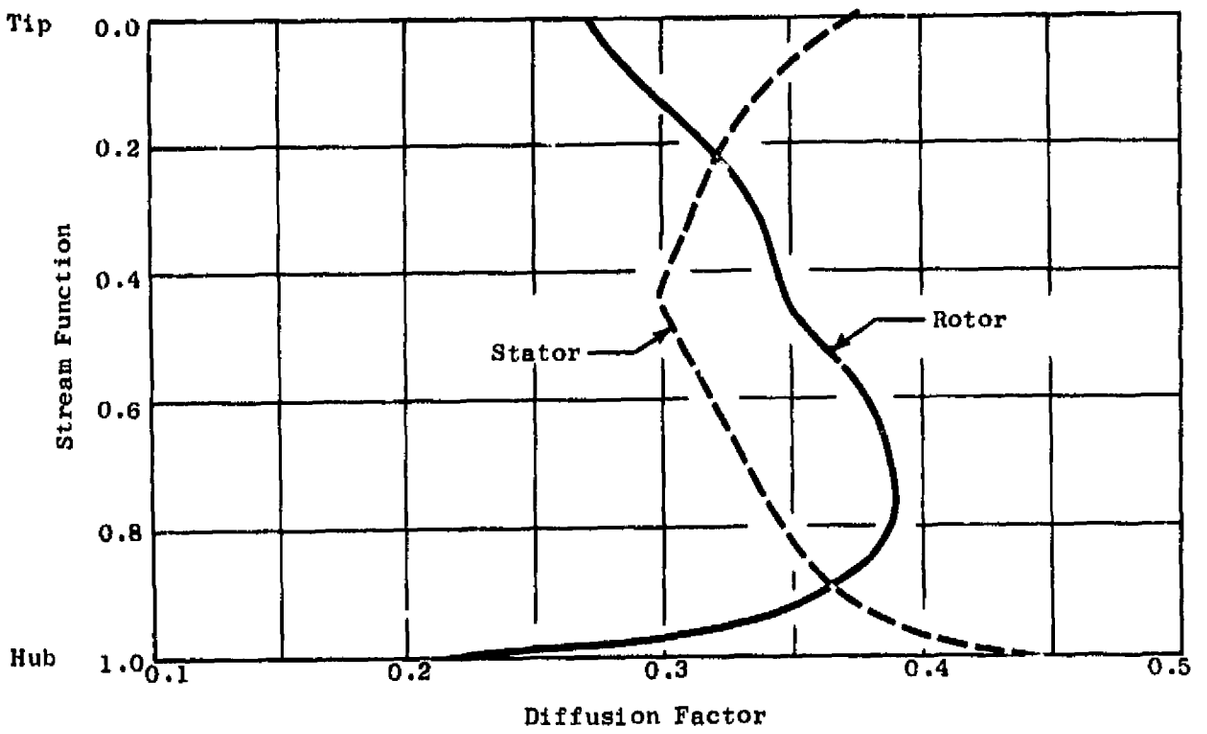

Figure 17. Diffusion Factor Profiles.

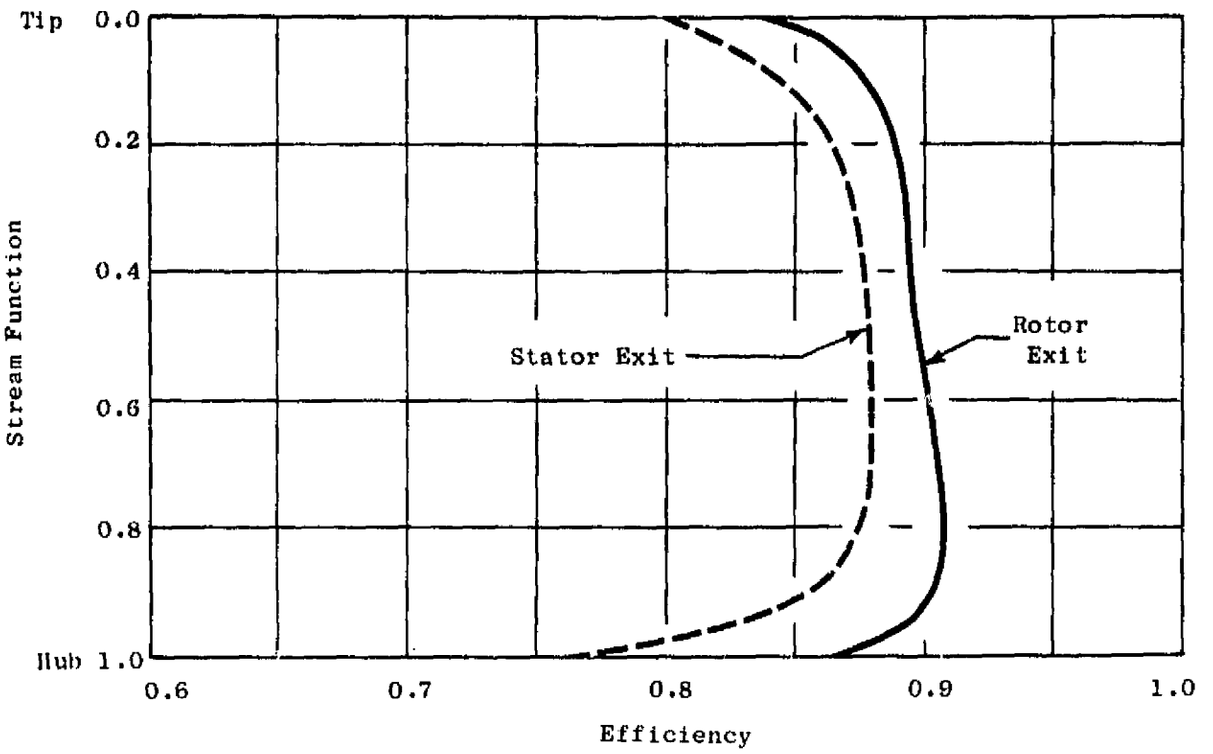

Figure 18. Fan Efficiency Profiles.

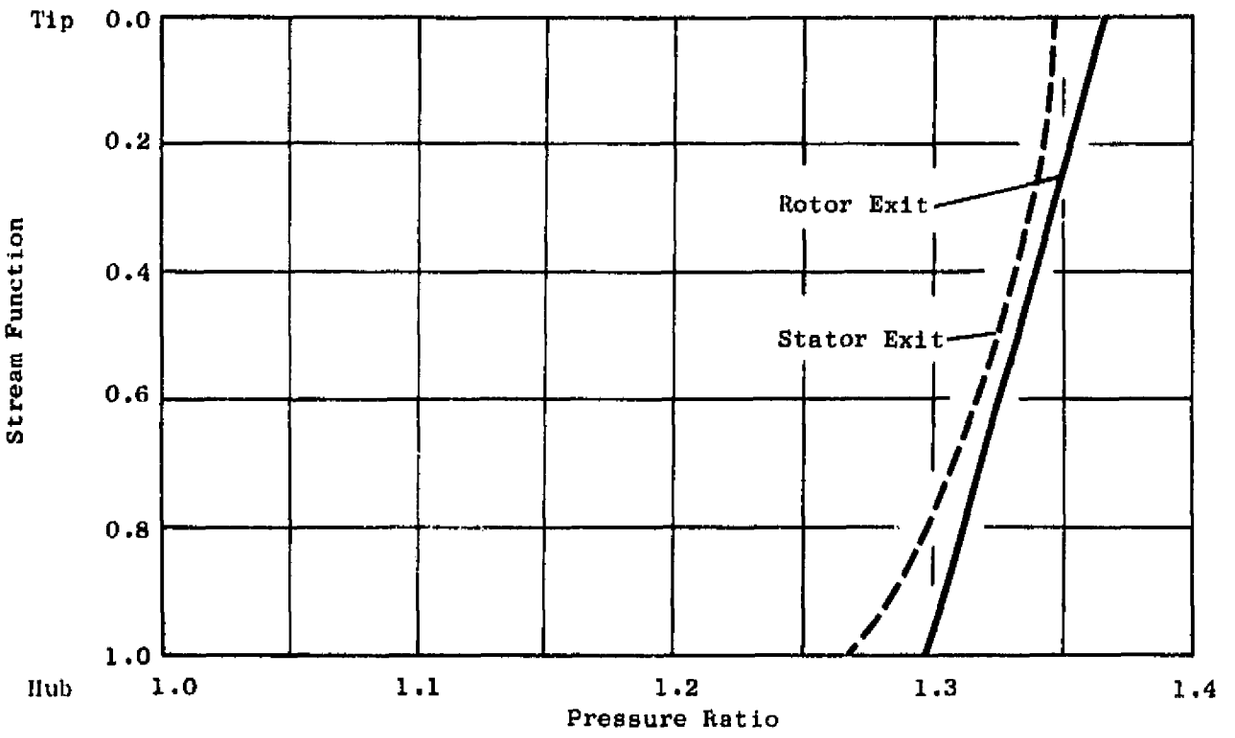

Figure 19. Total Pressure Profiles.

Table VII. Turbine Aerodynamic Design Parameters.

Inlet Temperature, K (° R)	1144 (2060)
Inlet Gas Flow, kg/sec (lbm/sec)	32.05 (70.66)
Inlet Pressure, kN/m^2 ($lbf/in.^2$)	357.4 (51.85
Total-to-Total Pressure Ratio	2.85
Exit Mach Number	0.55
Exit Total Temperature, K (° R)	917 (1651)
Adiabatic Efficiency	0.86
Design Energy, J/g (Btu/lbm)	260.6 (112.1)
Tip Diameter, m (in.)	1.684 (66.30)
Radius Ratio	0.9392
Blade Length, cm (in.)	5.12 (2.014)
Number of Nozzle Vanes	138
Number of Blades	364
Number of OGV's	9
Blade Aspect Ratio	2.10
Pitch-Line Wheel Speed, m/sec (ft/sec)	384.6 (1261.9)
Stage Work Coefficient, $gJ\Delta h/2w^2$	0.88
Stage Velocity Ratio, μ/Vo	0.46
Admission Arc, degrees	360
Hub Reaction, percent	10
Tip Reaction, percent	20

guide vanes are not needed to straighten the exhaust flow. At the cruise operating point, exit swirl angles and reaction levels are similar to the design point. At reduced power settings, such as the loiter operating point, the reaction tends to decrease toward the impulse condition. Thus, incorporating some reaction at the turbine design point helps to prevent part-speed turbine efficiency from dropping as rapidly as it would with an impulse design. For positive reactions, blade aerodynamic loading parameters decrease, thus allowing lower blade solidities compared to an impulse stage.

The design-point vector diagram analysis was carried out by an axisymmetric, through-flow analysis which utilizes both streamline slope and curvature. Leakage and coolant-flow injection or extraction was included at stations between the blade rows. Such flows have been shown to have significant local effects, depending on their penetration into the main flow.

Table VIII gives turbine flow-path coordinates, and Figure 20 shows the aerodynamic flow path with the analysis stations and the resulting flow streamlines. Simulation of the flow into the turbine from the scroll will be discussed in Section 4.2.3. The final vector diagrams, based on nomenclature given in Figure 21, are presented graphically in Figures 22 through 24. Radial distributions of nozzle and blade efficiencies used in the analysis were generated using a General Electric Evendale cascade correlation technique and are presented in Figure 25. The turbine was designed in such a way as to produce a constant total pressure profile at the stage exit. This required a blade which was "decambered" at the endwalls and overdesigned in the low loss regions away from the endwalls. The nozzle swirl profile is very close to a free-vortex type of distribution.

Three distinct nozzle vane airfoils are required for this turbine, due to the way in which flow enters the nozzle diaphragm from the scroll. This is shown schematically in Figure 26. At the turbine design point, the nozzle pitch-line total-to-static pressure ratio is 2.76. The nozzle vane airfoils were therefore designed as convergent-divergent sections to take advantage of the higher cascade efficiencies and more uniform exit profiles available from this configuration at elevated pressure ratios. However, previous analyses of this type of nozzle indicated that, if the convergent-divergent portion was designed for the full design pressure ratio, turbine part-speed performance would be poor due to overexpansion in the nozzle. For this reason, the divergent portions of the nozzles were designed to a pressure ratio of 2.5 at the pitch line. The same percentage reduction in pressure ratio was maintained at hub and tip.

All three vane airfoil families are geometrically similar from the throat to the trailing edge, as shown in Figure 27. Since each vane family is designed for a different inlet angle, each has its own optimum solidity as determined by the requirement that the compressible Zweifel loading parameter be equal to 0.34. Axial width for the nozzle vane is set by mechanical considerations at 4.3 cm (1.7 inches) for all three families. The spacing of each family was adjusted to give the required solidity. Figure 28 presents hub and tip sections for each vane family; the vane profiles are

Table VIII. Turbine Flow-Path Coordinates.

Tip:

Axial Station (cm)	Axial Station (in.)	Radius (cm)	Radius (in.)	
7.4930	-2.9500	87.8840	34.6000	-Point "A" in Figure 20
7.3792	-2.9052	87.2444	34.3482	
7.0411	-2.7721	86.6244	34.1041	
6.4892	-2.5548	86.0425	33.8750	Ellipsoidal
5.7399	-2.2598	85.5167	33.6680	Transition
4.8163	-1.8962	85.0626	33.4892	
3.5560	-1.4000	84.6422	33.3237	-Nozzle L.E.
2.5629	-1.0090	84.4136	33.2375	
1.3012	-0.5123	84.2569	33.1720	
0.0000	0.0000	84.2010	33.1500	
0.7620	0.3000	84.2010	33.1500	-Nozzle T.E.
3.7338	1.4700	84.2010	33.1500	-Blade L.E.
6.1722	2.4300	84.2010	33.1500	-Blade T.E.
11.938	4.7000	84.2010	33.1500	-Diffuser L.E.
28.702	11.3000	83.2980	32.7949	-Diffuser T.E.
35.56	14.0000	82.8568	32.6208	-Exit

Hub:

14.3022	-5.6308	79.6166	31.3451	-Point "B" In Figure 20
11.7940	-4.6433	79.5373	31.3139	
6.4038	-2.5212	79.0844	31.1356	
3.5560	-1.4000	79.0844	31.1356	-Nozzle L.E.
0.7620	0.3000	79.0844	31.1356	-Nozzle T.E.
3.7338	1.4700	79.0844	31.1356	-Blade L.E.
6.1722	2.4300	79.0844	31.1356	-Blade T.E.
7.1120	2.8000	79.0844	31.1356	
8.6360	3.4000	79.0722	31.1308	
10.1600	4.0000	79.0092	31.1060	
11.9380	4.7000	78.8706	31.0514	-Diffuser L.E.
16.2560	6.4000	78.3369	30.8413	
28.7020	11.3000	76.1312	29.9729	-Diffuser T.E.
35.5600	14.0000	74.9536	29.5093	-Exit

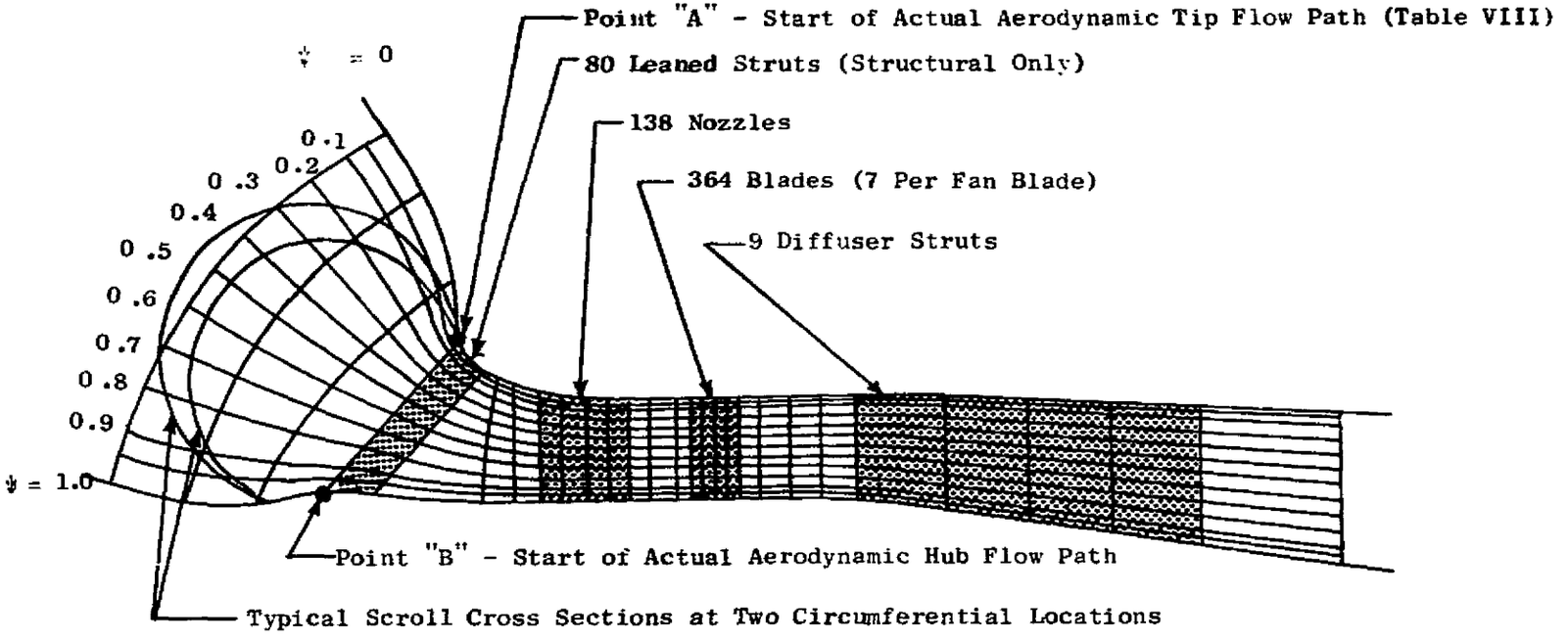

Figure 20. Turbine Aerodynamic Flow Path.

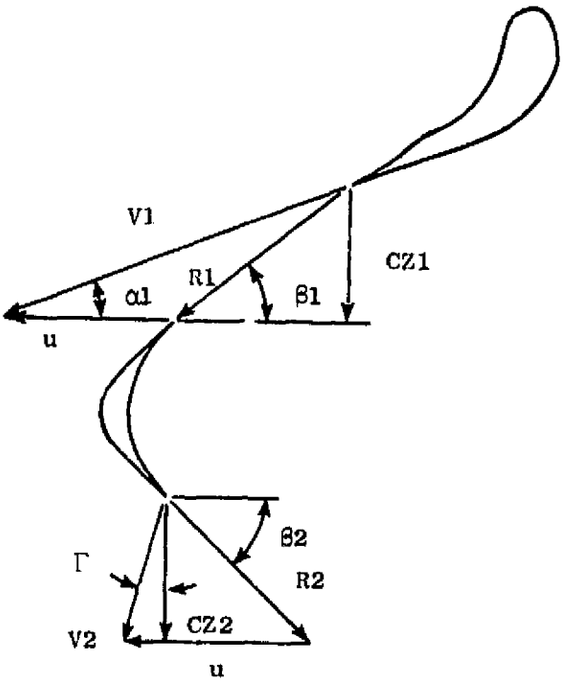

Station

1 Nozzle Exit/Blade Inlet

2 Blade Exit

Figure 21. Turbine Velocity Diagram Notation.

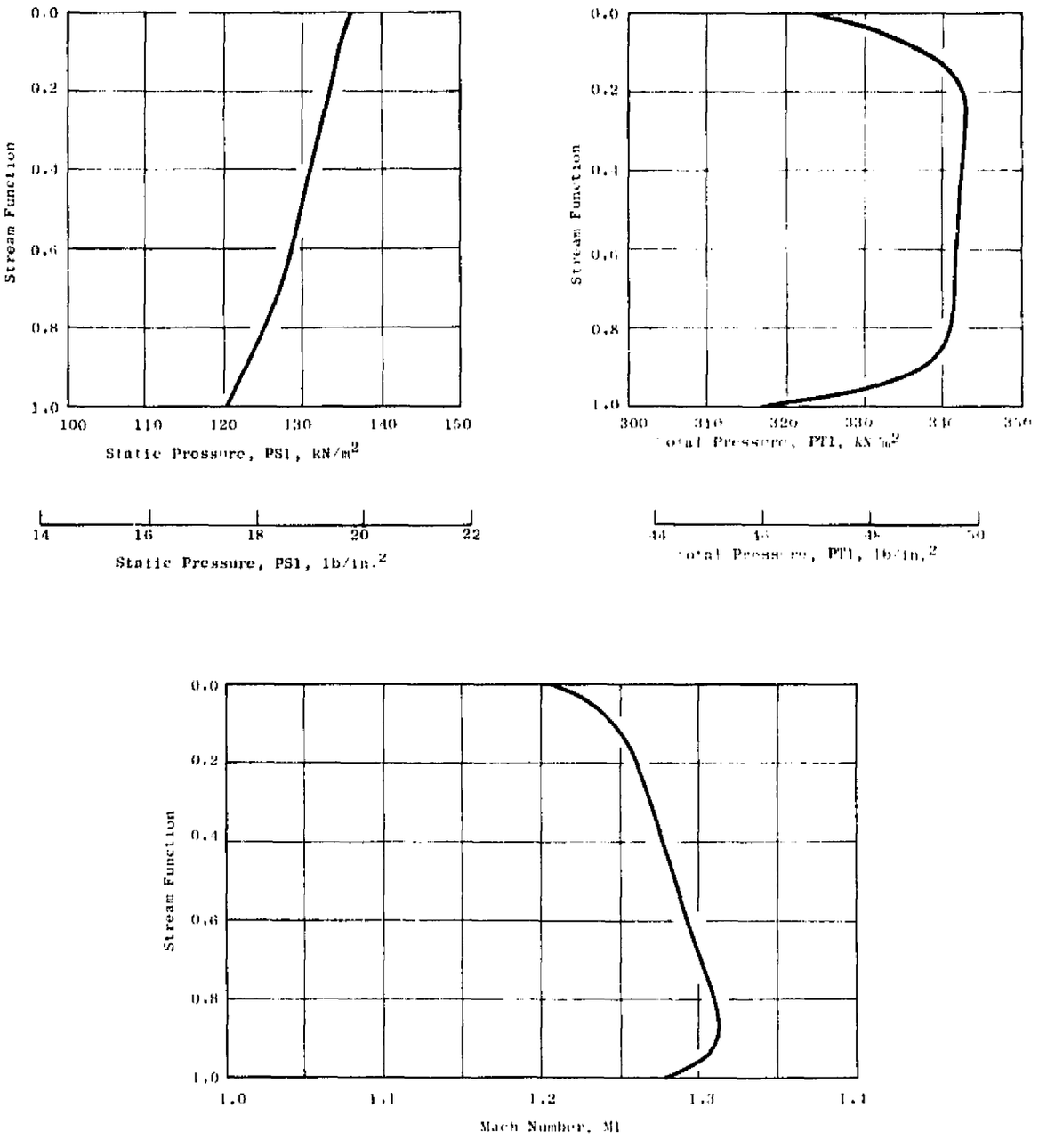

Figure 22. Turbine Vector Diagrams; Nozzle Exit.

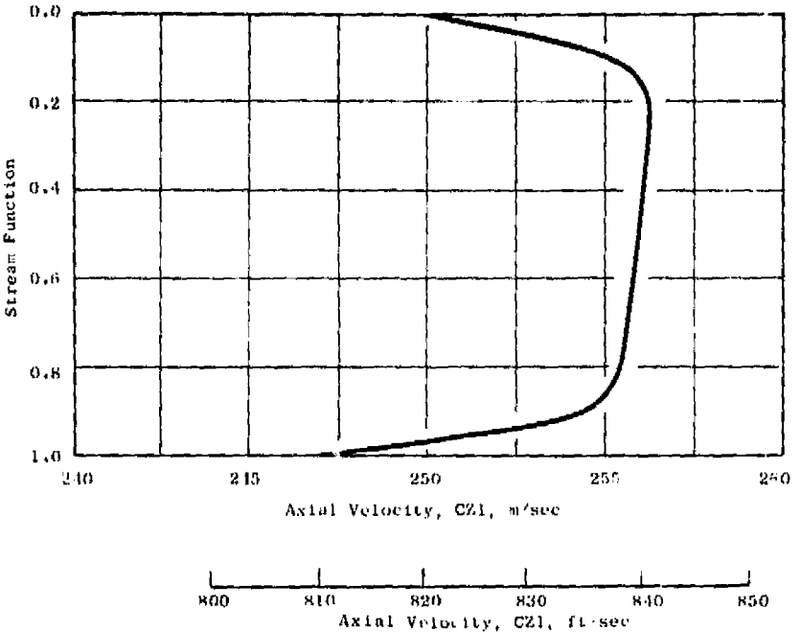

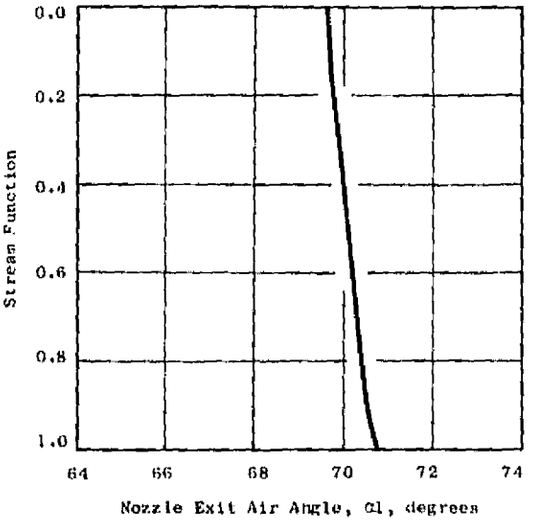

Figure 22. Turbine Vector Diagrams; Nozzle Exit (Concluded).

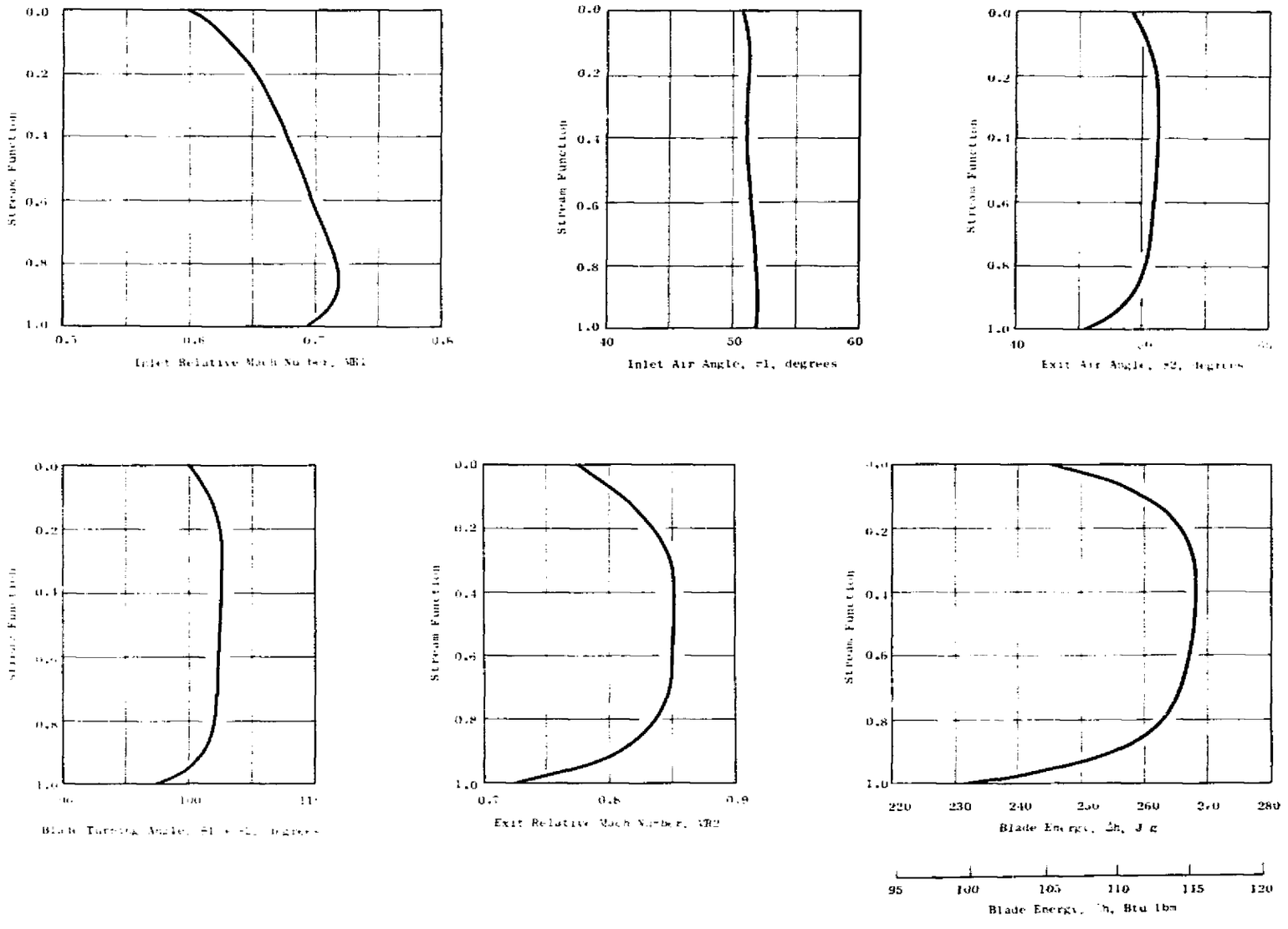

Figure 23. Turbine Vector Diagrams; Blade.

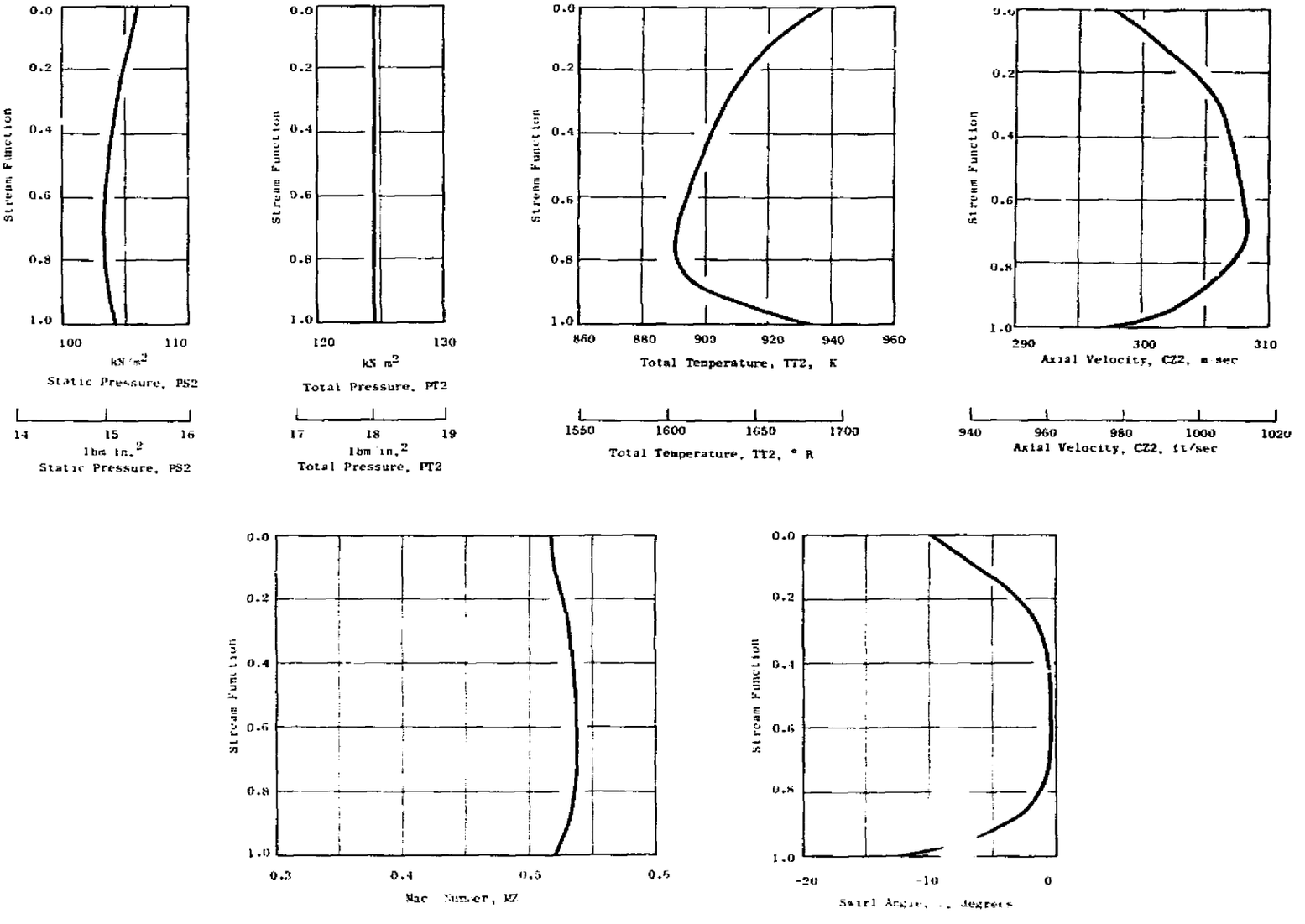

Figure 24. Turbine Vector Diagrams; Stage Exit.

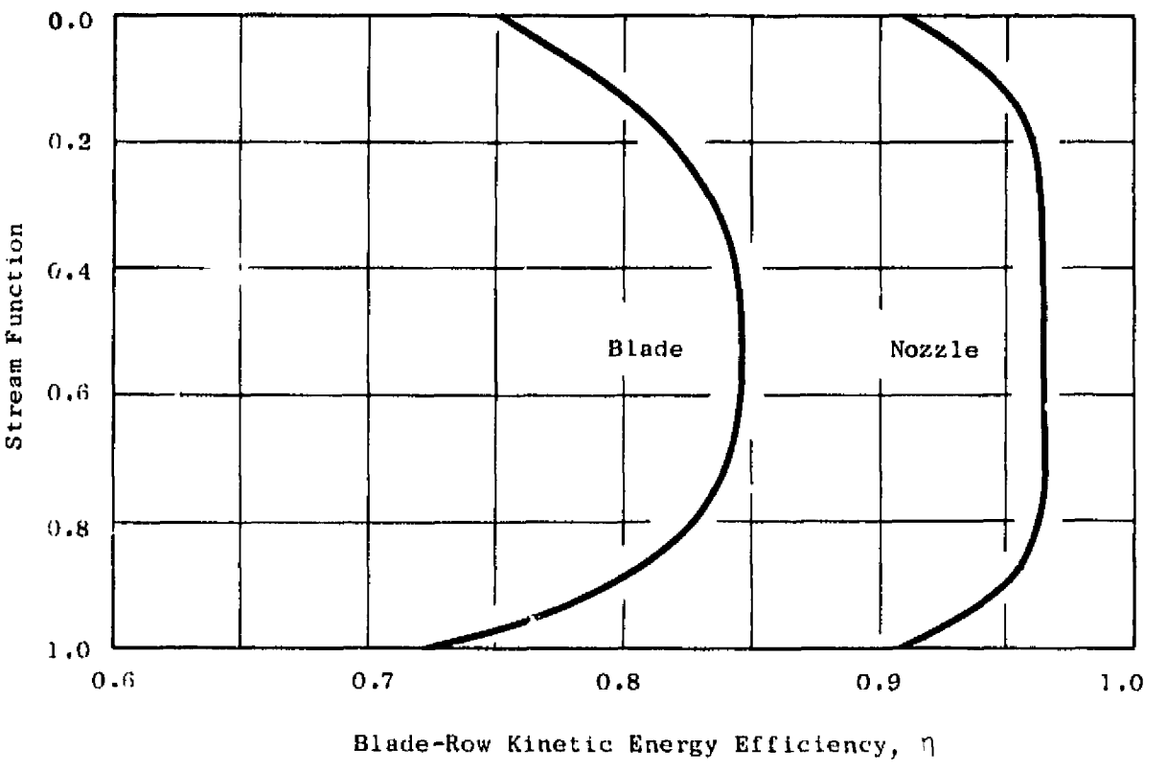

F'gure 25. Turbine Blade-Row Efficiencies.

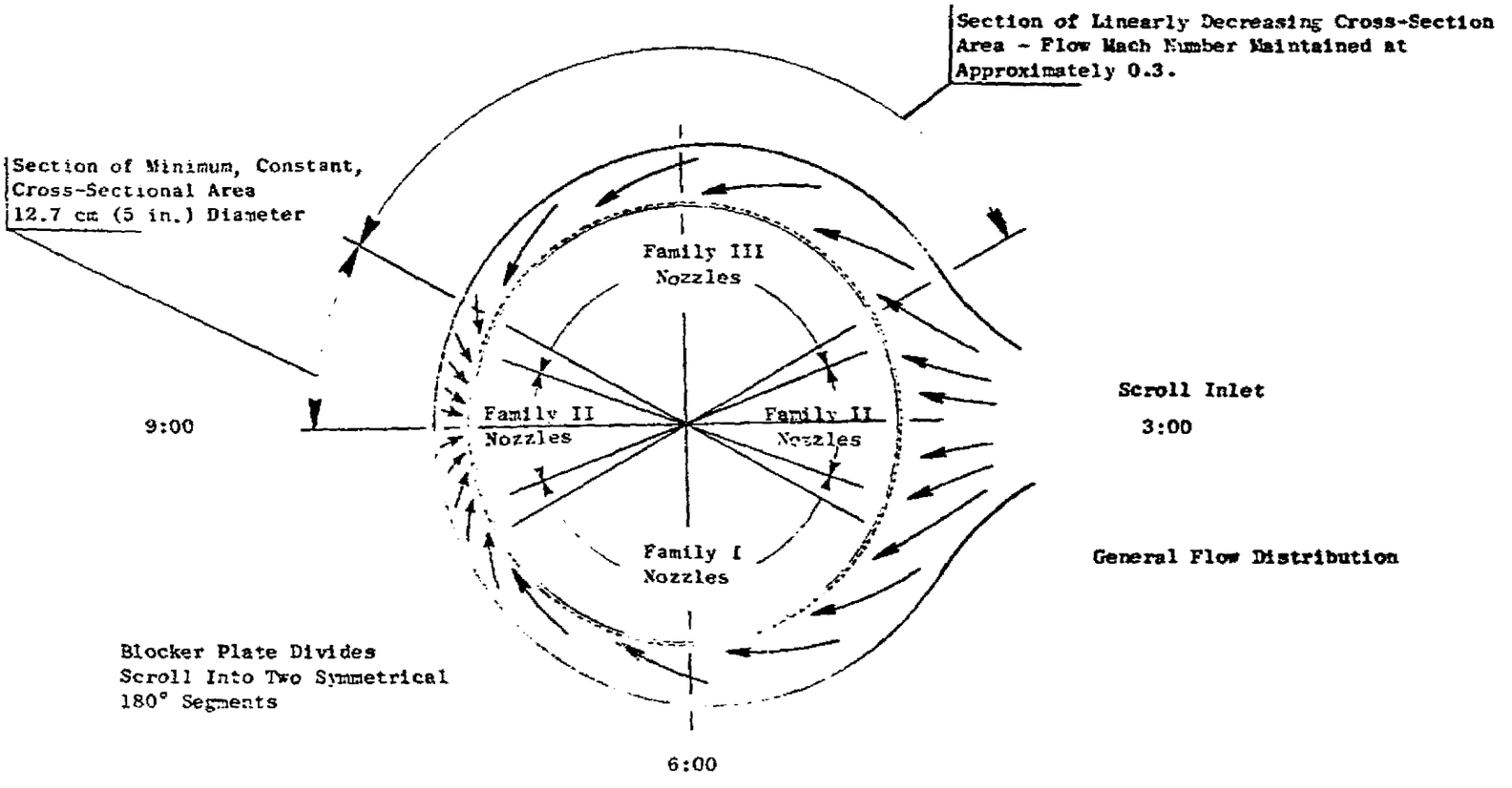

Figure 26. Schematic Representation of Scroll Flow Distribution.

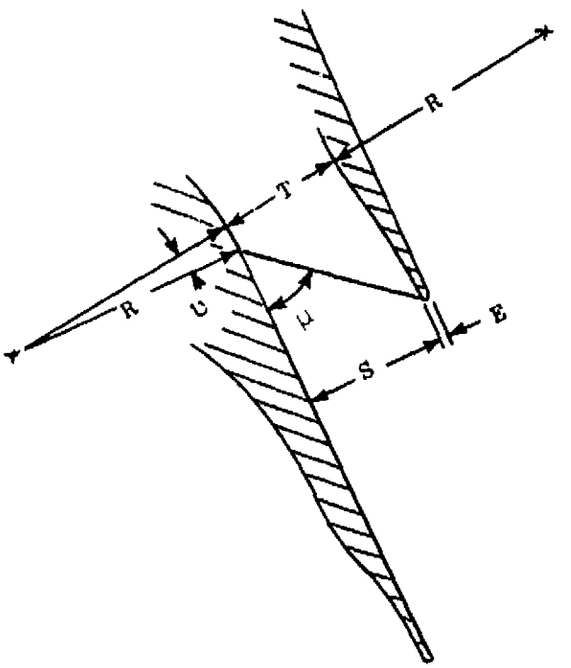

	Hub	Tip
R =	2T	2T
S	1.063T	1.033T
E =	0.06T	0.06T
μ	51.0 degrees	51.0 degrees
υ	5.8 degrees	3.6 degrees

Figure 27. Divergent Portion of Nozzle Passages.

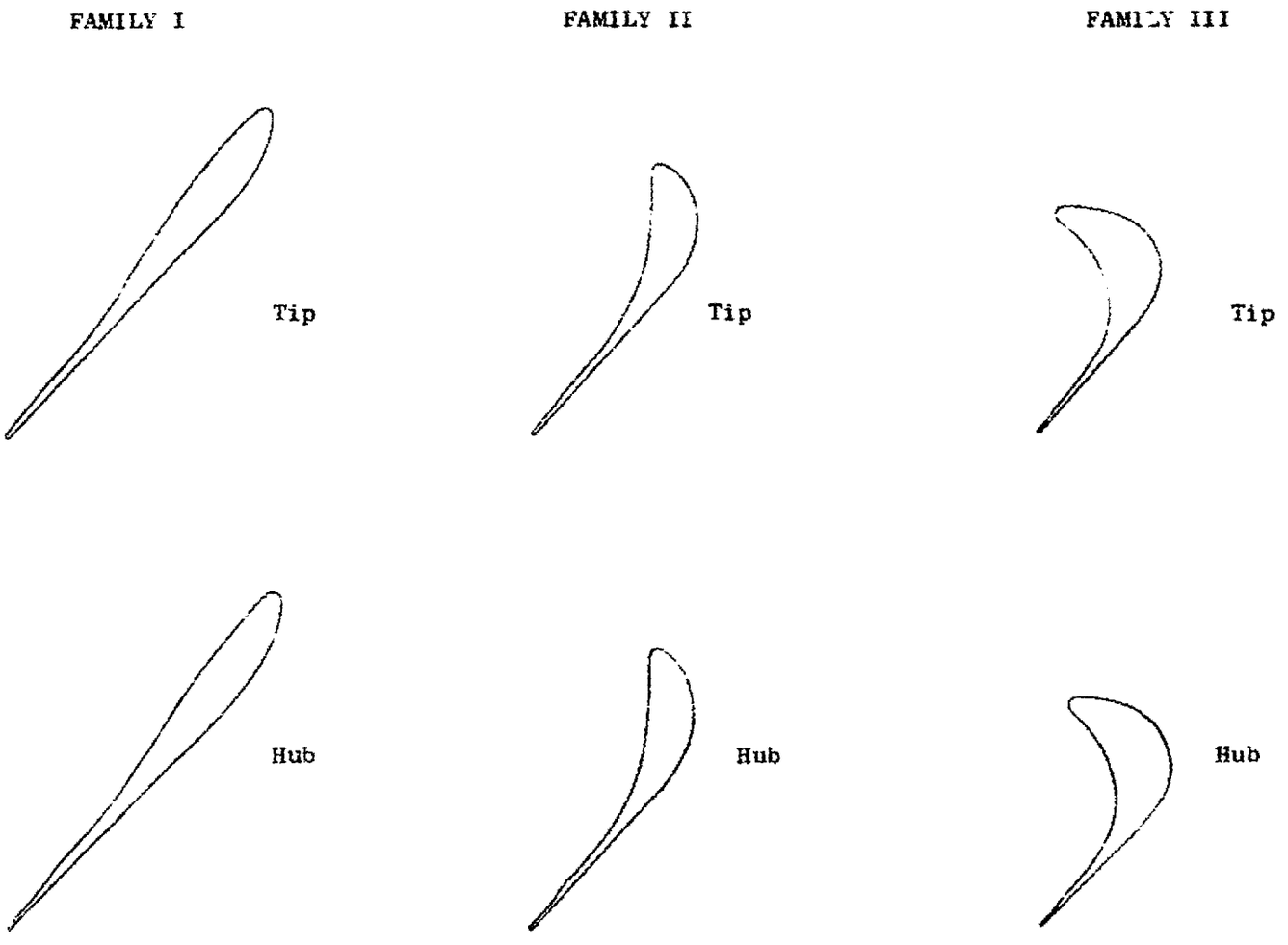

Figure 28. Nozzle Vane Profiles.

linear between hub and tip. Figure 29 is an unwrapped view of the nozzle diaphragm depicting vane airfoil placement.

Three blade sections and some pertinent design parameters are presented in Figure 30. This is the minimum number required to adequately define the spanwise variations in blade airfoil sections as dictated by the vector diagrams. A total of 364 blades (seven per each of the 52 fan blades) was selected as an acceptable number mechanically, and this number has been maintained. With spacing thus determined, blade axial width was calculated to meet solidity requirements based on a compressible Zweifel loading parameter of 0.8. The final blade axial width of 2.44 cm (0.96 in.) corresponds to a pitch-line solidity of 1.73, which is about ten-percent oversolid at design point. This higher solidity was chosen because the blade aerodynamic-loading coefficient increases at such off-design settings as VTO nominal and cruise, thus requiring solidities higher than the design-point, optimum value.

An exit diffuser system is located downstream of the turbine blades as shown in Figure 20. This system includes an expanding flow path with an area ratio of about 1.5 and nine equally spaced struts. The struts serve as structural members to carry stator loads.

4.2.3 Scroll

The general configuration of the scroll is illustrated and discussed further in Section 4.6. A blocker plate, located at 180° from the inlet, effectively divides the scroll into two 180° segments. Flow entering the scroll is divided evenly between each of the segments and turned circumferentially. The scroll segments are circular in cross section and are designed to maintain a flow Mach number of 0.3 in the circumferential direction by decreasing in cross-sectional area linearly from the inlet to a 12.7-cm (5 inches) diameter, constant-area section near the blocker plate. This is the minimum allowable area mechanically.

There are 80 leaned struts in the transition duct from the scroll to the nozzle diaphragm. These are for mechanical structure only since their solidity (less than 0.4) makes them ineffective as airfoil sections. The struts, however, are aligned to the general flow direction as determined by the axisymmetric flow analysis.

A realistic representation of the scroll and transition duct is important because both the level and radial distribution of flow angles at the struts and the nozzle vane leading edges were obtained from the axisymmetric analysis. The inner radius of the scroll ring is a constant 77.5 cm (30.5 inches) so that the decrease in scroll cross-sectional area is accomplished by decreasing the outer radius. This results in a stream function distribution around the scroll where streamline spacing is greater near the inner and outer flow path (less flow in these regions) and smaller in the central areas where higher flow rates are generated by the shrinking of the scroll skin. Two scroll cross sections have been superimposed on the flow path in Figure 20 in an attempt to illustrate this effect.

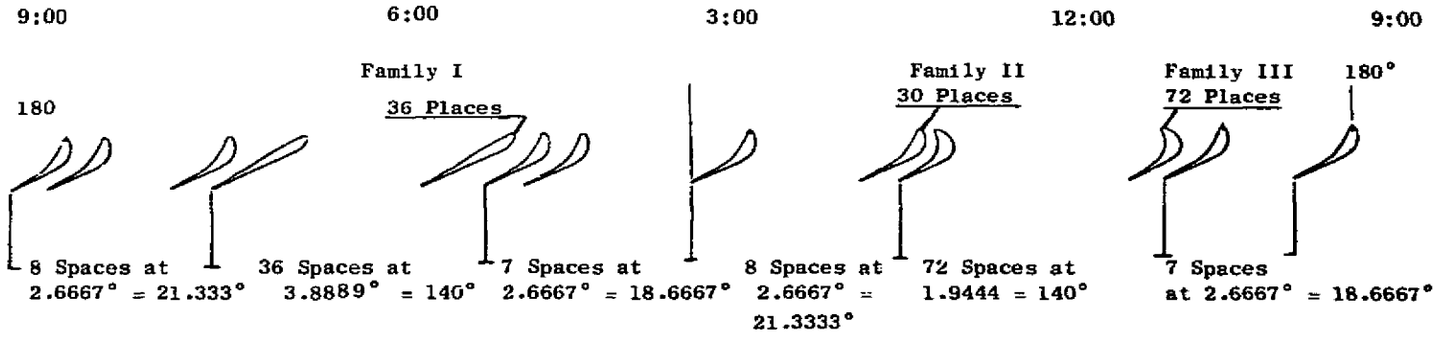

Figure 29. Unwrapped View of Nozzle Partitions.

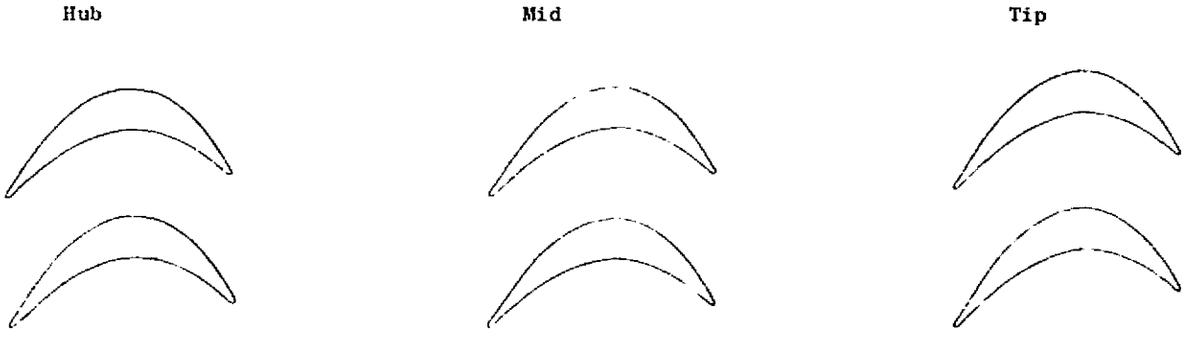

	Hub	Mid	Tip
Throat Dimension (D_o)	0.798 cm (0.3141 in.)	0.818 cm (0.322 in.)	0.818 cm (0.322 in.)
Unguided Turning	10°	10°	11°
Trailing Edge Diameter	0.051 cm (0.021 in.)	0.051 cm (0.020 in.)	0.051 cm (0.020 in.)

Figure 30. Turbine Blade Profiles.

The actual flow-path boundaries upstream of the struts in Figure 20 were determined from an incompressible-flow plot in which the streamlines were forced to their respective stream function values.

Special attention was paid to that portion of the inlet flow path from the strut-tip leading edge through to the vane throat to ensure that no diffusion took place anywhere in this high curvature, transition area.

Scroll pressure loss estimates have been made for the scroll with two inlet configurations representing a typical cruise fan installation. The scroll inlet diameter is 44.5 cm (17.5 inches) which gives a scroll inlet Mach number of approximately 0.30.

Scroll pressure losses are composed of the following components:

- Inlet bend loss
- Skin friction
- Strut drag
- Nozzle inlet transition loss
- Diffusion loss
- Valve loss

These pressure losses are then simply summed to get the total scroll pressure drop. This approach has been relatively successful in predicting pressure losses for several previous scroll model tests.

Table IX summarizes the pressure loss estimates. The inlet bend loss is not a large portion of the total loss (about 14 percent). Since the inlet configuration may differ for each installation, the total losses shown in Table IX should only be considered as typical values.

4.3 COOLING AND CLEARANCE CONTROL

The turbotip fan includes two unique design features that require special attention with regard to temperatures and cooling. The hot tip-turbine carrier is bolted to a titanium fan blade. Temperature limits for the titanium fan blade are around 315° C (600° F), as compared to turbine gas temperatures of 760° C (1400° F). The transfer of heat from the turbine to the fan must be carefully controlled. A carrier cooling system has been defined for the LCF459.

The second critical temperature area is the frame outer case and seal support. This large ring structure, approximately 1.78 m (70 inches) in diameter, supports the bearing structure and the fan and turbine tip seals. The outer case temperature must be controlled to minimize frame thermal

stresses because the major part of the frame runs cold; only the outer tip is hot. Frame growth must also be limited to provide acceptable turbine and fan tip clearances. This section of the report defines these cooling systems and includes an evaluation of the fan and turbine leakage flows with the associated corrections to performance.

Table IX. Scroll Pressure Loss Summary.

Percent of Inlet Total Pressure Loss	
	Cruise Fan
Inlet bend	0.4
Skin friction	1.6
Strut drag	0.2
Nozzle inlet transition loss	0.1
Diffusion loss	0.3
Valve loss	0.3
Total	2.9

4.3.1 Turbine Carrier Cooling

The method used to cool the turbine blade carriers extracts cooling air from between the fan stator vane tips, ducts it forward through the fan and turbine flow divider, then pumps it through the carriers by means of scoops attached to the carrier aft sides. This scheme is shown schematically in Figures 31 and 32 which show, respectively, the anticipated cooling flows and associated pressures at the design-point conditions. The cooling air is extracted from points near the fan stator vane trailing edge plane and near the vane pressure surfaces in order to maximize the available static pressure. Air scoops are provided at this location to recover a portion of the velocity head. The flows shown in Figure 31 are based on the clearances shown in Figure 33.

The following discussion and analysis describes the operation of this carrier cooling scheme.

During all steady-state operating conditions, the carrier cooling system must be able to maintain a forward seal cavity pressure equal to or greater than the turbine hub static pressure to exclude turbine hot gas from the carrier area. The most severe steady-state operating point in terms of the cooling system design is the aerodynamic design point where turbine reaction

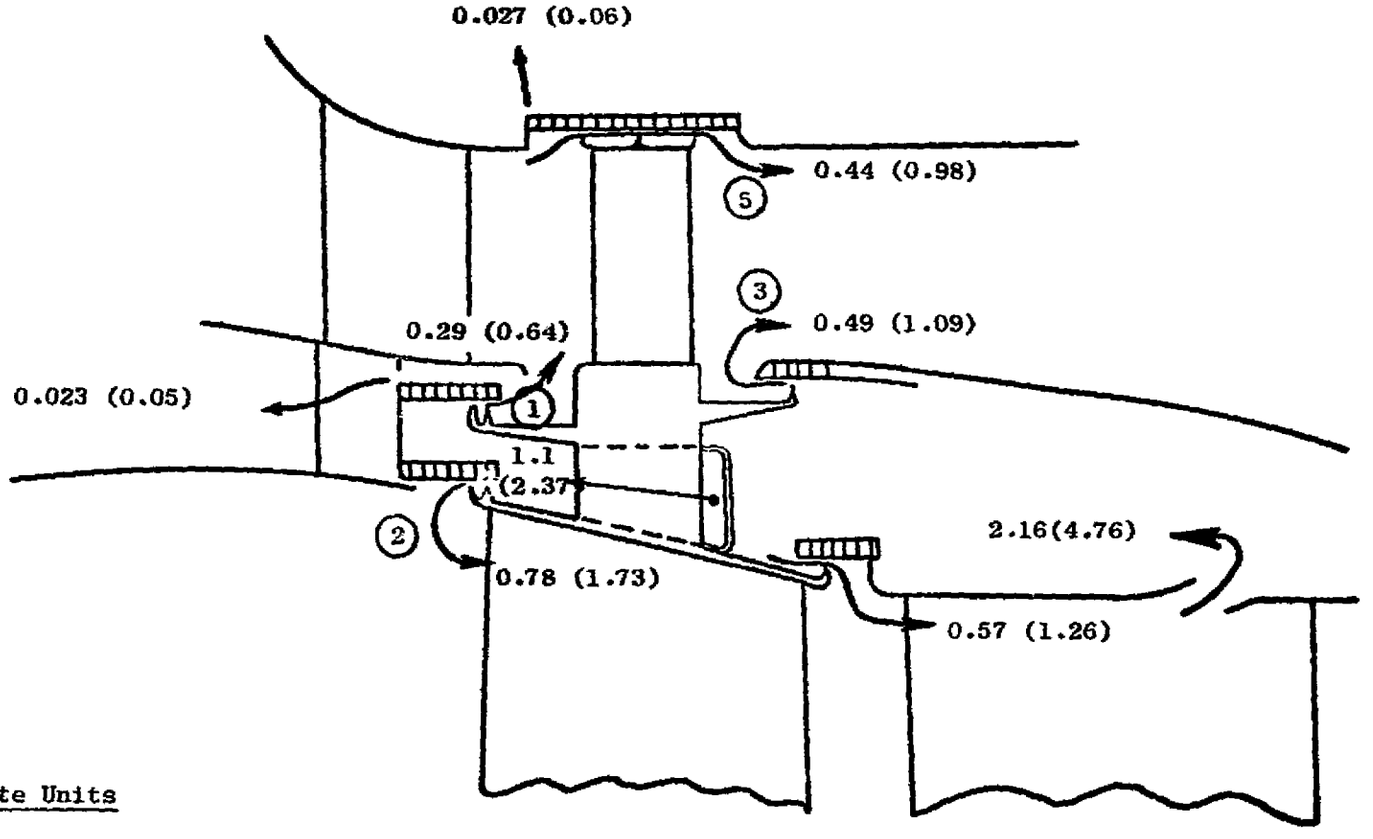

Flow Rate Units

kg/sec (lbm/sec)

Figure 31. Carrier Cooling System Flow Rates.

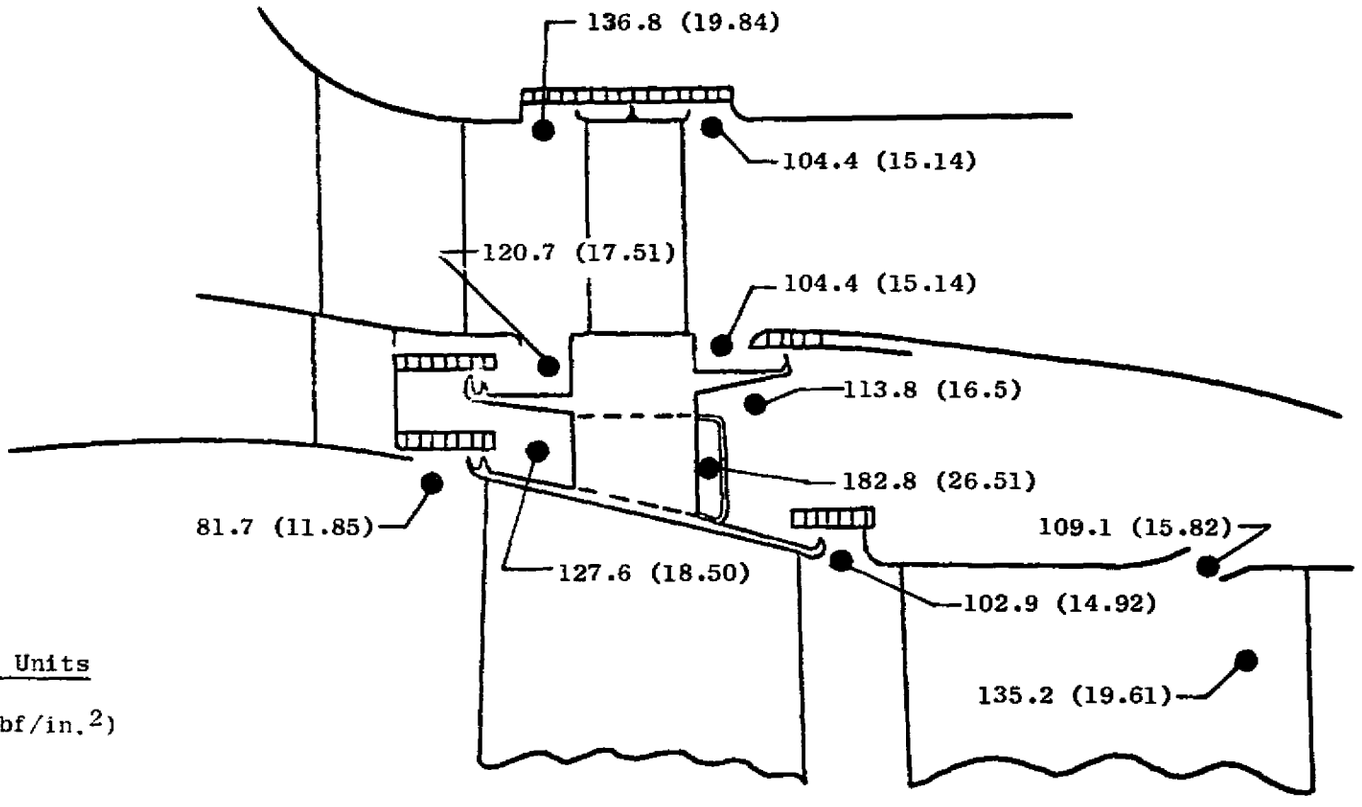

Figure 32. Carrier Cooling System Pressures.

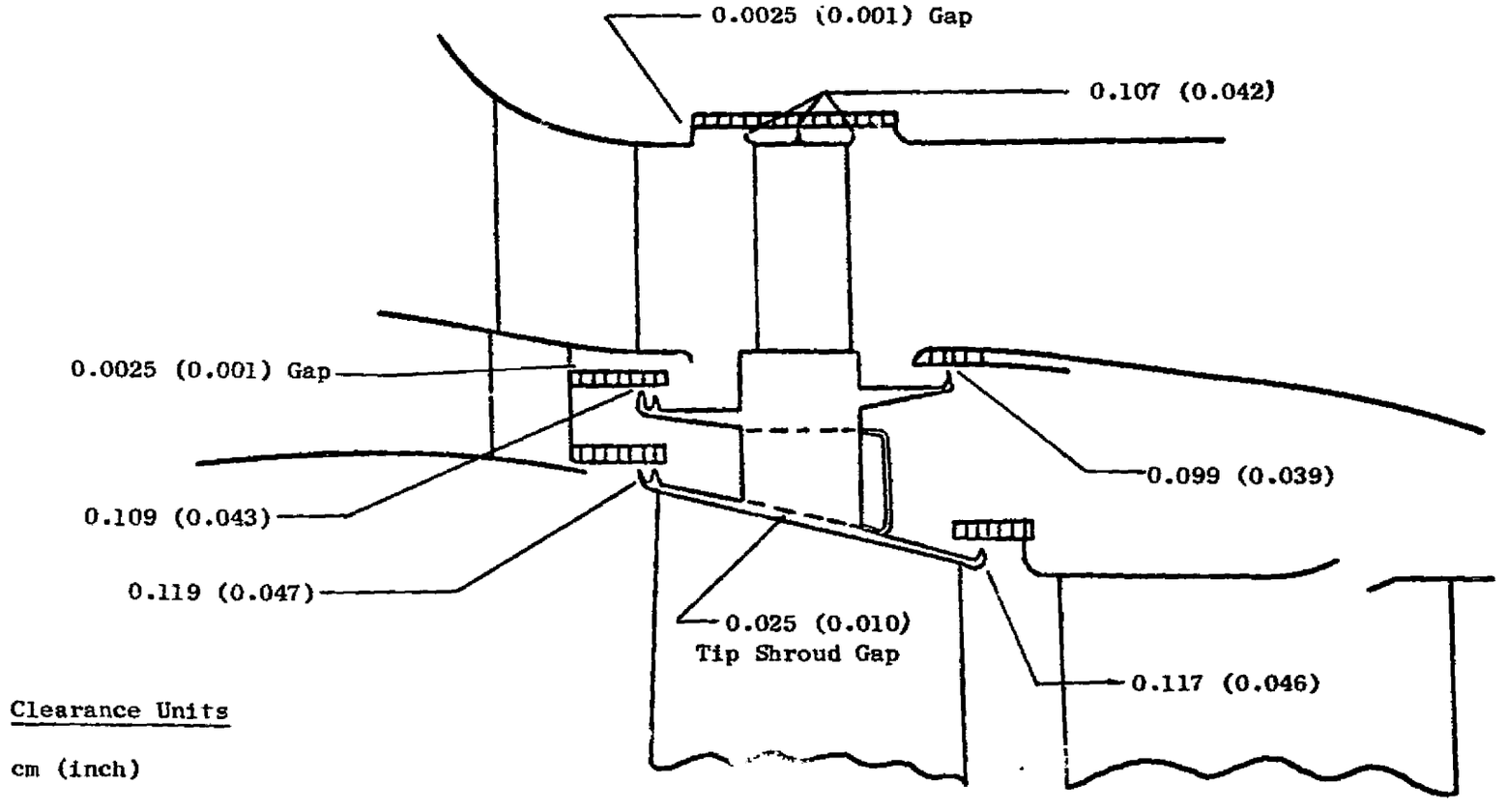

Figure 33. Turbine and Fan Clearances at Design Point.

is highest. The turbine hub static pressure at the design point is 120 kN/m^2 (17.51 lbf/in.^{2}). A design pressure of 127 kN/m^2 (18.5 lbf/in.^{2}) for the forward seal cavity was selected to ensure a positive pressure differential across the outer forward air seal at all times.

During initial start-up, and possibly during a very rapid acceleration, the turbine hub static pressure could briefly exceed the pumping capability of the carrier scoops, causing hot gas to backflow through the scoop and into the rear seal cavity. This is acceptable for a short period, but the scoop must be able to recover and start pumping cool air again even with the aft seal cavity filled with hot gas. Recovery will occur under these conditions if the static pressure on the aft side of the carrier exceeds that on the forward side so that the carrier scoops are not required to pump. Under backflow conditions the static pressure on the forward side of the carrier will be intermediate between the turbine hub and fan tip static pressures. The exact value depends on the relative clearance areas of the inner and outer forward seals and the amount of flow through the carrier scoop. Figure 34 shows the forward seal cavity static pressure as a function of relative clearance. For equal seal clearances the forward cavity pressure will be 105 kN/m^2 (15.4 lbf/in.^{2}). For the case where the outer seal clearance area is 50% larger than the inner seal clearance area, the curve gives a pressure of 114 kN/m^2 (16.5 lbf/in.^{2}) on the forward side of the carrier. Thus, if the static pressure on the aft side of the turbine blade carrier were 114 kN/m^2 (16.5 lbf/in.^{2}) at the aerodynamic design point, the cooling system would start flowing cool air even if the carrier scoops did not pump.

To summarize the requirements for this cooling system at the aerodynamic design point:

- the static pressure on the aft side of the carrier shall be at least 114 kN/m^2 (16.5 lbf/in.^{2}) to ensure starting and recovery from backflowing.

- the carrier scoop shall be able to pump the pressure from 114 kN/m^2 (16.5 lbf/in.^{2}) up to 128 kN/m^2 (18.5 lbf/in.^{2}) at a flow equal to the total leakage through both forward seals.

A time-share computer program was written to represent the cooling system. Compressible-flow analysis was used to derive the pressure drops and flow rates. The pumping characteristics of the carrier were represented using estimated recovery characteristics as a function of mass flow ratio as shown in Figure 35. In this analysis, the fan and turbine seal clearances were represented as a function of speed and temperature. Section 4.3.3 gives a detailed description of the operating clearances and representation used in the seal leakage calculation.

At the fan design point, the scoop and air extraction areas were sized to produce the design pressures of 114 kN/m^2 (16.5 lbf/in.^{2}) at the back side of the carrier and 128 kN/m^2 (18.5 lbf/in.^{2}) at the forward seal cavity. The final areas for the fan design are:

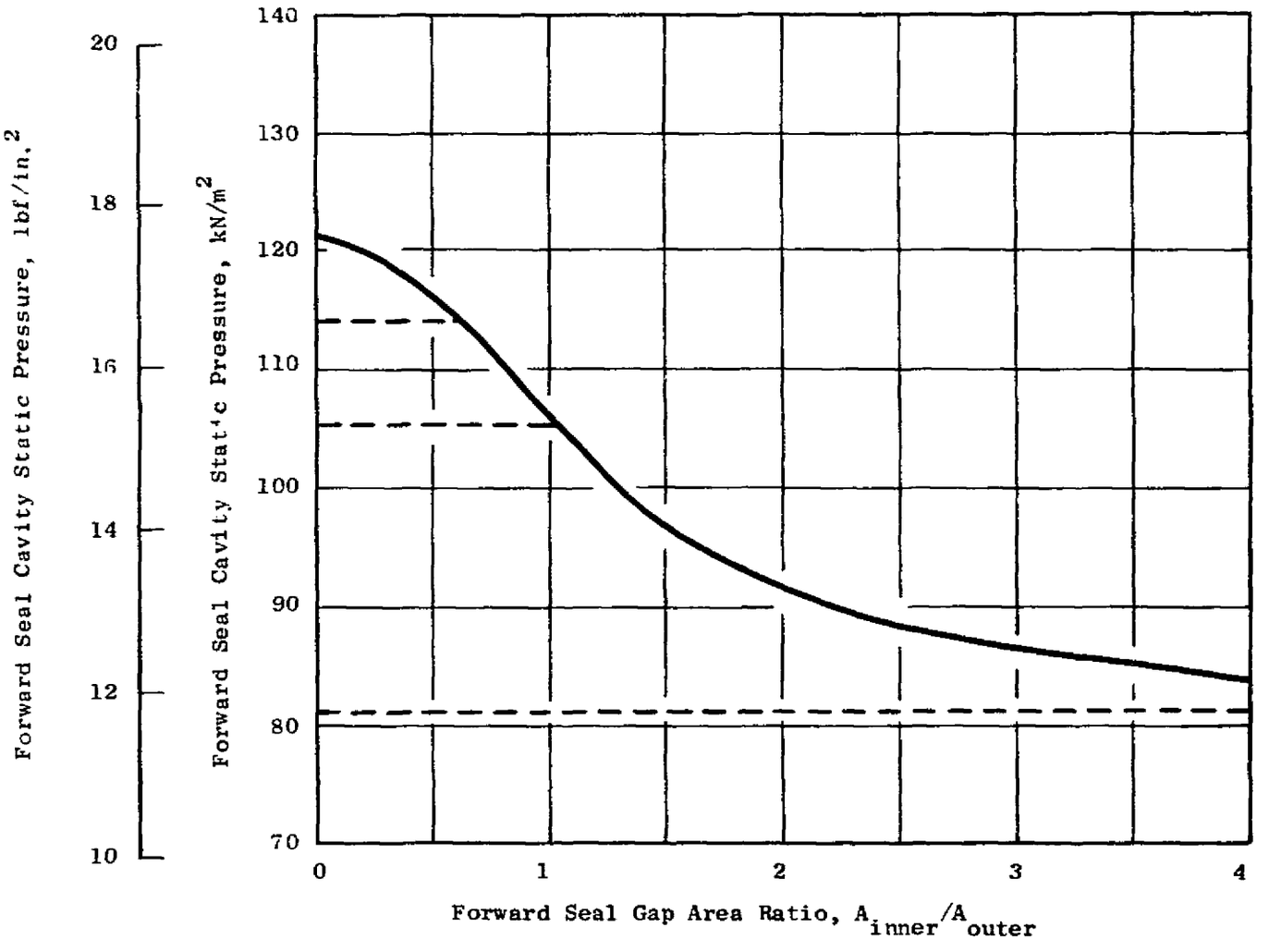

Figure 34. Forward Seal Cavity Pressure with No Carrier Scoop Flow.

- Pressure Recovery = (PS2 - PS1)/(PT1 - PS1)
- Mass Flow Ratio = V2/V1
  - 2 Denotes Scoop Inlet
  - 1 Denotes Free Stream

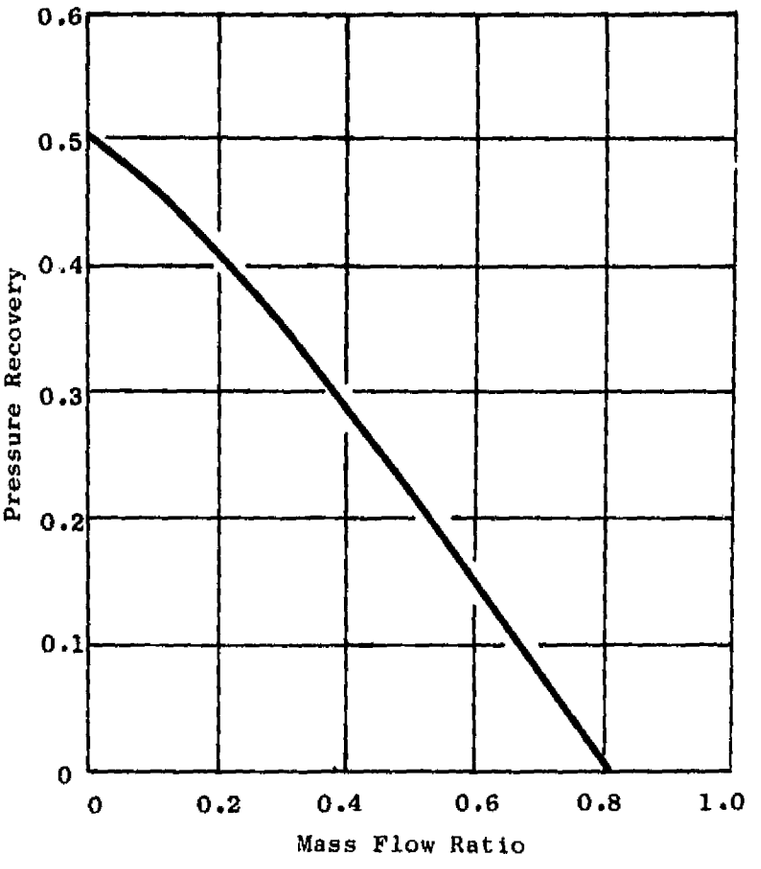

Figure 35. Carrier Pump Recovery Characteristics.

- Area of air extraction parts at stator vane trailing edge, 165 cm^2 (25.5 $in.^2$).
- Area at inlet of carrier scoops, 41.1 cm^2 (6.38 $in.^2$).
- Area at exit of carrier scoops, 48.4 cm^2 (7.50 $in.^2$).

The design-point leakage and cooling air flow rates and cavity pressures are shown in Figures 31 and 32. The effects of these leakage rates on fan and turbine performance will be presented in Section 4.3.4 of this report.

4.3.2 Frame Cooling

The need to maintain favorable fan tip seal clearances and reasonable frame thermal stresses requires cooling of the outer rings and casings of the fan frame. Without cooling, the total radial growth of the fan case would be about 0.64 cm (0.25 in.), and excessive seal clearances would occur. Frame cooling is therefore required to provide seal clearance control. Outer case impingement cooling is a method utilized on the CF6 engine for case cooling and low pressure turbine clearance control. This method was selected for the LCF459. The impingement cooling system uses manifolds with many small holes to direct air jets onto the structure to be cooled. For the LCF459, this arrangement was designed to maintain a frame temperature of 232° C (450° F).

Low frame temperatures are also desired for low thermal stresses. The outer casing is attached to the fan bearing using nine radial struts. The bending stresses in the struts are proportional to the relative frame casing and strut growth. Large growth of the struts does not occur because about 80 percent of the structure is within the cold fan flow path. The 232° C (450° F) frame temperature, as selected for good seal clearances, also yields acceptable thermal stresses.

The frame impingement system consists of air scoops and manifolds that direct the air onto the fan frame structure. Four scoops are used to extract 5.3 kg/sec (2.4 lbm/sec) of air from the fan discharge stream. This air is then distributed to the critical areas of the structure. Frame temperatures and radial growth at off-design conditions were evaluated and used in the detailed calculation of seal leakage as described in Section 4.3.3.

4.3.3 Clearances and Leakages

The evaluation of leakage flows during off-design, fan-operating conditions is a situation that involves combinations of frame thermal growth, rotor growth, aerodynamics of the cooling systems, and effects of maneuver loads on rotor-to-frame clearances.

The rotor total growth includes blade, disk, and turbine growth due to both centrifugal and thermal effects. Rotor system total growth as evaluated at the fan design condition is given in Table X. For the off-design

Table X. Rotor Growth.

- Rotor Speed = 4370 rpm
- Turbine Inlet Temperature = 1144 K (2060° R)
- Blade Relative Temperature = 972 K (1750° R)

Centrifugal Growth

	(mm)	(in.)
Disk	0.70	0.0275
Fan Blade	1.29	0.0506
Turbine Blade	0.01	0.0005
	2.00	0.0786

Thermal Growth - Relative to 21° C (70° F)

	(mm)	(in.)
Fan Blade	0.08	0.0030
Turbine Blade	0.67	0.0263
	0.75	0.0293

Temperatures

	(K)	(° R)
Fan Blade	333	600.2
Turbine Blade	972	1750

calculation of rotating seal diameters, the following relationships were used:

- Centrifugal growth varies with physical speed squared.
- Fan blade thermal growth scales using fan exit total temperature.
- Turbine blade thermal growth scales with blade relative temperature, where Relative Temperature = $T51[1-0.150\ (rpm/4473)^2]$.

The diameters of the stationary seals at the fan and turbine tips are established by the temperatures of the seal supporting structure. The diameter of the seals increase proportional to the seal diameter and the structure temperature at a rate of 1.07×10^{-5} cm/cm K (0.594×10^{-5} in./in. ° R). The frame temperatures can be estimated using a constant cooling effectiveness of 0.675 where:

$$\text{Effectiveness} = \frac{\text{gas temperature - metal temperature}}{\text{gas temperature - coolant temperature}}$$

For this calculation the gas temperature is the turbine discharge temperature and the coolant is fan discharge. At the fan design point, this level of effectiveness gives a frame temperature of 232° C (450° F).

A buildup clearance was defined to provide adequate seal clearance to avoid seal rubs during typical aircraft maneuvers. Figure 36 shows the relative rotor-to-frame deflections for a combination of gyro precession rates and acceleration forces normal to the axis of rotation. Based on these characteristics, a fan tip buildup clearance of 0.11 cm (0.045 in.) was selected. The turbine tip clearance was set at a larger gap of 0.18 cm (0.071 in.) to account for the additional centrifugal and thermal growth of the turbine blades. These clearance levels were then used in the evaluation of seal leakages during off-design operation.

The previous discussion has given the analytical methods and procedures used to determine seal leakages during steady-state operation. The six leakage flows that were calculated include:

- WL1 - leakage from forward seal cavity into turbine blade inlet station.
- WL2 - leakage from forward seal cavity into fan inlet station.
- WL3 - leakage from aft seal cavity into turbine diffuser inlet station.
- WL4 - leakage from aft seal cavity into fan station between rotor exit and stator inlet.
- WL5 - Total leakage flow extracted from fan flow; combination of WL1 through WL5.

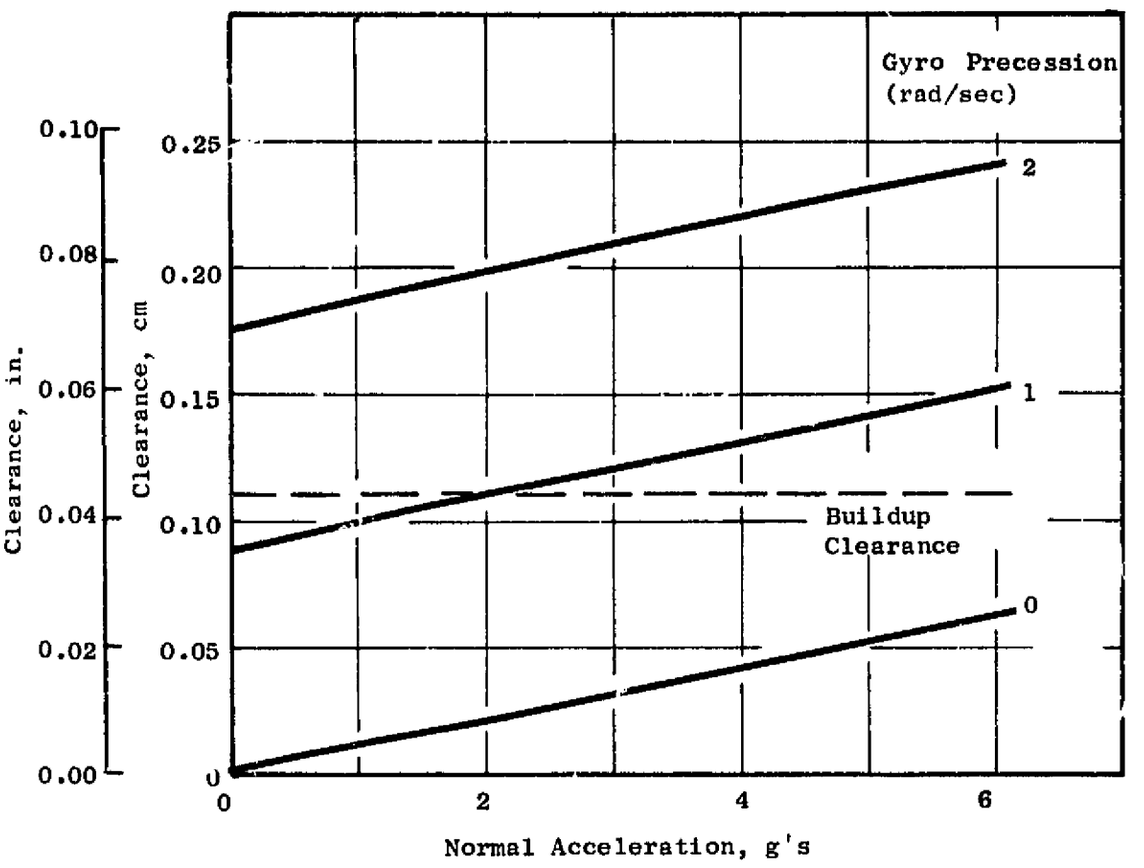

Figure 36. Maneuver Envelope Based on Seal Clearance.

- WL6 - Turbine tip seal leakage from turbine blade inlet to turbine blade exit.

All of the seal leakages appeared to be a function of only fan physical speed and flight altitude and almost independent of flight Mach number. Figure 37 shows the leakage flow rates as determined through these analytical methods.

4.3.4 Performance Corrections

Leakage flows not only represent a flow lost from the system, but also represent significant changes of performance of the individual components. In the analysis of fan performance, the effects of the individual leakages are accounted for in the following manner.

Leakage into the turbine blade inlet, WL1, was assumed to have no detrimental effect on turbine performance. The leakage flow does occupy some area within the blade row which changes the turbine velocity diagrams slightly; however, this flow does do some work as it passes through the turbine. Previous turbine test experience has shown that this type of leakage has negligible effects on turbine performance, except for the flow lost from the system.

Fan inlet seal leakage, WL2, is known to have a large effect on fan efficiency. Tests of large and scale-model fans have defined the efficiency decrements as shown in Figure 38. A large change of fan efficiency, five times the percent leakage, is shown.

Figure 39 shows the correction of fan efficiency due to rear seal leakage, WL4. There was no actual data base for estimating this performance derivative. A conservative estimate of one-third of the inlet air seal effect was used.

Tests of diffusers with leakage at the inlet have shown that the leakage rates have small performance effects on the diffusion pressure loss but do represent large changes of the diffuser effective area ratio. The diffuser flow path has been sized with corrections for the calculated levels of flow leakage.

Turbine tip seal leakage, WL6, is treated on a one-for-one basis. The leakage flow is assumed to contribute nothing to the turbine work, and thus the performance corrections as shown in Figure 40 can be derived.

One additional correction to performance accounts for the work done in pumping the carrier cooling flow. In the cooling analysis, this work was calculated and compared to the total turbine power. A constant ratio of 1.2 percent of turbine power was determined as a typical level for performance corrections.

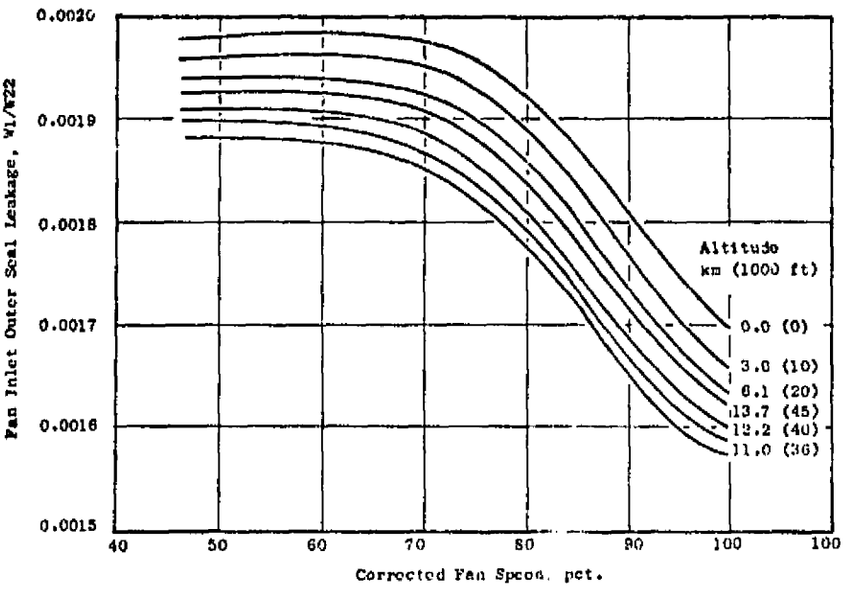

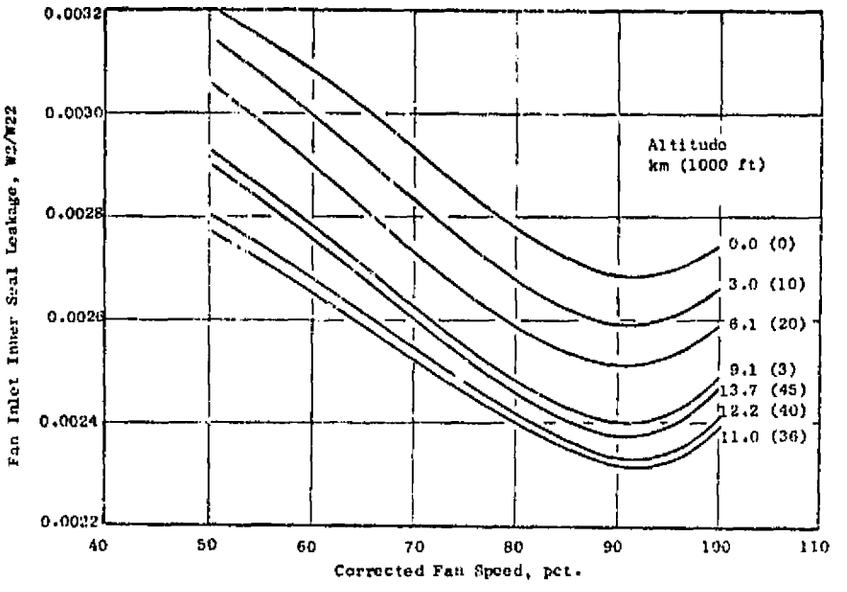

Figure 37. Seal Leakage Maps.

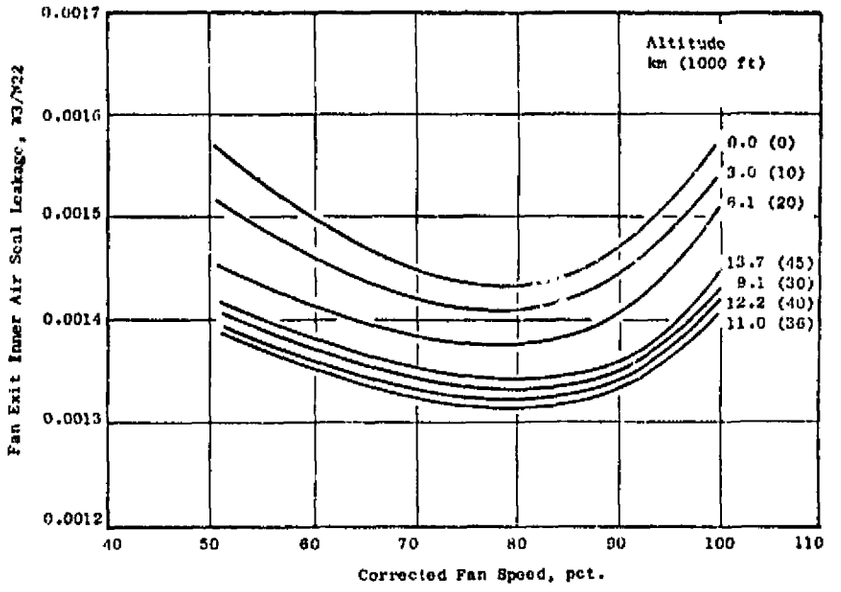

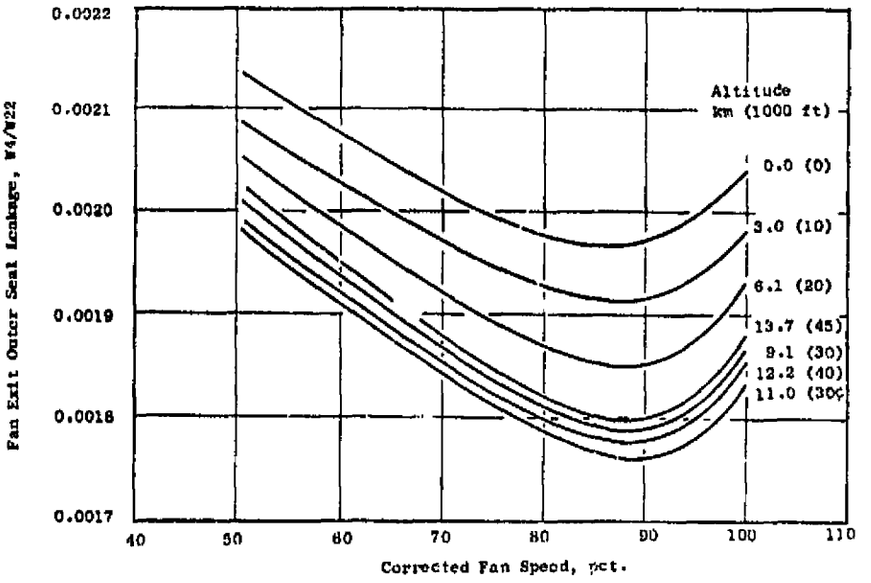

Figure 37. Seal Leakage Maps (Continued).

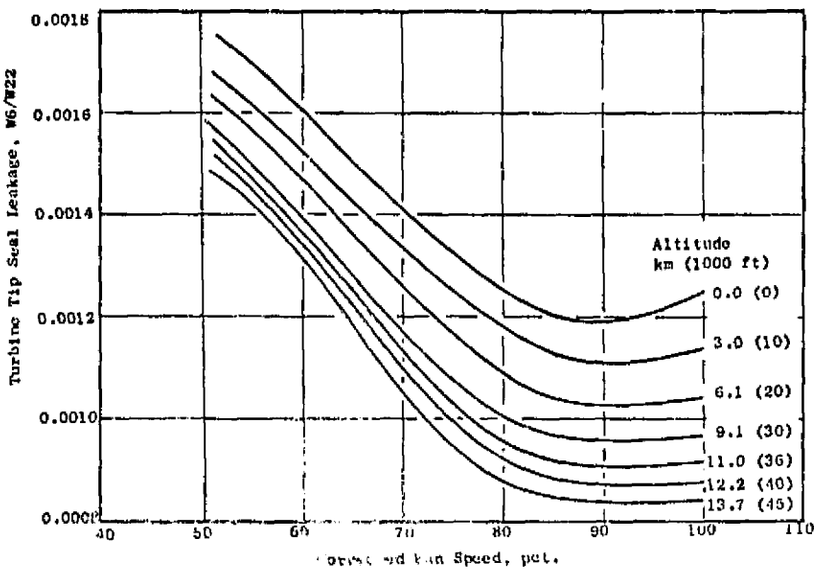

Figure 37. Seal Leakage Maps (Concluded).

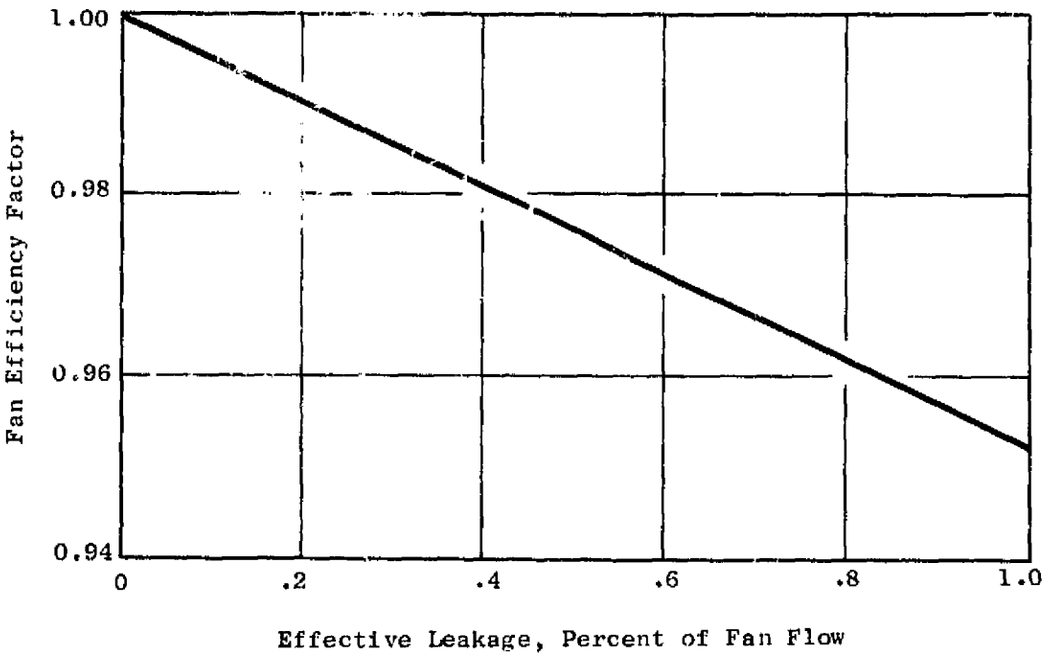

Figure 38. Fan Forward Seal Leakage Effect.

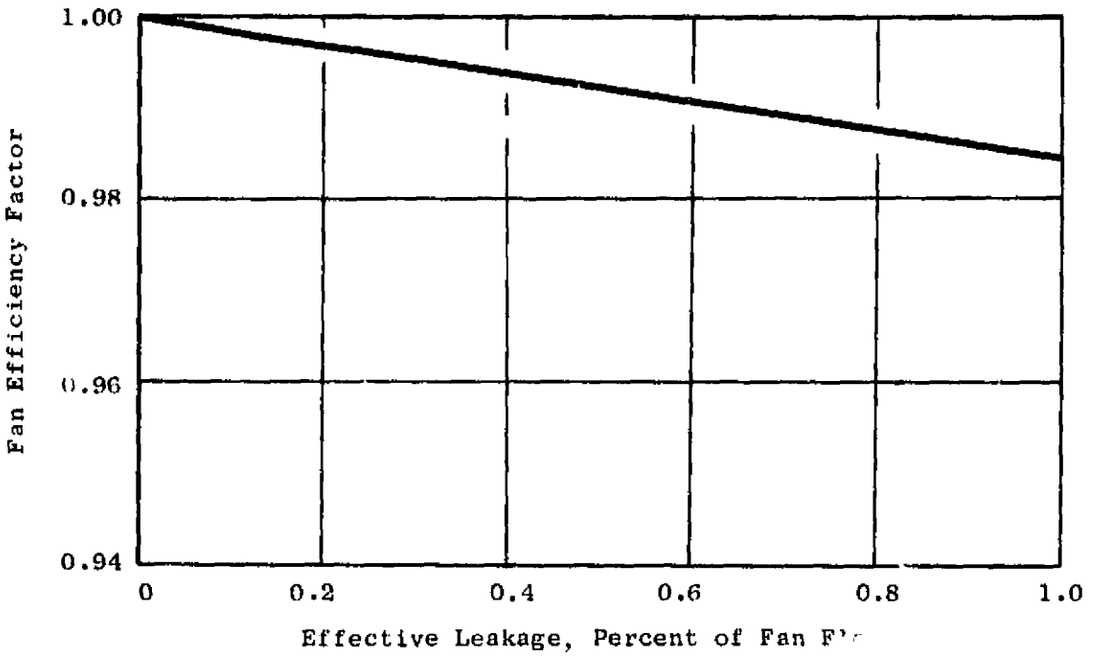

Figure 39. Fan Rear Seal Leakage Effect.

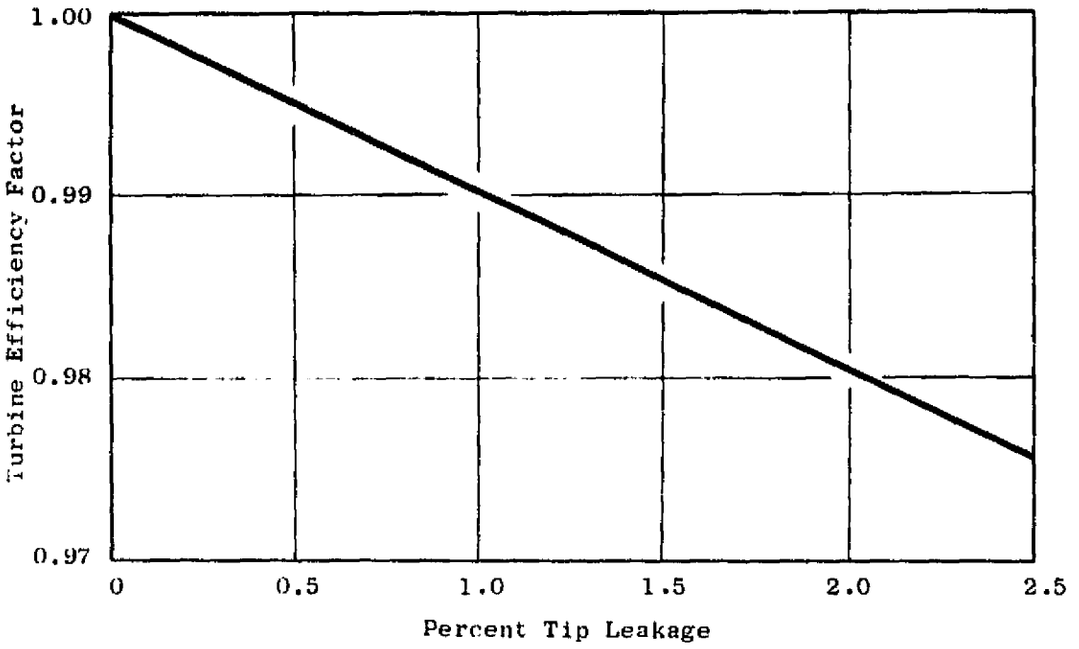

Figure 40. Turbine Tip Leakage Corrections.

4.4 ROTOR ASSEMBLY

4.4.1 Design Requirements

The fan rotor was designed to meet the requirements imposed upon the LCF459 fan assembly by the Research and Technology Aircraft. The objectives which have a direct influence on the rotor design are:

- Aerodynamic design requirements
- 1200 hours and 14,400 idle-to-takeoff-to-idle cycle operations
- Bird-strike tolerance
- Rapid response to changes of thrust (minimum inertia)
- System vibratory stability margin of 15 percent over two-per-revolution sources at 100-percent speed
- Torsional and flexural flutter stability (blade flutter shall not occur prior to fan stall)
- Stresses less than 0.2-percent yield strength
- Stresses within stress range diagram for 10^7 cycles
- 15-percent margin on blade natural frequencies over anticipated excitation sources
- Burst speed greater than 122-percent design speed
- Disk dovetail capable of retaining adjacent blades with one blade out (domino-type, disk-post failures)
- Single blade removal on wing
- On-wing fan rotor balance
- Axial fan blade retention capability of 30 percent of fan blade centrifugal loading
- Low manufacturing costs

4.4.2 Basic Design Features

Figure 41 is a detailed layout of the fan rotor showing the salient features. The rotor contains 52 fan blades of titanium 6-4 material. The blades are retained by a conventional, single-web disk and driven by a tip turbine. The disk material is also titanium 6-4. The fan blades incorporate

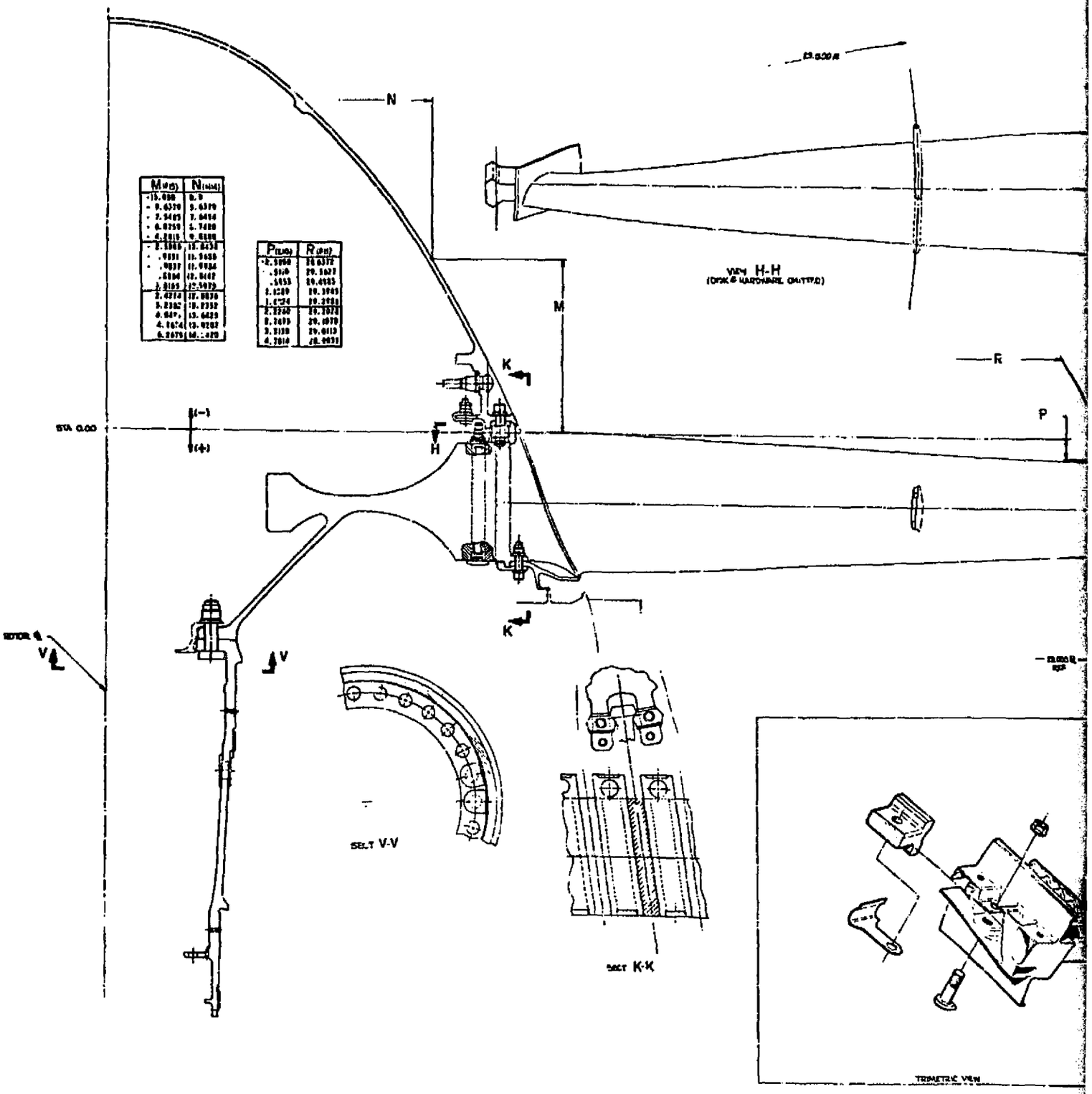

Figure 41. Rotor Ass

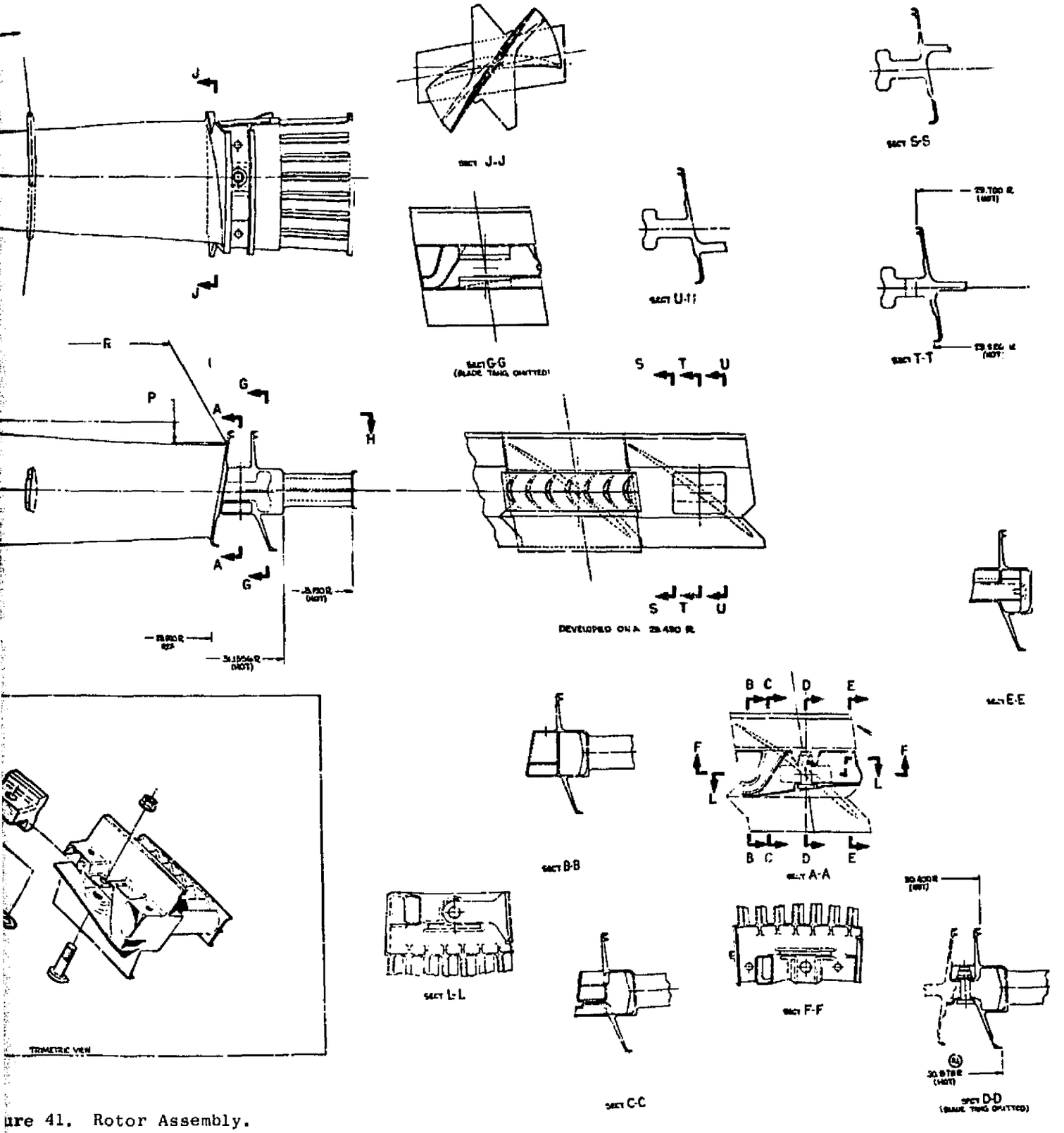

ure 41. Rotor Assembly.

single, part-span shrouds for vibrational stability and bird-strike resistance. An integral tip shroud is employed to define the fan outer flow path and provide a seal against hot gas leakage into the fan stream. The fan blade incorporates integral platforms to form the inner flow path. The disk retains the blades using single-hook dovetails with a drop-down slot for single blade removal. Spacers below the dovetail are used for blade retention. An aluminum spinner is rigidly attached to the disk to provide structural stability for increased blade-disk mode frequency margin. The spinner also includes provisions for on-wing field balance without rotor disassembly through the addition of radial balance weights. A bolted flange joint allows separation of the disk and shaft for ease of maintenance. The tip turbine contains 52 cast René 80 carrier assemblies, each having a tip shroud to define the outer flow path. Seven airfoils are attached to a box structure retained by a rabbeted, fan-blade-to-turbine attachment. The box structure has protruding seals to shield the fan stream and blade from the hot gas.

4.4.3 Design Analysis

Using combinations of analytical methods and comparison with similar operating rotor experience, the selected rotor configuration was shown to be capable of meeting all of the objectives. The rotor was analyzed consistent with design criteria used for large commercial turbofan engine rotors.

The fan blade was designed in Ti 6-4 for low cost and weight. Figure 42 presents the blade airfoil geometry. The geometry was selected for low weight and reasonable stress levels in view of foreign object damage and cyclic life requirements. Figure 43 gives the airfoil stress distributions, Figure 44 shows the blade dovetail stresses, and Figure 45 4.4-5 depicts the various blade stress levels in comparison to the strength levels of Ti 6-4.

A part-span shroud at a 65% spanwise location provides stability from torsional stall and flutter, higher blade-disk system frequency, better bird-strike resistance, and lighter airfoil weight over a nonshrouded airfoil. Torsional stall instability is characterized by large oscillatory vibrations at the blade torsional frequency. A nondimensional "reduced velocity parameter" predicts the susceptibility of a blading design to instability. Figure 46 compares the blade inner and outer panel reduced velocity parameters with a stability boundary derived from numerous compressor and fan tests. A large stability margin is indicated.

Figure 47 presents the blade frequency diagrams of both the in-phase and out-of-phase modes for the case with an assumed rigid disk. Noted on the figures are possible sources of excitation. Figure 48 shows the combined blade and disk frequency diagram. The two-nodal frequency margin of the blade-disk system over the two-per-revolution excitation is less than the design objective of 15 percent at design speed. Not included in this margin is the increased stiffness effect of the structural spinner. The concept of a structural, rotating, fan-inlet spinner bolted directly to the disk rim was

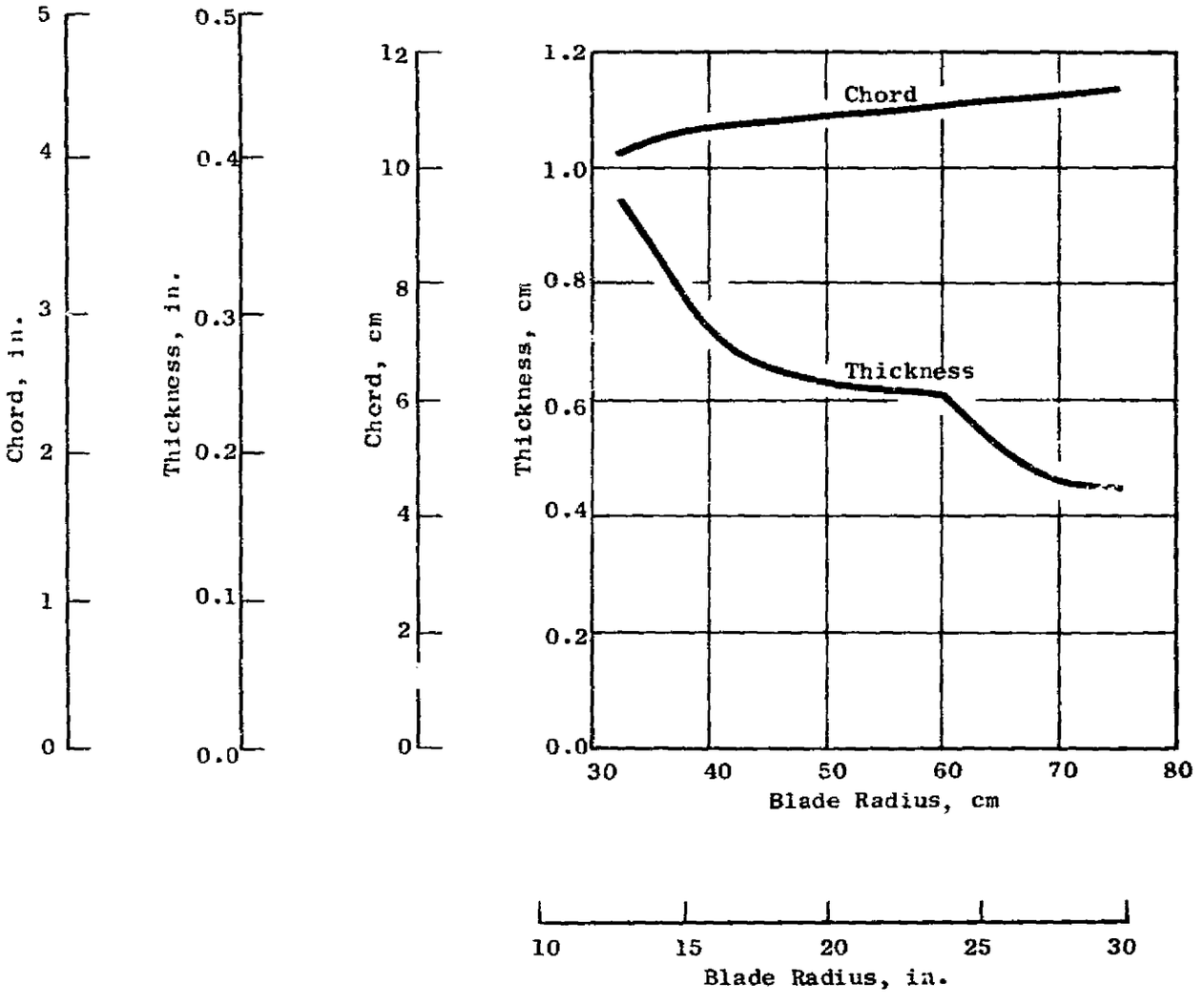

Figure 42. Fan Blade Airfoil Geometry.

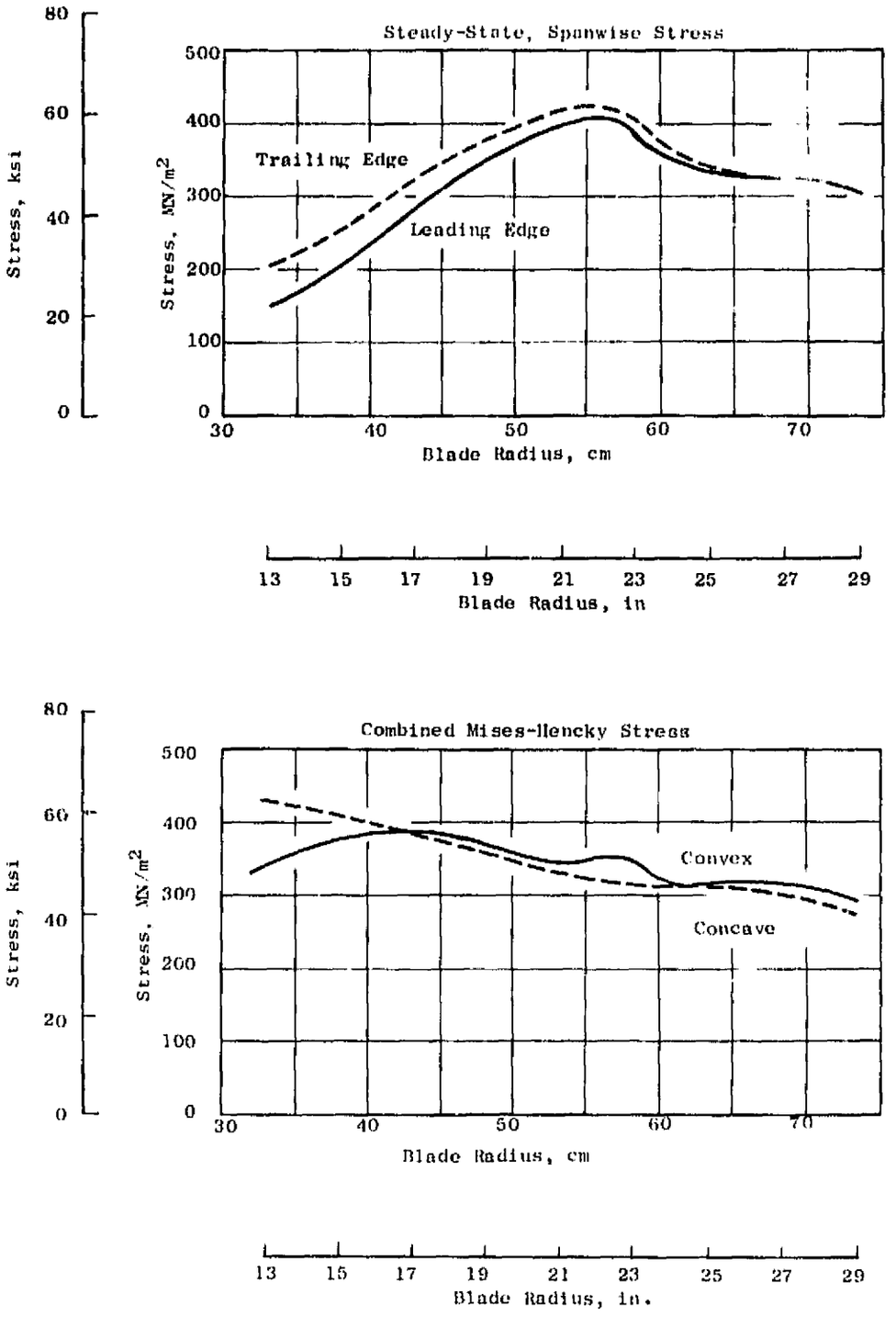

Figure 43. Fan Blade Airfoil Stress Distributions.

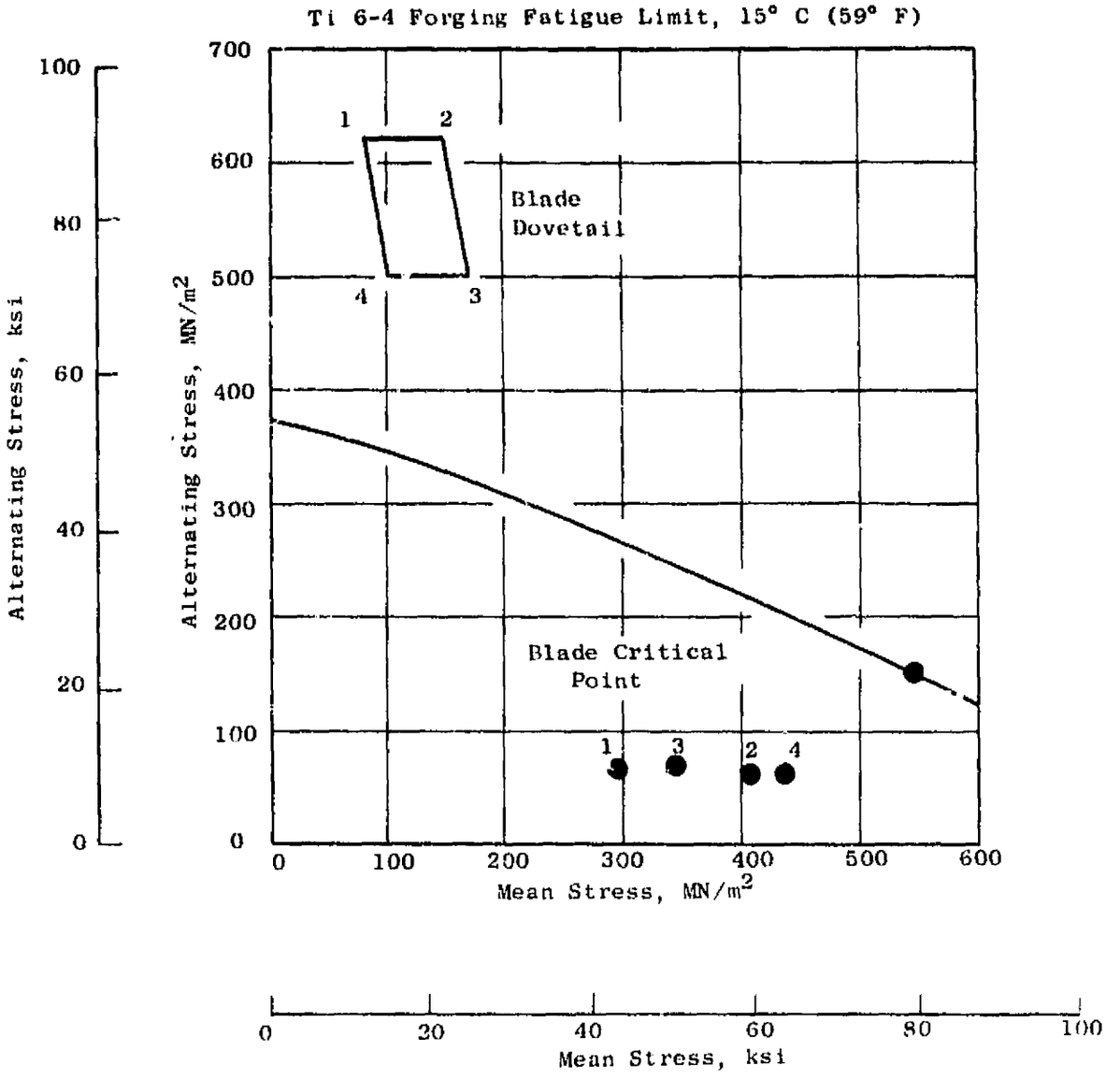

Figure 44. Fan Blade Stress Range Diagram.

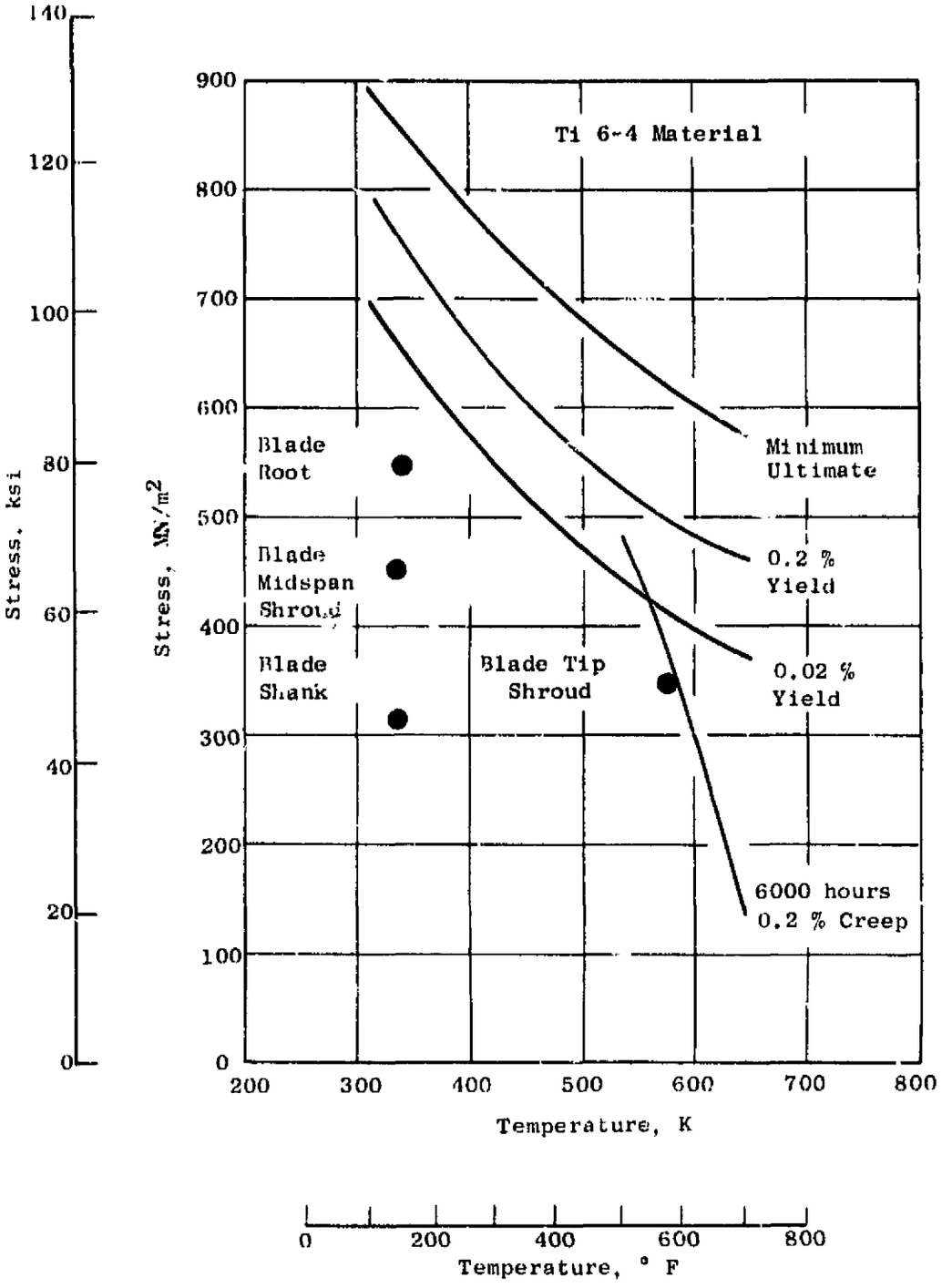

Figure 45. Fan Blade Material Properties.

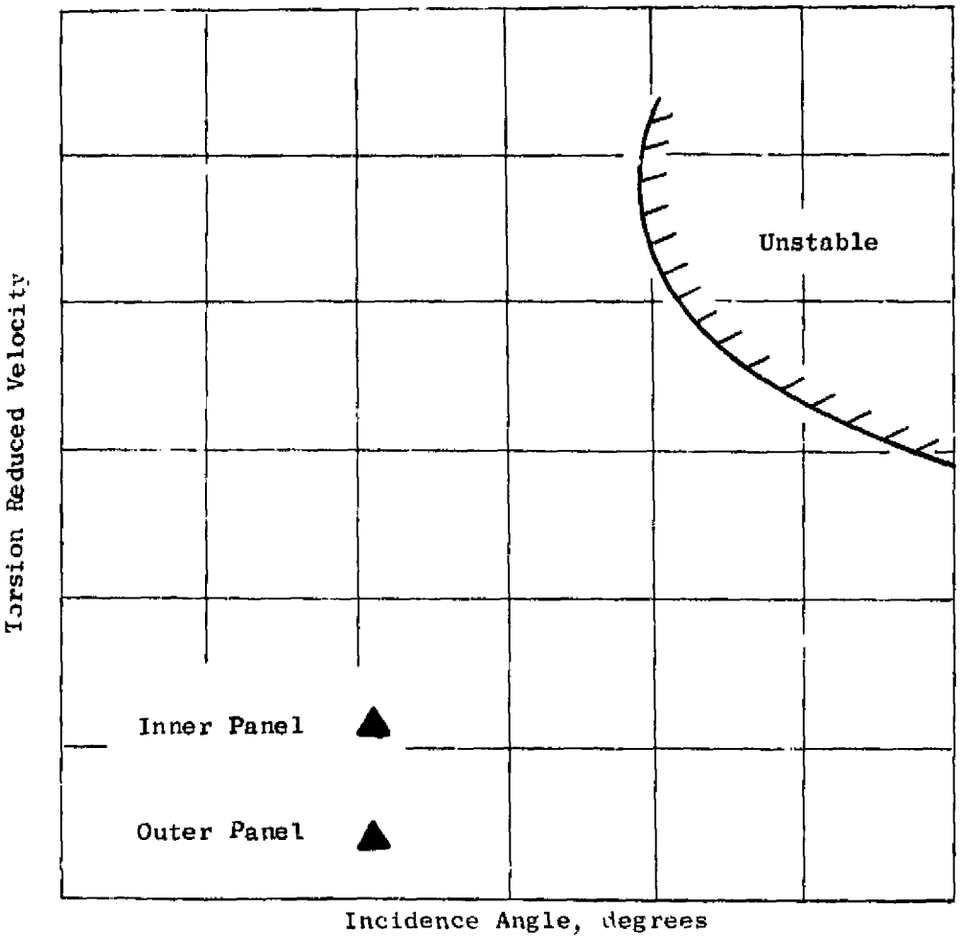

Figure 46. Fan Blade Torsional Stability.

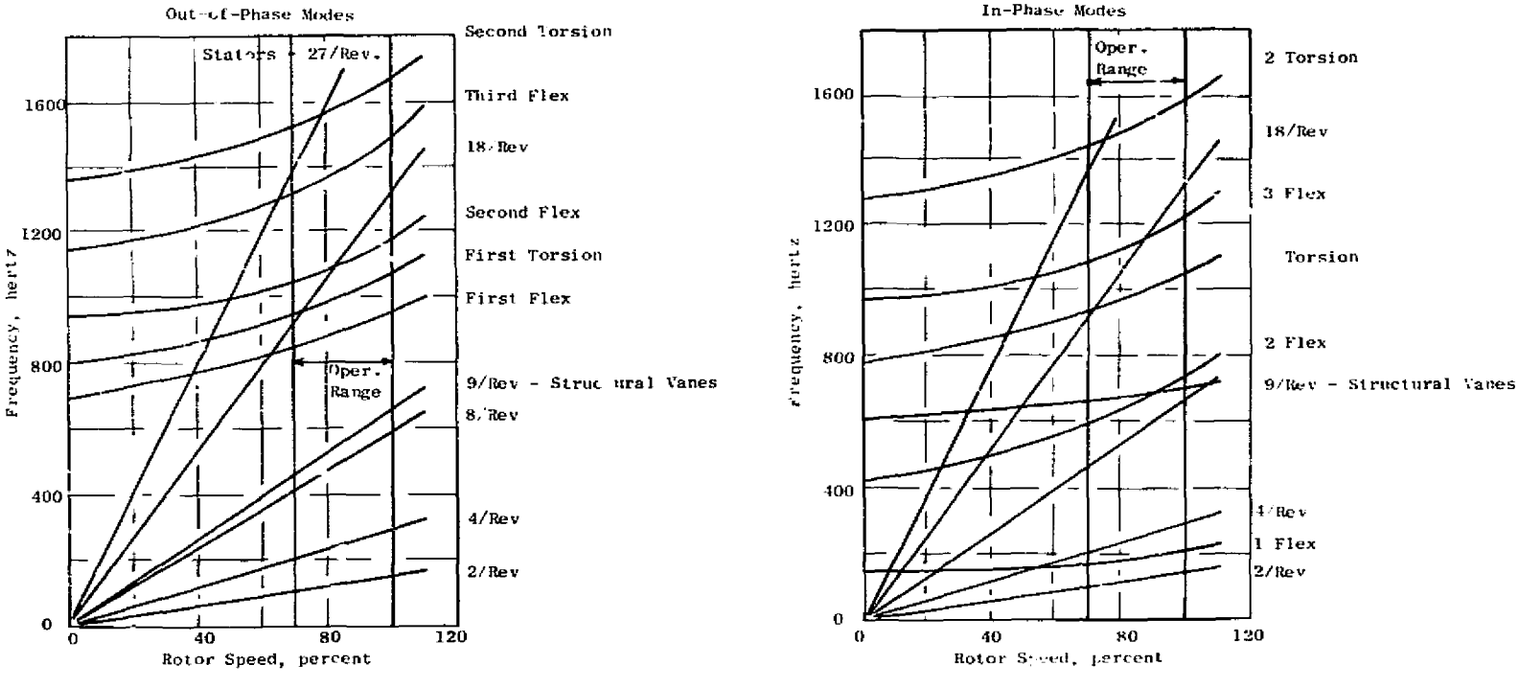

Figure 47. Fan Blade Rigid Disk Frequency Diagram.

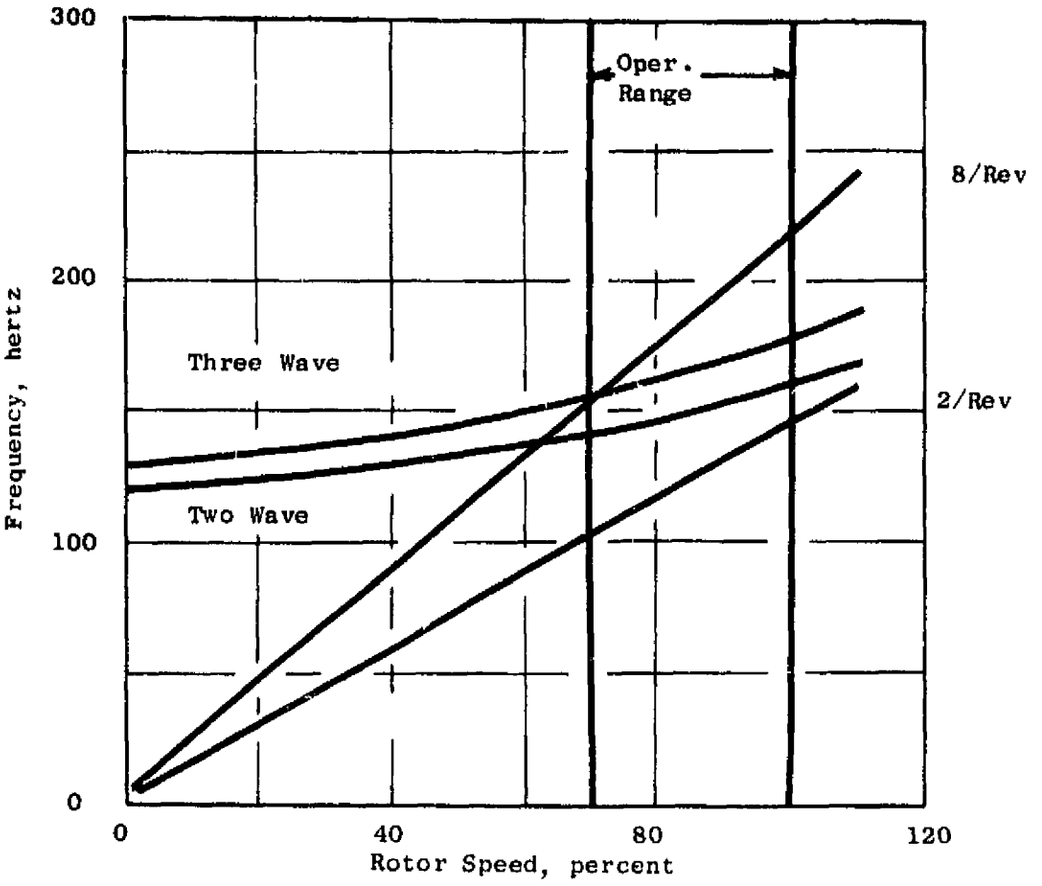

Figure 48. Fan Blade Disk Mode Frequency Diagram.

initially demonstrated on the CF6-50 turbofan engine. This combination of spinner and disk provides a unified structure which exhibits a significant increase in the blade root retention stiffness over the disk alone and, thus, increased margin over the two-per-revolution excitation. The margin at design speed for the blade-disk-spinner system is increased to 16 percent. Acceptable margins for safe operation exist either with or without the added stiffness of the bullet-nose structure.

The bird-strike capability of the blade was evaluated using an analytical procedure which employs a semiempirical method based on energy balance theory. The method has consistently been able to predict, with good correlation, the bird-impact results for new fan designs. Empirical data from static and whirligig impact tests and actual bird ingestion incidents on previous, fixed-pitch, fan designs such as the CF6-6, CF6-50, TF34, and TF39, in conjunction with analytical simulation of the incidents, was used to determine a damage boundary. The ability of the LCF459 fan blade design to sustain bird strikes when compared to this boundary is shown in Figure 49. Torn or missing pieces from the blade could result if a 0.45 kg (1 lbm) bird strike occurs. Adjustments in the blade geometry during the detail design phase can be used to improve the strike capability with the objective of meeting the 1.0 kg (2.2 lbm) criteria. These adjustments are:

- Generous blends to hard-point locations, tip and midspan shrouds, to reduce stress concentrations.
- Local thickness distribution changes to improve susceptible areas of the blade.
- Chordwise location of the midspan shroud away from the leading edge so that chordwise plastic deformation can absorb some of the impact energy.

A conventional, single-web, disk design was selected for the LCF459. This type of disk design was selected based on light weight and low cost. The disk mean-line stress distribution is presented in Figure 50. Figure 51 shows the disk material fatigue strength. A comparison with the blade dovetail fatigue stress and material properties reveals that both the disk and the blade dovetails have more than adequate stress margins.

The tip turbine contains 52 integrally cast, tip-shrouded carriers, each having seven hollow turbine airfoils. The tip shroud is employed to control tip clearance for increased performance. The airfoil wall thickness is 0.0635 to 0.1016 cm (0.025 to 0.040 in.) which is applicable to thin-wall casting techniques. High resistance to foreign object damage is provided with adequate material strength.

The carriers have a simplified forward seal pressurization scheme utilizing air scoops on the aft face of each carrier which pump cool aft cavity air through an internal passage into the forward cavity. The scoops add some weight and inertia to the turbine, but the addition is justified in light of the more simplified pressurization scheme over that offered by other

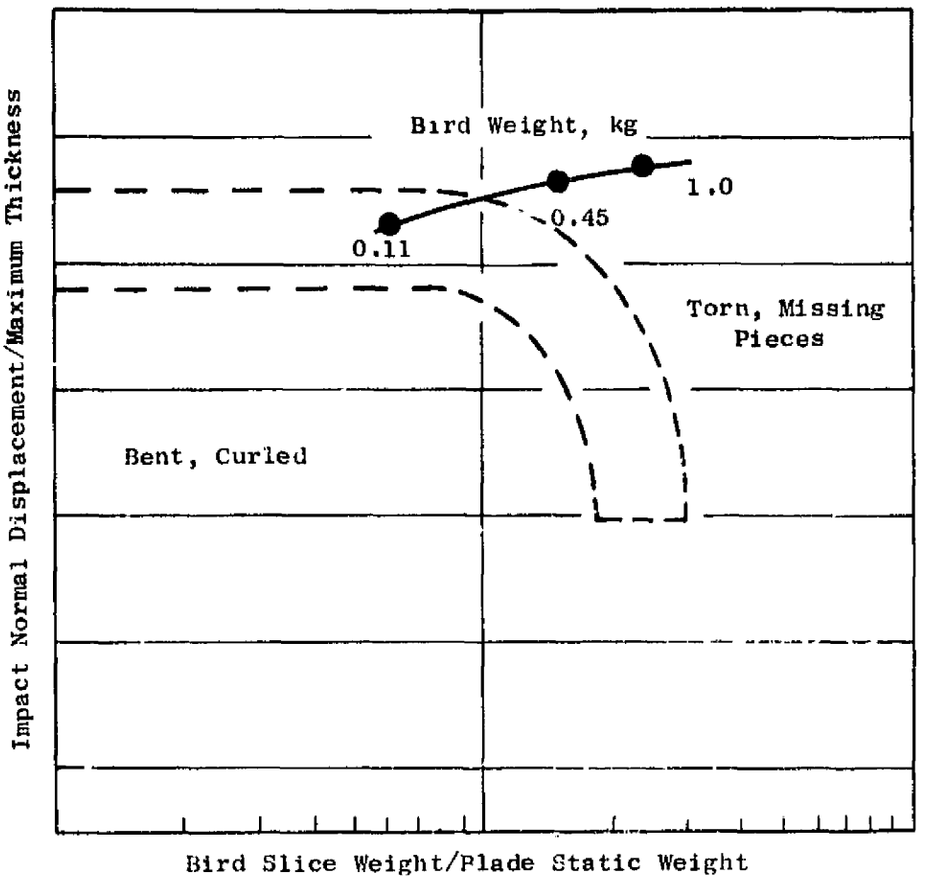

Figure 49. Fan Blade Bird Strike Capability.

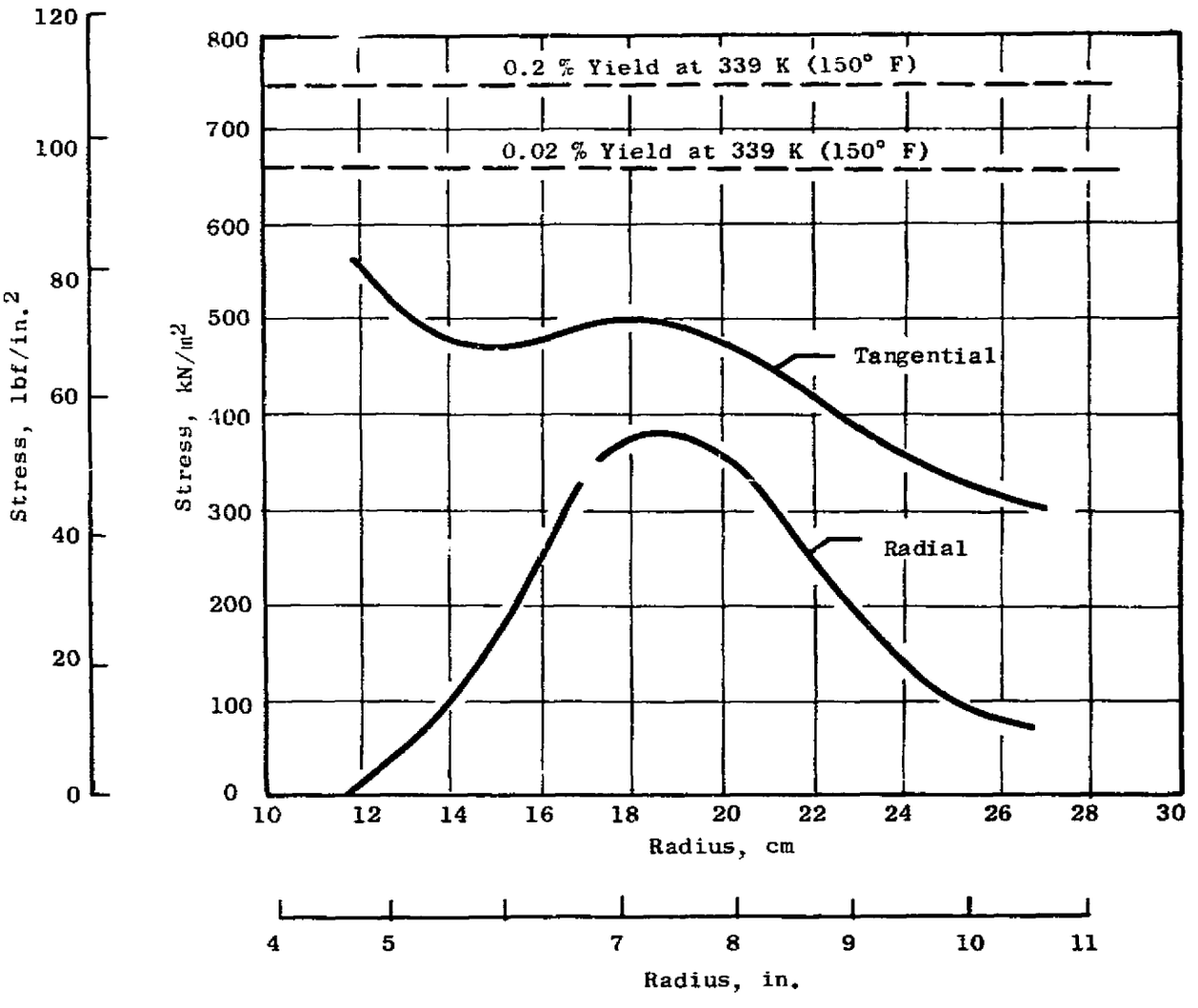

Figure 50. Disk Mean-Line Stress Distribution.

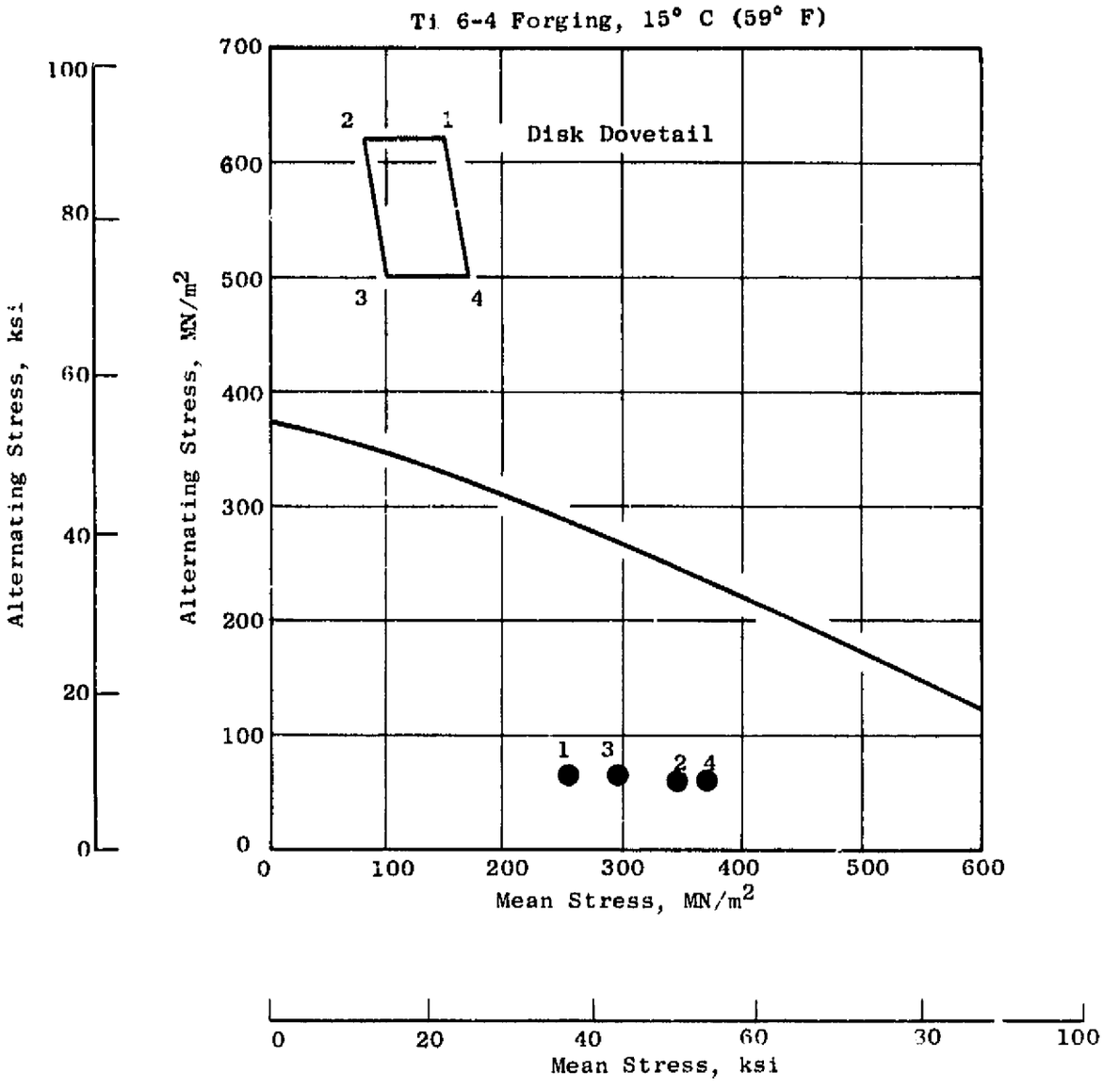

Figure 51. Disk Dovetail Stress Range Diagram.

external pressurization methods. The carrier is retained by a rabbet joint on the tip of the fan blade as shown in Figure 52. This type of carrier-to-blade joint does not require bolt preload and the associated clamping action for carrier retention.

Figure 53 compares the principal turbine blade vibratory frequencies with the potential sources of excitation. Adequate frequency margins exist within the normal speed operating range. Figure 54 compares the blade maximum root stress with the material properties of the blade material. At the design speed, the material vibratory strength is three times the anticipated blade vibratory stress.

4.4.4 Weights and Inertias

The rotor system weight at the conclusion of this design was 150 kg (329 lbm). The rotor polar moment of inertia was calculated to be 35.54 N-m-sec^2 (26.2 lbf-ft-sec^2). Table XI gives a detailed breakdown of the contributions of the rotor components to the total weight and inertia.

Table XI. Rotor Weights and Inertias.

Component	Weight		Inertias	
	kg	lbm	N-m-sec^2	lbf-ft-sec^2
Tip Turbine	19.3	42.4	11.9	8.8
Fan Blade	69.2	152.2	19.5	14.4
Disk	41.9	92.1	2.4	1.8
Spinner	5.2	11.4	0.3	0.2
Shaft	4.7	10.3	0.04	0.03
Miscellaneous	9.3	20.6	1.4	1.0
Total	149.6	329.0	35.5	26.2

4.5 BEARINGS AND LUBRICATION

4.5.1 Design Requirements

The LCF459 sump system was designed to meet the following requirements:

- The system shall withstand the loading caused by steady-state, frequent, and maximum maneuvers, and blade-out conditions.
- Design life shall be 1200 hours for the research aircraft duty cycle as defined.

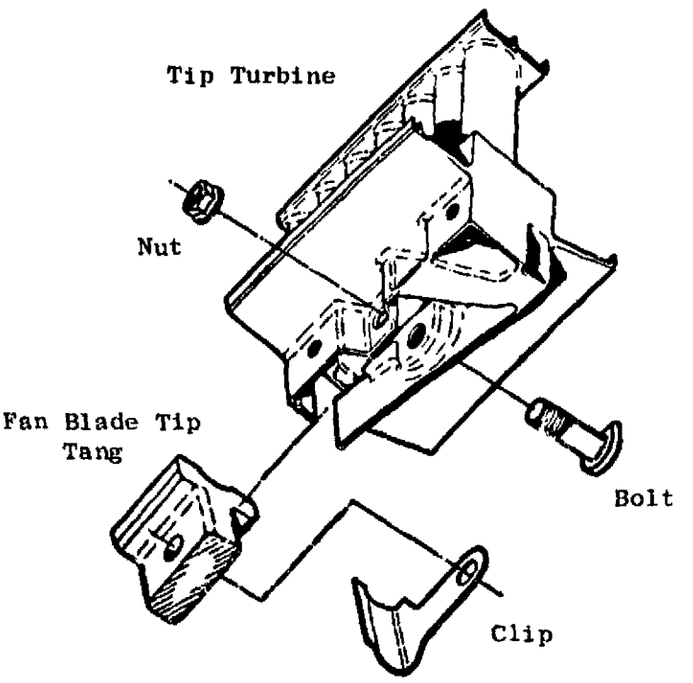

Figure 52. View of Tip Turbine Carrier.

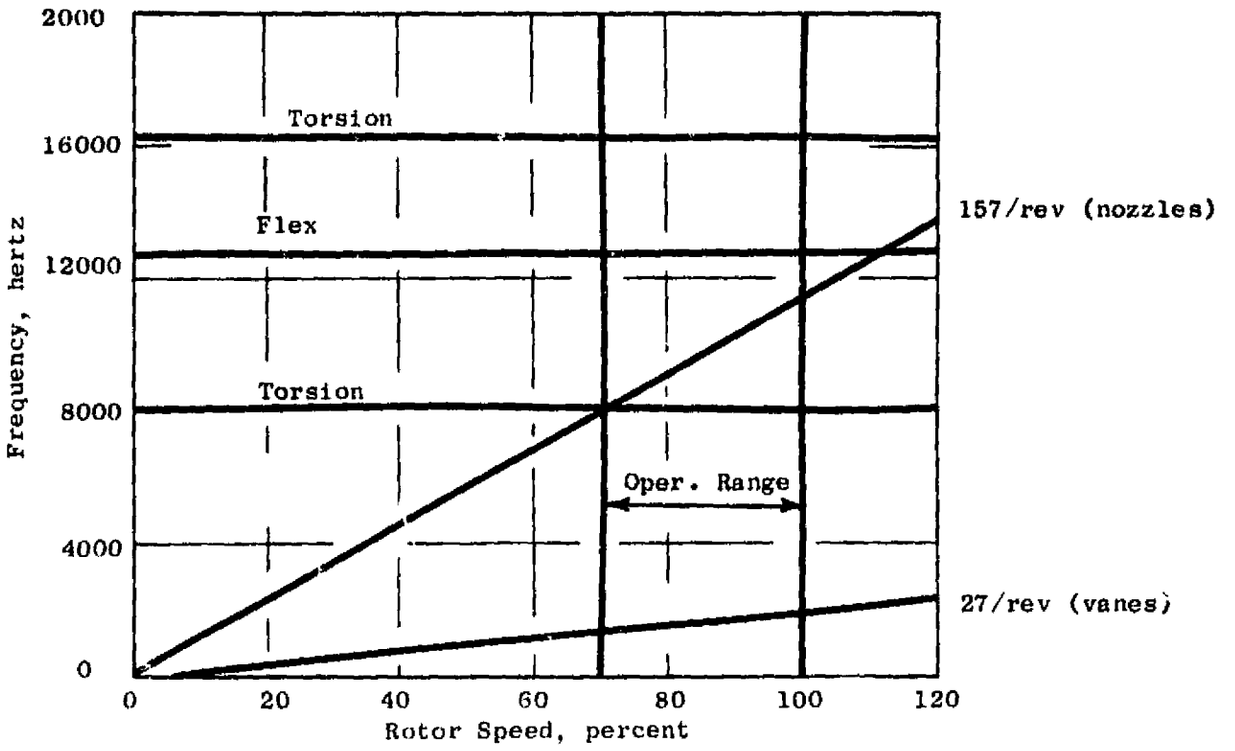

Figure 53. Turbine Blade Frequency Diagram.

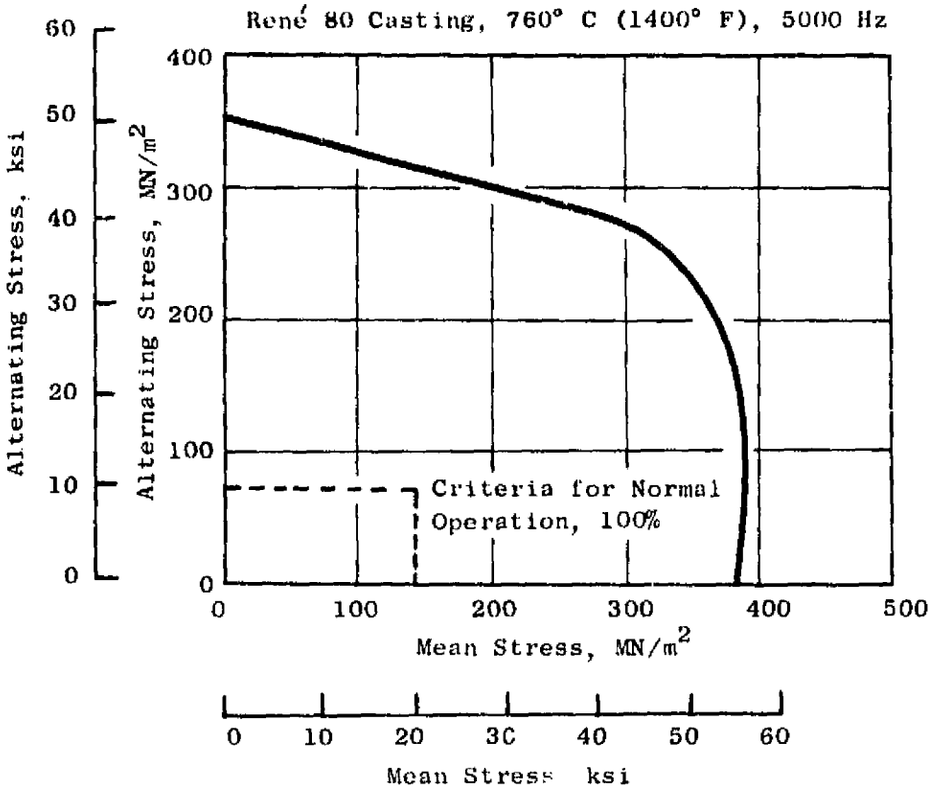

Figure 54. Turbine Blade Stress Range Diagram.

- The design shall meet the attitude requirements shown in Figure 55.

- A single design concept shall be capable of both vertical and horizontal installation.

4.5.2 Sump Design Features

The LCF459 rotor is supported by a roller and ball bearing as shown in Figure 56 and 57. Design practices successfully used on current General Electric engines have been used for these bearings. The roller and ball bearing are retained in the sump housing by a retainer ring and lock nut respectively. Tangs are provided between the roller bearing outer race and sump housing to prevent rotation. Both the roller and ball bearing inner race are clamped by individual lock nuts. These bearings feature standard cross sections allowing utilization of some existing tooling.

An aspirating-bore, carbon seal is provided forward of the roller bearing to prevent oil leakage into the aft fan cavity. This carbon seal is identical in size to the F101 No. 5 seal but does contain certain unique features pertinent to this design.

A splined shaft to drive the accessory gearbox for the horizontally installed configuration is attached to the aft end of the fan rotor shaft. The aft cover housing incorporates a gearbox mounting rabbett and a carbon seal for the drive shaft. Spline lubrication is to be obtained from the accessory gearbox. A cover is provided for the vertically installed system where the accessory drive is not used.

A steel investment casting is used for the sump housing. Internal coring is kept to a minimum to simplify the casting design. Welded-in oil tubes are used to transfer oil to and from the collector tank. Bearing reaction loads are transmitted to the fan frame directly by two structural cones terminating at the fan frame forward and aft flange. The entire sump assembly can be removed by removing bolts at the forward flange and nuts at the aft flange. Boroscope provision is provided for internal inspection.

Heat transfer capability is maximized by utilizing radiating fins in the oil collector/heat exchanger which is configured between the two structural support cones.

The main rotor shaft, in addition to supporting the rotor loads, provides the following functions:

- Collects any lube system debris in a specially provided separator.

- Transfers oil to inner races of bearings.

- Provides a drive for the accessory gearbox.

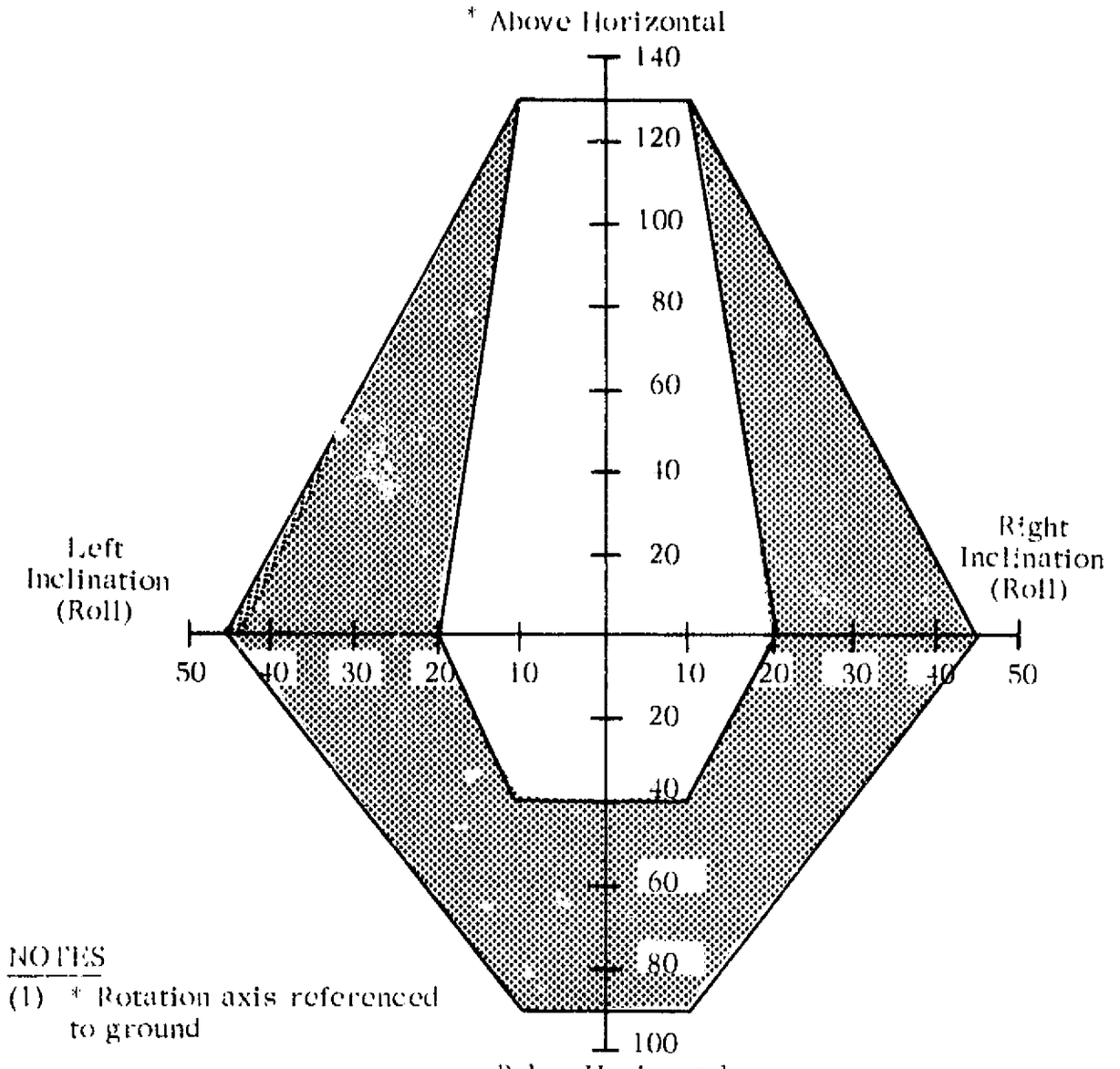

NOTES

(1) * Rotation axis referenced to ground

(2) Clear area - Continuous operation

(3) Shaded area - 30-second limitation

Figure 55. Lubrication Attitude Envelope.

FOLDOUT FRAME

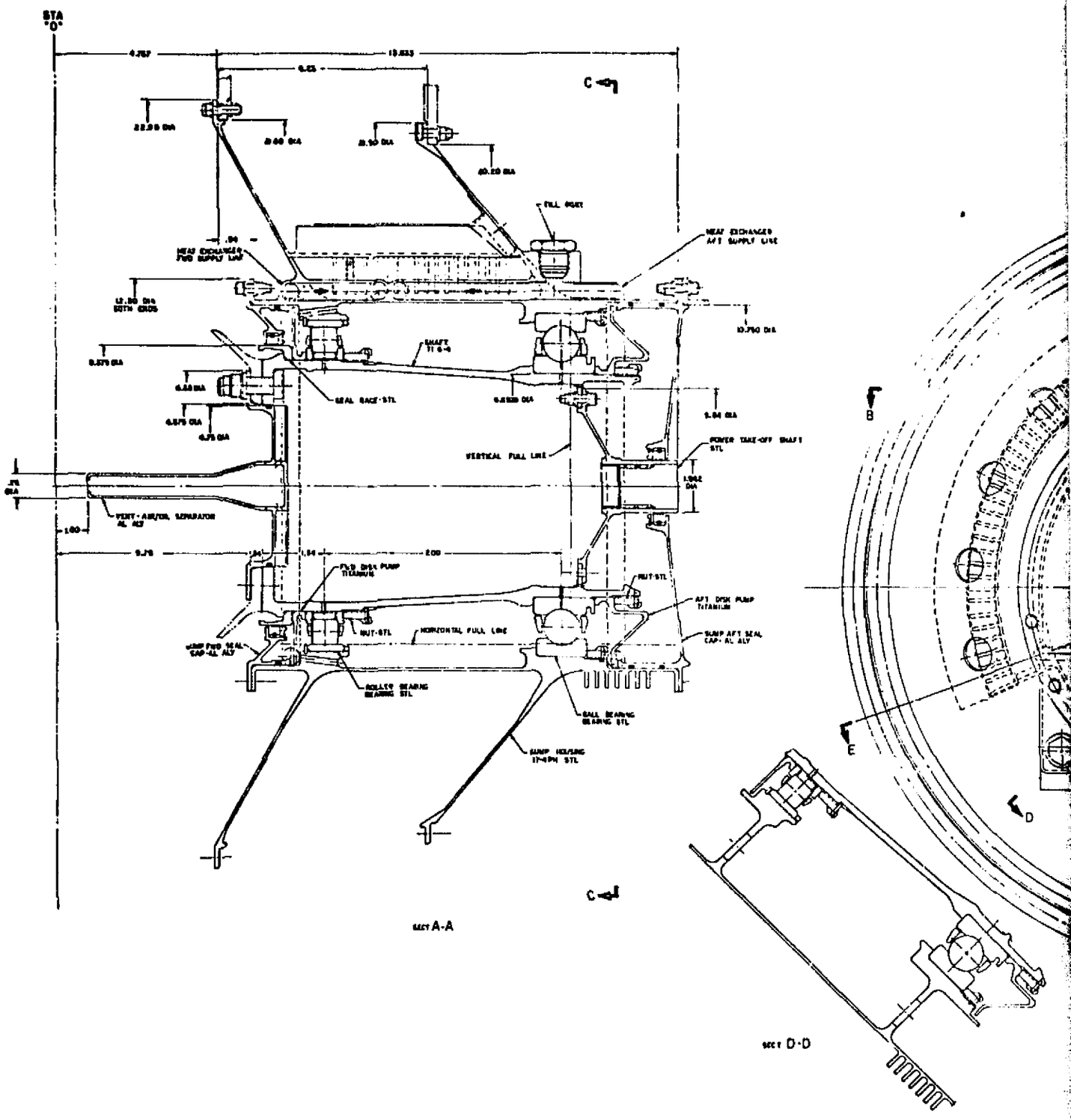

Figure 56. Sump Sys

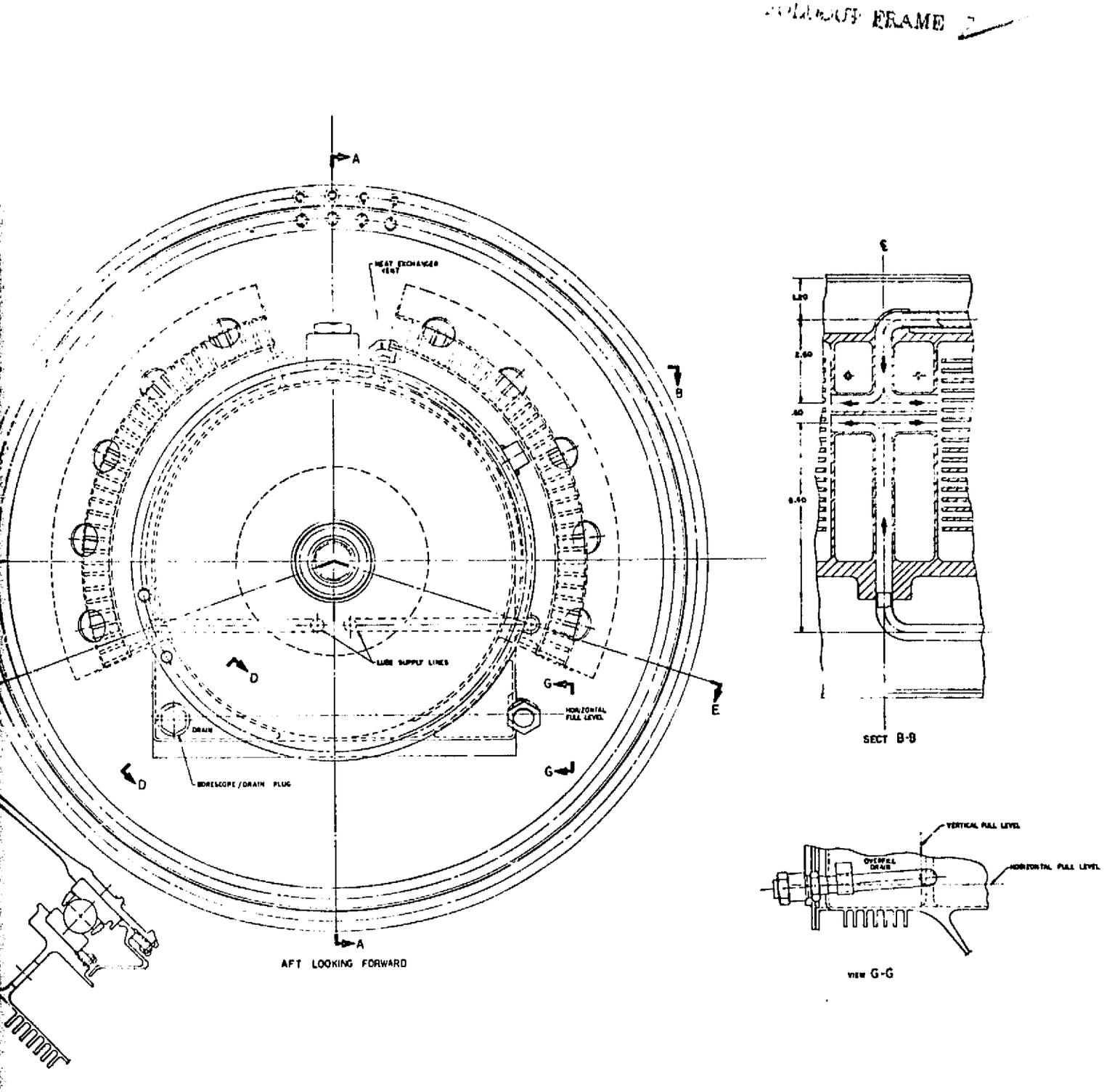

ure 56. Sump System Layout.

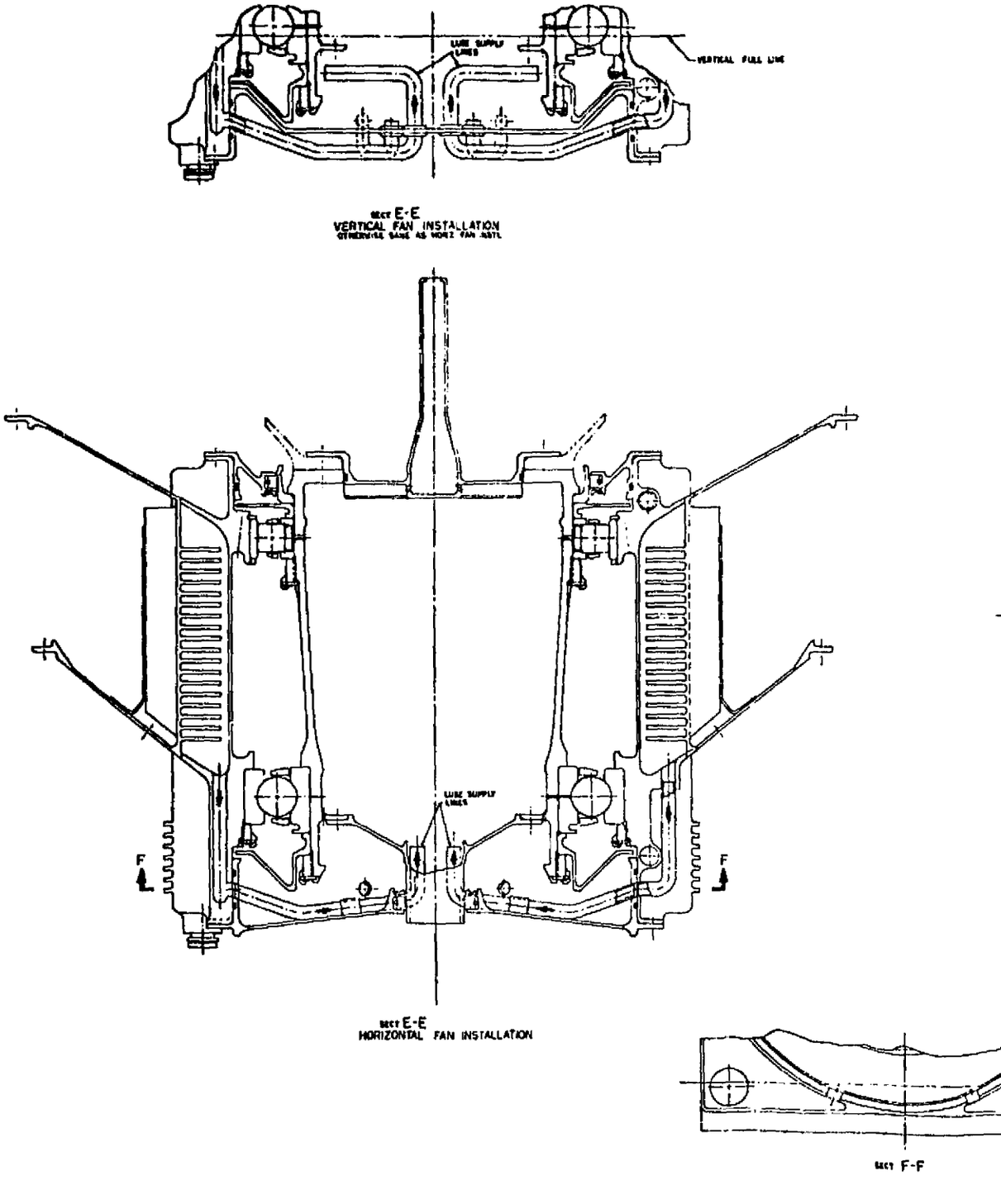

Figure 56. Sump System Layout

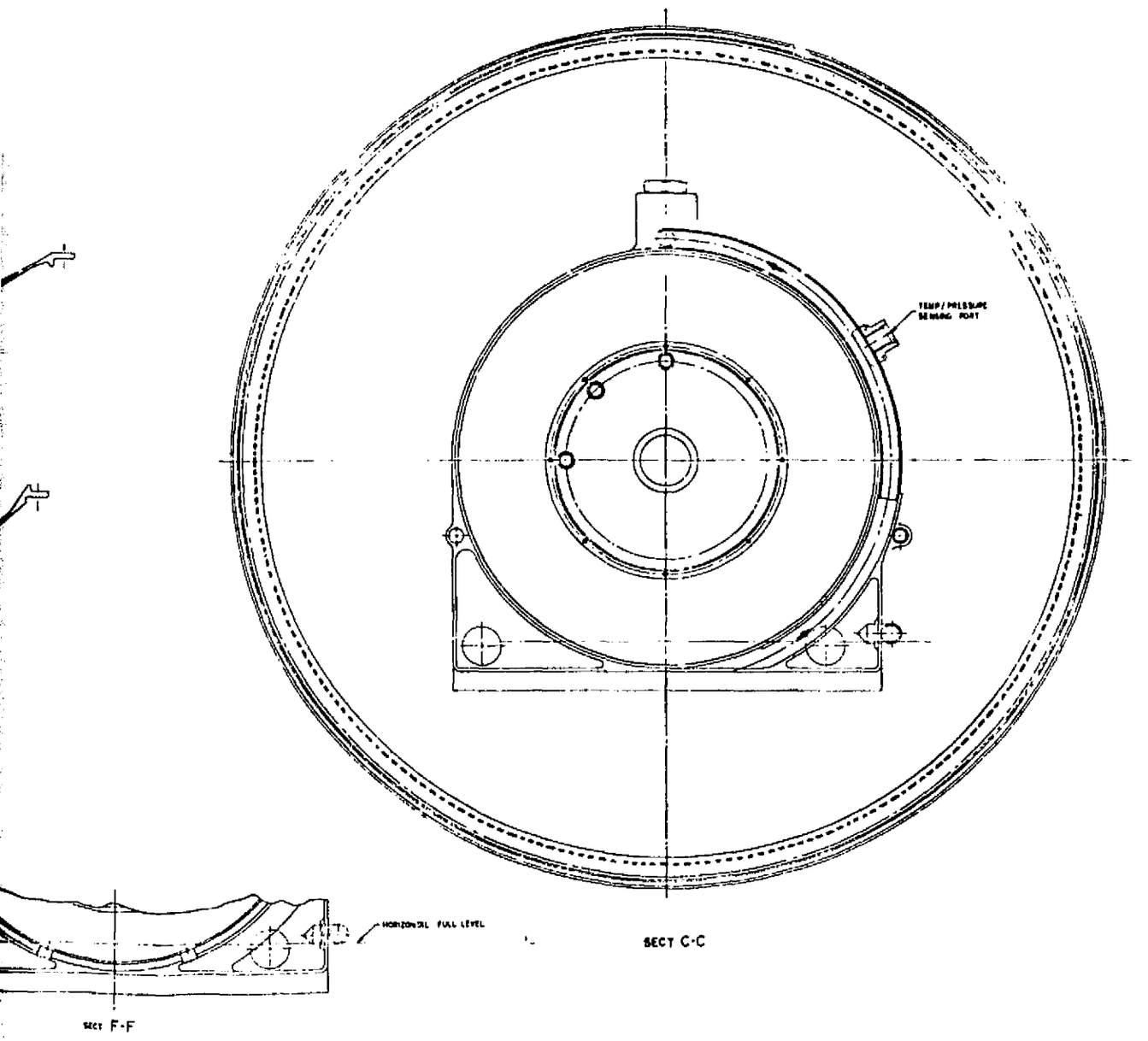

Sump System Layout (Concluded).

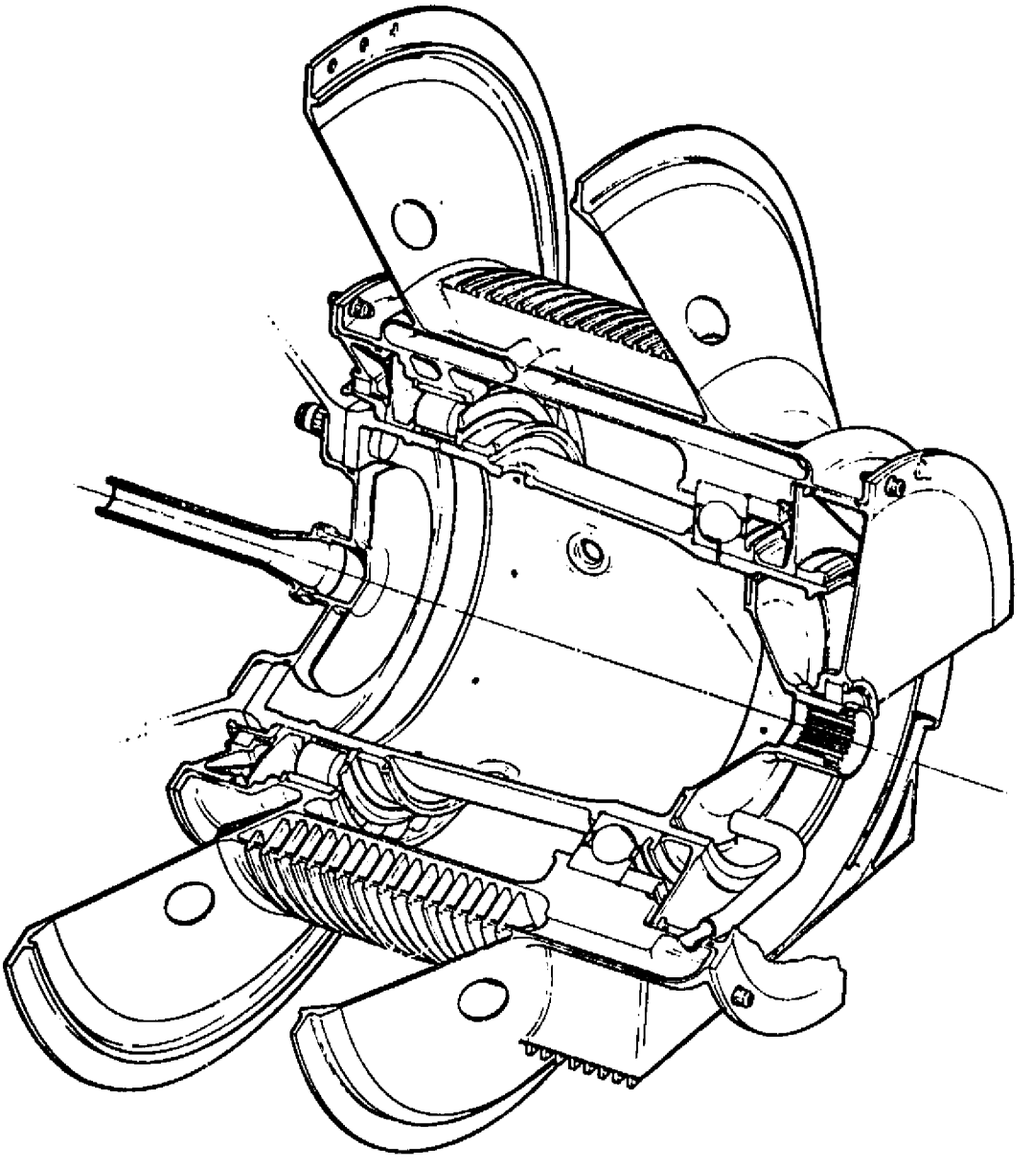

Figure 57. View of Sump System.

- Rabbetts the sump vent tube assembly.

Figure 56 shows the selection of materials used in the sump design.

The lube system is shown schematically in Figure 58 and includes the following features:

- Forward and aft viscous disk pumps to scavenge oil at all required attitudes.
- Under race lubricated bearings allowing the use of a low pressure lube supply system.
- Oil collector/heat exchanger integrated into a cast sump housing.
- Oil reservoir incorporated into sump housing.
- Debri separator integrated with rotor shaft.
- Sump vent which includes dynamic air-oil separator.

During operation, the lubricating and cooling oil is pumped by the aft and forward viscous disk pump from the oil reservoir located in the lower portion of the sump into the oil collector-heat exchanger. The oil reservoir is sized for approximately 0.00189 m^3 (0.5 gallons) of useable oil in either a horizontal or vertical installation. The disk pump concept is similar to that used successfully in the "D" sump of the CF6 engine. The oil collector/heat exchanger is sized to remove the heat generated by the bearings and seals and incorporates cooling fins to increase the effective heat-radiating-surface area. Holes are provided in the sump support cones to allow for cooling air flow. Cooled oil from the collector is directed by gravity through a dual-tube system to the end of the fan support shaft. The tube is sized to flow the required oil at a minimum oil head height of approximately 2.54 cm (1.0 inch). Sizing the tubes in this manner will also allow orificing the exit area if needed, based on test data from a planned sump development test program.

A centrifugal separator has been incorporated into the aft end of the fan shaft. This separator will trap debris, not allowing it to enter bearings. Holes are provided in the shaft to introduce oil as a function of fan speed at a rate necessary to adequately lubricate and cool the bearings. This oil is then returned to the disk pump inlet for recirculation.

The sump is vented forward to the spinner cavity by an air/oil separator bolted to the fan disk.

4.5.3 Bearing Design Analysis

Figures 59 and 60 summarize the basic design configuration, design loads, and calculated life of the fan rotor support bearings.

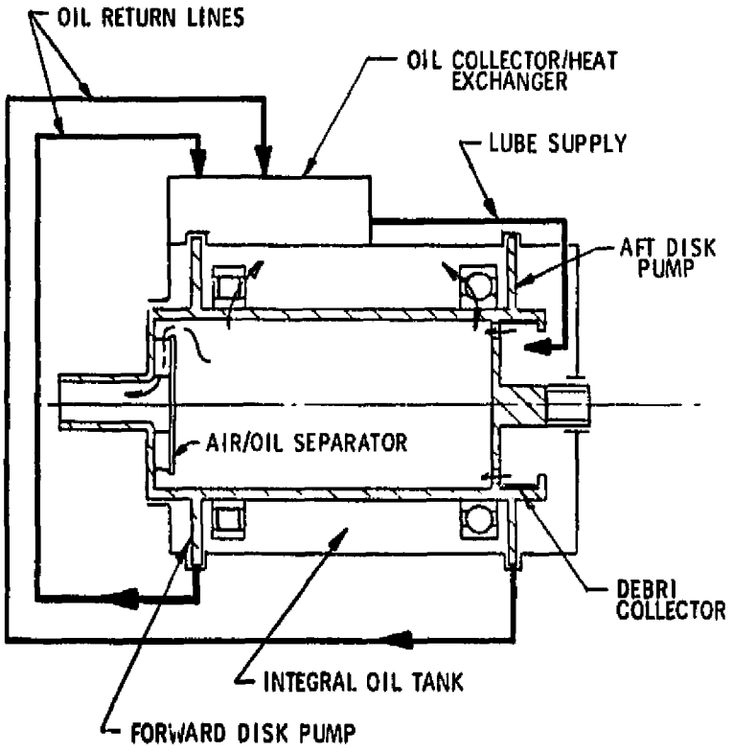

Figure 58. Lubrication Schematic.

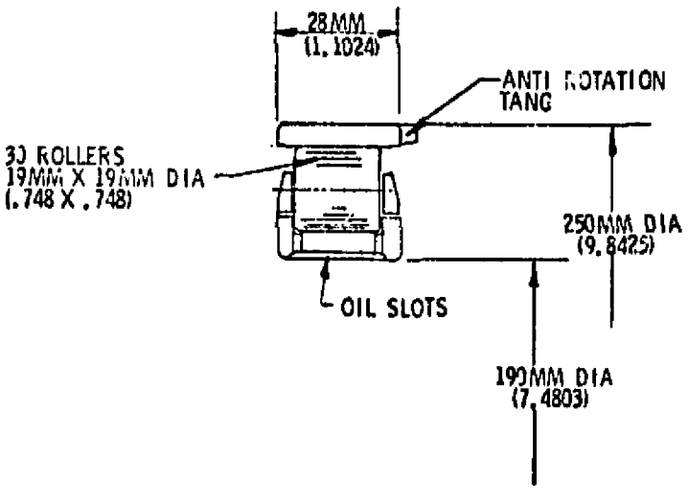

Materials

Outer Ring	M-50
Inner Ring	M-50
Rolling Elements	M-50
Cage	A1S1 4340 (AMS 6414)
Cage Plating	Silver (AMS 241C)

Loading

Condition	Radial Load (N)	(lbf)	Calc. Life (hrs)	Pct. Life
Steady State	9,733	2,188	760,000	99.2
Frequency Maneuver	150,750	33,890	82	0.7
Max. Maneuver	187,200	42,090	40	0.1
Dynamic Capacity	224,800	50,540		

Equivalent Life = 8,950 hours

Figure 59. Roller Bearing Design Summary.

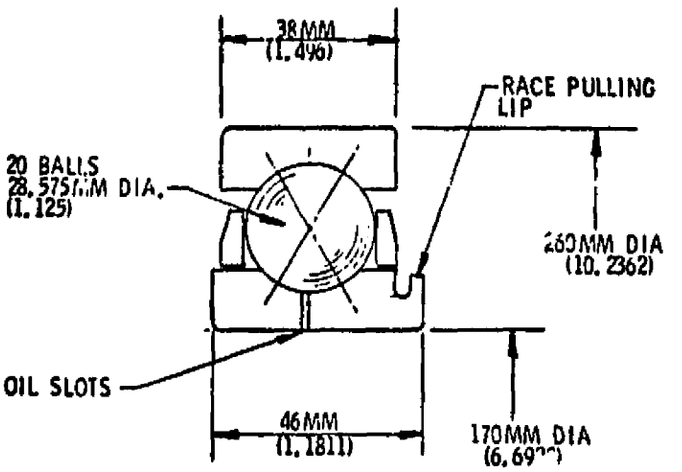

Materials

Outer Ring	M-50
Inner Ring	M-50
Roller Elements	M-50
Cage	AISI 4340 (AMS 6414)
Cage Plating	Silver (AMS 2410)

Loading

Condition	Radial Load (N)	Radial Load (lbf)	Calc. Life (hrs)	Pct. Life
Steady State	4,390	987	279,100	99.2
Freq. Maneuver	135,060	30,360	64	0.7
Max. Maneuver	180,390	40,550	27	0.1
Dynamic Capacity	145,000	32,600		

Equivalent Thrust Load	9,100 N (2045 lb)
Equivalent Life	6670 hrs

Figure 60. Thrust Bearing Design Summary.

The steady-state loads have been determined by combining the fan rotor reaction loads with the calculated vibratory load components. The methods used to combine these loads are current General Electric design practices. The frequent-maneuver load is a combination of the moment caused by a 1.4-radian-per-second maneuver rotation in combination with a 10-g sideload and 2-g vertical load. The maximum maneuver load is determined from a 2.0-radian-per-second maneuver rotation combined with a 4-g sideload and 6-g vertical load.

A cubic-mean-thrust load has been determined and used in the calculation of the thrust bearing life.

The life has been calculated for each of the loading conditions, and an equivalent life has been calculated using the following relationship.

$$L = \left[\sum_{1}^{i} \frac{Ni}{Li} \right]^{-1}$$

where

L = mission life in hours

N_i = fraction of time at i-th point of mission. The percentage used is based on General Electric design practices representative of military missions.

$$\sum_{i}^{1} N_i = 1$$

L_i = Antifriction Bearing Manufactures Association (AFBMA) calculated design life

The AFBMA calculated design life includes a "Life Improvement Factor" of 12.0 for the ball bearing and 5.0 for the roller bearing. The "life factors" include the effects of materials, lubrication film thickness, and hardness. These concur with the American Society of Mechanical Engineers document: "Life Adjustment Factors for Ball and Roller Bearings." The roller bearing life factor of 5.0 was selected because of the limited test data available. The material to be used in these bearings is vacuum-induction-melted/vacuum-arc-remelted M-50 (VIM-VAR M50). In testing to date, this material has outperformed the recommendations of the above reference. The calculated lives shown are therefore conservative.

General Electric engine and laboratory experience and computer techniques have been used to determine the internal geometry and cage design criteria. It is currently General Electric practice to use one-piece, steel, silver-plated cages, and these will be used for the LCF459.

The static bearing capacities of the ball and roller bearings are 173,570 N (39,020 lbf) and 208,000 N (46,760 lbf), respectively, which are adequate to handle the loads induced by a one-blade-out condition. Limited laboratory testing has shown that bearings can withstand three to four times their static capacity without fracture.

4.5.4 Shaft Seals

Figure 61 is a section view showing the typical construction of the aspirating-bore, carbon seals which are to be used in the LCF459. Most GE engines, including the F101, utilize seals of similar construction. Millions of successful hours in field service have demonstrated the mechanical integrity of this construction.

The carbon element is segmented circumferentially. The segment ends are overlapped in tongue-and-socket joints which are precisely fitted to form a positive seal. Circumferential clearance at the end gaps allows the seal ring to expand and contract diametrally with the seal race and to ride on the bore without arch-binding. An extension spring encompassing the seal carbon element outside diameter provides an inward radial force to close the segment end gaps in the free state and holds the segments like so many keystones in an arch. Axial compression springs hold the carbon elements against the transverse face of the seal housing.

Figure 62 shows the forces acting on the circumferential carbon elements. Axial coil springs, plus an unbalanced axial pressure, force the elements against the transverse face of the stationary housing. An extension spring around the outside diameter of the seal elements, and an unbalanced radial pressure, radially force the elements against the rotating seal race. This inward radial force is supplemented by the aspirating effect of a reversed-direction, hydrodynamic bearing to prevent bore hydroplanning. Hydrodynamic bearings are machined into the bore of the element wear pads; the closed end of the bearing is downstream of the pocket in the direction of shaft (or race) rotation. Oil being dragged out of these pockets by the shearing action of the rotating race depresses the pressure in the bearing pockets and aspirates the seal bore onto the surface of the race.

4.5.5 Heat Generation

The amount of heat rejected by bearings is dependent on bearing rotational speed, load, lube flow to the bearing, and lube viscosity. Since the bearing speeds and loads are determined by the cycle and configuration requirements, the only variable available to reduce bearing heat generation is lube flow and viscosity. The lube flow supplied to the bearings reflects this design intent. Table XII shows the amount of heat generated by the

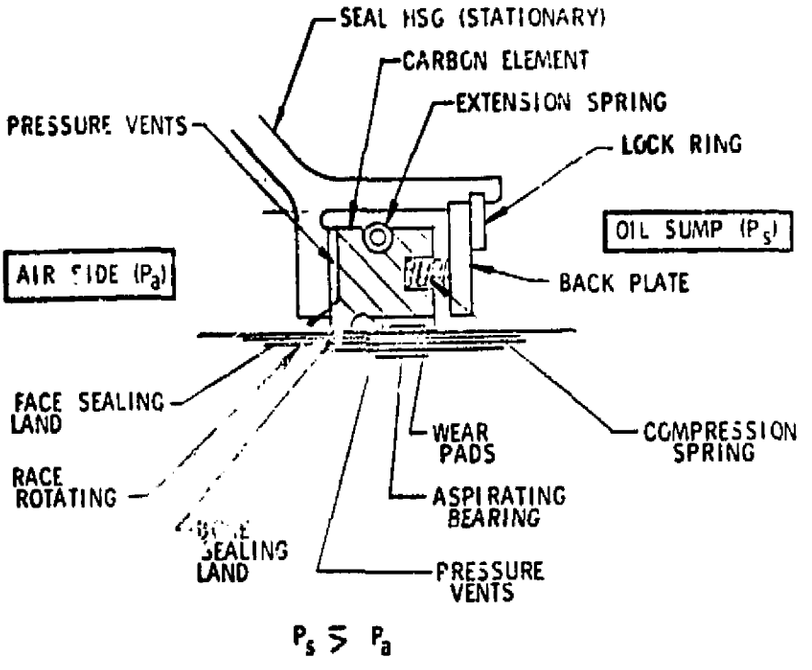

Figure 61. Construction of Aspirating Bore Carbon Seals.

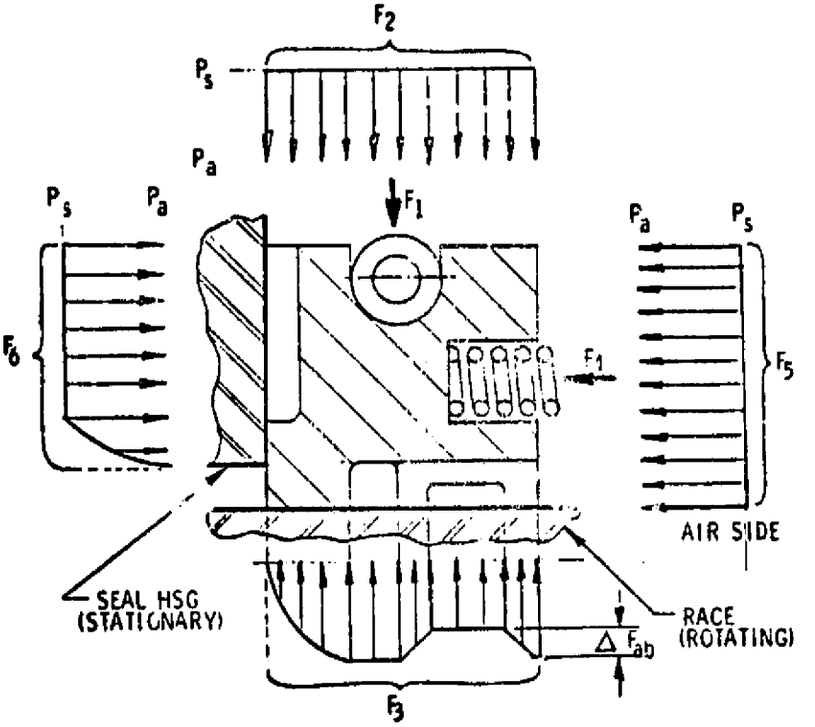

Figure 62. Aspirating Bore Seal Element Forces.

bearings under maximum cycle conditions and the amount of lube oil to be supplied.

The oil flows shown in Table XII are conservative based on tests run on a CF6-50 No. 4 roller bearing with simulated LCF459 loads and speeds. Figure 63 shows that, at an oil-in temperature of 106.3° C (223° F) and with the flow reduced from approximately 2500 cm^3/min (0.661 gpm) to 500 cm^3/min (0.132 gpm), the bearing outer race temperature increased less than 11.1° C (20° F).

The integral heat exchanger has been sized to dissipate the generated heat by forced convection conditions. Radiating fins and a thin, sheet-metal, air-flow baffle are utilized to increase the effectiveness of the heat exchanger. Maximum scavenge oil temperature should stabilize at approximately 149° C (300° F) for the configuration shown.

4.5.6 Viscous Pump Performance

The lube supply and sump scavenge system have been combined by utilizing a viscous disk pump to convey the oil out of the sump to the oil collector/heat exchanger. The design of this viscous disk pump is based on a similar pump used both in the TF39 and the CF6 engines which have accumulated over two million successful engine hours. A comparison between the CF6 pump and the LCF459 pump is shown in Table XIII.

Figure 64 shows discharge pressure versus pump peripherial speed using data from CF6 testing. These data have been extrapolated to include the speed range of the LCF459 at takeoff. A component test will be required to verify the extrapolation. It should be noted that the minimum required pump discharge pressure is 2.2 to 6.9 kN/m^2 (0.032 to 1.0 $lbf/in.^2$) for all speed ranges. Figure 65 shows pump discharge flow versus discharge pressure. The LCF459 flow requirement is 0.00756 m^3/min (2.0 gpm) at takeoff conditions.

4.5.7 Sump Housing

The sump housing performs the following functions.

- Contains a lube tank and heat exchanger integral with housing
- Supports the rotor structure
- Transfers maneuver loads into fan frame
- Provides mounting rabbett for an accessory gearbox
- Contains integral oil manifolding for bearing cooling and lubrication

Table XII. Bearing Heat Generation.

Component	Heat Generation		Lube Flow	
	Watts	Btu/min	m^3/min	gal/min
Roller Bearing	1810	103	0.00378	1.0
Thrust Bearing	1845	105	0.00378	1.0
Total	3655	208	0.00756	2.0

Table XIII. Disk Pump Comparison.

	TF39 and CF6	LCF459
Pump Diameter, mm (in.)	203 (8.0)	269 (10.6)
Pressure, kN/m^2 ($lbf/in.^2$)	103 (15)	262 (38)
Speed, rpm	2500	4370

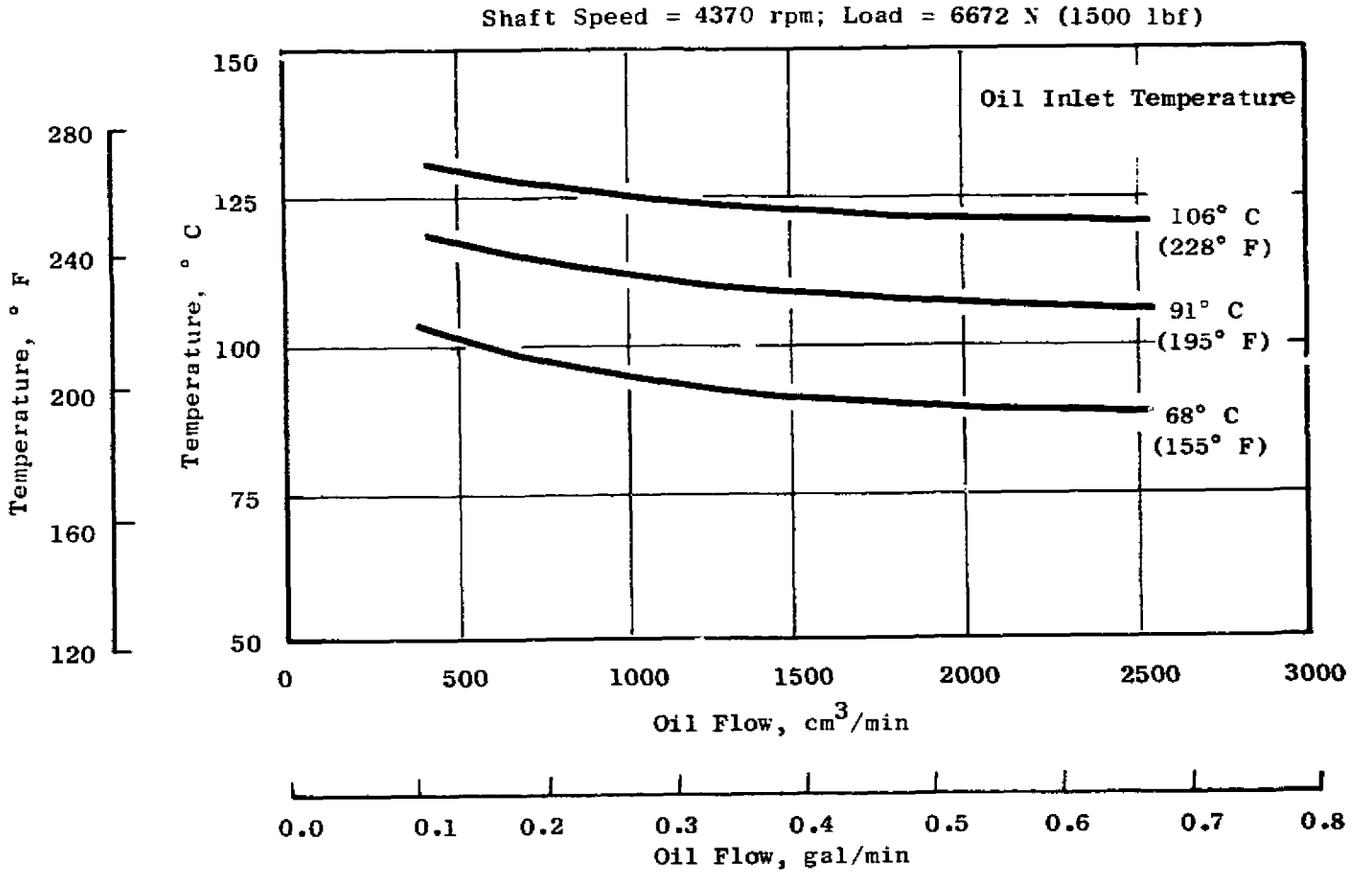

Figure 63. Bearing Race Temperatures.

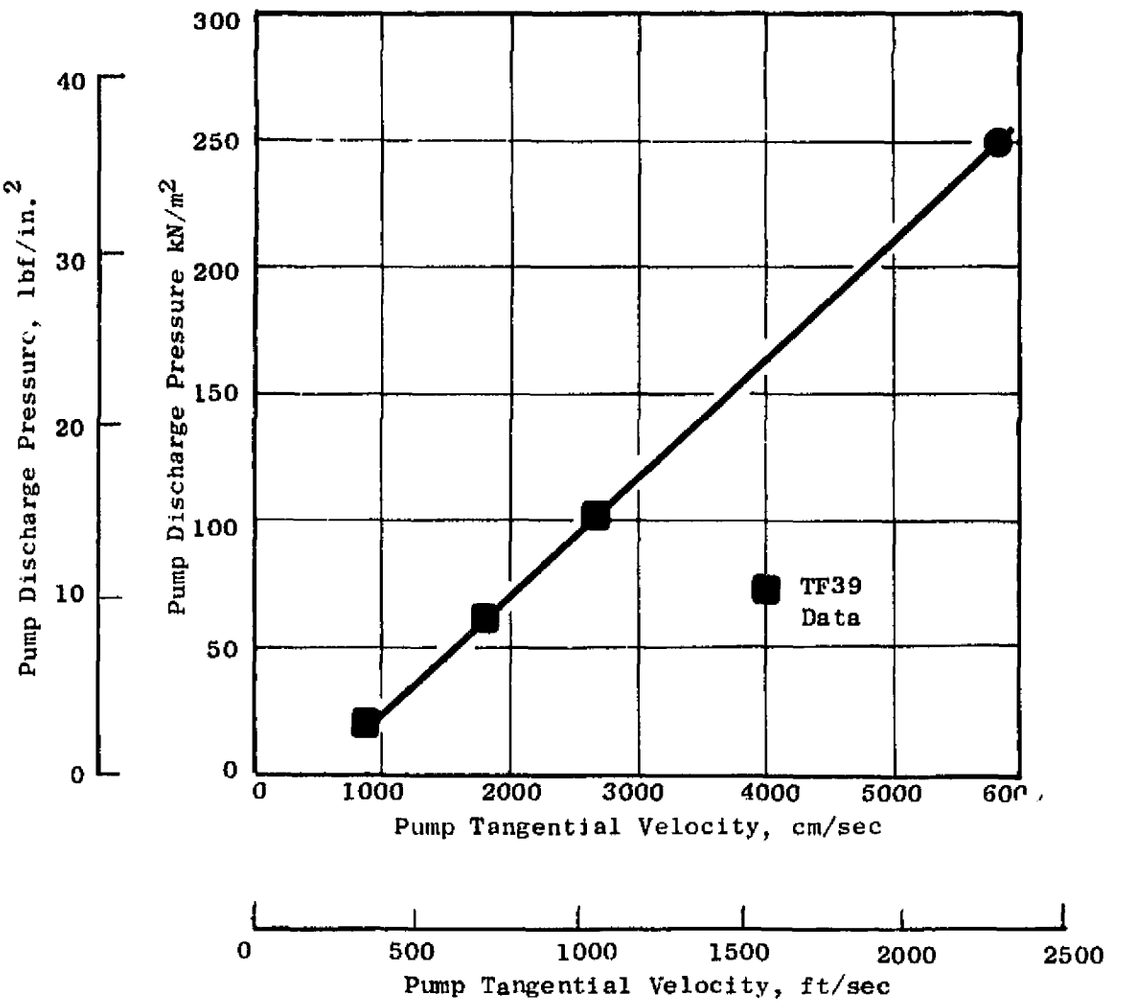

Figure 64. Disk Pump Discharge Characteristics - No Flow.

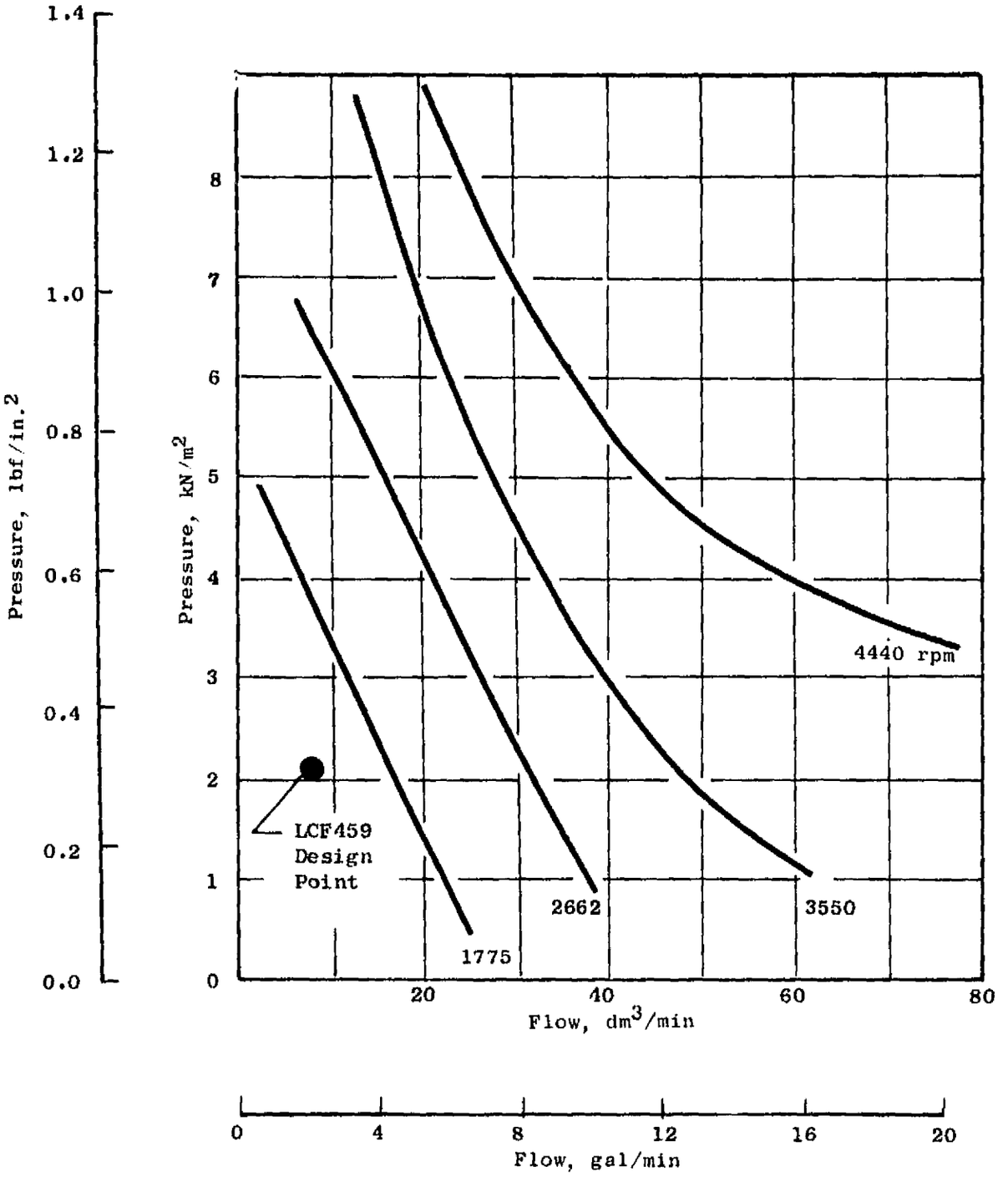

Figure 65. Pump Discharge Pressure/Flow Characteristics.

To meet the requirements of all these functions, a cast steel and sheet welded construction is being utilized. Figure 66 shows the induced bearing reaction loads and stresses at various critical areas for a 2-radian-per-second maneuver condition.

4.5.8 Fan Shaft Stress Analysis

Design practices which have been previously applied to main shaft configurations used in the CF6 and F101 engines have been used in designing the rear fan shaft. Titanium (Ti 6-4) material has been selected considering strength, weight, thermal compatibility with the fan rotor, and corrosion resistance to a salt environment.

Stresses, as shown in Figure 67, were calculated for the 2-rad/sec maneuver condition and are compared with allowable material properties. Stress concentration factors have been applied where holes and small radii are necessary to meet secondary functions of the shaft.

4.5.9 Accessory Drive

Figure 68 shows a typical accessory package. The gearbox is spline-driven from the rear fan shaft. The spline is lubricated by the accessory gearbox with a shaft seal to prevent leakage. Hardened splines are utilized to minimize wear. A large rabbett is provided on the sump housing to support the overhung moments of the accessory package.

Accessory drive requirements vary from application to application, and the arrangement shown in Figure 68 provides a 5000 rpm hydraulic pump and an 8260 rpm constant-speed-drive generator pad. Lube system requirements must be provided in the gearbox.

4.5.10 Weights

The weights of the components of the bearing and lubrication system are listed in Table XIV. The total weight of the system at the conclusion of these design studies is 33.3 kg (73.5 lbm).

Table XIV. Bearings, Sumps and Lubrication Weights.

	kg	lbm
Sump Housing Assembly	17.2	38.0
Disk Pump	1.0	2.2
Bearings, Seals, and Hardware	15.1	33.3
Total	33.3	73.5

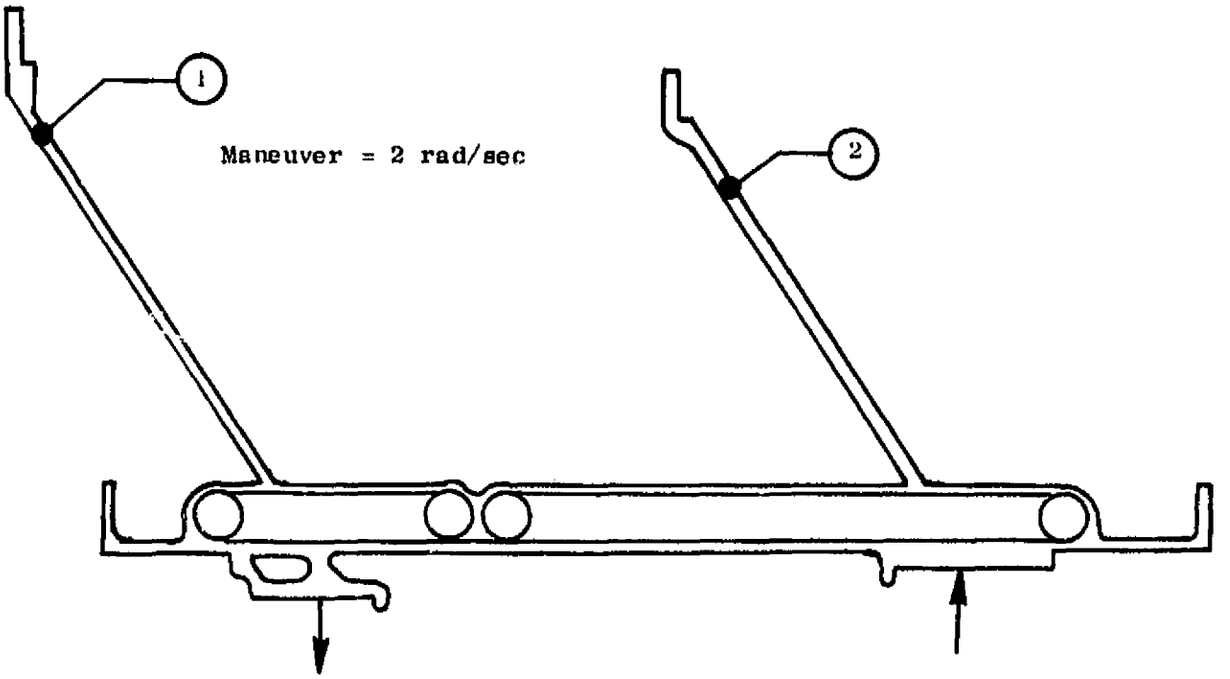

Location	Stress	
	(kN/m^2)	($lbf/in.^2$)
1	134.1	19,500
2	156.8	22,800

Figure 66. Housing Loads and Stresses.

Maneuver = 2 rad/sec

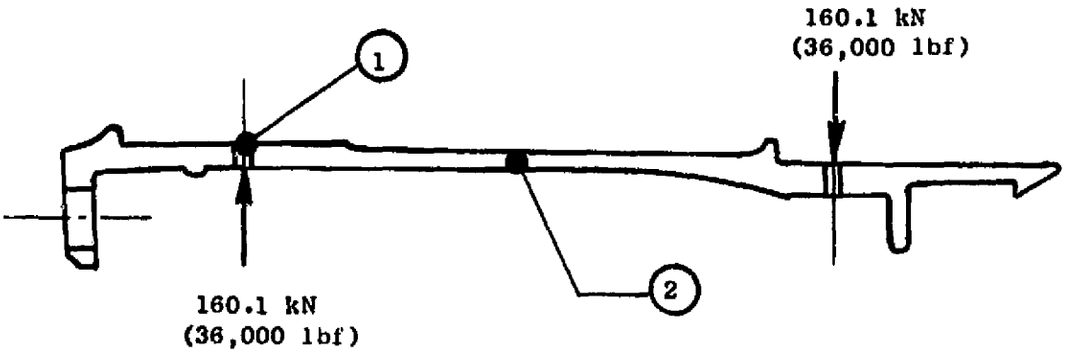

Location	Stress	
	(kN/m^2)	($lbf/in.^2$)
1	503.3	73,000
2	146.9	21,300

Stresses Include K_T Factors

Figure 67. Shaft Loads and Stresses.

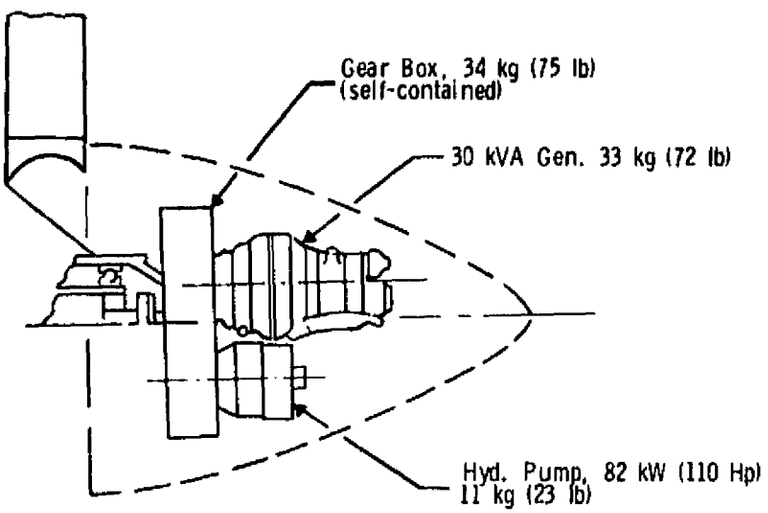

1g Loads
Shear - - - 77 kg (170 lb)
Overhung Moment - - - 283 N-m (2500 lb-in)

Figure 68. Turbine Aircraft Accessory Package.

4.6 SCROLL

The scroll has the function of efficiently distributing the gas generator exhaust to the tip turbine. This requires a flow passage with an approximately constant velocity and a minimum of internal flow obstructions or blockages which would result in high pressure losses. The end of the scroll flow path forms the nozzle discharge passage for the tip-turbine annulus.

The scroll for the Research Technology Aircraft was selected from a number of configurations which were studied and compared on the basis of performance, weight, installation compatibility, reliability, and cost. General Electric experience in scroll design for tip-turbine fans has been well factored into the RTA design so that development can proceed with confidence. This report will cover only the selected scroll configuration.

The selected scroll, which is illustrated in Figure 69, is a single-bubble concept. The scroll body is made from HS188, a relatively low cost, heat-resistant material.

4.6.1 Design Requirements

The scroll is designed to satisfy the design life, cyclic, and engine-out operation requirements consistent with Section 3.0. Summarizing the design criteria pertinent to the scroll:

- Design life - 600 hours
- Stress (short time)

  0.02% Yield Strength
  2/3 Ultimate

- LCF

  Life = 2 × Mission Requirements
  12 Cycles per Mission
  600 One-hour Missions
  2 × 600 × 12 = 14,400 Cycles

- Rupture

  Rupture Life $\geq$ twice mission requirement
  2 × 600 one-hour missions = 1200 hours

- Pressure Vessel Proof Test

  Twice maximum operating pressure at rated temperature without bursting. Some permanent distortion acceptable.

In addition to gas pressure loads shown in the free-body diagram, Figure 70, a maneuver loading of 10-g down (4-g fore and aft) has been factored into the design analysis. The inlet is designed to take a 13.3 kN (3000 lbf) additional applied load from the ducting maneuver. The inlet gas pressure load is reacted through the inlet to the ducting as pipe stress.

4.6.2 Basic Design Features

The scroll configuration as shown in Figure 71 indicates the principal features of the design. In the mechanical design of the scroll, emphasis has been placed on cost, durability, weight, maintainability, sealing, and life. The scroll body as shown consists of a circular membrane and gooseneck. The internal flow areas are designed for a Mach number of 0.30. The scroll is symmetric about a line through the inlet, with the flow area linearly decreasing on either side to a minimum 12.7-cm (5 in.) diameter section. This arrangement allows the larger, drag-contributing sections to be buried in the airframe with the inlet and ducting. The scroll body and inlet skins are manufactured by stretch-forming, and the scroll body skins are common to typical wing- and nose-fan scroll installations. Different inlet designs may be required to produce ducting attachments tailored to fit the confines of the aircraft. Because of the symmetry, this scroll design can be installed on either the left- or right-side arrangements. To achieve minimum weight while providing the necessary weld-joint reinforcement, the formed scroll sections are masked and chem-milled to minimum thickness after forming.

The scroll is made of HS188 material. This material is a heat-resistant, cobalt-base alloy commonly used in exhaust system components. It is readily field-weld repairable and significantly lower in cost than the age-hardening superalloys. Previous General Electric scroll manufacturing experience with cobalt-base alloys makes this material a good choice for the RTA design.

In the gooseneck area, just upstream of the turbine nozzle vanes, 80 struts are used to continue the hoop tension load path of the circular membrane across the annular nozzle flow path. The struts are brazed into ring sections and oriented with the flow to minimize blockage. The turbine stator row at the aft end of the gooseneck consists of 138 hollow nozzle vane partitions. The vane shapes are varied circumferentially as required to accommodate the varying nozzle-inlet angles of attack and provide an efficient tip turbine. Ferrules are used at the vane ends to increase the braze-joint area so that they may be securely joined to the thin, sheet-metal, scroll structure.

The scroll is attached to the fan structure by links. The network of links reacts both the axial thrust load, 15.30 kN (3440 lbf), and the tangential thrust load, 24.42 kN (5490 lbf). The links also allow for free radial expansion of the hot scroll with respect to the cooler fan casing. A piston-ring-type seal on the outside diameter of the gooseneck prevents exhaust gas leakage into the surrounding aircraft cavity. This seal seats on a machined flat that runs continuously around the scroll and is held captive to the fan casing by a sheet-metal retainer.

FRAME

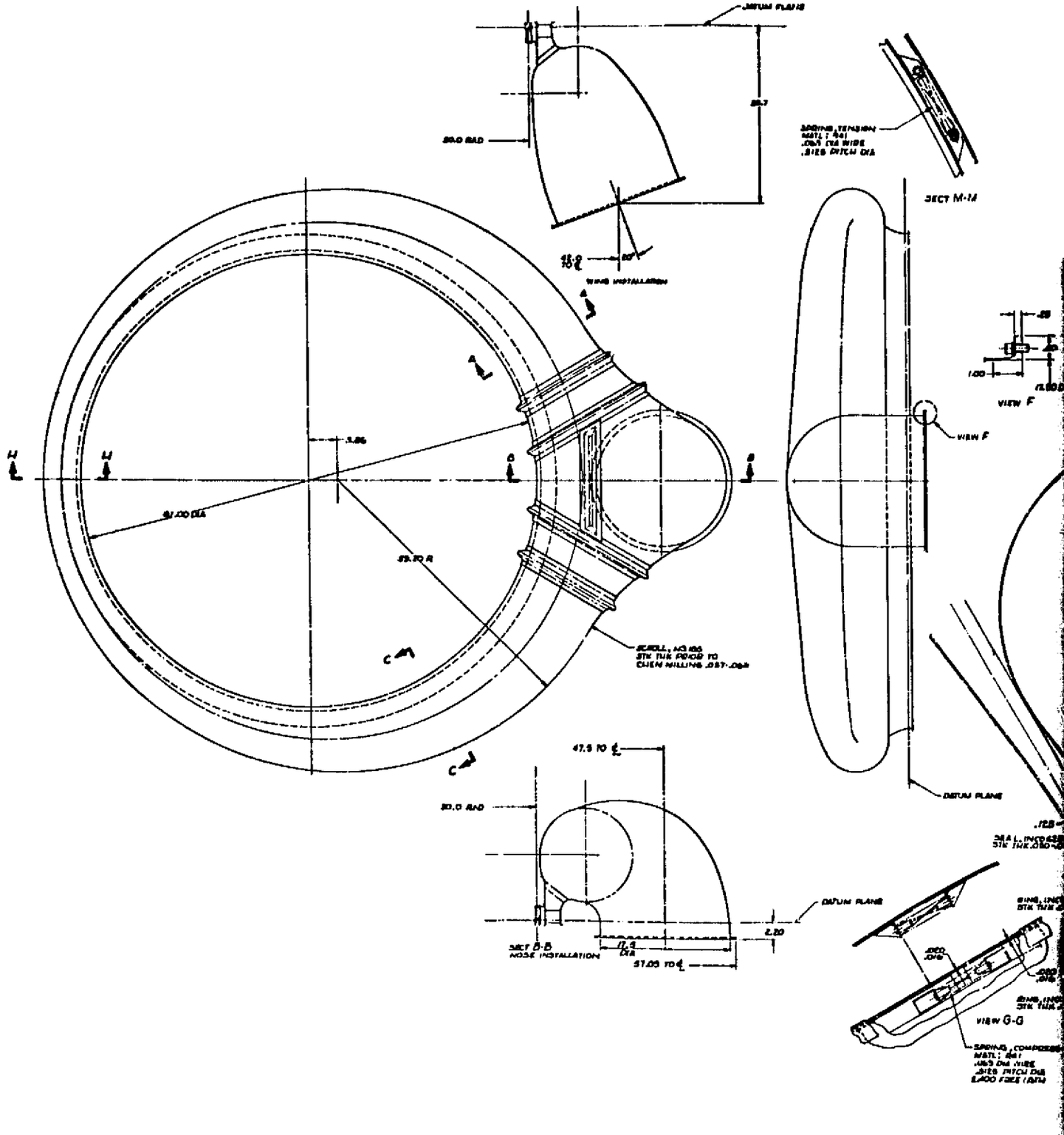

Figure 69. Scroll

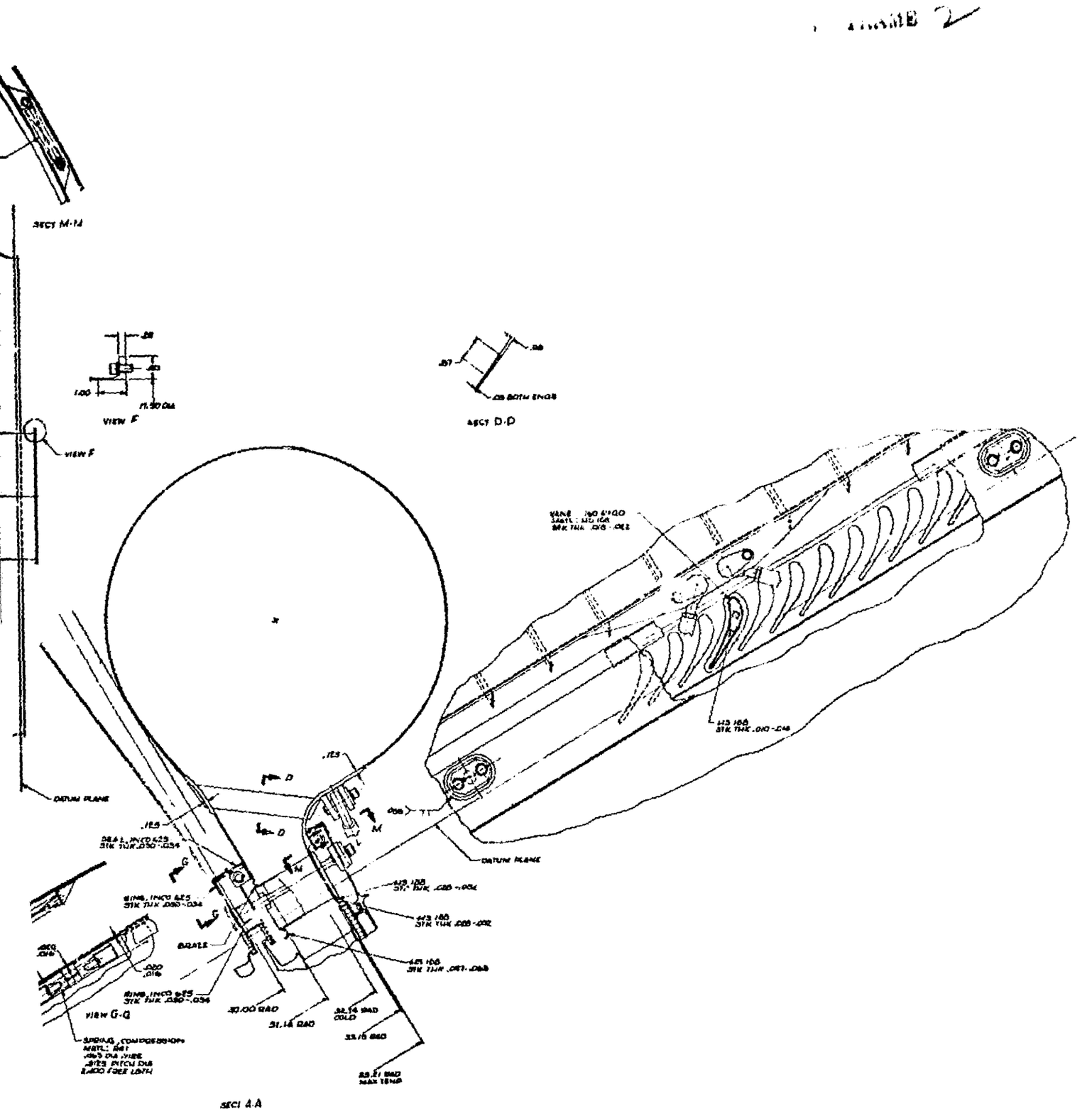

69. Scroll Layout.

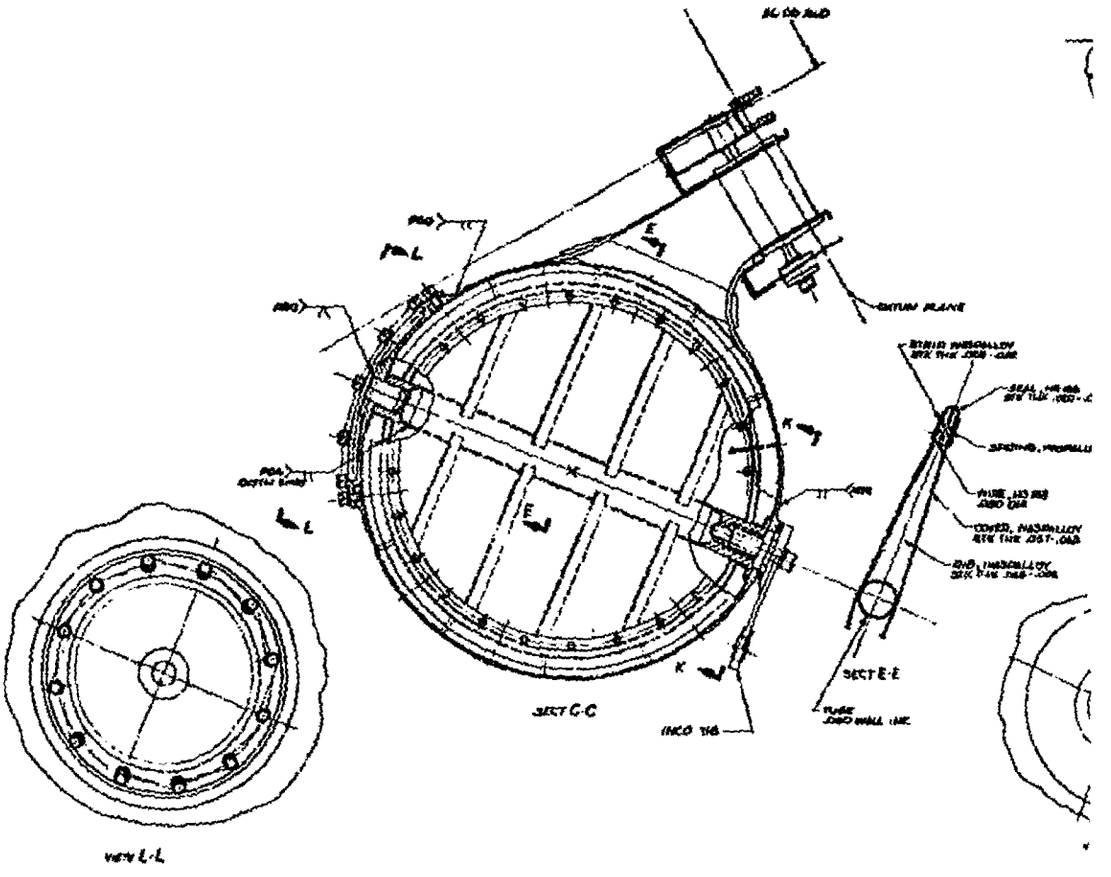

Figure 69. Scroll I

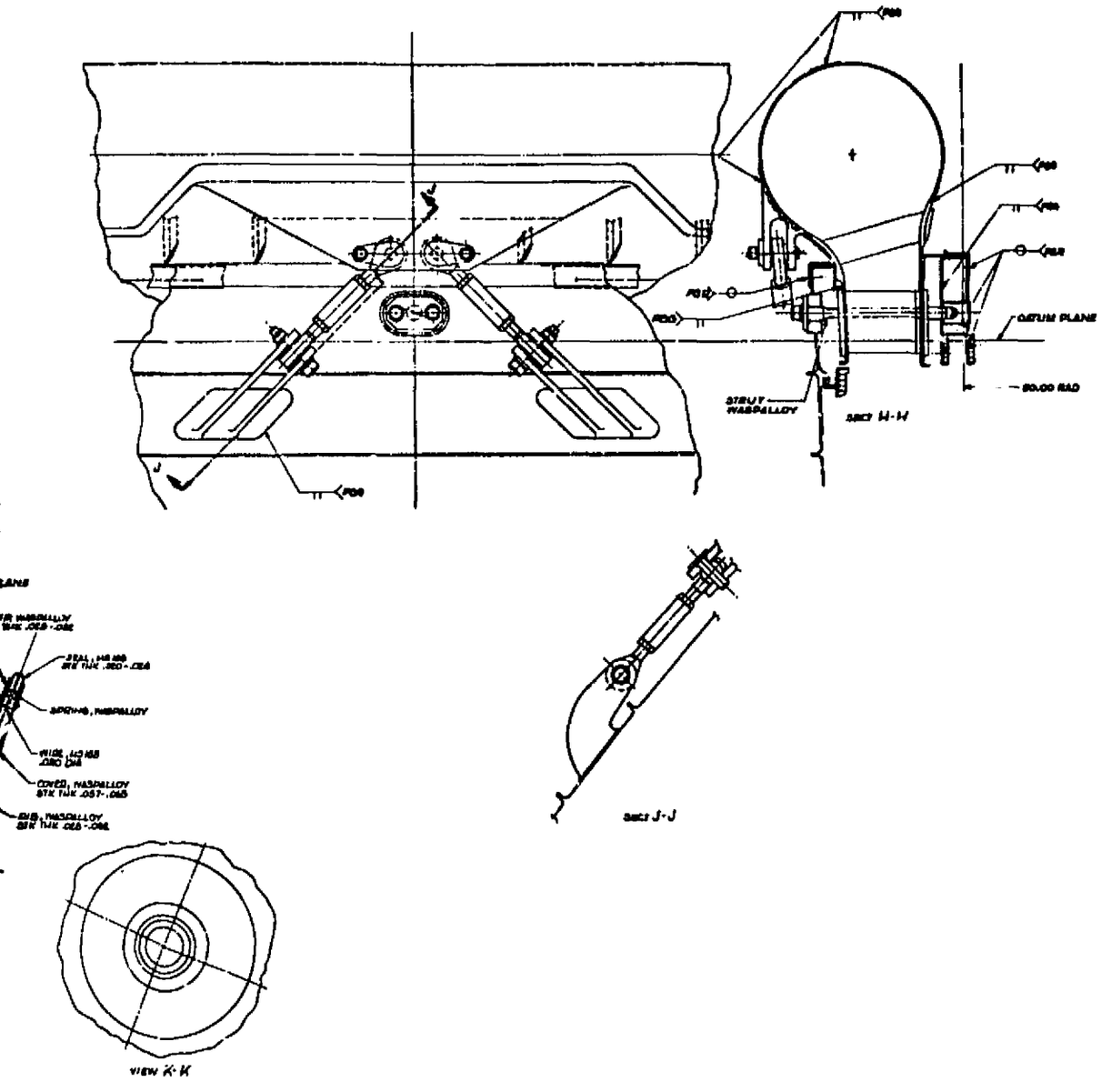

). Scroll Layout (Concluded).

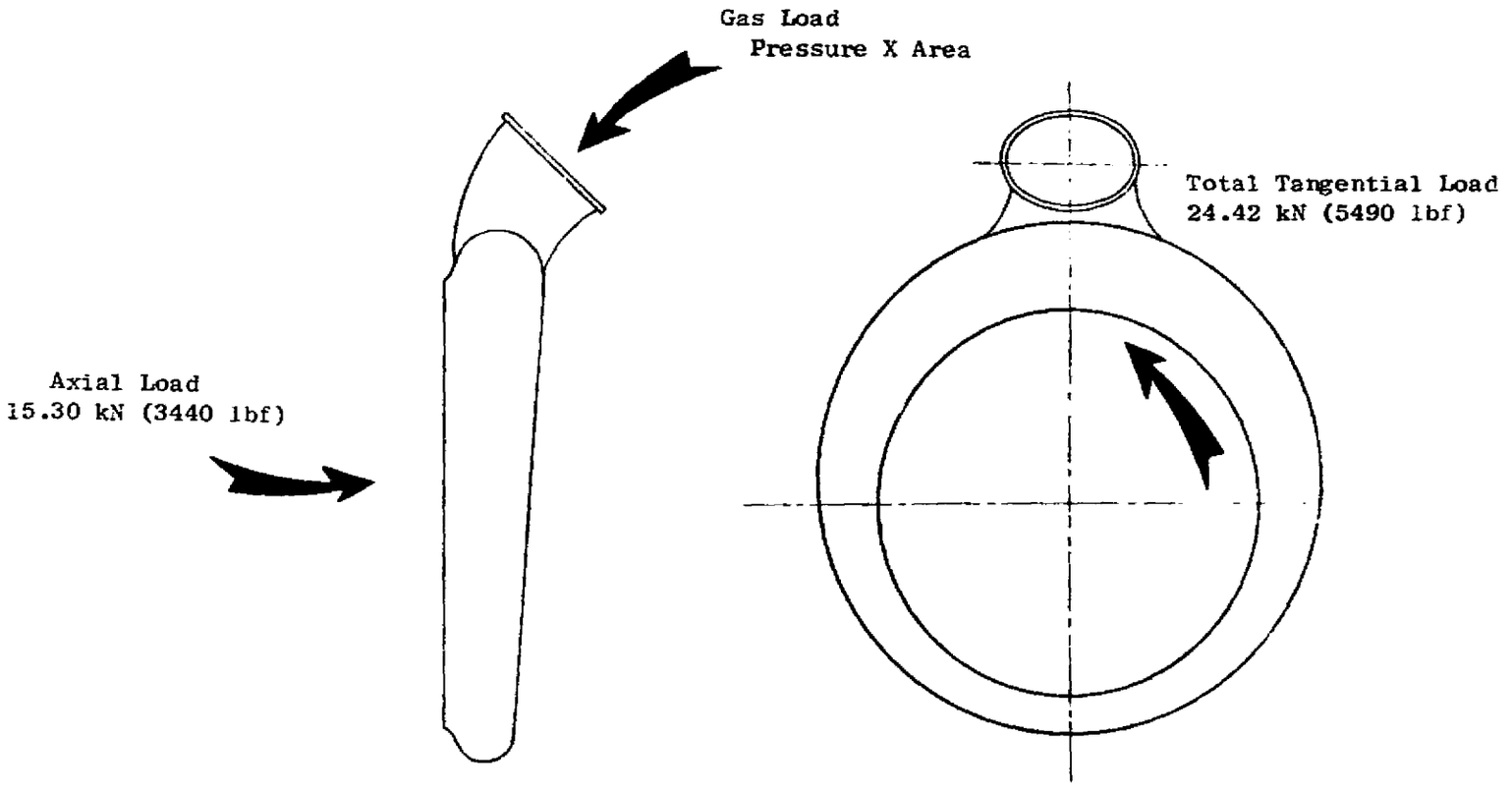

Figure 70. Scroll Gas Loads.

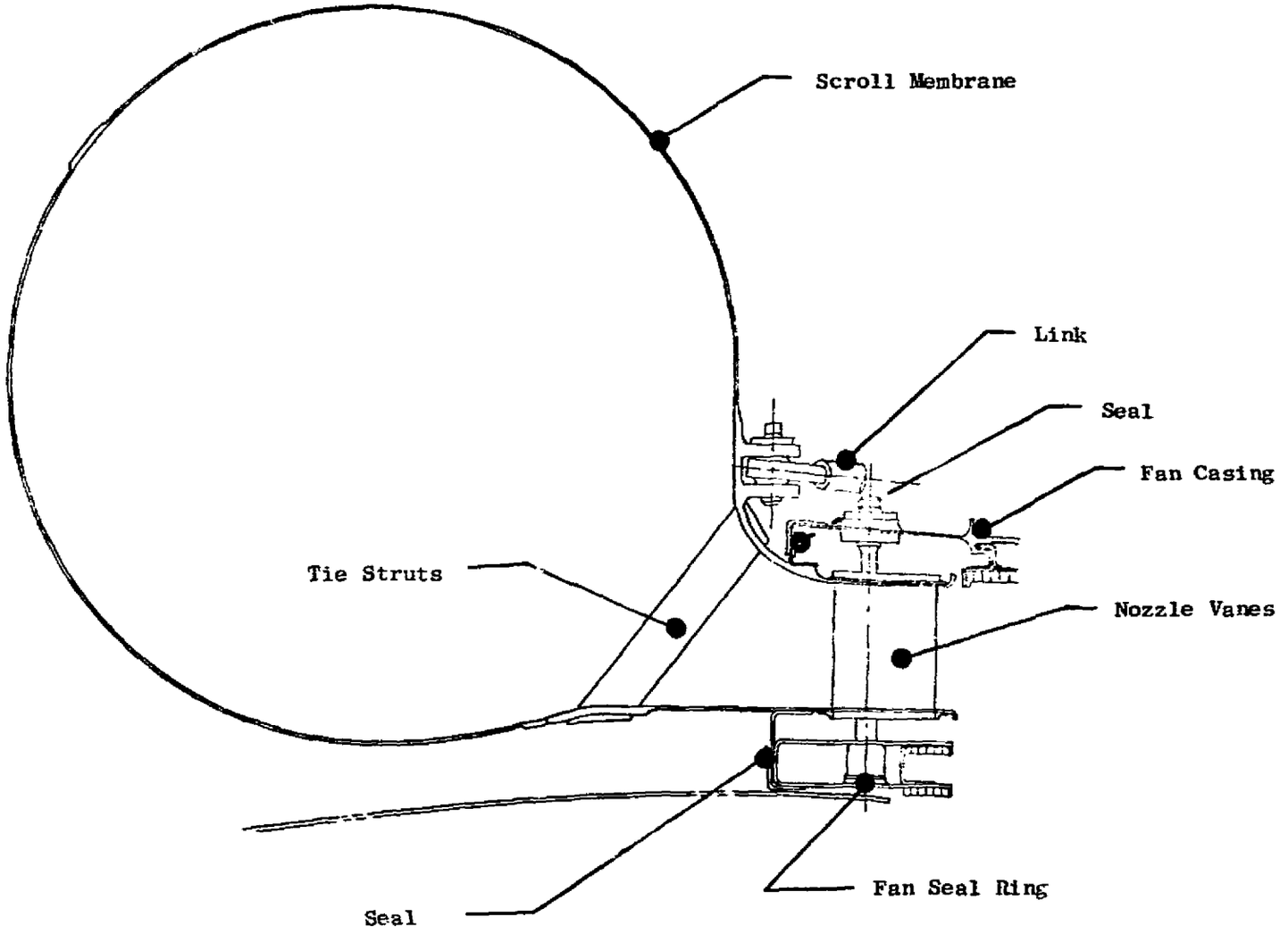

Figure 71. Scroll Configuration.

The forward fan seal ring is attached to the fan casing by 18 equally spaced rods as shown in Figures 71 and 72. The rods pass through the hollow turbine nozzle vanes, isolating the fan seal from the large thermal migrations of the scroll. Mounting the seal ring in this manner provides a dimensionally stable mounting base for the honeycomb seals. The fan seal cavity is pressurized by cooling air pumped through the fan rotor carrier assembly. This pressurized air prohibits hot turbine gases from entering into the seal cavity; as a result, the seal will operate close to the fan discharge air temperature. At the forward edge of the seal ring is a piston-ring-type seal that keeps gases from leaking around the fan seal into the airframe cavity. This seal follows the scroll radial growth to prevent leakage at all flight conditions. Figure 73 compares the scroll and seal relative locations for both the cold and the operating-temperature conditions.

The outer surface of the scroll will be covered with insulation. This insulation, shown in Figure 69, is 0.635-cm (0.25 in.) thick Min-K enclosed in a quartz cloth blanket. Calculations show that the outside surface temperature can be kept below 180° C (350° F) even though the gas temperature inside the scroll is as hot as 870° C (1600° F). The weight of the insulation is not included because it is intended that this item will be furnished by the aircraft manufacturer.

4.6.3 Design Analysis

Figures 74 and 75 give the maximum stresses at various locations in the scroll. These stresses were used in the life analysis. Where applicable, the stresses include the effects of maneuver loading and stress concentration factors.

The link network used to attach the scroll to the fan casing is shown in Figure 76. The links are adjustable for flow-path alignment during assembly. The maximum stresses in the link network as determined for the maximum maneuver load condition are shown in the figure.

During the emergency, engine-out condition, the scroll must operate with less than a 360-degree active arc. Part of the scroll is shut off in order to maintain the choked flow condition in the turbine nozzles. As a consequence, the scroll will experience a start-up, thermal transient creating thermal stresses. The peak stresses experienced during this transient are shown in Figure 77.

The results of a life analysis of the scroll are given in Table XV. The life analysis for both the time- and the cycle-dependent conditions make use of the linear damage assumption common to all General Electric life calculations. In this type of analysis, the mission profile is broken up into common life-consuming points such as takeoff, landing, climb, and cruise. For each life-consuming point, calculations are made to determine the stress and life expectancy. By this procedure the overall mission life is calculated. The cyclic life analysis is done in much the same way, using load cycles

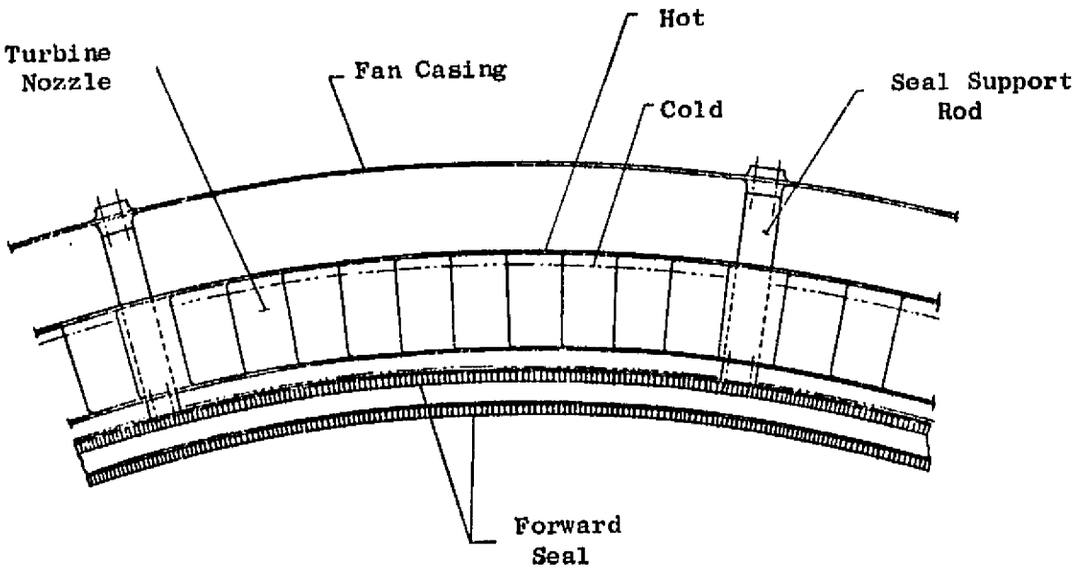

Figure 72. Forward Seal Mounting.

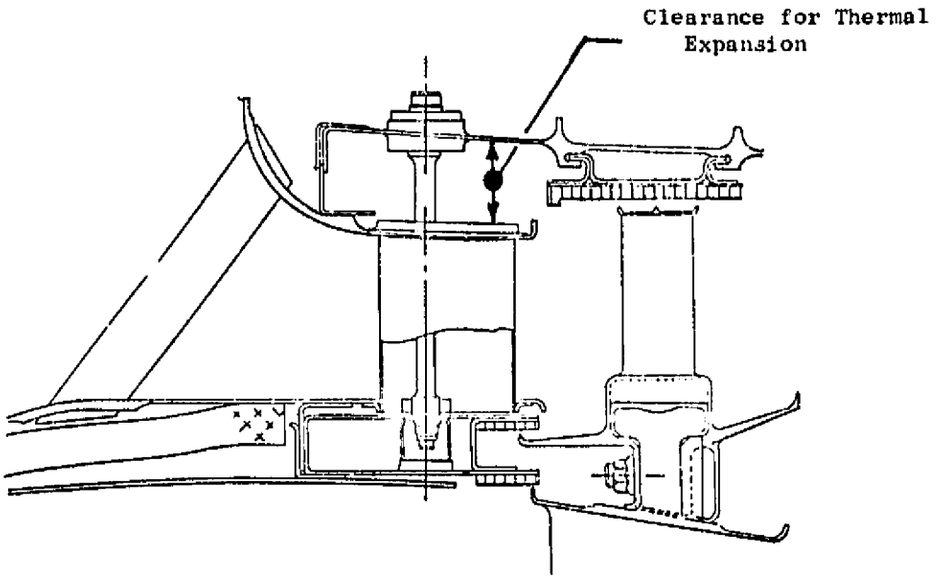

(a) Cold

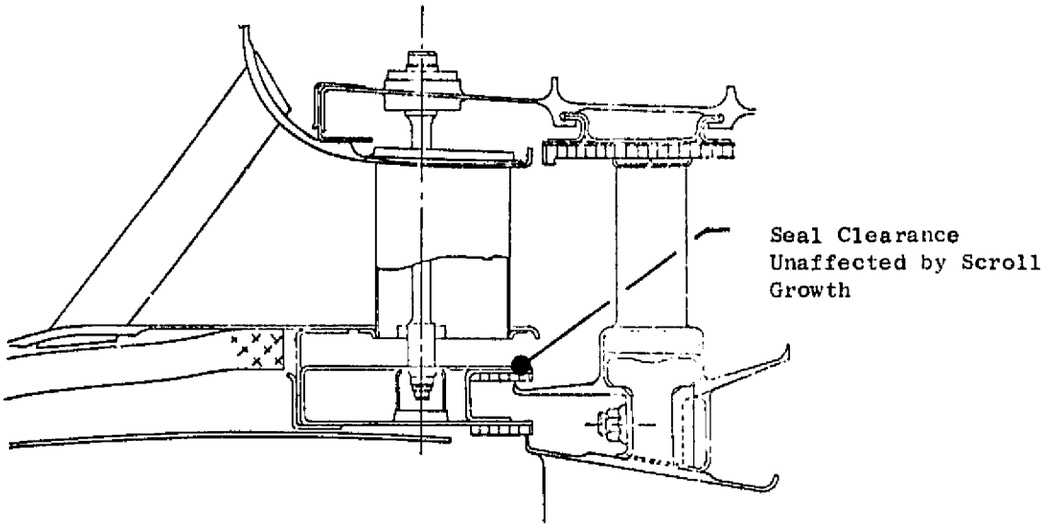

(b) Hot

Figure 73. Scroll Alignment; Hot and Cold.

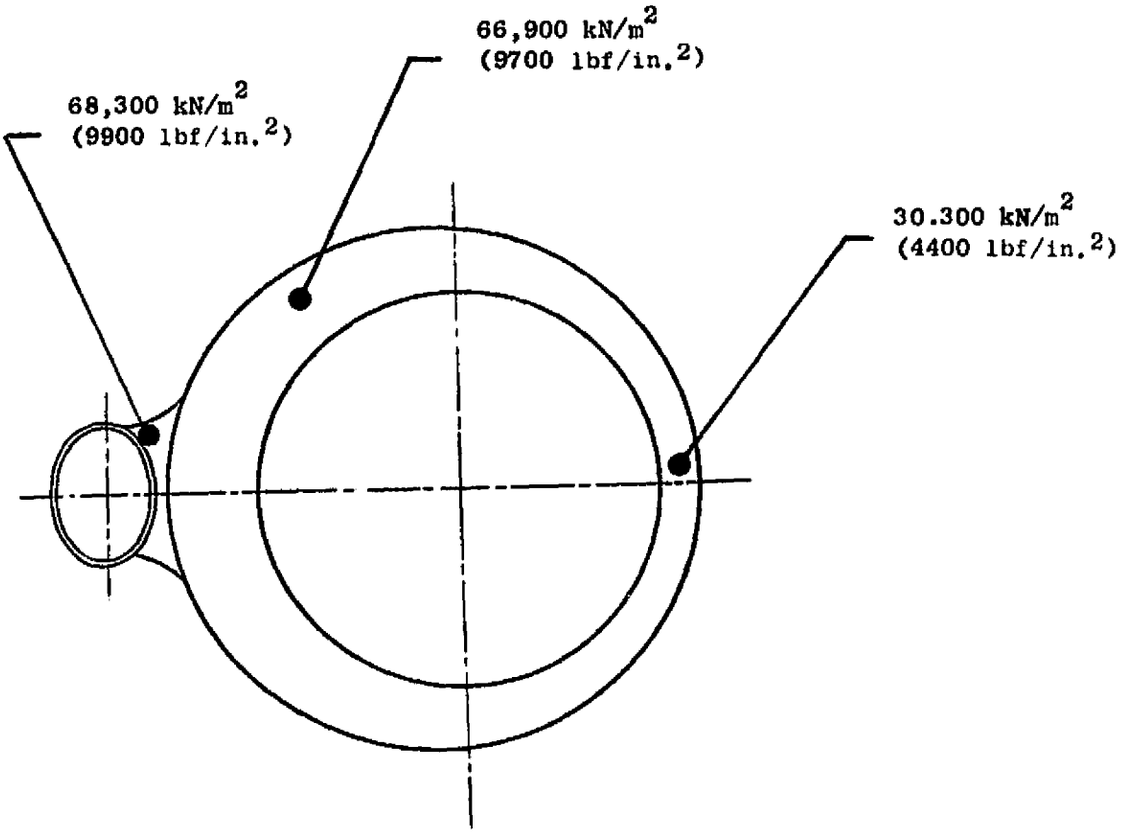

Figure 74. Scroll Membrane Stresses.

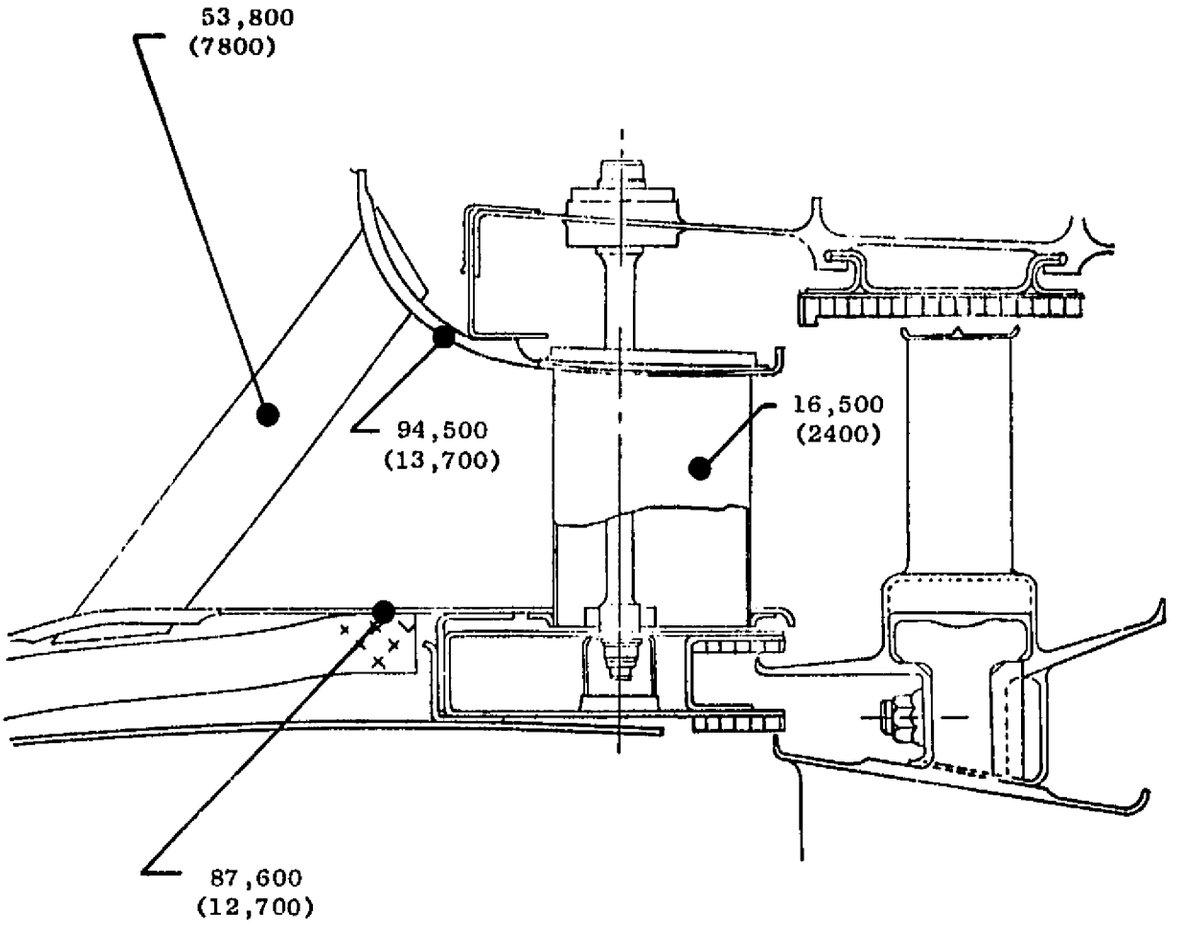

Stress: kN/m^2 ($lbf/in.^2$)

Figure 75. Scroll Gooseneck Stresses.

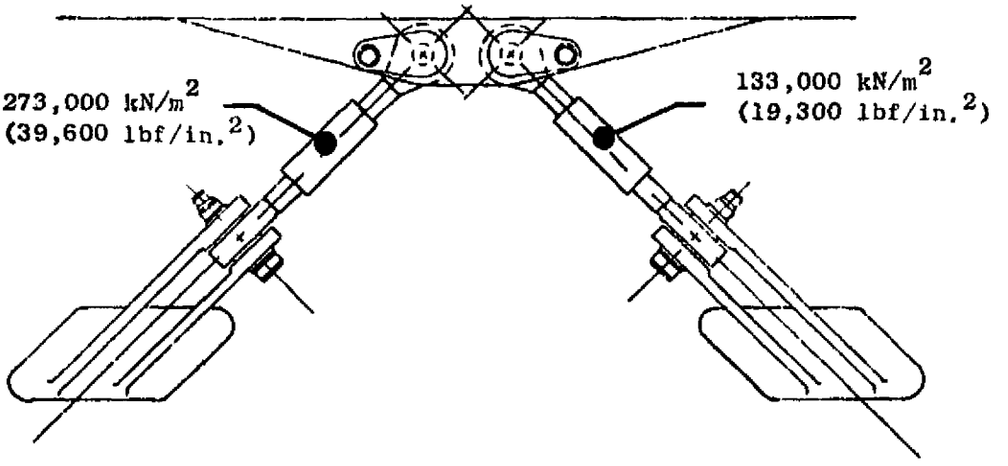

Figure 76. Scroll Mounting Arrangement.

LCF459 Scroll for Partial Arc Operation

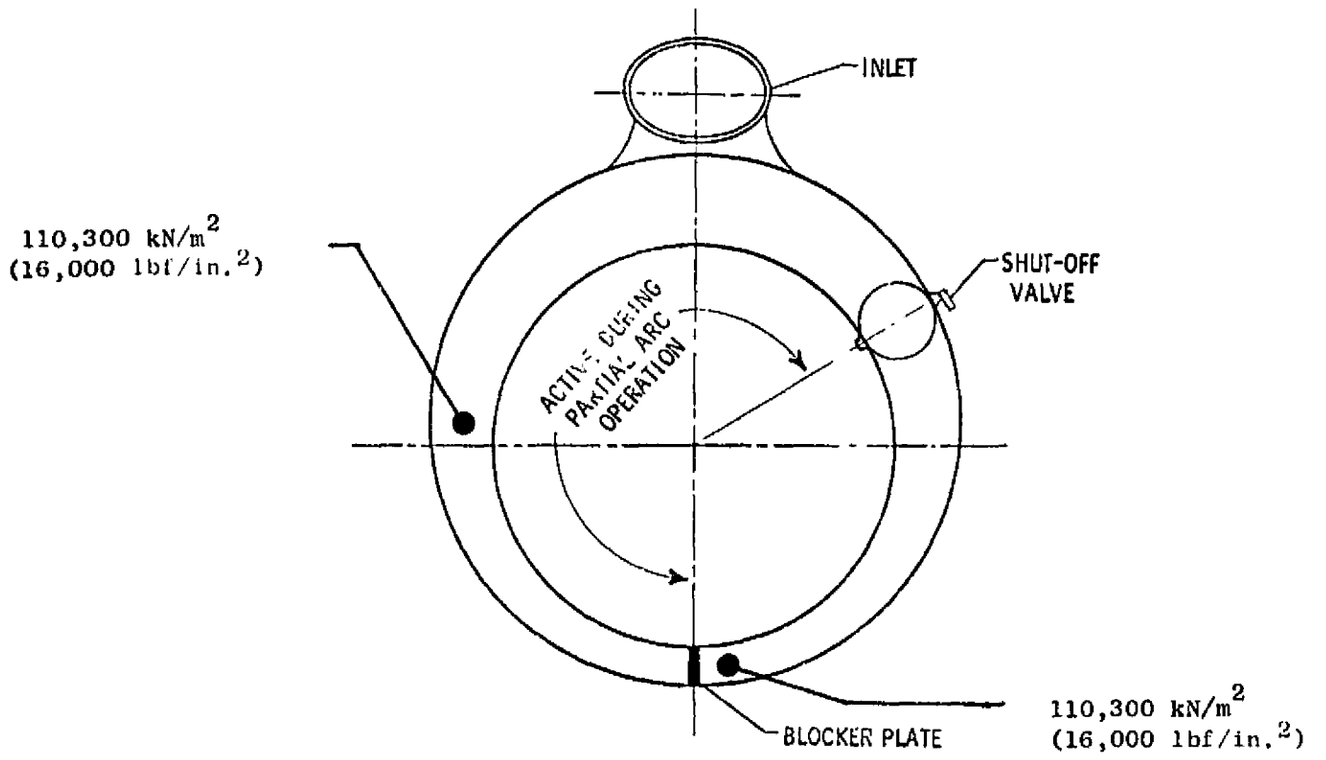

Figure 77. Scroll Stresses During Engine-Out.

Table XV. Scroll Life Analysis.

Flight Condition	Temperature K	Temperature ° R	Pressure kN/m^2	Pressure lbf/in.^{2}	Stress kN/m^2	Stress lbf/in.^{2}	Time Hours	Percent Life Used 10% Creep	Percent Life Used Rupture
Control	1144	2060	356	51.6	68,300	9,900	14	60	27
Takeoff	1089	1960	334	48.5	62,700	9,100	52	21	9
Climb	1019	1835	327	47.4	60,700	8,800	80	--	--
Cruise	905	1630	274	39.8	46,200	6,700	250	--	--
Pattern	962	1733	301	43.6	53,800	7,800	130	--	--
Landing	1077	1940	330	47.8	61,400	8,900	74	--	--
							Total	15/96	7/43
Low Cycle Fatigue - For 7200 Idle to Maximum Control Cycles = 34.8% Life Used.									
Engine-Out Operation - 2-min. Duration with 427° C (800° F) Warmup = 0.43% Life Used.									

rather than mission points. The mission includes twelve idle-to-maximum control cycles per hour of life. The intermediate or lower range of load cycles can be ignored because the alternating stress range is small. The partial arc operation life usage is calculated separately, based on the design analysis mentioned earlier and severe estimates of duration at temperature. The design critera and analytical methods used assure a light-weight, reliable, cost-effective, scroll design for the research technology aircraft.

4.6.4 Weight

The calculated weight of the total scroll assembly including items such as the fan inlet seals, outer casing, and shutoff valve is 116 kg (256 lbm). This weight does not include the shutoff valve actuation system or insulation blanket, both of which are aircraft furnished. Table XVI gives a weight breakdown of the scroll components.

Table XVI. Scroll and Fan Casing Weights.

	kg	lbm
Scroll skin	25.2	55.5
Nozzle assembly	36.3	80.1
Fan seal and struts	9.2	20.4
Fan casing	37.6	82.8
Valve, fastners, and small parts	7.7	16.9
Scroll Total	116.0	255.7
Insulation	9.9	21.9
Total	125.9	277.6

4.7 FRAME

In addition to being the main fan structural component, the vane frame functions as the exit stator vane for the fan. The turbotip fan is a single-frame propulsion unit; thus, the frame must support both the rotor and the scroll, provide the propulsion mounting points, and collect all aerodynamic and mechanical loads.

4.7.1 Design Requirements

The frame was designed to meet all of the requirements established for propulsion in a research and technology aircraft. The specific requirements as translated into frame requirements are as follows:

- The frame shall be designed for 1200 hours of operation in the RTA duty cycle, which translates into 14,400 LCF cycles.

- The frame shall be designed to the specified maneuver loading criteria with adequate stiffness to maintain favorable seal clearances and stator roundness.

- The frame shall be capable of operating for at least 30 seconds under the vibratory loading developed due to the unbalance associated with a missing blade and carrier assembly.

- The first-flexural and first-torsional frequencies of the fan stator vanes shall not be intersected by the rotor blade passing frequency within the engine operating range.

4.7.2 Basic Design Features

The basic design features and construction of the frame are shown in Figures 78 and 79.

The frame is a welded fabrication consisting of an inner hub, outer casing, nine leaned structural struts, and 18 leaned fan stator vanes. The inner hub consists of nine cast segments incorporating the structural strut ends and welded into a 360° ring. Two forged rings form the outer flanges with sheet stock welded between the rings. Each structural strut is composed of two hollow castings welded together. The strut assemblies are then welded to the inner hub and outer rings.

Molded nylon liners, bolted to the inner hub, form the inner flow path. The outer fan flow path and the two turbine flow paths are formed by ribbed liners attached to the struts by a slip-fit key. This allows for a differential thermal growth between the liners and struts. Insulation is installed between the outer turbine liner and the outer case to minimize the effective heat transfer of the turbine exhaust gas to the outer case.

The outer rings are cooled by impingement-cooling tubes to maintain reasonable thermal stresses. The outer strut is impingement cooled to maintain the material within operating limits.

Three equally spaced mounting points are provided to attach the fan assembly to the aircraft structure. Adequate ribbing of the outer casing is provided to ensure reasonable distribution of the frame loads among the struts.

The nonstructural fan stator vanes are solid, forged-aluminum airfoils. The vanes are bolted to the inner hub and outer fan liner.

The listing of the materials used in fabrication of the major frame components is given in Table XVII.

Table XVII. Frame Materials.

Outer Ring	17-4 PH
Outer Strut	17-4 PH
Inner Ring	17-4 PH
Inner Strut	17-4 PH
Fan Stator Vane	7075 aluminum
Inner Fan Liner	Nylon
Outer Fan Liner	17-4 PH
Turbine Liners	17-4 PH
Fan Casing	INCO 706

4.7.3 Design Analysis

The design analysis of the frame structure was evaluated using a three-dimensional stress analysis. An existing computer program was used; wherein, the frame structure was represented by an array of beam and plate elements. A series of conditions, including maneuver, thermal, and aerodynamic loading, were imposed on the frame model. The maximum component stresses for the most critical cases are summarized in Table XVIII. The yield and fatigue limits of the frame materials are included in the tabulation. A comparison of calculated and allowable stress levels indicates that the frame has adequate strength to meet the most severe loading conditions.

The frame analytical model is also capable of determining the frame stiffness factors. These data are necessary for the evaluation of the system critical frequencies and deflections during maneuver loading and rotor unbalance. The three stiffness factors or spring constants as determined are listed in Table XIX. These factors are based on deflections of the frame inner hub relative to the mounting points. The application of these data in the vibration analysis of the complete fan system will be described in Section 4.8 of this report.

Vibratory frequency analyses were performed for the frame stator vanes and flow-splitter panels to ensure resonance-free operation. Figure 80 shows the frequency diagram for the exit stator vanes. Resonance-free operation is indicated by the lack of synchronism of the predominant frequencies with known sources of excitation. The two strongest excitations are the one per revolution associated with rotor unbalance and the 57 per revolution due to the blade passing frequency.

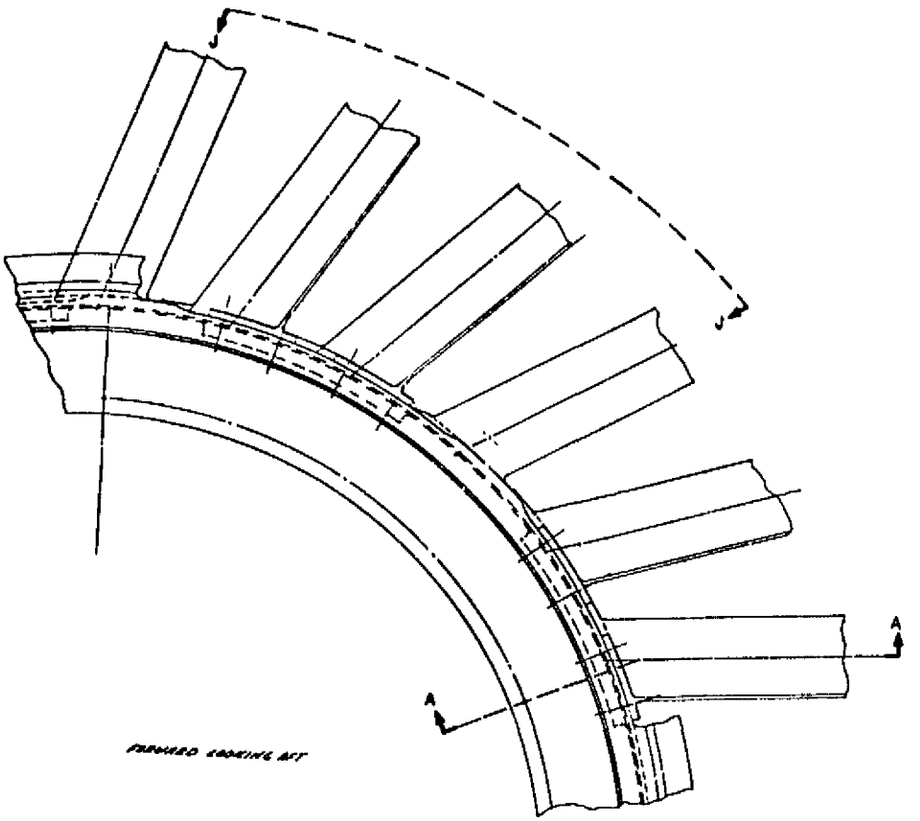

Figure 78. Frame Layout.

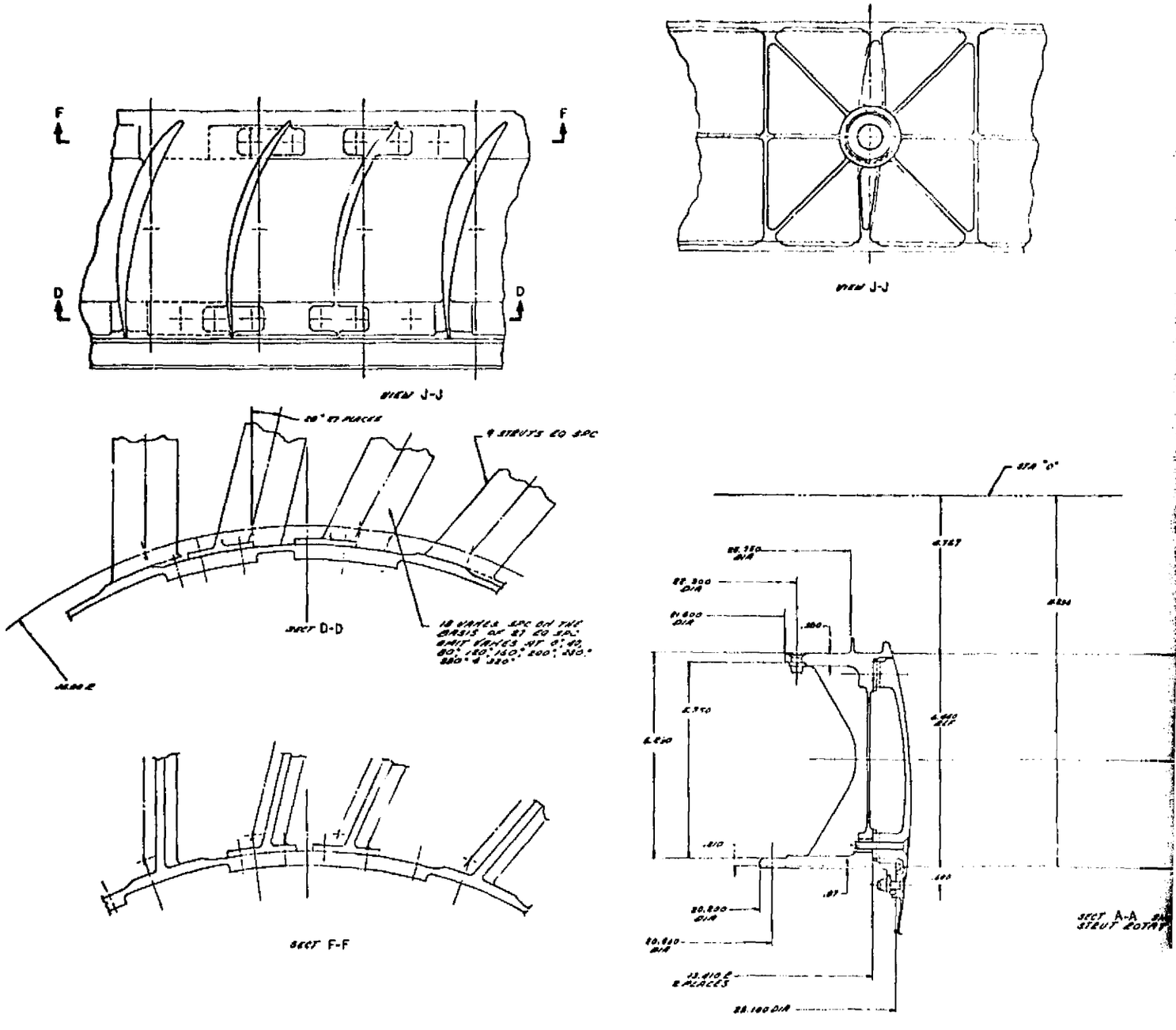

Figure 78. Frame Layout

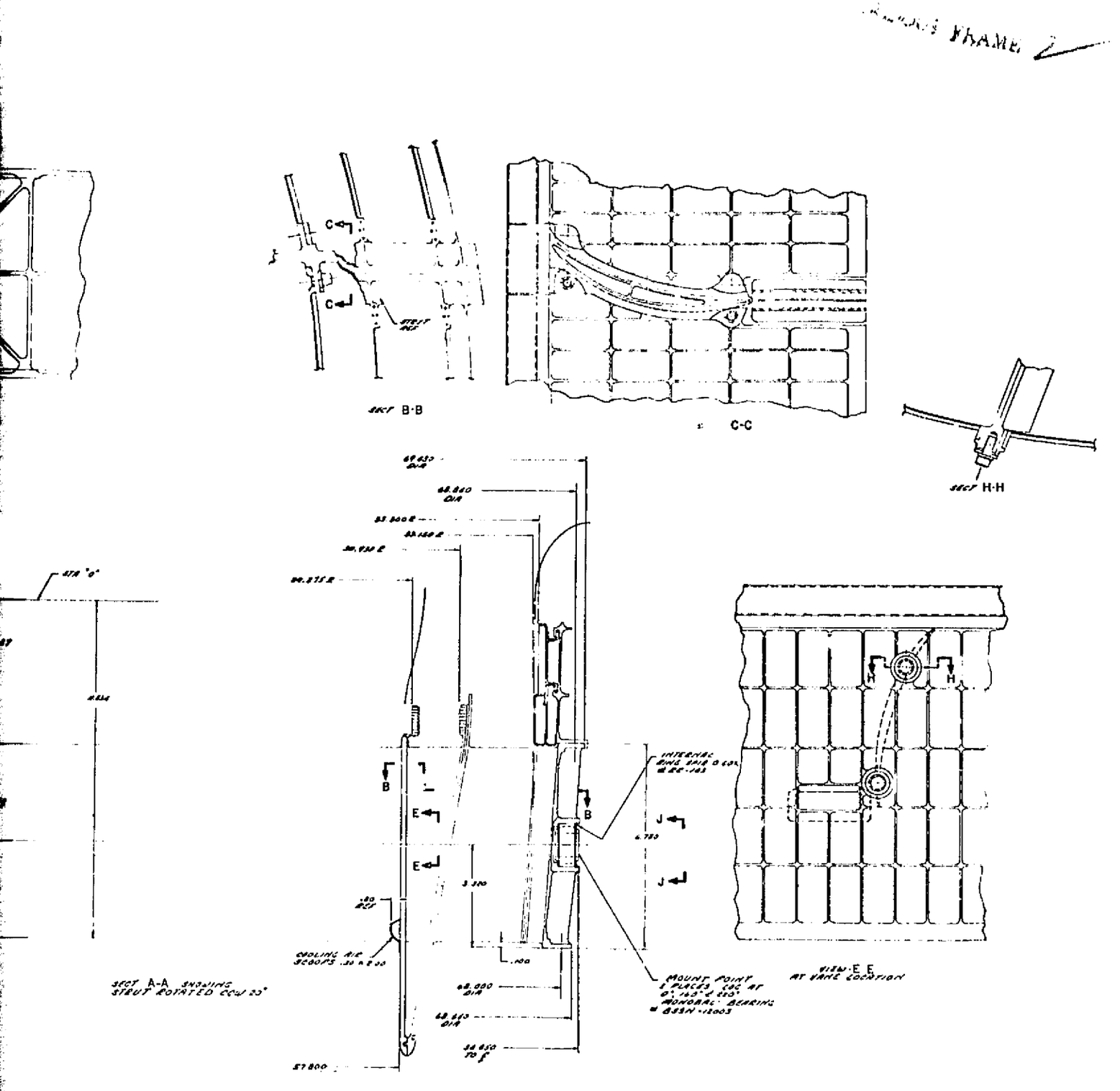

78. Frame Layout (Concluded).

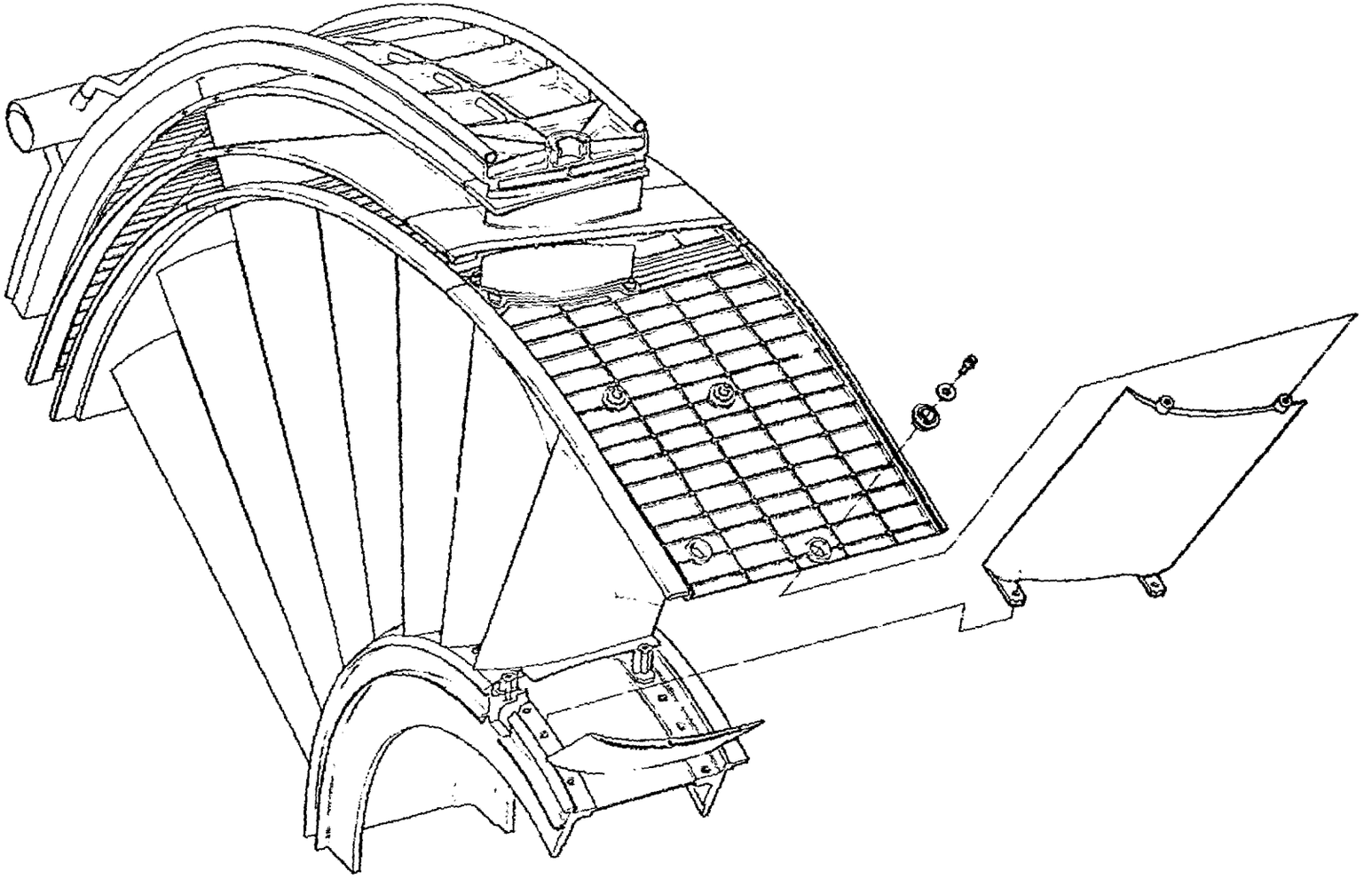

Figure 79. Frame Configuration.

Table XVIII. Rear Frame Stresses.

	I		II		III		IV		V		14,400 Cycle Limit		0.2% Yield Point	
	kN/m^2	(ksi)	kN/m^2	(ksi)	kN/m^2	(ksi)	kN/m^2	(ksi)	kN/m^2	(ksi)	kN/m^2	(ksi)	kN/m^2	(ksi)
Inner Ring	455070	66	310275	45	461960	67	248220	36	117210	17	827400	120	710185	103
Outer Ring	565390	82	592970	86	6250550	90	517120	75	317170	46	965300	140	655025	95
Inner Strut	655025	95	668810	97	696390	101	517129	75	330960	48	827400	120	710185	103
Outer Strut	455070	66	386120	56	455070	66	337850	49	220640	32	758450	110	620550	90

Case I - 2 rad/sec, Any Axis - 1-g Down - Max Thrust - Thermal Load

Case II - 1.4 rad/sec, Any Axis - 10-g Down - 2-g Side - 4-g Forward - Max Thrust - Thermal Load

Case III - 2 rad/sec, Pitch - 6-g Down - 4-g Side - 2-g Forward - Max Thrust - Thermal Load

Case IV - 10-g Down - 2-g Side - 4-g Forward - Max Thrust - Thermal Load

Case V - Thermal Load

Table XIX. Frame Spring Constants.

Radial	1.769×10^8 N/m (1.01×10^6 lbf/in.)
Overturning	5.853×10^6 N-m/rad (5.18×10^7 lbf-in./rad)
Axial	9.120×10^6 N/m (5.205×10^4 lbf/in.)

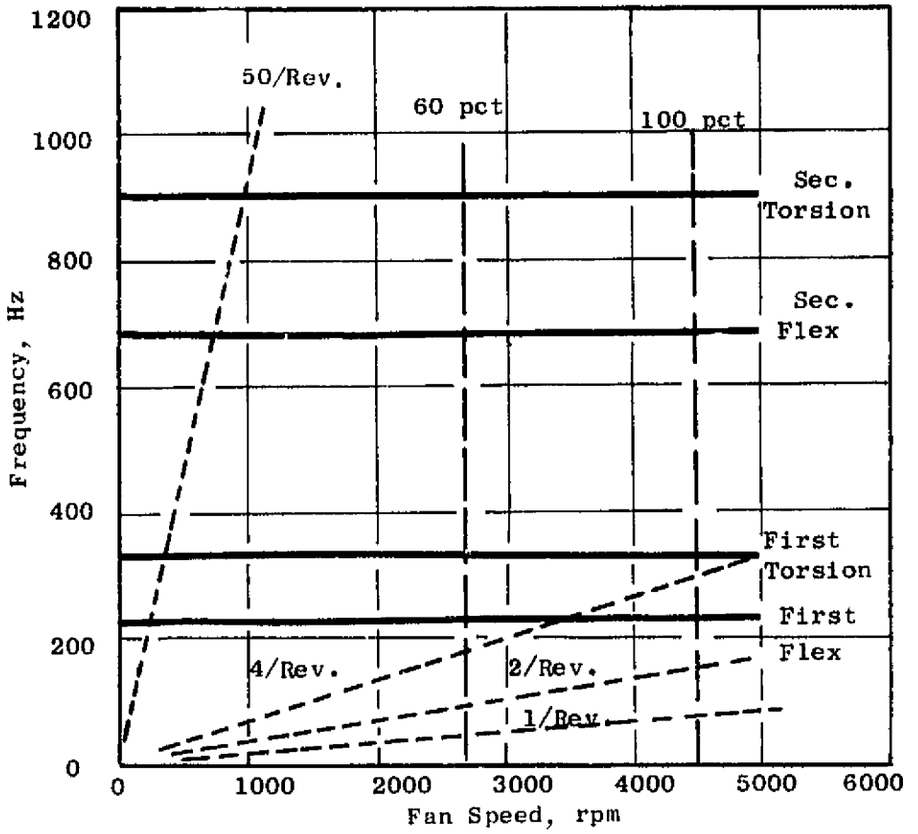

Figure 80. Fan Stator Vane Frequency Diagram.

Similar vibratory characteristics for the flow-splitter panels are shown in Figure 81 and are also indicative of resonance-free operation.

4.7.4 Weight

The weight of the total frame assembly including the cooling system manifolds was calculated at 122 kg (270 lbm). Table XX gives a detailed breakdown of the individual component weights.

Table XX. Frame Weights.

	kg	lbm
Frame Structure	68.5	151
Cooling System	5.4	12
Flow-path Liners	16.8	37
Fan Stator Vanes	14.5	32
Fan Casing	12.7	28
Turbine Seal	4.5	10
	122.4	270

4.8 VIBRATION ANALYSIS

A vibratory analysis of the complete engine system is required to ensure a smooth-running, resonance-free configuration. Such an analysis was performed as part of the LCF459 design studies. The analysis techniques used not only predict system resonant conditions, but are also used to determine system response to maneuver loading and forces due to rotating component unbalance.

A similar analysis was conducted for the YJ97 engine as part of the studies. The results of this analysis will be presented in Section 5.4 of this report.

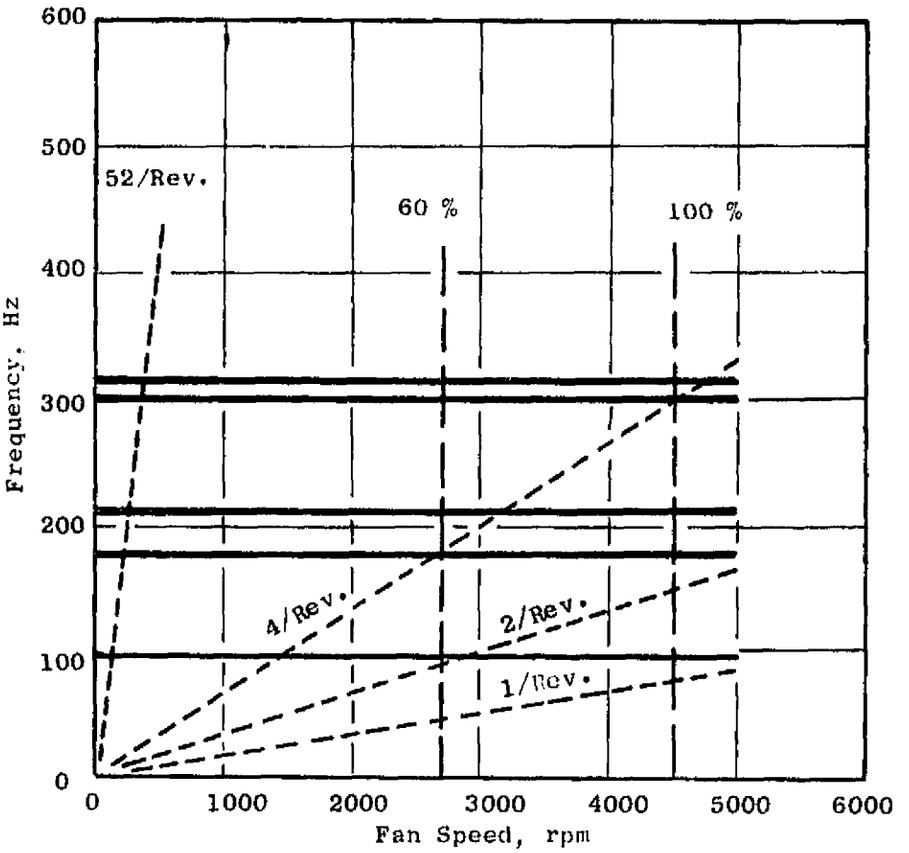

Figure 81. Flow-Path Liner Frequency Diagram.

4.8.1 Analysis Method

The fan system was analyzed using an existing General Electric computer program called VAST (Vibration Analysis System) which is used to calculate system critical speeds and vibratory response for known unbalances. The VAST program has been in use at General Electric for a number of years and has consistently demonstrated the capability of accurately predicting engine critical speeds and responses for many types of engines and test vehicles. A mathematical model of the engine system is constructed which includes all rotor components plus all static components supported from the fan frame. The modeling procedure establishes the geometric and physical properties of the various components as a series of lumped or point masses connected by flexible beam, cone, and spring elements. For more complex structures, such as a fan frame or a bearing, special finite-element models must be constructed or tests of actual hardware be performed to determine the deflection characteristics. In summary, the basic assumptions made in a VAST analysis are as follows:

- The structure is axisymmetric, and all deflections and vibration modes will be based on beam-type behavior. No shell modes are considered.
- Linear elastic behavior of materials for all elements modeled as beams or cones.
- Elements modeled as beams follow classical beam small-deflection theory in bending; shear deformation in beams is also considered.
- All spring-type elements exhibit linear load-deflection characteristics.
- Rotors exhibit gyroscopic stiffening due to whirling.
- Damping coefficients are assumed to be constant. The structural damping factor is not considered to be a function of velocity.
- Mass properties are considered as lumped at discrete points and are interconnected by weightless, generalized, elastic or spring elements.
- A VAST analysis is an extension of the Prohl-Myklestad method of calculating the critical speeds of flexible rotors represented by beams.
- The effects of flexible supports, multiple branches, and energy distribution scheme are also considered.

Critical speeds are calculated assuming an undamped system; however, estimated actual vibratory deflections and loads can be calculated by including damping coefficients for the various components along with possible fan unbalance.

4.8.2 Vibration Model

The basic model of the LCF459 configuration is shown schematically in Figure 82. In this model, the fan frame structure is represented by a lumped spring constant. Table XIX gives the spring constants determined during the analysis of the frame structure. The two fan bearings were also modeled as lumped spring constants. The remainder of the fan system was modeled by a series of flexible cones and lumped masses. The analysis indicated critical frequencies at 5897 and 7701 revolutions per minute, both of which are well above the normal operating speed of the system. Table XXI gives a summary of critical frequencies, modal descriptions, and maximum deflections locations which were determined for the fan system. In addition, the maximum system response is given for an unbalance of 25 g-cm (10 g-in.) at selected rotor planes. Computer-generated plots of the system schematic with superimposed modal deflection patterns are shown in Figures 83 and 84. Also shown on these diagrams is a percentage distribution of kinetic and potential energies. This graphic output assists in identifying deflection patterns, and the energy distribution shows which parts are bending (high potential energy) and which parts are subject to highest g-loads (high kinetic energy). The maximum deflection point of the modal patterns corresponds to the maximum value listed in Table XXI.

Maneuver forces and moments were also determined for the fan system. The values are shown in Figures 85 through 87 for 1-g, 1-rad/sec, and 1-rad/sec^2 maneuver cases. The forces and moments for larger maneuver cases can be scaled directly from the figures. For example, a 10-g maneuver case would have a shear force of 29.89 kN (6720 lbf) in the front bearing, as compared to a 2.99 kN (672 lbf) force for a 1-g maneuver case.

The forces and moments as established by this analysis provided the inputs for the load analysis of the fan component, particularly the fan frame structure.

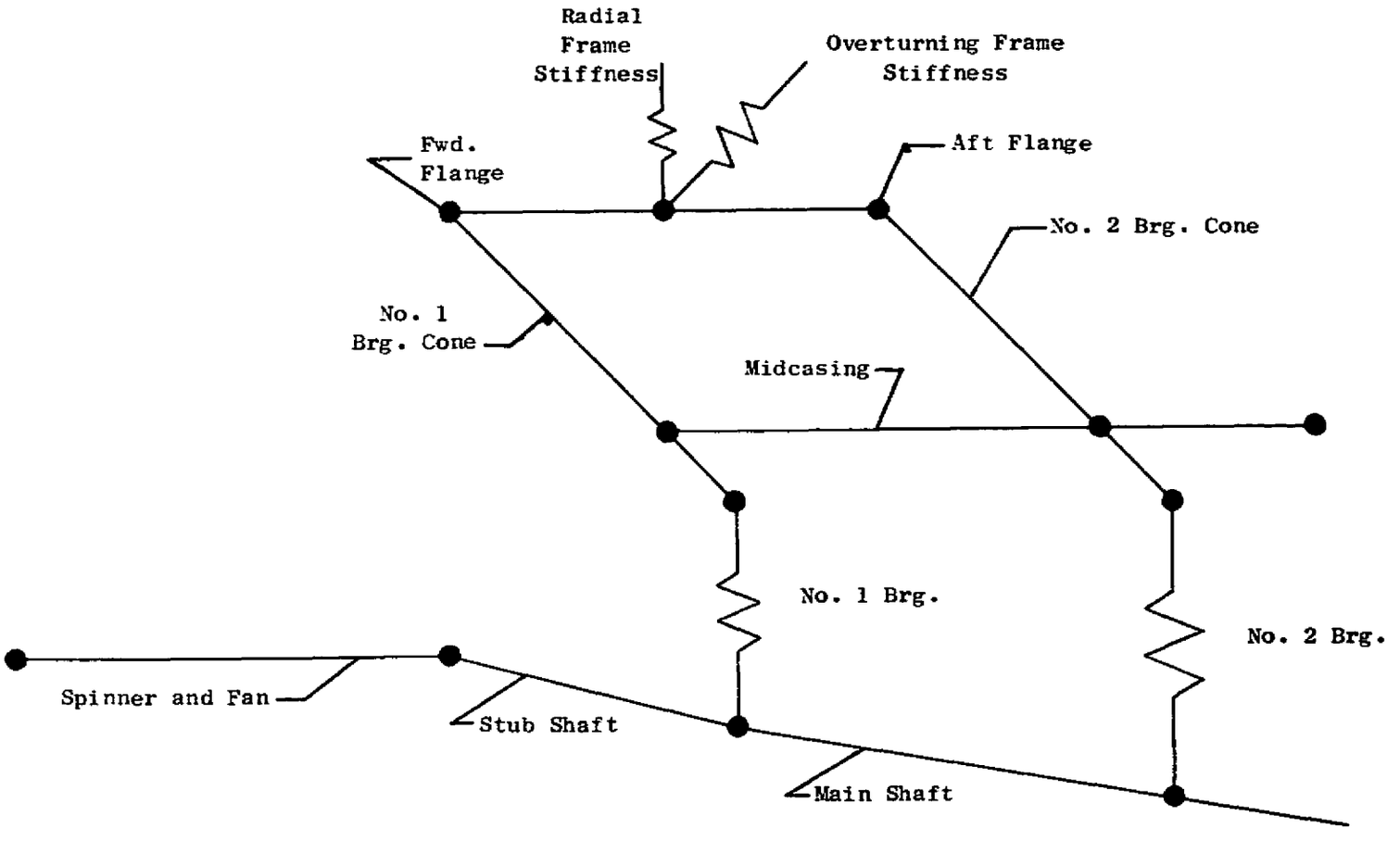

Figure 82. Fan Vibration Analysis Model.

Table XXI. Lift Cruise Fan Critical Frequency Summary.

Crit. No.	Speed (rpm)	Mode Description	Max. Deflection Location	Max Unbal. Resp. cm	in.	Location*
1	5897	System bouncing off the fan frame, rotation about the fan frame. The roller bearing is also active.	Front End of the Spinner	0.0020 0.0013	0.0008 0.0005	1-2 2-2
2	7701	System rotating about the fan frame slight bending of the stub shaft and both bearings are lightly active.	Front End of the Spinner	0.0028 0.0008	0.0011 0.0003	1-2 2-2

*Unbalance Locations

1-2 25.4 g-cm (10 g-in) at the Fan Centerline

2-2 25.4 g-cm (10 g-in) at the Middle of the Main Shaft

Approximate Engine Speeds

	rpm
Cruise	2400
Maximum	4370

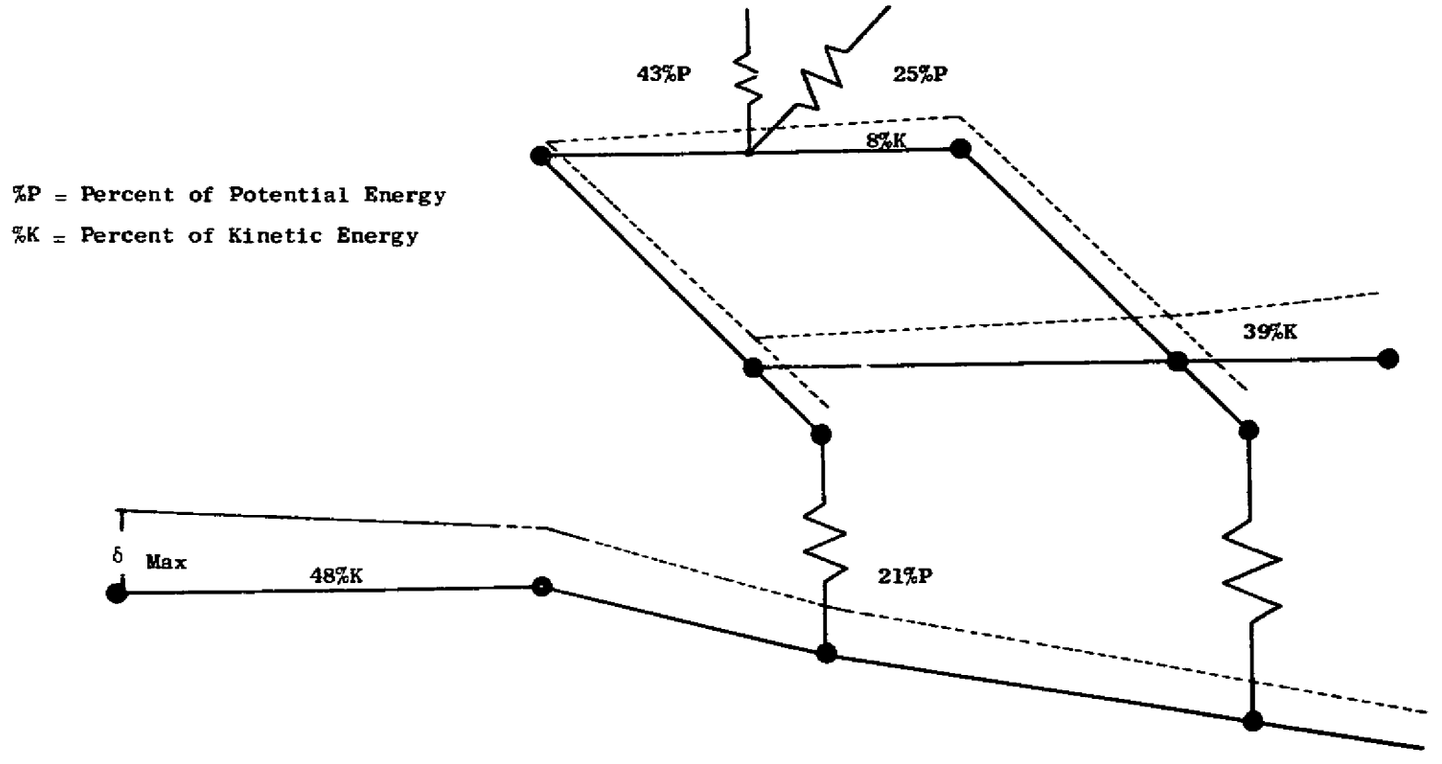

Figure 83. System Critical Modal Deflection Pattern - 5897 rpm.

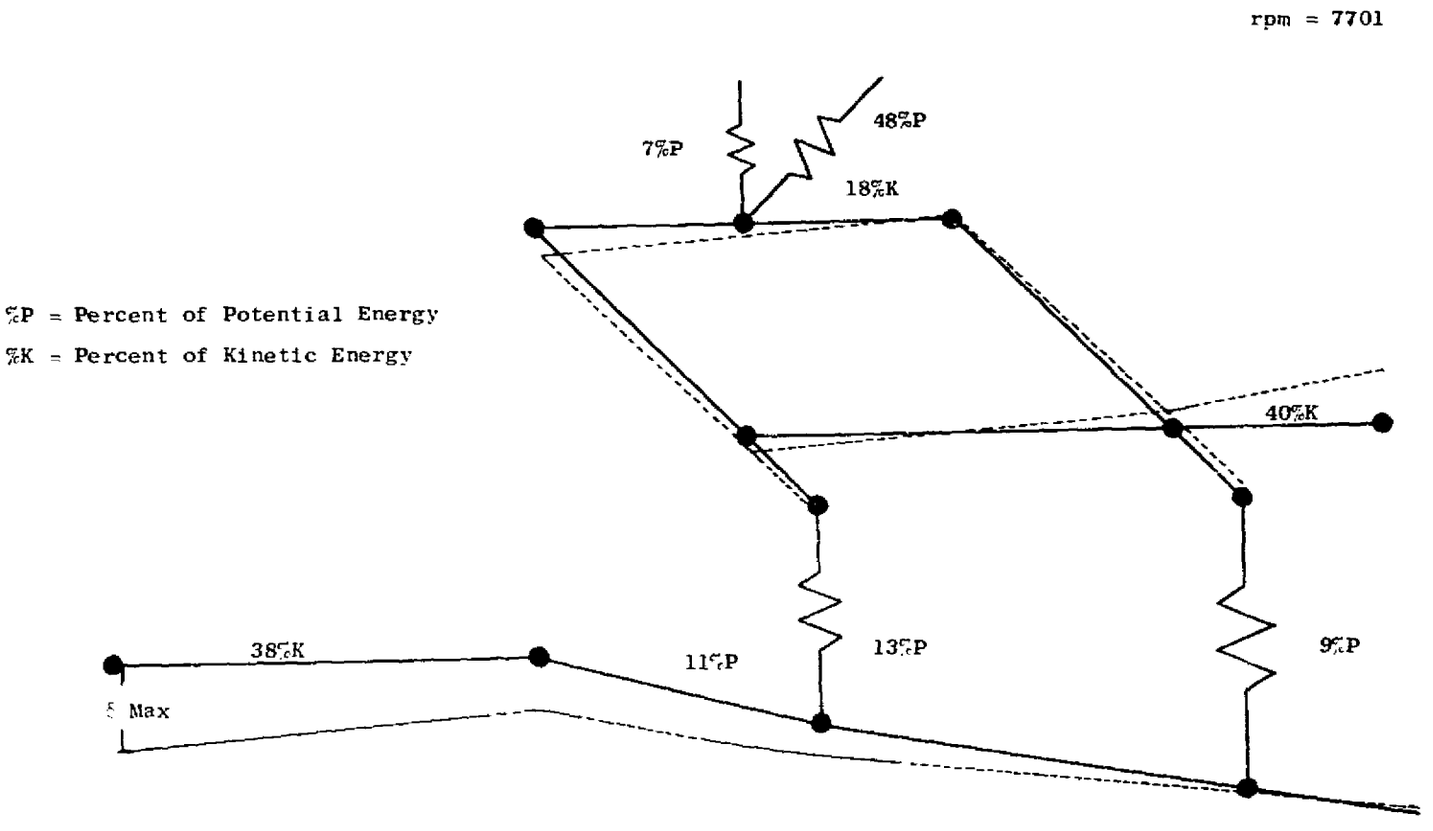

Figure 84. System Critical Modal Deflection Pattern - 7701 rpm.

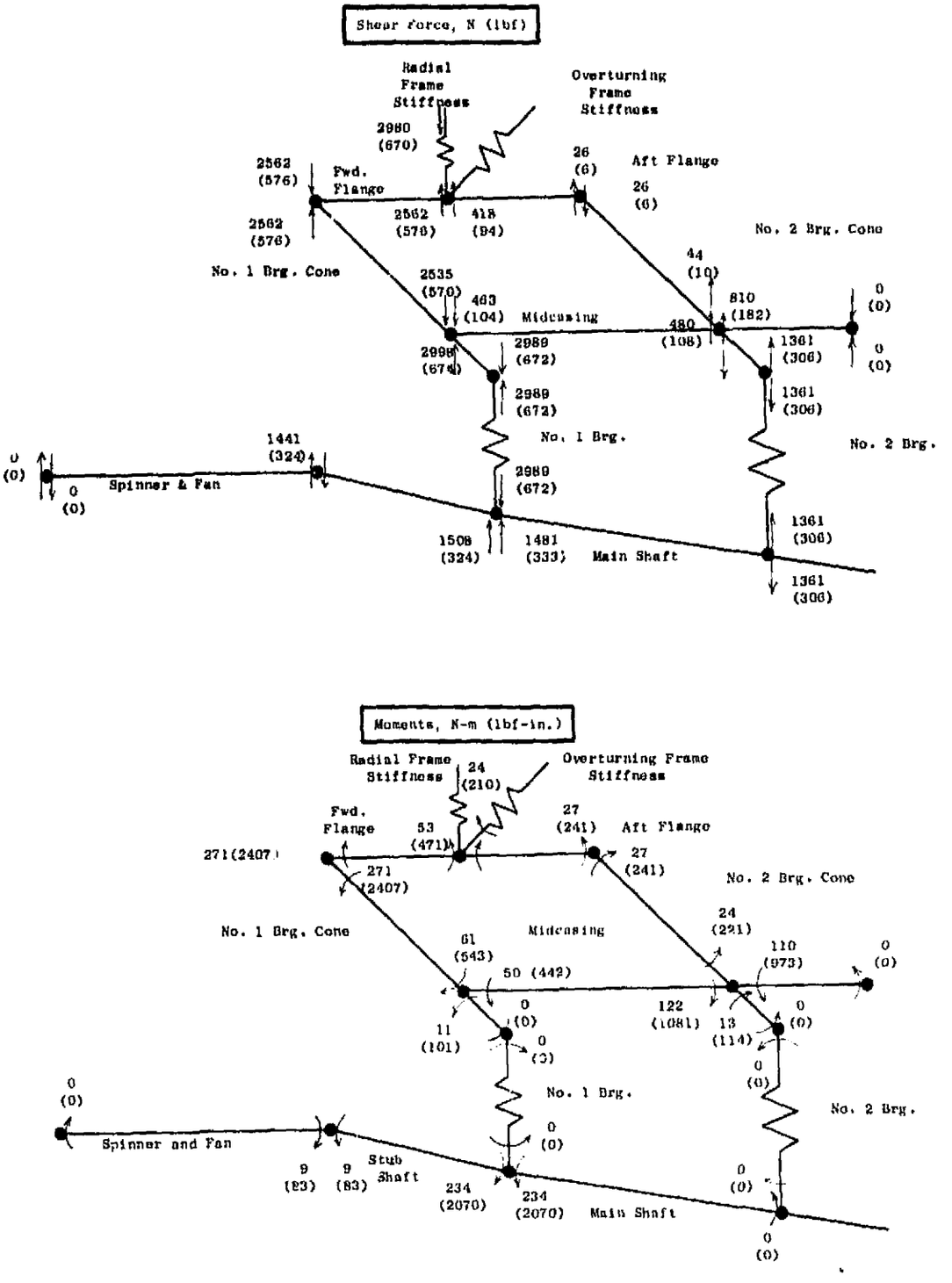

Figure 85. Shear and Moments - 1-g Down Maneuver.

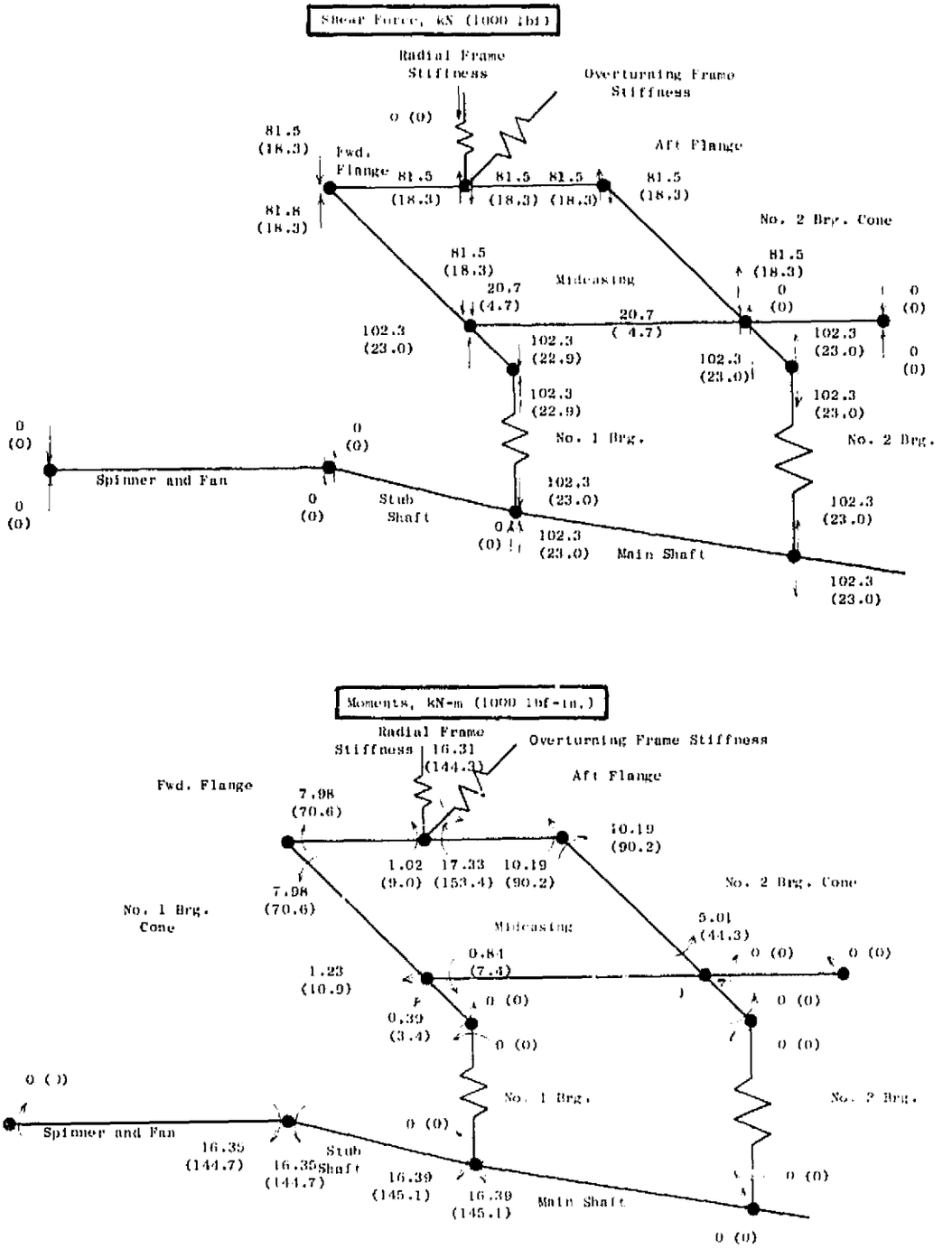

Figure 86. Shear and Moments - 1-Radian-per-Second Maneuver.

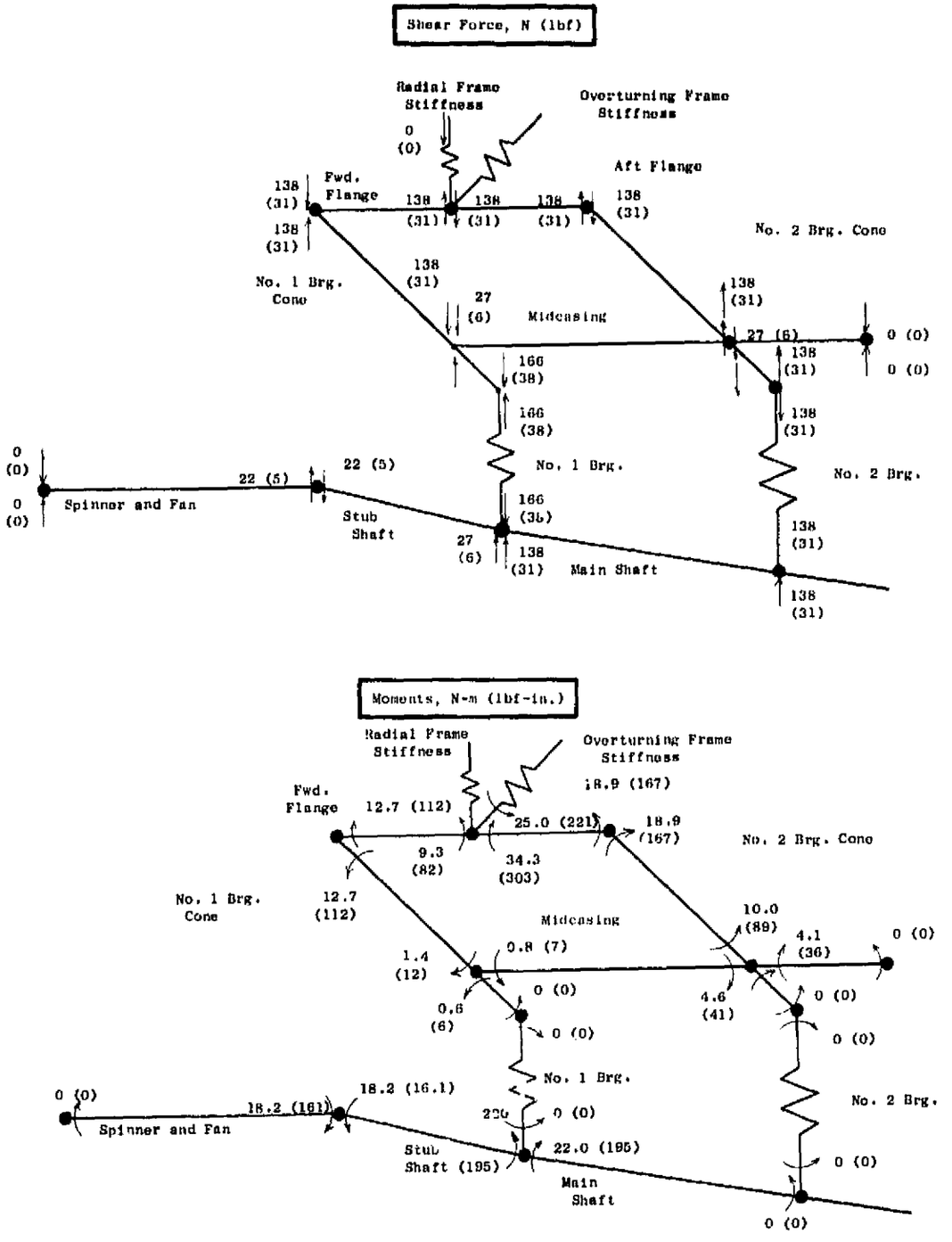

Figure 87. Shear and Moments - 1-Radian-per-Second-Squared Maneuver.

5.0 YJ97 ENGINE

The engine selected to power the turbotip fans in the Research and Technology Aircraft is the YJ97-GE-100. This engine was selected based on availability, low cost for refurbishment, and good match of engine size. The YJ97-GE-100 engine had completed a 60-hour preflight rating test (PFRT) in 1970, Reference 8. Production of this engine was never initiated. A different model, the YJ97-GE-3, was put into limited production. There are presently 22 of these engines available. Based on the engine records, 18 of these are serviceable, low-time engines. The modifications required for conversion from the -3 to the -100 model, which are minor, will be discussed in detail in this section of the report.

5.1 BASIC FEATURES

The J97 engine is a conventional turbojet engine with a single-spool compressor and two-stage turbine. The compressor develops an overall pressure ratio of 14 to 1. The compressor has 14 stages with variable inlet guide vanes and variable stators of stages 1 through 5. Compressor flow is 31.4 kg/sec (69.2 lbm/sec). The turbine contains two stages, one cooled and the second uncooled. The engine turbine inlet temperature is in the 1388 K (2500° R) class. Table XXII lists the significant engine performance parameters at two levels of engine power setting. This rating is consistent with those used for conventional engine systems; a discussion of the special V/STOL ratings will be presented in Section 7.3. A photograph of the engine is shown in Figure 88.

Table XXII. YJ97-GE-100 Engine Performance.

(Sea Level Static, Standard Day)

Rating	Military	Normal
Compressor Speed, percent	101.5	99.6
Compressor Speed, rpm	13,855	13,589
Inlet Airflow, kg/sec (lbm/sec)	31.39 (69.20)	30.98 (68.30)
Compressor Pressure Ratio	14.07	13.68
Turbine Inlet Temperature, K (° R)	1382 (2487)	1343 (2417)
Exhaust gas pressure, kN/m^2 (lbf/in^2)	365.2 (52.97)	354.7 (51.44)
Exhaust gas temperature, K (° R)	1019 (1835)	989 (1780)
Exhaust gas flow, kg/sec (lbm/sec)	32.00 (70.54)	31.55 (69.56)
Thrust* kN (lbf)	23.44 (5270)	22.69 (5100)
Fuel Flow, kg/hr (lbm/hr)	2187 (4822)	2082 (4590)

*With convergent nozzle

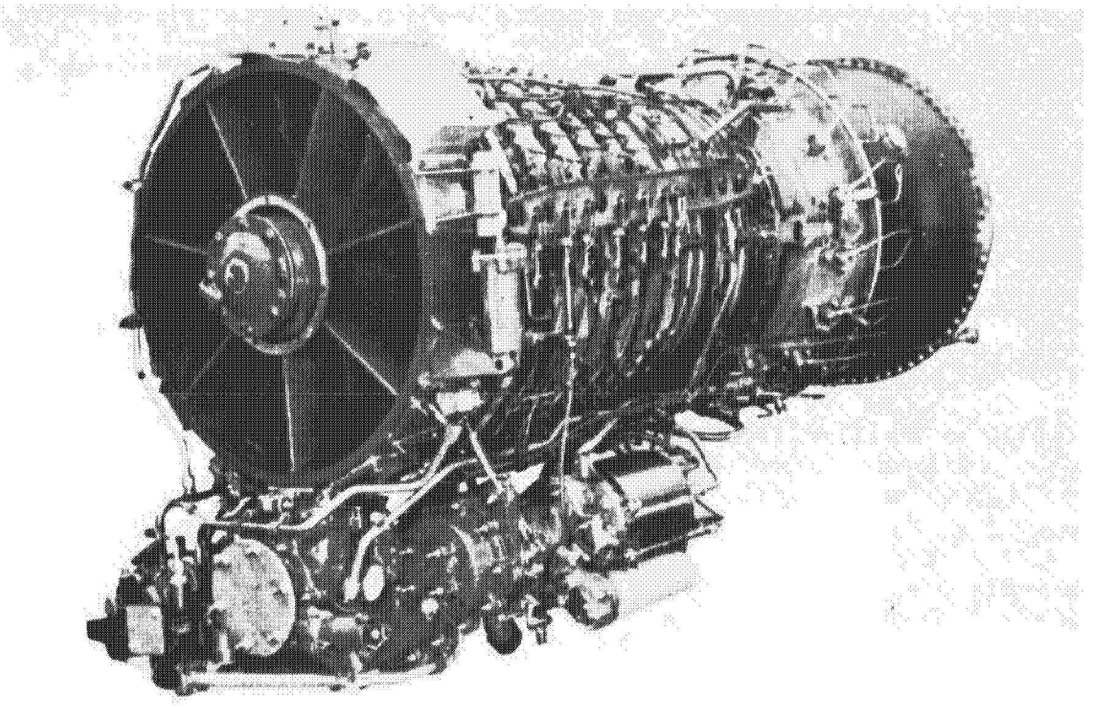

Figure 88. YJ97-GE-100 Engine.

5.2 ENGINE AVAILABILITY

At the present time, 22 YJ97-GE-100 engines are being stored in the General Electric Facilities at the Edwards Flight Test Center for possible use in the NASA/Navy Research and Technology Aircraft program. The records provided with the engines have been reviewed to determine the serviceability of each engine. Based on this survey, 18 engines are definitely serviceable, two are unserviceable, and two have records which do not adequately define the status. Table XXIII gives a listing of the engines by serial number, the total engine operating time, and time since last overhaul. The records show that most of the engines have low operating times, less than 25 hours.

The engines presently are in the -3 configuration and must be modified to the -100 configuration for operation at sea level conditions. The changes and modifications have been made on several engines prior to this time. The engine used for the PFRT was a -3 engine converted to a -100; in addition, two serviceable engines exist in the -100 configuration. These engines were used in the McDonnell/NASA energy-transfer-control tests as summarized in References 7 and 8. The engines presently are in the custody of NASA Ames Research Center. These two engines have high operating times and are not planned for use in the research aircraft program.

With at least 18 low time, serviceable engines, adequate numbers of engines are available for a research program. A two-aircraft program, with three engines per aircraft, would require about 11 to 13 engines. This number of engines is required to provide adequate spares to support the aircraft program and to provide engines for the 500 to 700 hours of development testing required to bring a new propulsion component, such as the turbotip fan, up to flight status.

5.3 MODIFICATIONS

The modifications for conversion of the available -3 engines to the -100 configuration are minor. During some early studies using the YJ97 engine, water injection was considered as a method for thrust augmentation during V/STOL operation, primarily for the one-engine-inoperative case. Modification of the engine for water injection would be costly and is not a simple task. Recently, the use of water injection for the RTA has been abandoned. Three engines without water injection, even with one engine inoperative, appear to provide adequate power for the research application.

The modifications required for this engine conversion, excluding water injection, are as follows:

- The present -3 engine fuel control is not designed for high power setting operation at sea level. The fuel system capacity is inadequate. Internal fuel control orifice size changes are required.

Table XXIII. YJ97 Engine Record Summary.

S/N	Estimated Engine Condition	Total Time, hours	Time Since Overhaul, hours	Remarks
447-052	Serviceable	64.55	8.05	
447-053	Unserviceable	58.82	34.39	Involved in crash, condition unknown.
447-059	Unknown	Unknown	Unknown	Serial number on records do not agree with container serial number.
447-060	Serviceable	47.1	53.3	
447-061	Serviceable	46.1	46.1	
447-062	Unserviceable	24.6	24.6	Involved in crash, requires major repair.
447-063	Serviceable	16.5	16.5	
447-064	Serviceable	16.7	0	
447-065	Serviceable	16.4	0	
447-066	Serviceable	19.5	19.5	
447-067	Serviceable	14.1	14.1	
447-068	Serviceable	15.4	0	
447-070	Questionable	50.1	1.4	Involved in crash, repaired but has had problems.
447-071	Serviceable	36.7	4.1	
447-073	Serviceable	54.5	54.5	
447-074	Serviceable	32.1	32.1	
447-075	Serviceable	50.4	50.4	
447-079	Serviceable	17.1	17.1	
447-080	Serviceable	21.3	21.3	
447-081	Serviceable	23.4	23.4	
447-082	Serviceable	1.4	1.4	Early engine records apparently lost.
447-083	Serviceable	14.14	14.14	

- The -3 engine incorporates an exhaust temperature cutback; the output from the exhaust gas temperature harness is fed into an amplifier which, in turn, commands a flow cutback in the fuel control. Part of the fuel control changes involves deactivation of this function. External engine modifications include removal of the amplifier mounted on the engine front frame.

- To provide a better rotor thrust balance at sea level operation, the seal pressurization air bleed must be changed from the 14th to the 8th stage of the compressor. The compressor cases incorporate a pad with this bleed capability at the 8th stage. The engine modifications require replacement of an external bleed pipe and blank-off of the existing bleed ports.

- The engine presently has a single, vertical mount point at the top of the front frame. A stronger, forward mount arrangement is desirable for applications where large maneuver loads are anticipated. A different forward mount arrangement has been designed and will be incorporated during the engine modifications. The single forward mount will be replaced with two mount points spaced 26 degrees from top center of the engine. The mount loads are transmitted to two points on the frame which are in line with two of the seven front frame struts.

The above modifications can be made without engine disassembly. Incorporation of the fuel control changes and seal pressurization are the only two changes required to provide -100 engines for static testing. Two other engine modifications which require disassembly are required to achieve a flight static configuration.

- A number 2 ball bearing with higher load capacity is required for increased engine life. The replacement bearing has been designed and can be procured for these engine modifications.

- The number 1 bearing carbon seals must be changed to provide increased clearance around the oil jet.

The above modifications are minor, and the YJ97-GE-3 engine has operated well in its application without these changes. Operation during the development of the -100 configuration through the PFRT program has been equally successful. The YJ97-GE-100 engine can be expected to perform equally well in the research aircraft application. These engines will also be used as the gas supplier during the 500 to 700 hours of fan development testing, terminating in a flight-worthiness test as a complete propulsion system, including both fans and engines. The background and operating experience generated during these tests will further verify the operational capabilities of the engine.

Some other engine configuration items that should be considered for the RTA application include:

- The engine does not have an integral oil tank. An aircraft-furnished component is required.

- Ignition excitation is not included with the engine.

- The struts and inlet guide vanes of the front frame do not contain anti-icing provisions. Modification for anti-icing is a large design change. For a research application, operation without an anti-icing capability should be acceptable.

5.4 VIBRATION ANALYSIS

As part of these design studies, a vibration analysis of the YJ97 was performed. The purpose of this analysis was to evaluate potential engine-system, resonant-condition characteristics of the application with a turbofan and to provide a basis for the establishment of rotor tip clearances during engine refurbishment. The original YJ97-GE-3 application did not subject the engine to large maneuver loads; thus, very close clearances were used to achieve peak performance. Wider clearances will probably be required for the RTA application. The following discussion describes this vibration analysis study and presents results of the resonant-frequency search, deflection during maneuver loads, and relative compressor clearance changes.

The J97 engine is supported at two points by mounts located at the forward and aft frames. The front frame is a seven-strut, aluminum frame which supports the number one and two bearings. The rear frame is a six-strut, cast, Inconel 718 frame; it supports the number 3 bearing. A two-dimensional computer model composed of curved and straight beams was used to determine spring constants of the two frames. Table XXIV lists the spring constants as determined by this analysis. The analytical techniques used for the J97 engine dynamics were the same as those used for the fan analysis.

Table XXIV. Engine Spring Constants.

Front Frame	
Radial:	1.91×10^6 N/m (1.09×10^5 lbf/in.)
Overturning:	2.26×10^5 N-m/rad (2.0×10^5 lbf-in./rad)
Rear Frame	
Radial:	4.9×10^6 N/m (2.8×10^5 lbf/in.)
Overturning:	6.33×10^6 N-m/rad (5.6×10^6 lbf-in./rad

The vibration model, including component descriptions, is shown in Figure 89. Table XXV gives a summary of critical frequencies, modal descriptions, and maximum deflection locations determined for the engine system. Response sensitivities to unbalance at selected rotor planes are also shown. Computer-generated plots of the system schematic with superimposed modal deflection patterns are shown in Figure 90. Also shown on these diagrams is a percentage distribution of kinetic and potential energies.

This graphic output assists in identifying deflection patterns. The energy distributions show which parts are subjected to bending (high potential energy) and which parts are subject to the highest g-loads (high kinetic energy). The maximum deflection point of the modal patterns corresponds to the maximum value listed in Table XXV. Since no rotor-dominated modes exist near the operating range of the engine, vibration levels for normal operation should be low.

Response of the engine system to maneuver condition was also determined. Figures 91 through 93 present shear force and moment diagrams for maneuvers of 1-g acceleration, 1-radian-per-second precession, and 1-radian-per-second-squared angular acceleration. These forces and moments, translated into change of rotor clearance, are given in Table XXVI. For a set of design maneuvers, these data can be used to establish the compressor and turbine buildup clearances.

Based on the results of this initial study, the YJ97 will experience low vibration levels and should maintain structural integrity during normal aircraft maneuvers.

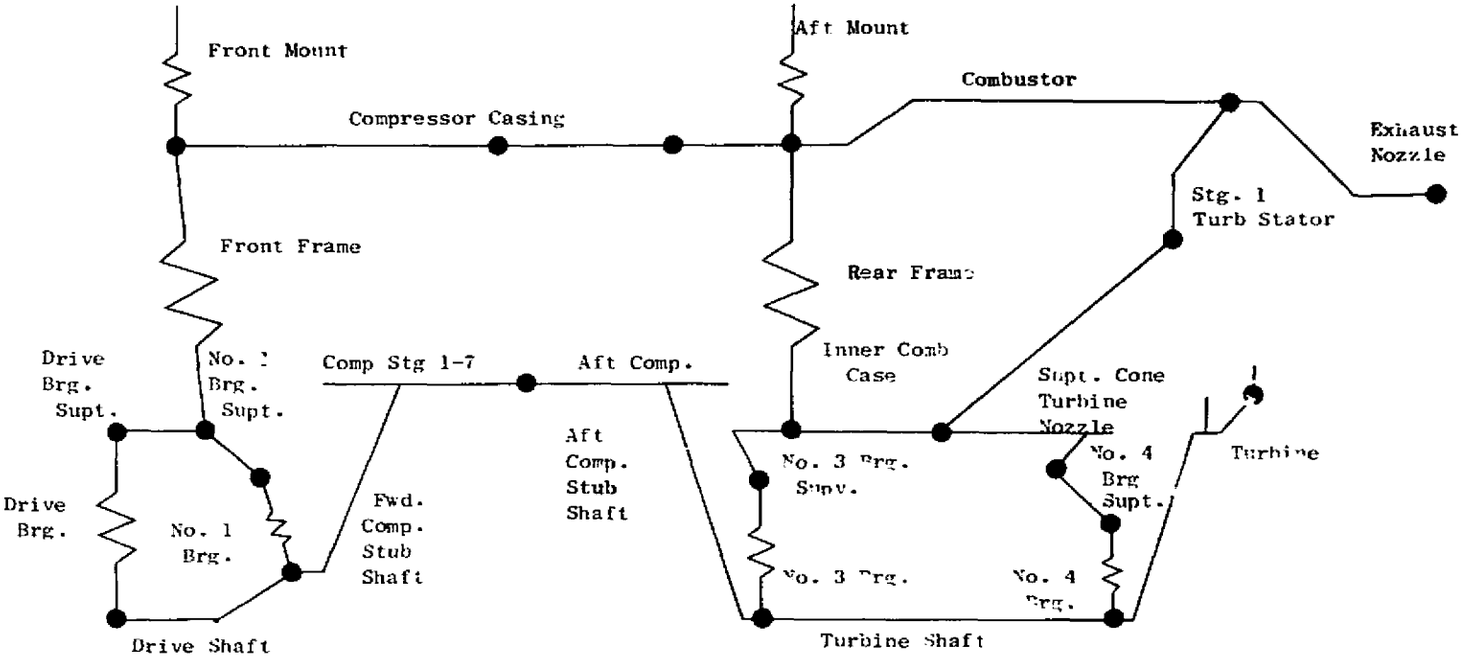

Figure 89. YJ97 Vibration Model Schematic.

Table XXV. J97 Critical Frequency Summary.

Crit.	Speed	Mode Description	Max. Deflection Location	Max Unbal. Resp.		
				cm	in.	Location
1	1,745	Aft Mount Mode and Exhaust Nozzle	Aft End of Exhaust Nozzle	0.0069	0.0023	5-5
2	2,940	Front Frame and Drive Shaft	Front End of Drive Shaft	0.0076	0.0030	1-5
3	3,541	Front Mount Mode	Front End of Drive Shaft	0.0041	0.0016	1-5
4	8,092	Exhaust Nozzle, Turbine, and Lightly Active No. 4 Bearing	Aft End of Exhaust Nozzle	0.0137	0.0054	5-5
5	9,191	Exhaust Nozzle and Active Frames	Aft End of Exhaust Nozzle	0.0066	0.0026	3-5
6	10,076	Exhaust Nozzle, Front Frame, and Bending of the Turbine Casing	Aft End of Exhaust Nozzle	0.0116	0.0046	1-5
7	13,927	Exhaust Nozzle and Rear Frame	Aft End of Exhaust Nozzle	0.0124	0.0049	3-5
8	19,128	Exhaust Nozzle, Outer Casings, and Rear Frame	Aft End of Exhaust Nozzle	0.0056	0.0022	3-5

* Unbalance Locations — 25.4 g-cm (10 g-in.) at the:

1-5 Stage 1 Compressor
2-5 Stage 7 Compressor
3-5 Stage 14 Compressor
4-5 Middle of the Turbine Shaft
5-5 Stage 2 Turbine

Approximate Engine Speeds

	rpm
Idle (60%)	8,400
Maximum	14,000

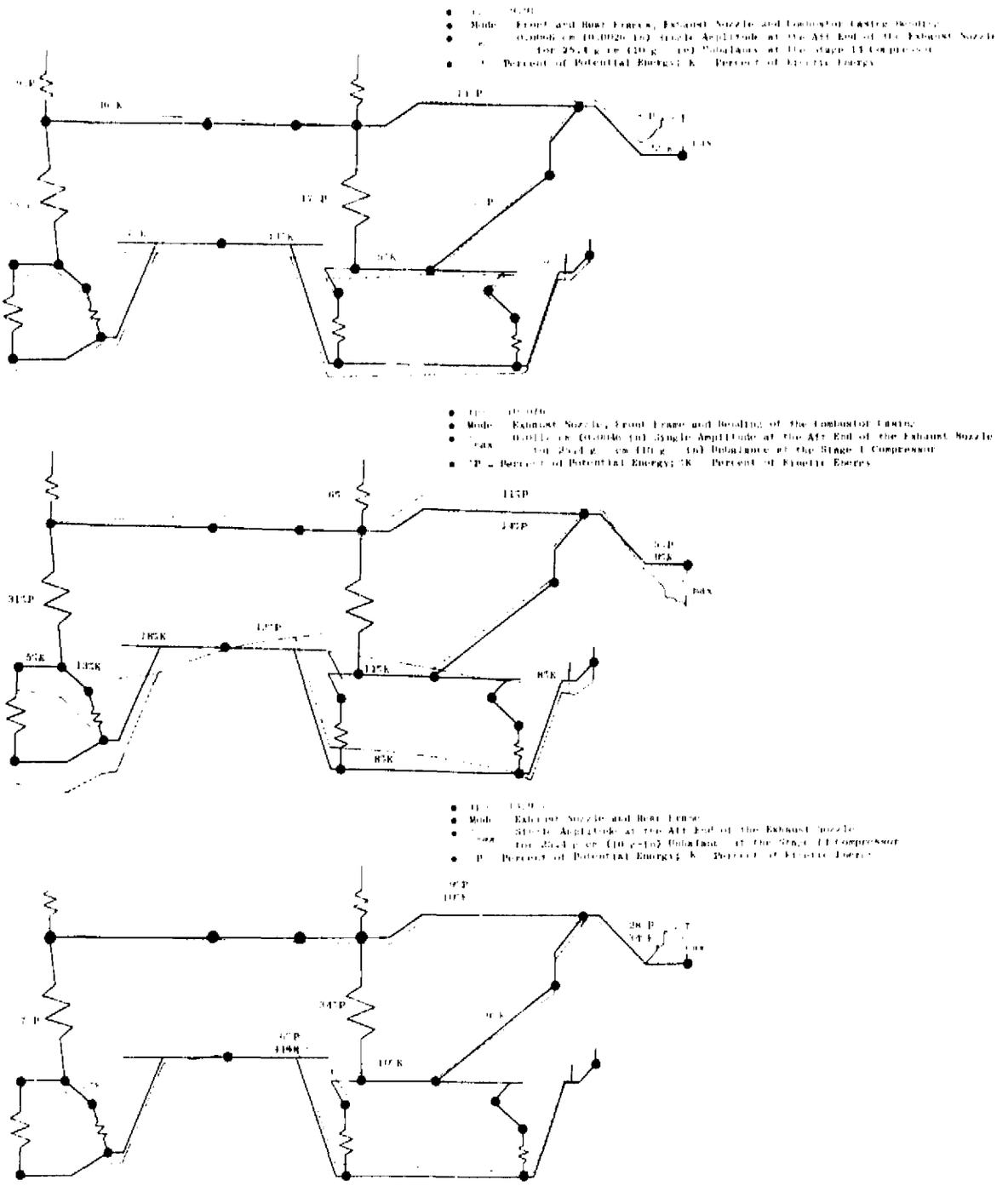

Figure 90. YJ97 Engine Criticals.

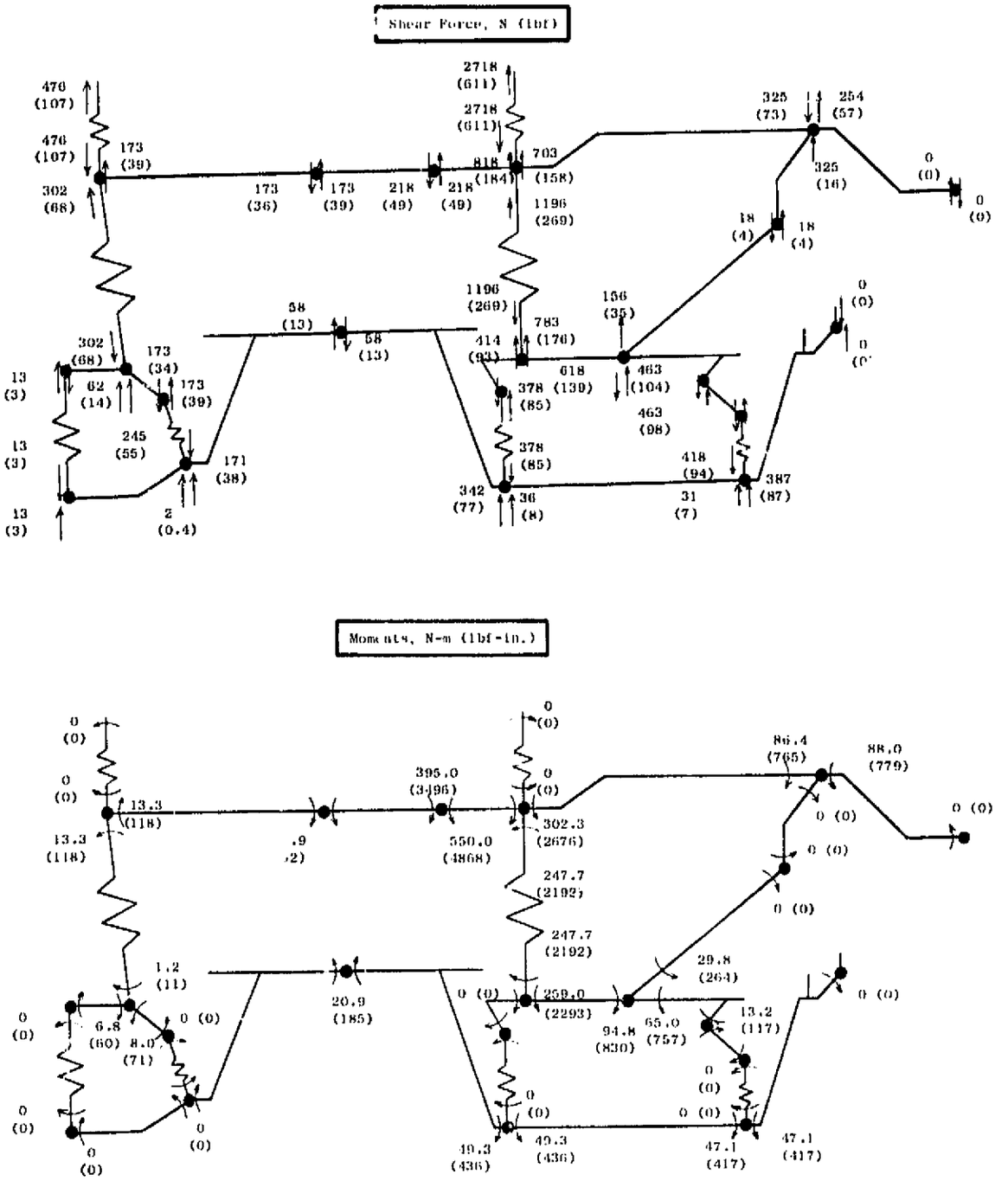

Figure 91. Engine System Maneuver; Vertical Acceleration.

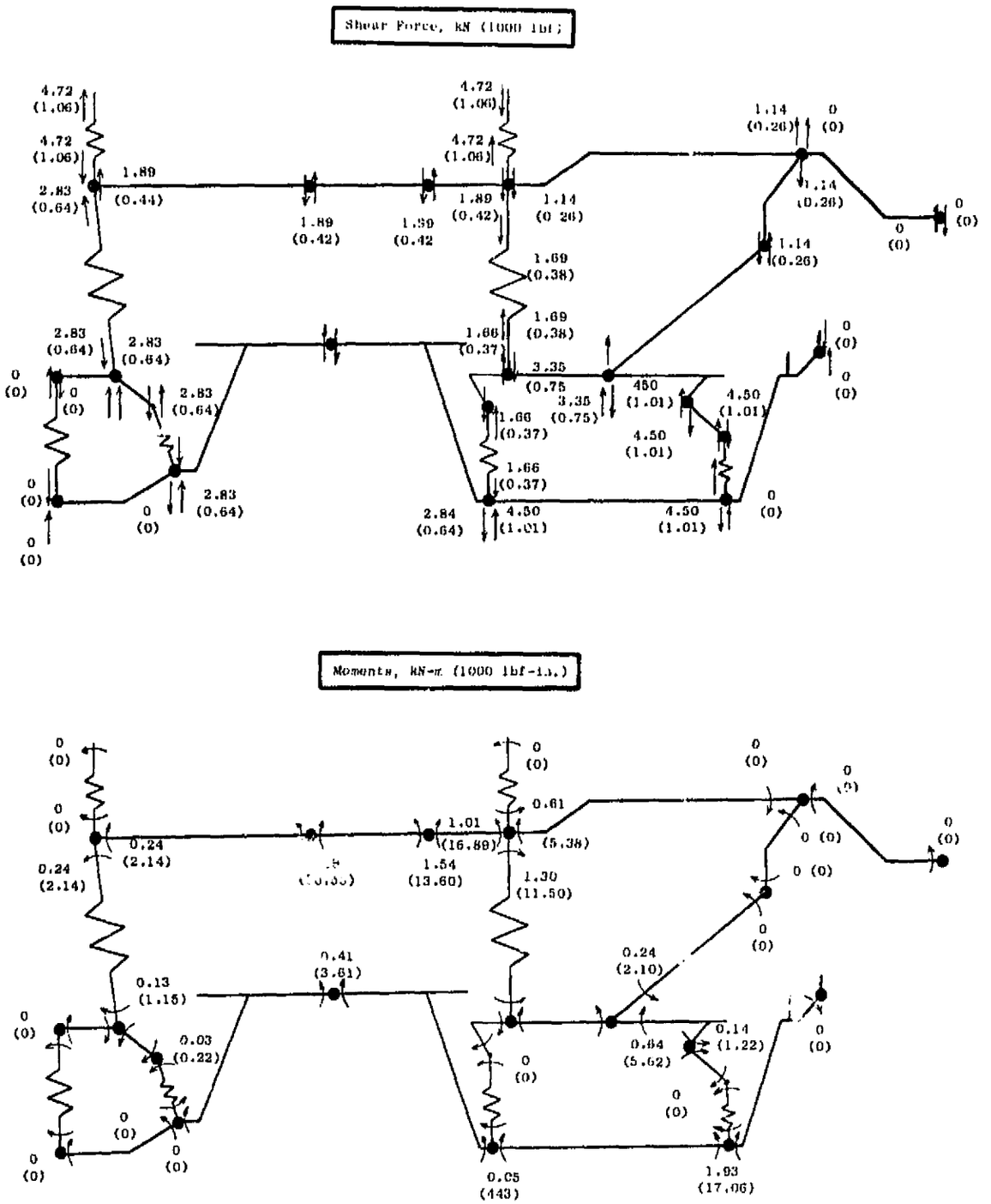

Figure 92. Engine System Maneuver; Precession.

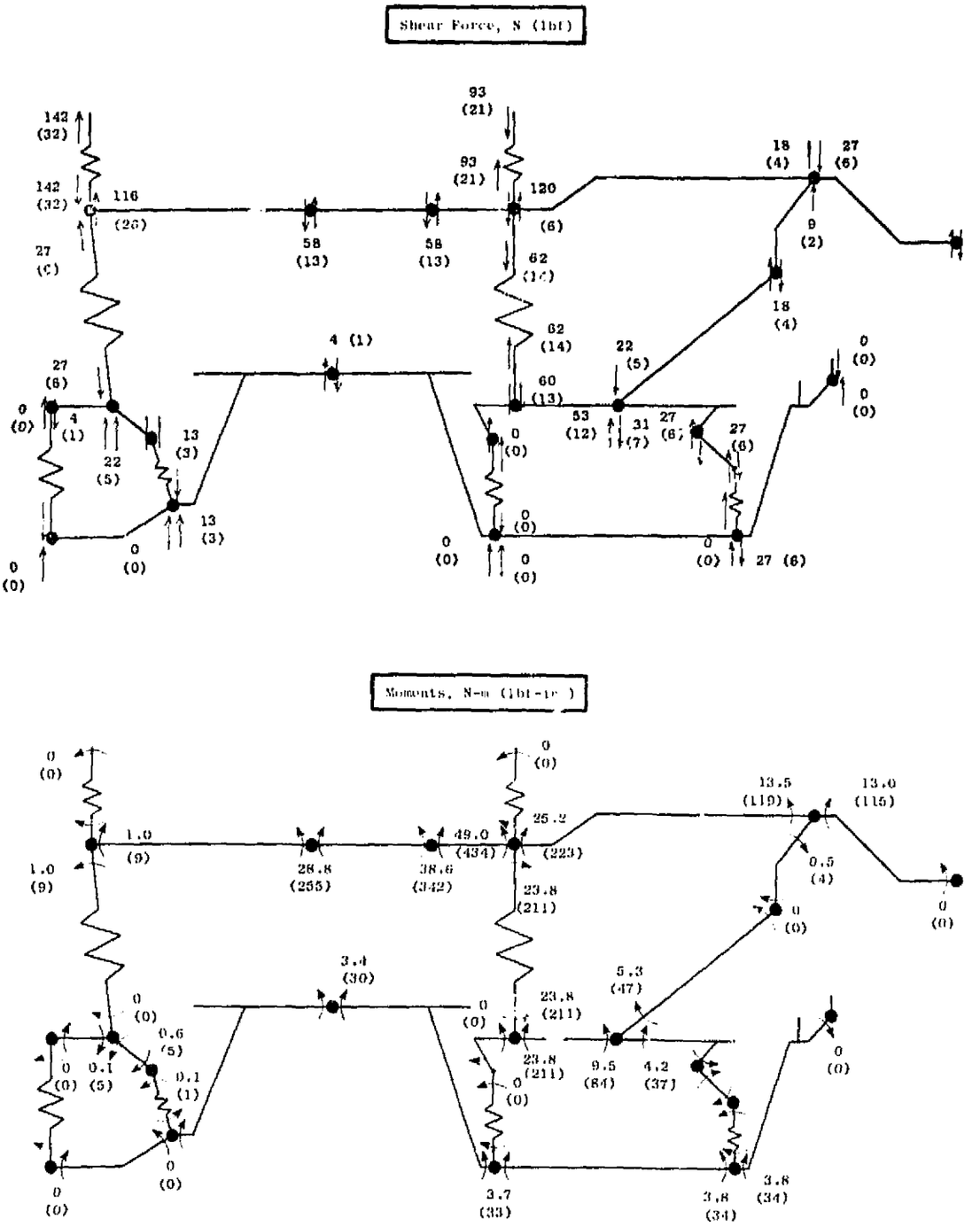

Figure 93. Engine System Maneuver; Angular Acceleration.

Table XXVI. Maneuver Load Relative Deflections for the YJ97.

Compressor

Maneuver	Stage Deflection, mm/100 (in./1000)				
	1	2	3	4	5
1-g	0.51(0.20)	0.74(0.29)	0.53(0.21)	0.10(0.04)	0.13(0.05)
1-rad/sec$_2$	2.5.(0.99)	1.09(0.43)	1.75(0.69)	3.37(1.33)	3.02(1.19)
1-rad/sec^2	negligible				
	6	7	8	9	10
1-g	0.54(0.23)	0.48(0.19)	0.45(0.18)	0.46(0.18)	0.46(0.18)
1-rad/sec$_2$	0.97(0.38)	1.14(0.45)	1.12(0.44)	1.02(0.40)	0.84(0.33)
1-rad/sec^2	negligible				
	11	12	13	14	
1-g	0.41(0.16)	0.38(0.15)	0.36(0.14)	0.33(0.13)	
1-rad/sec$_2$	0.84(0.33)	0.79(0.31)	0.66(0.26)	0.64(0.25)	
1-rad/sec^2	negligible				

Turbine

	1	2
1-g	0.99(0.39)	1.45(0.57)
1 rad/sec$_2$	-25.9(-10.2)	-38.9(-15.3)
1 rad/sec^2	negligible	

6.0 HAZARD ANALYSIS

A preliminary hazard analysis, as described in Reference 14, paragraph 5.8.2.1, was performed as part of these design studies. The intent of such an analysis is to qualitatively evaluate the relative safety of a system design. The results of the study can then be used to establish safety criteria to be imposed on performance or design specifications.

The LCF459 system consists of turbotip fans, YJ97 engines, interconnect ducts, nozzles, inlets, and control devices. Since this design effort was for the fan system only, the preliminary hazard analysis was limited to this component.

In the evaluation, four categories (levels) of the hazard are defined as follows:

I. Negligible - will not result in personnel injury or system loss.

II. Marginal - can be counteracted or controlled without injury to personnel or major system damage.

III. Critical - will cause personnel injury or major system damage or will require immediate corrective action for personnel or system survival.

IV. Catastrophic - will cause death or severe injury to personnel or system loss.

Table XXVII gives the results of this hazard analysis. The hazards are broken down into three types:

1. Identification of Energy Sources
   - Rotating Machinery and Pressurized Vessels
   - Combustible Fluids
2. Control of Energy Sources
   - Rotor Speed Controls
   - Variable Pressure Controls
3. Turbotip Fan Environmental Constraints
   - Foreign Object Damage
   - Maneuver Loads

Table XXVII. Hazard Analysis.

• Section 1 - Identification of Energy Sources

Potential Hazard	Safeguards and Design Considerations/Recommendations	Hazard Level
A. Rotating Machinery and Pressurized Vessels Rotating structures contain potential energy which becomes kinetic energy if released by structural failure or if failure or if by external means.	The general design philosophy for all rotating disks and blades is to provide sufficient strength for limited operaton at overload conditions such as overspeed or impact with foreign objects. Rotating structures are designed to cause the least possible release of kinetic energy (high velocity projectiles) when excessive loads occur and cause structural failure.	
LCF459 Fan Rotor		
(1) Fatigue failure of the thrust bearing would result in vibrations and possible rotor radial shift, probably would result in turbine rub, involuntary shutdown, and noisy coast-down.	(1) To minimize failure, the bearings are designed for long life under normal operating loads. The calculated life for the LCF459 thrust bearing under this loading is approximately 279,000 hours. Small, isolated, bearing spalls should not result in rotor radial shift. Oil condition monitoring should identify pending deterioration of the bearings. The vibration monitoring system could also be utilized to detect spalls and warn of impending bearing fatigue failure.	Category I
(2) If a single-fan-blade failure occurs during high speed operation of the fan it can create a high energy projectile comprised of the failed portion of the fan blade and attached turbine carrier segment. If this projectile is not contained it may cause damage to aircraft structure fluid carrying components, flight controls, or personnel.	(2) The fan with the attached turbine carrier is basically a tip-shrouded blade design which helps to prevent a failed blade from piercing the case. Local containment shielding, external to the fan frame, will be provided for protection to critical aircraft components and personnel. The static and rotating engine structures are designed to withstand the vibration caused by the loss of one fan blade at the dovetail at maximum engine rpm for at least 30 seconds and be safely shut down.	Category II
(3) If multiple fan-blade and/or fan-disk failures occur, high energy projectiles are generated. If these projectiles are not contained they may create a hazard to tip-turbine accessories, aircraft structure, or personnel. Projectile paths can be forward and penetration of the scroll with release of hot gases to surrounding aircraft structure possible. Release of hot gases may create a hazard to aircraft structure, tip-turbine structure, fluid-carrying components, flight controls, or personnel. Blade dovetails or disk dovetails need not fail to eventuate multiple blade failures. These may occur as a result of a prying or wrenching motion as with multiple large bird strikes, etc.	(3) The fan containment shield to be provided will be designed to contain single-blade failures but may not contain simultaeous multiple blade and/or disk failures. Disk failures are very unlikely since a higher strength margin is designed into the part to help in preventing disk failure as a result of blade failure. Experience shows that simultaneous multiple blade failure is very unlikely, unless severe FOD/DOD is encountered. Multiple blade failure will result in immediate fan shutdown. The following design features and considerations provide safeguards against this potential hazard: • Fan disk designed burst speed is 120%. • Axial blade retention is 30% of centrifugal load, minimizing possibility of multiple blade loss. • Improved blade tolerance to bird strike or FOD. (a) Generous blends to hard-point locations, tip and midspan shrouds, to reduce stress concentrations. (b) Local thickness distribution features to improve susceptible areas of the blade. (c) Chordwise location of the midspan shroud away from the leading edge so that chordwise plastic deformation can absorb some of the impact energy.	Category III when in the VTOL mode.

Table XXVII. Hazard Analysis (Continued).

• Section I - Identification of Energy Sources (continued)

Potential Hazard	Safeguards and Design Considerations/Recommendations	Hazard Level
LCF459 Fan Rotor (continued)		
	• Disk-to-shaft bolt joint designed to withstand combined maneuvers and blade-out loadings. • Thicker turbine walls, resulting from casting process, improve FOD/DOD resistance. Sustained release of hot gases to surrounding aircraft structure is remote because performance deterioration of the fan would be detected even if the rotor structural failure leading up to the penetration was not detected immediately.	
LCF459 Turbine Carrier		
(1) Turbine carrier separation failure from the fan blade can create a high energy projectile. If this projectile is not contained it may cause damage to aircraft structure, fluid-carrying components, flight controls, or personnel and also would release hot gases with possible impingement upon nacelle surfaces or structure.	(1) Local containment shielding external to the fan frame will be provided to protect critical aircraft components and personnel. Fan shall be capable of sustained operation after loss of only one turbine carrier.	Category III
B. Combustible Fluids		
LCF459 Scroll, Turbine Nozzles, Exhaust Nozzles		
The tip-turbine fan body and nacelle does not house any of the fuel systems.		
(1) Fuel from external to the tip-turbine fan could find its way into the hot gas path and into the scroll, turbine nozzle, and exhaust nozzle areas if the gas generator was experiencing starting difficulties resulting in a "wet" start. This source of combustible fluid in the tip-turbine, hot gas stream could result in a fire which would release a considerable amount of thermal energy in a short period of time. Most of this sudden thermal energy release would be dissipated aft out of the exhaust nozzle but may result in damage to the scroll or turbine or to deterioration of tip-turbine parts.	(1) Fuel in the scroll, turbine nozzle, and exhaust nozzle area is only a remote possibility but the following precautions are taken: • Fuel drains will be provided in all scroll, ducting and propulsion areas where fuel accumulation is possible. • Procedures will be established and documented in the flight manual and maintenance manual to reduce hazards following a "wet" start.	Category I

Table XXVII. Hazard Analysis (Continued).

Potential Hazard	Safeguards and Design Considerations Recommendations	Hazard Level
• Section I - Identification of Energy Sources (continued)		
LCF459 Turbotip Fan Lube Sump System The supply of lube system fluid provides a limited source of energy if released. The fan lube sump is isolated physically from the tip turbine so that a sump fire autoignited by the turbine is too remote to consider.		
(1) If the forward or aft disk pump should rub or fail, or should structure failure occur, or should contamination permit airflow through the sump to increase the temperature and decrease the oil/air ratio sufficiently; autoignition may occur within the sump.	(1) Disk pump running clearances are large and are designed not to rub during mission maneuvers. Review of internal GE data indicates the danger of a fire in this sump is minimal. Expected sump temperatures will be approximately 121 - 146° C (250 - 300° F) below the autoignition temperature for oil/air. The oil temperature sensor should provide adequate warning of impending lube system failure. Failure of lube supply pumping or any other partial or total interruption of pressure will be indicated in the cockpit. Action by the pilot may prevent secondary turbotip fan damage.	Category II
(2) Damage to the sump forward seal or aft seal or to the sump housing could provide an oil leak path to the tip turbine under static conditions. This may result in autoignition upon subsequent operation. Such a leak may also result in small quantities of oil traveling to adjacent aircraft structure.	(2) A sump overboard drain will be provided. An oil retention channel will be provided on the forward and aft seal housings. A drain overboard from this channel will also be provided.	Category II
• Section II - Control of Energy Sources		
A. Rotor Speed Controls		
(1) Failure of LCF459 fan rotor speed control system could result in an overspeed condition which might lead to rotor failure.	(1) Under normal operation, the gas generator cannot deliver sufficient power to overspeed the rotor. Overspeed capabilities are designed into all rotor structures. The control function of the gas generator adjusts fuel flow to limit power to the tip turbine to prevent fan speed from exceeding a safe limit. Redundant rotor speed sensors and control limiters will be provided in the aircraft and gas generator control and condition-monitoring systems. Based on this redundancy of design features, it is expected that rotor overspeed failure due to control system failure is highly unlikely.	Category I (if only rotor speed occurs) Category III (if rotor failure should result from overspeed)

Table XXVII. Hazard Analysis (Continued).

Potential Hazard	Safeguards and Design Considerations/Recommendations	Hazard Level
• Section II - Control of Energy Sources (continued)		
B. Variable Pressure Control (1) A loss of control of the scroll butterfly valve could result in inadvertent closure of the valve and unwanted change in fan thrust.	(1) The following safeguards and design features limit the possibility of this hazard: • The scroll butterfly valves will be designed to remain open following loss of actuation forces. • Valve closure is required only following failure of a gas generator. Combined failures of both the gas generator and the valve actuation system are remote. • Inadvertent valve closure without engine failure can be corrected by the pilot or automatic engine power setting reduction through a T_4 limiter. • Valve actuation will be monitored as part of preflight checkout. Redundancy will be provided both in the hydraulic and in the electrical controls.	Category II
• Section III - Turbotip Fan Environmental Constraints		
A. Foreign Object Damage Damage to fan blades and vanes as a result of ingestion of foreign objects may occur. The foreign objects may be ingested from runway debris or from environmental sources such as birds, rocks, sand, or ice. Carelessness in maintenance could also result in the ingesrion of loose objects from the inlet duct. FOD generally results in only minor nicks and dents, but it may cause major blade and/or vane damage.	The following design procedures were utilized to provide improved tolerance to bird strike or FOD: • Generous blends to hard-point locations, tip and midspan shrouds to reduce stress concentrations. • Local thickness distribution features to improve susceptible areas of the blade. • Chordwise location of the midspan shroud away from the leading edge so that chordwise plastic deformation can absorb some of the impact energy. • Disk-to-shaft bolt joint designed to withstand combined maneuvers and blade-out loadings. Information will be provided for repair procedures to relieve stress risers from minor FOD and for maintenance procedures and operating procedures to minimize and avoid FOD.	Category II

Table XXVII. Hazard Analysis (Concluded).

• Section III - Turbotip Fan Environmental Constraints (continued)		
B. Maneuver Loads	Safeguards and Design Considerations/Recommendations	
Maneuver loads in excess of those for which the turbotip fan is designed may cause: (1) fan mount failure or, (2) temporary heavy rotor rubs.	The following safeguards and design features apply: • Fan mounting systems are designed for blade-out loads which are two-times greater than design maneuver loads. • Fan seals and rub surfaces will contain adequate material to permit rubs equivalent to twice the maneuver loads without fan distress, except for the seal and rub material. Continued operation with a small degradation in performance will result. • Fan mount failure is considered to be very unlikely.	Category II (for heavy rotor rubs) Category III (for remote possibility of fan mount failure)

The majority of the hazards fall into levels I and II. The category level III hazards represent very remote possibility of occurrence. No category IV hazard levels have been identified.

As a benefit of this analysis, several fan design changes have been, or will be, considered to enhance the safety of the Garbotip fan concept. Typical design changes considered were:

- Fuel drains will be provided in all areas of the fan where fuel can collect. For example, the lower part of the scroll and vane frame.

- An oil retention channel, with overboard drains, will be provided to collect oil in the event of bearing sump seal leakage.

- Fan speed control limits and redundant speed indicators will be provided to ensure accurate fan speed measurements and to initiate gas generator power reductions should a fan overspeed occur.

- The scroll partial-arc shutoff valves will be designed to remain fixed in the original position following loss of actuation forces.

7.0 PERFORMANCE

7.1 INTERCONNECT SYSTEM

The trend in V/STOL propulsion systems is to use power interconnect between the various energy sources. These interconnect arrangements perform two major functions:

- They provide a method of power transfer between units to modulate or change thrust for aircraft attitude control.
- They provide a method of redistribution of power throughout the aircraft in the event of an engine failure.

The interconnect method used for the turbotip fan uses hot gas flow through a ducting system. A typical arrangement for a three-fan, three-engine system, as being considered for the research aircraft system, is shown in Figure 5. The ducting system contains two starting valves that are closed to isolate the three engines during start-up. There is a control valve located at the inlet to the scroll of each fan. These control valves are used to provide power transfer for aircraft control. A third set of valves is operated only in the event of an engine failure or shutdown. When an engine fails, the corresponding engine backflow valve is closed, and all three scroll valves are closed. The closure of the scroll valves reduces the total fan nozzle area to about two-thirds of the original area, which provides a match for the two operating engines. This type of ducting system was considered during development of performance and in the ducting representation in the LCF459 customer deck.

The pressure losses of the complete ducting system were evaluated for the condition where all three engines are operating with no power transfer. The pressure losses with a duct diameter of 0.44 m (17.5 in.) are given in Table XXVIII.

Table XXVIII. Estimated Ducting Pressure Losses.

	Percent of Total Pressure
Lift/cruise engine to lift/cruise fan.	4.2
Third engine to nose fan.	6.5
Lift/cruise fan scroll.	2.9
Nose fan scroll.	5.9

7.2 CONTROL SYSTEM

The gas-interconnected, turbotip fan system uses a method of gas power transfer to generate differential thrust levels for aircraft attitude control. This control concept was originally proposed by the McDonnell Aircraft Company and has been demonstrated using two interconnected YJ97-GE-100 engines. The results of this NASA/McDonnell test program are given in References 7 and 8. A description of the operating characteristics of this control system, both transient and steady state, is given in these references.

This gas power transfer control system is used to provide control moments both in the pitch and the roll axis of the aircraft. Height control is obtained using engine throttles to change power settings, with vanes or louvers located in the fan efflux to generate yaw control moments.

The distribution of gas flow during control in the pitch and roll axes are shown in Figure 94. The levels of flow transfer are shown for a 20-percent thrust increase for one of the fan systems. The flow split is also established for no interaxis coupling; that is, roll control does not produce a pitching moment. Thrust spoiling will be required on the down-going fan for generation of the control moment at a constant total system thrust. Figure 95 gives the flow transfer requirements for various levels of control thrust.

7.3 RATINGS AND LIMITS

The weight of V/STOL aircraft is very sensitive to engine short-time ratings, particularly the one-engine-inoperative (OEI) contingency rating. The number of engines used in the system is also important; the larger the number of engines, the lower the required ratings. In the three-engine technology aircraft, two of the YJ97 engines can operate to provide the high levels of system thrust during the engine-out condition.

Ratings established for the YJ97 engine, which are consistent with present limitations of rotor speeds and turbine inlet temperature, are given in Table XXIX. The three ratings established are the one-engine-inoperative (OEI) rating, the V/STOL takeoff rating, and the maximum control (MC) rating when flow transfer is used for aircraft control. The normal engine "Military" rating is also given for comparison. These ratings as established for the engine are a good match with the scroll and turbine limitations of the turbotip fan system, without requiring the use of exotic materials or cooling. The only other limit imposed on the turbotip fan system, other than those established by the engine, is a speed limit of 100-percent, steady-state and 105-percent, short-time rating consistent with the control duty cycle.

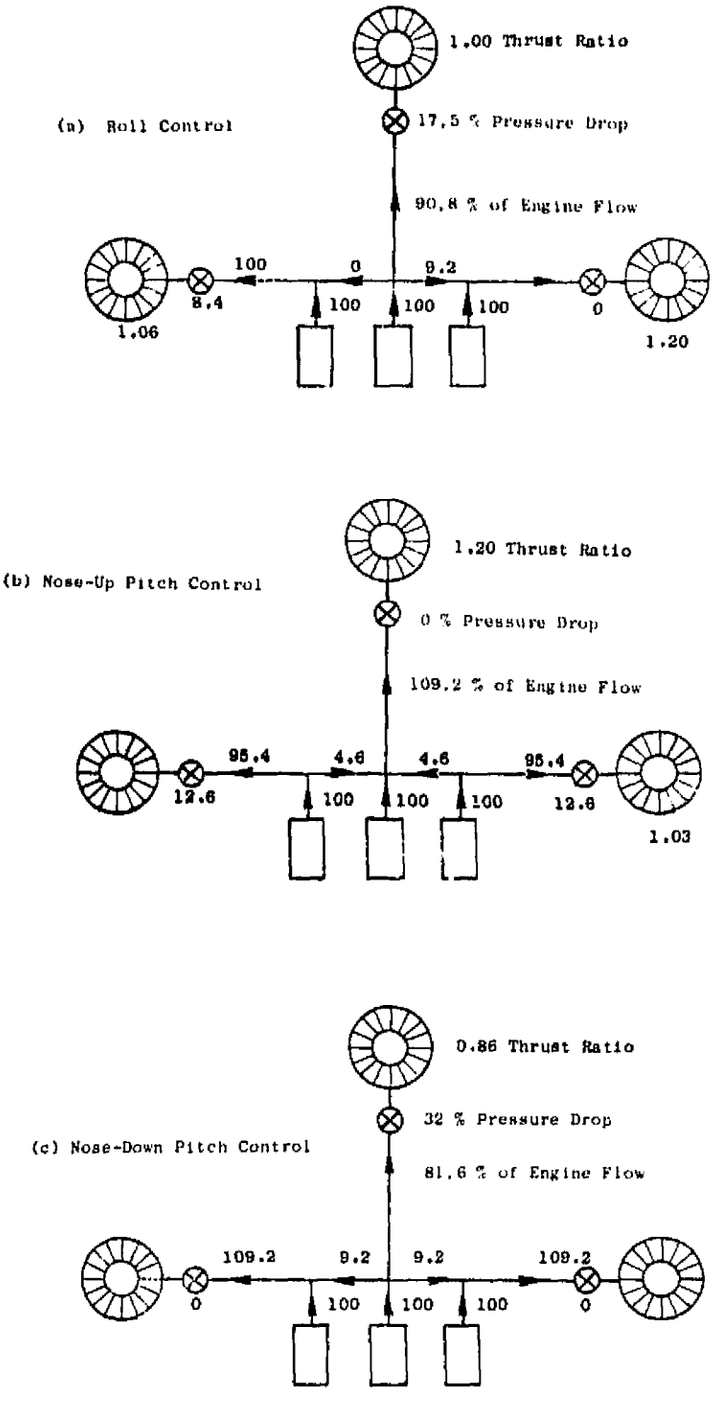

Figure 94. Flow Distribution for Control.

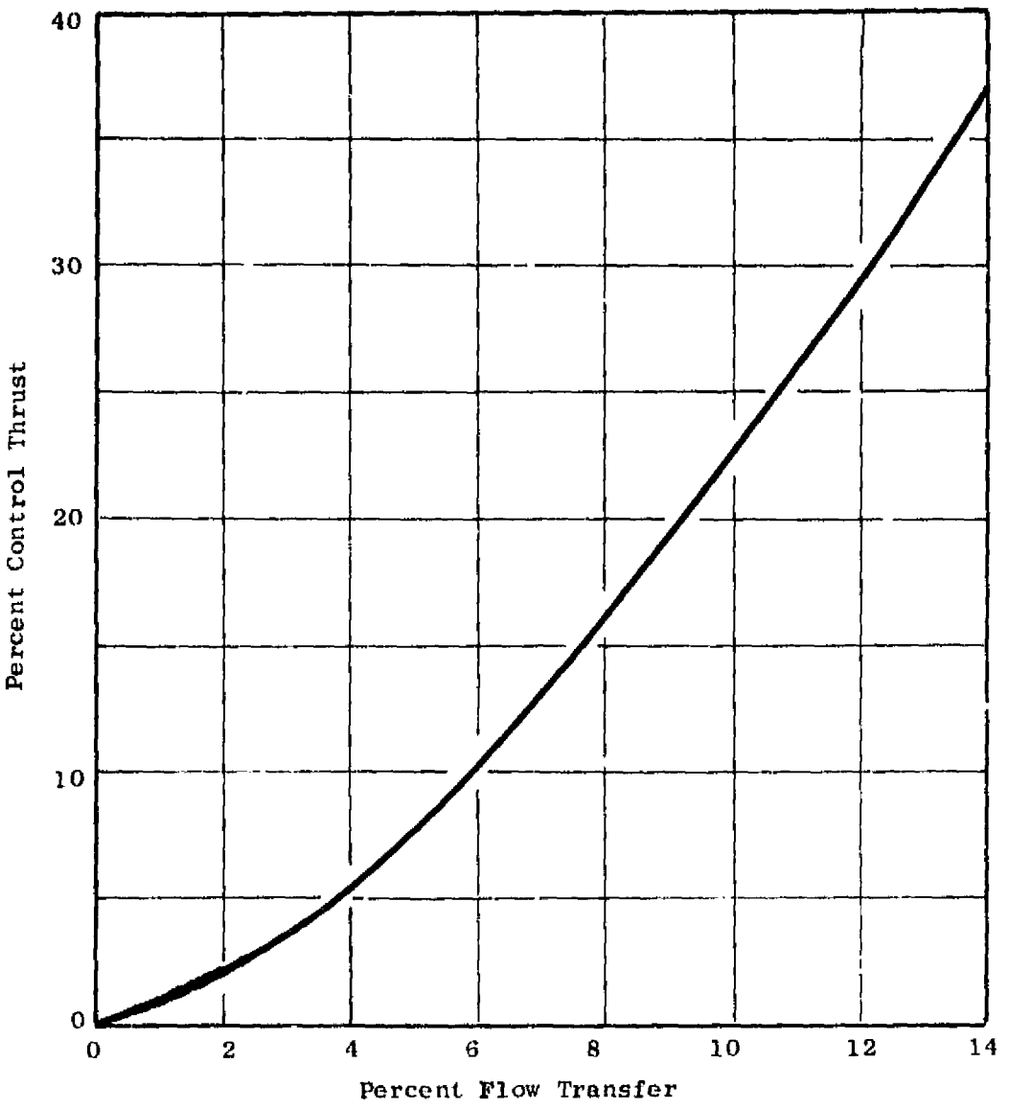

Figure 95. Flow Transfer Requirements.

Table XXIX. YJ97-GE-100 Ratings.

(Sea Level Static)

Rating:	V/STOL	MC	OEI	MIL
Ambient Temperature, K (° R)	305.4 (549.7)	305.4 (549.7)	305.4 (549.7)	288.1 (518.7)
Physical Rotor Speed, percent	102.7	102.7	107.5	101.5
Turbine Inlet Temperature, K (° R)	1433 (2580)	1521 (2738)	1540 (2772)	1383 (2490)
Turbine Discharge Temperature, K (° R)	1060 (1909)	1144 (2060)	1144 (2060)	1019 (1835)

V/STOL - one-minute takeoff rating

MC - maximum condition during power transfer, 100 percent control

OEI - one-minute contingency rating in event of engine failure

MIL - normal military power rating

7.4 MATCH POINT

The fan design point established during the preliminary design studies, Reference 1, was retained for the turbotip fan. The fan has a tip diameter of 1.50 m (59 in.) and a design-point pressure ratio of 1.32. Table XXX lists the significant fan design parameters.

In the aircraft installation, three of these fans are supplied power by three YJ97-GE-100 engines. The condition for maximum power delivery to one fan occurs at the power transfer condition. The gas conditions supplied at the scroll inlet are listed in Table XXXI. These gas conditions are based on a three-percent duct pressure loss between the engine discharge and the scroll inlet. In the RTA, these losses will probably be different because of the particular installation and duct pressure loss. For these conditions, the original fan and turbine design point will be retained; differences in duct pressure losses, including the scroll, will be taken into account through adjustment of the scroll nozzle areas for engine trim. This change can be incorporated easily during the hardware manufacturing cycle.

The turbine design point was established to provide adequate power to give a fan corrected speed of 100 percent on a hot day. The rotor physical speed at this condition is 102.9 percent. Table XXXII lists the significant turbine design-point parameters.

7.5 V/STOL PERFORMANCE

Performance in the V/STOL mode of operation was determined for a typical system consisting of three fans are three engines. The performance was determined for installed conditions using the factors given in Table XXXIII. Performance is shown in Figures 96 through 98.

7.6 CRUISE PERFORMANCE

Cruise performance was determined for a single engine/fan configuration. The installation factors given in Table XXXIV were used in the data generation. Performance data are given in Figures 99 through 104 using corrected parameters referenced to standard pressure and temperature. These performance data are developed for a configuration employing a continuously variable-area nozzle. For this design pressure ratio, the penalties associated with a fixed nozzle area are intolerable. A two-position configuration may be acceptable; additional performance data must be obtained to evaluate this approach. An engine computer deck with this capability will be available for use in aircraft studies.

Table XXX. Fan Design Point.

Tip Diameter, m (in.)	1.50 (59.0)
Pressure Ratio	1.319
Corrected Airflow, kg/sec (lbm/sec)	293 (646)
Corrected Tip Speed, m/sec (ft/sec)	343 (1125)
Adiabatic Efficiency, percent	86.0
Flow per Annular Area, kg/sec-m^2 (lbm/sec-ft^2)	1.72 (40.8)
Flow per Frontal Area, kg/sec-m^2 (lbm/sec-ft^2)	1.43 (34.0)
Fan Exit Mach Number	0.55
Inlet Radius Ratio	0.407

Table XXXI. Scroll Inlet Gas Condition.

Flow, kg/sec (lbm/sec)	32.05 (70.66)
Pressure, kN/m^2 (lbf/$in.^2$)	372.2 (53.99)
Temperature, K (° R)	1144 (2060)
Fuel/Air Ratio	0.0228

Table XXXII. Turbine Design Point.

Flow, kg/sec (lbm/sec)	32.05 (70.66)
Pressure, kN/m^2 ($lbf/in.^2$)	357.5 (51.85)
Temperature, K (° R)	1144 (2060)
Pitch Line Reaction, percent	15
Speed, rpm	4500
Energy Function, J/g K (Btu/lbm ° F)	0.228 (0.0544)
Efficiency	0.86
Exit Mach Number	0.55
Annular Area, m^2 ($in.^2$)	0.242 (375)

Table XXXIII. V/STOL Installation Factors.

	Lift/Cruise Fan	Nose Fan
Gas generator recovery	0.985	0.985
Gas generator bleed, percent	0.5	0.5
Gas generator power extraction, kW, (hp)	19 (25)	19 (25)
Ducting pressure loss, percent	4.2	6.5
Scroll pressure loss, percent	2.9	5.9
Fan inlet recovery	0.985	0.985
Fan power extraction, kW (hp)	38 (50)	0 (0)
Nozzle velocity coefficient	0.940	0.950

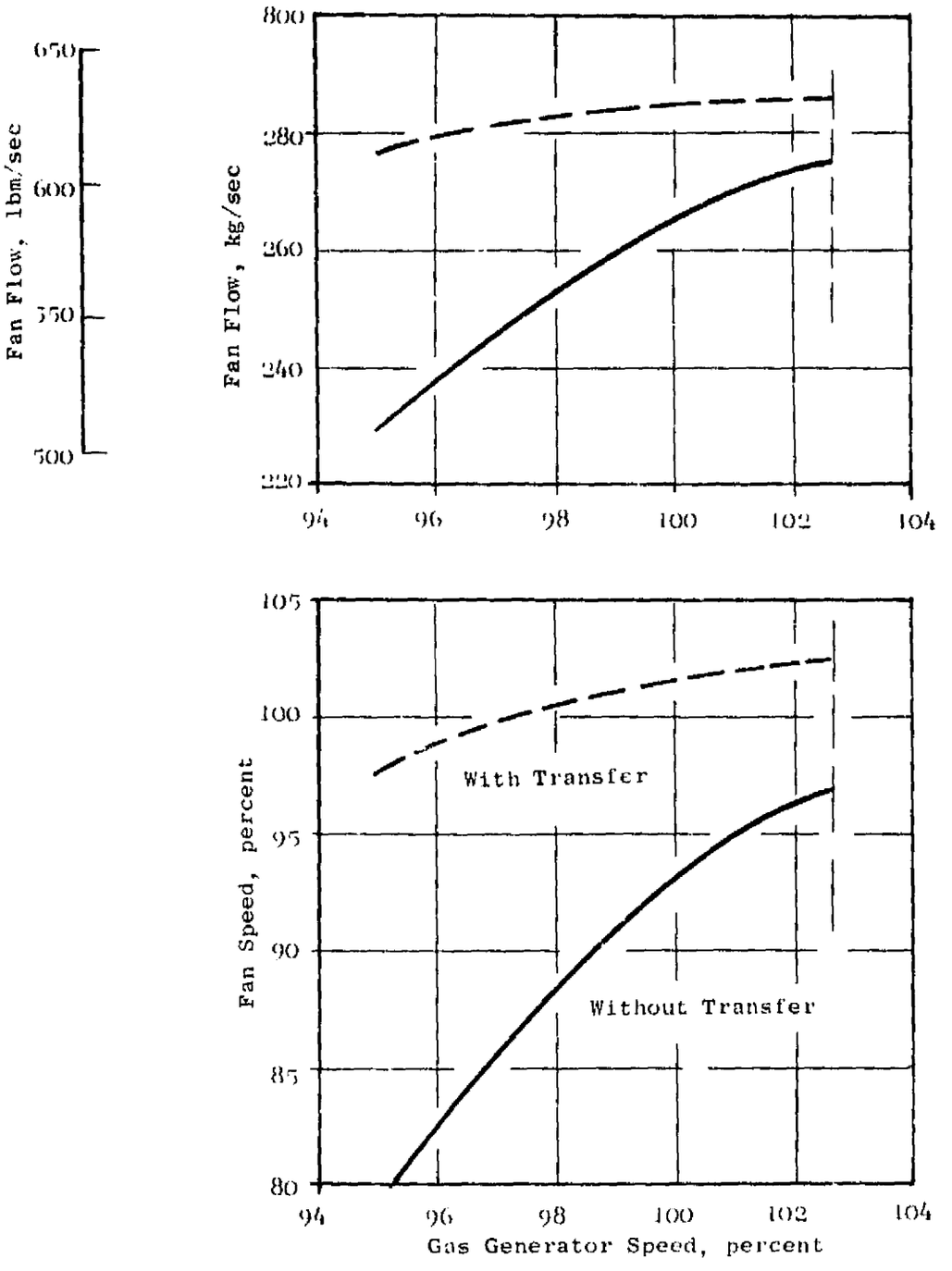

Figure 96. V/STOL Performance; Lift/Cruise Fan.

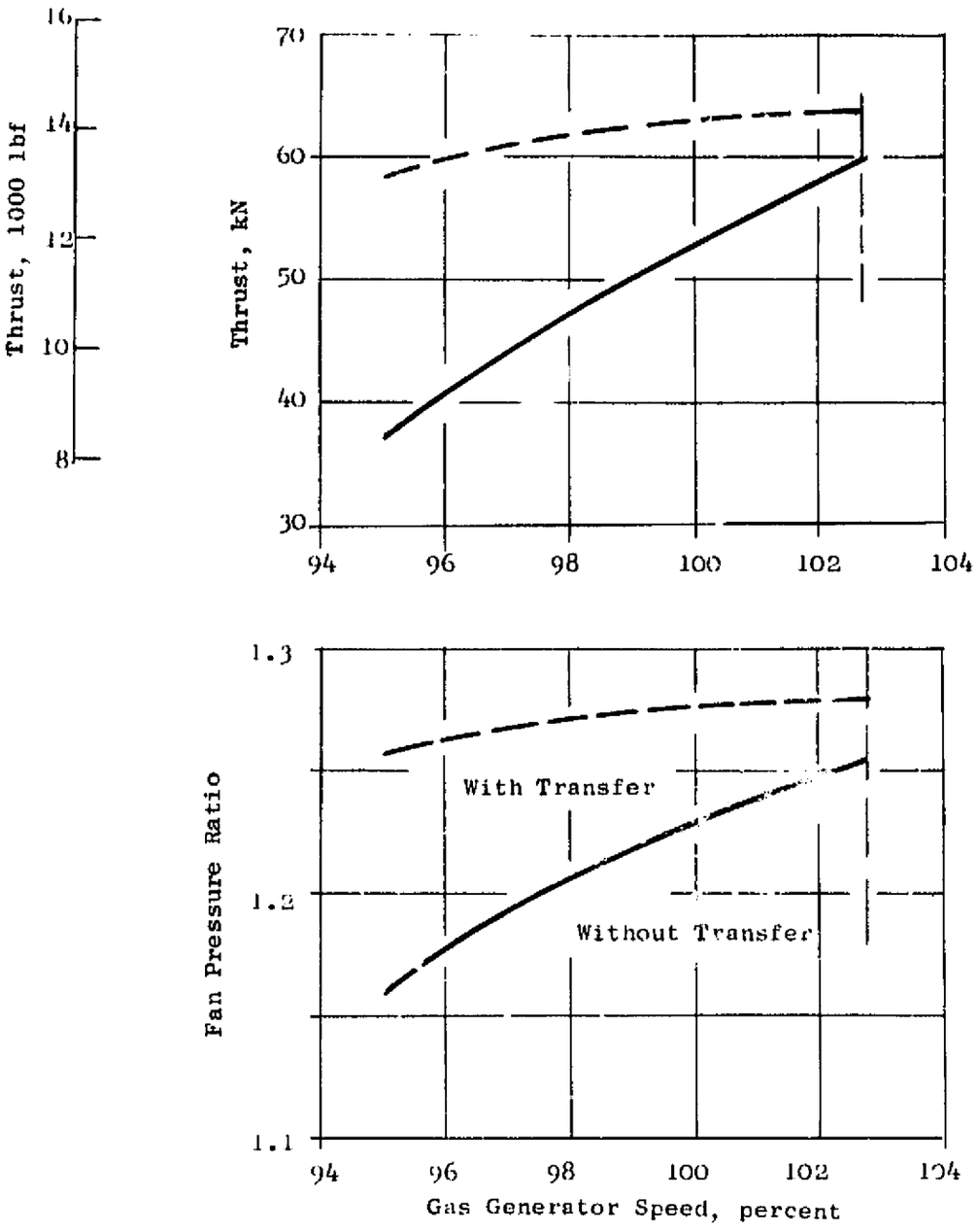

Figure 96. V/STOL Performance; Lift/Cruise Fan (Concluded).

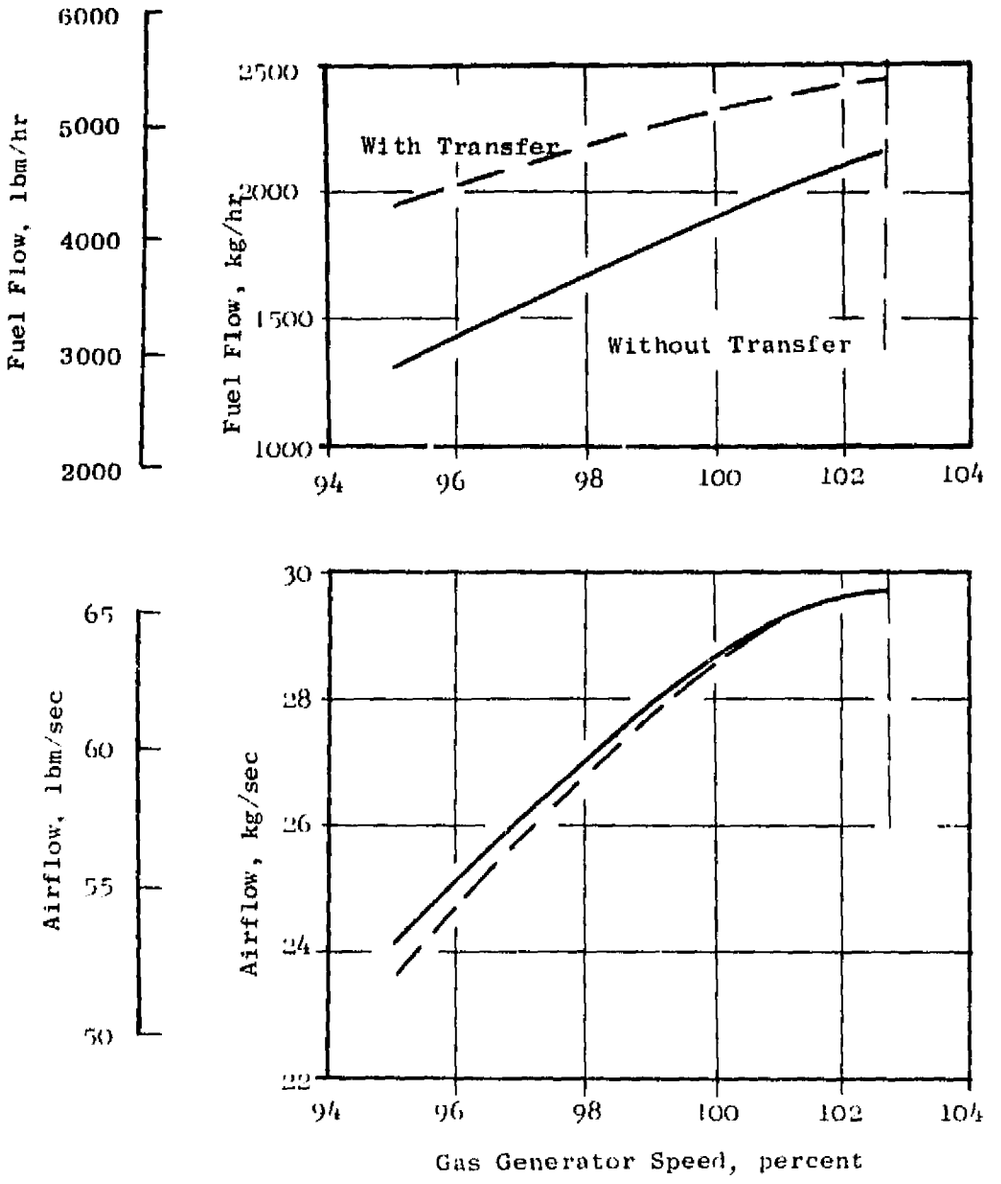

Figure 97. V/STOL Performance; YJ97-GE-100 Engine.

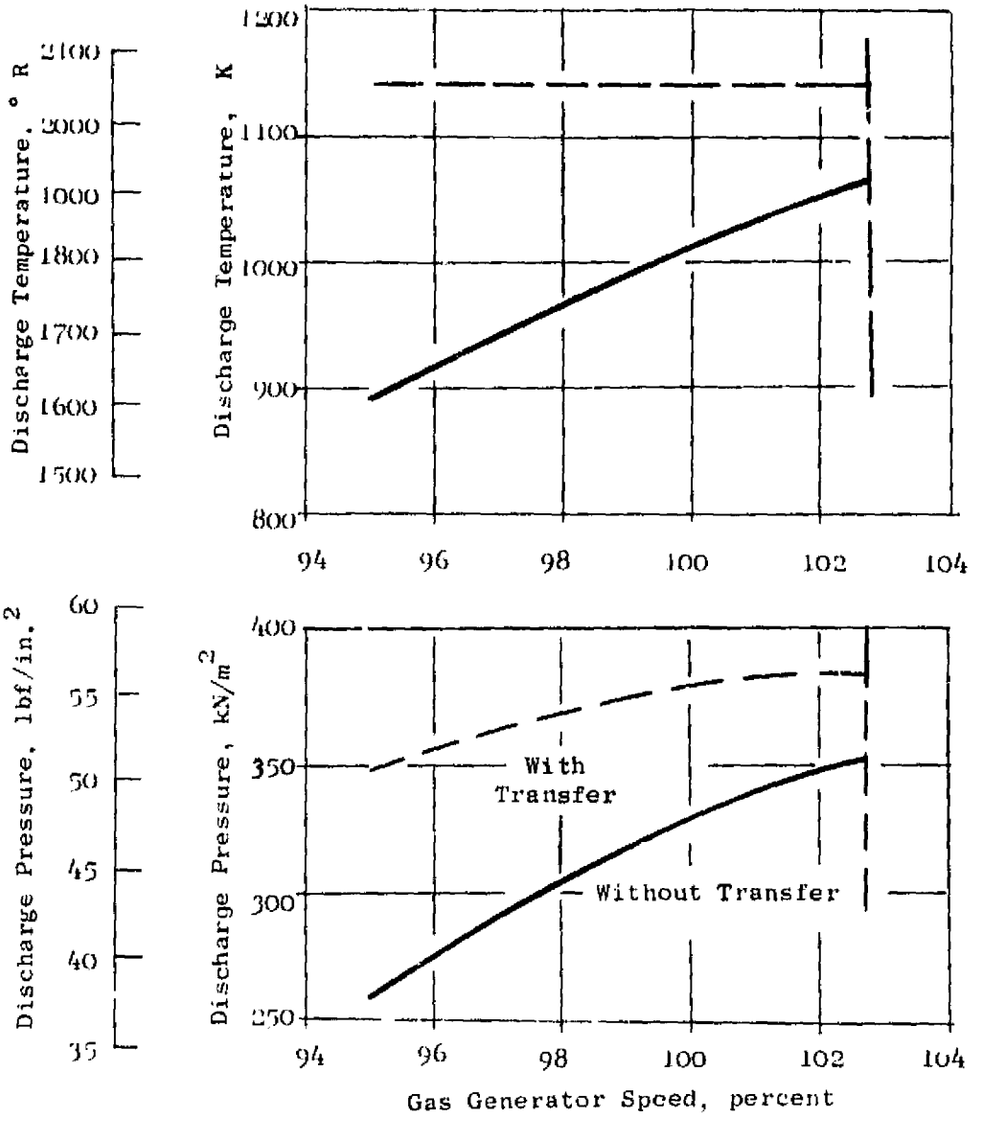

Figure 97. V/STOL Performance; YJ97-GE-100 Engine (Concluded).

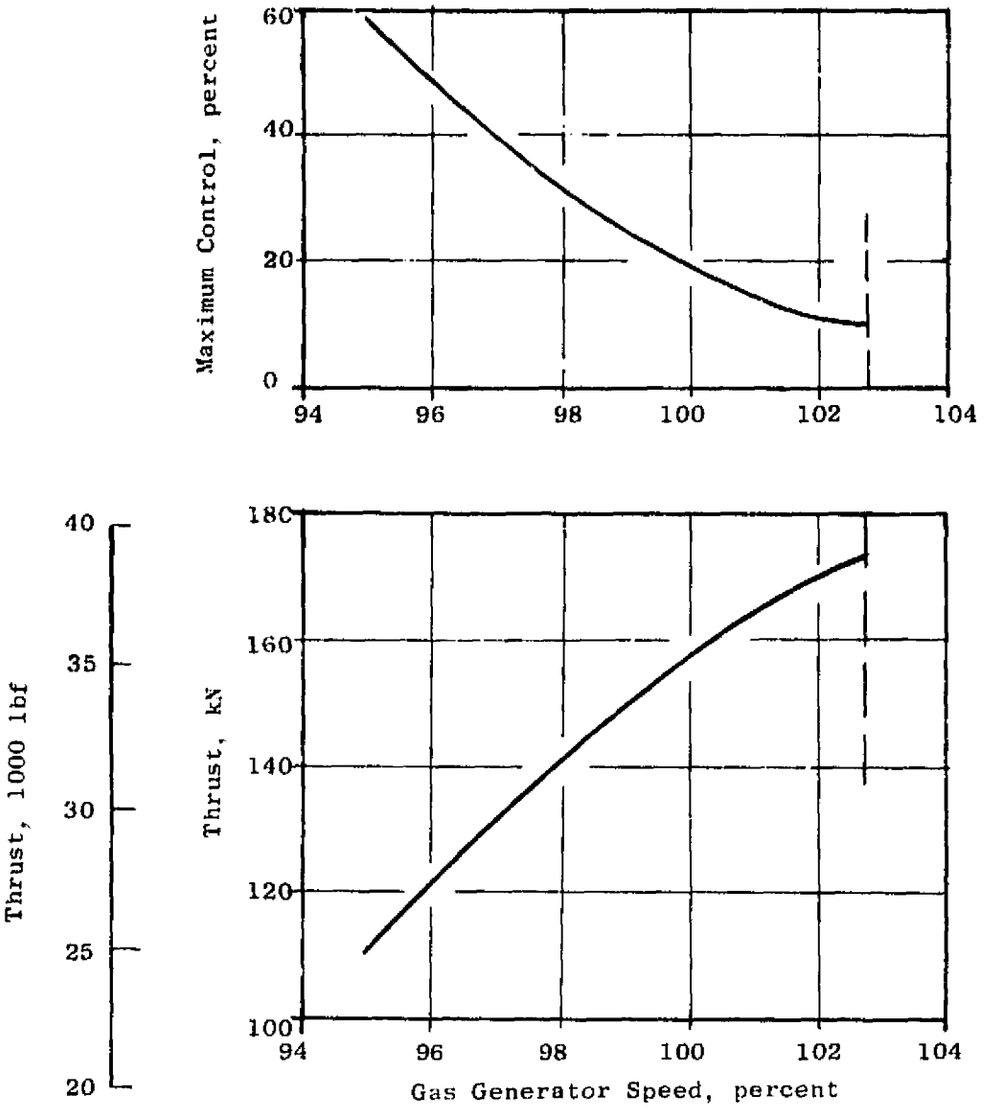

Figure 98. V/STOL Performance; Three-Fan System.

Table XXXIV. Cruise Installation Factors.

Engine Inlet Recovery	see tabulation
Compressor Bleed, percent	1.0
Engine Power Extraction, kW(hp)	19(25)
Fan Inlet Recovery	see tabulation
Directing Pressure Loss, percent	---
Scroll Pressure Loss, percent	2.9
Fan Power Extraction, kW(hp)	38(50)
Nozzle Thrust Coefficient	0.980

Mach Number	Engine	Fan
0.0	0.985	0.985
0.2	0.989	0.993
0.4	0.990	0.995
0.6	0.990	0.994
0.8	0.987	0.980
0.9	0.984	0.970

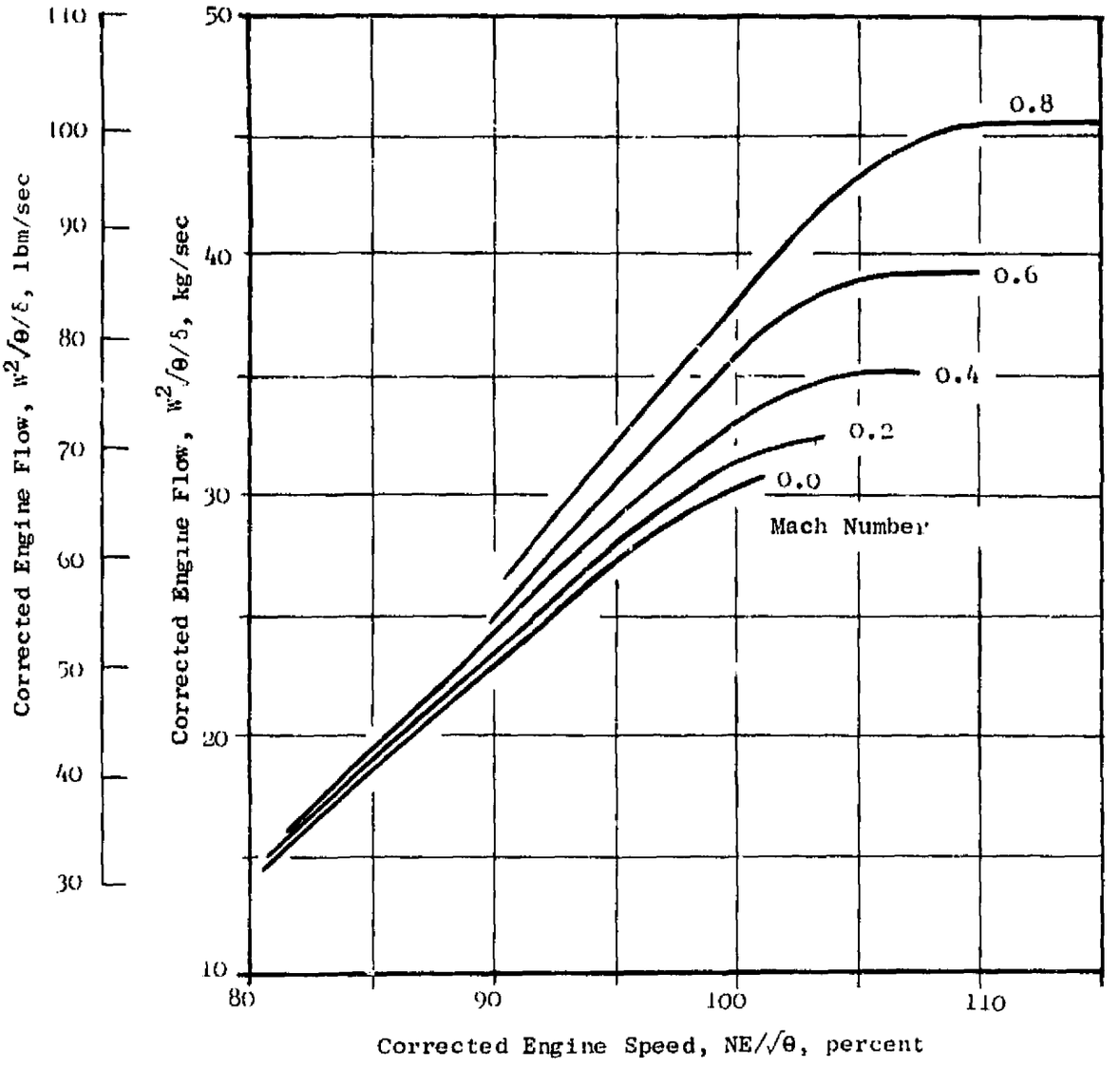

Figure 99. Cruise Performance; Engine Airflow.

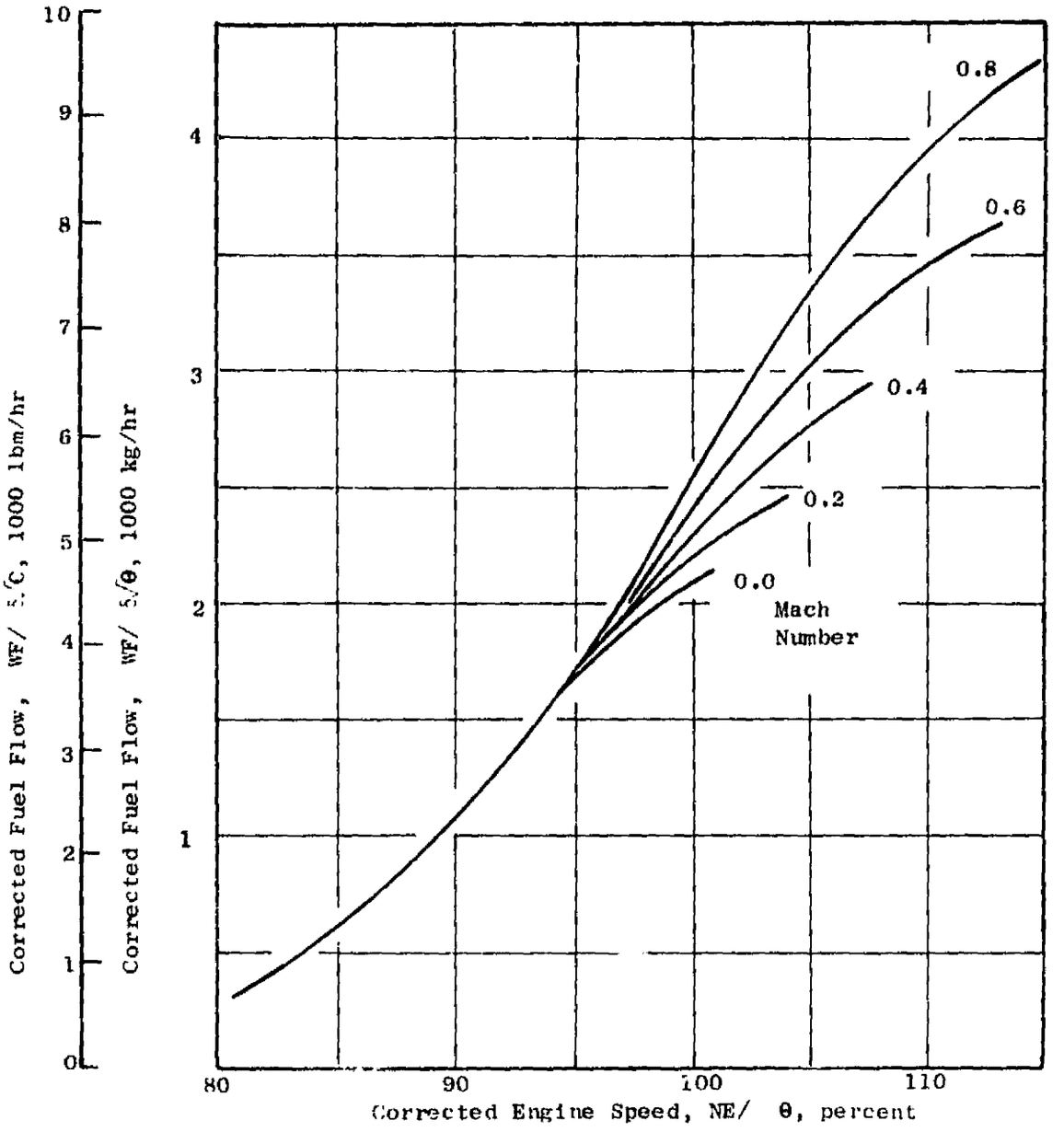

Figure 100. Cruise Performance; Fuel Flow.

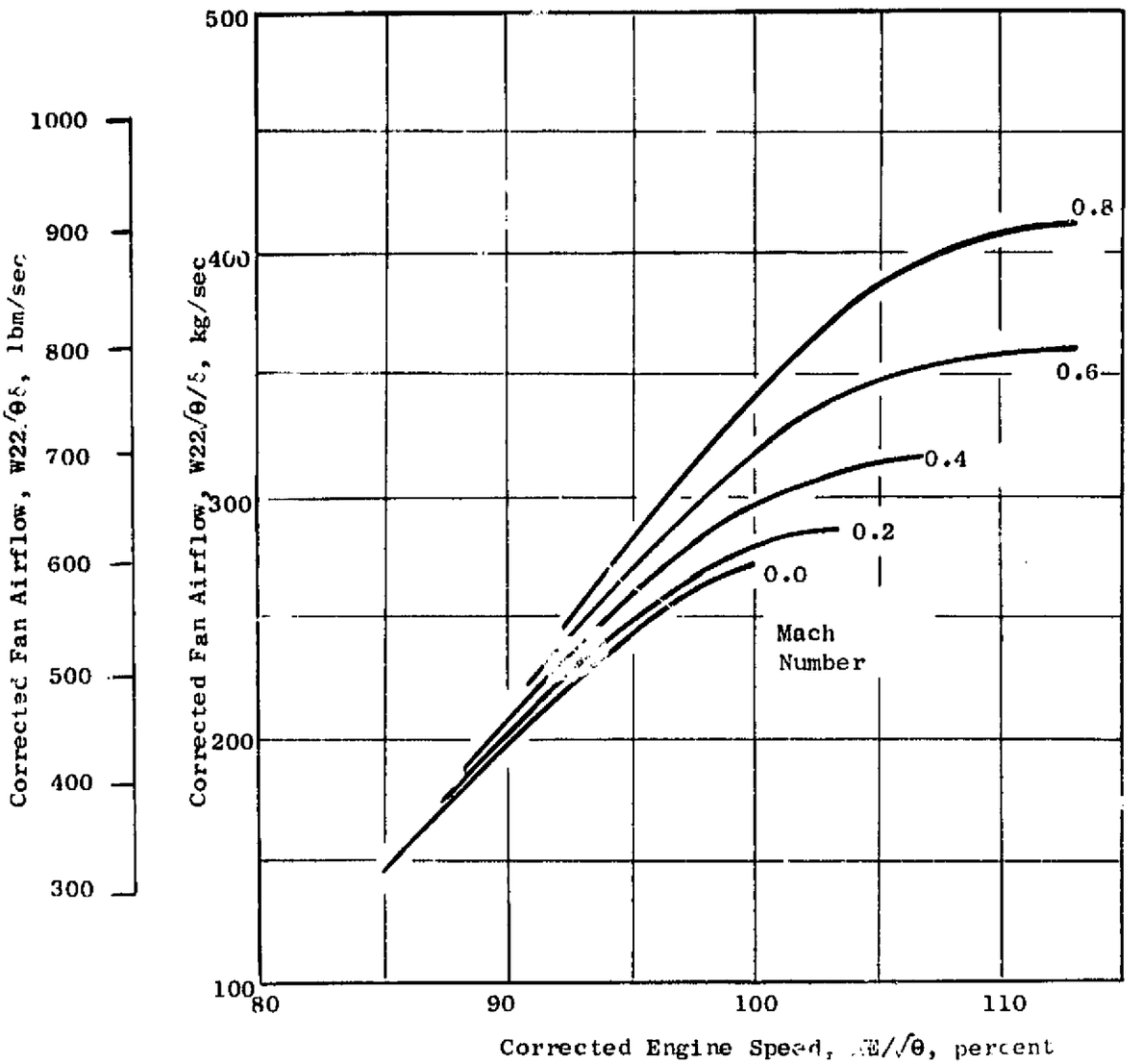

Figure 101. Cruise Performance; Fan Airflow.

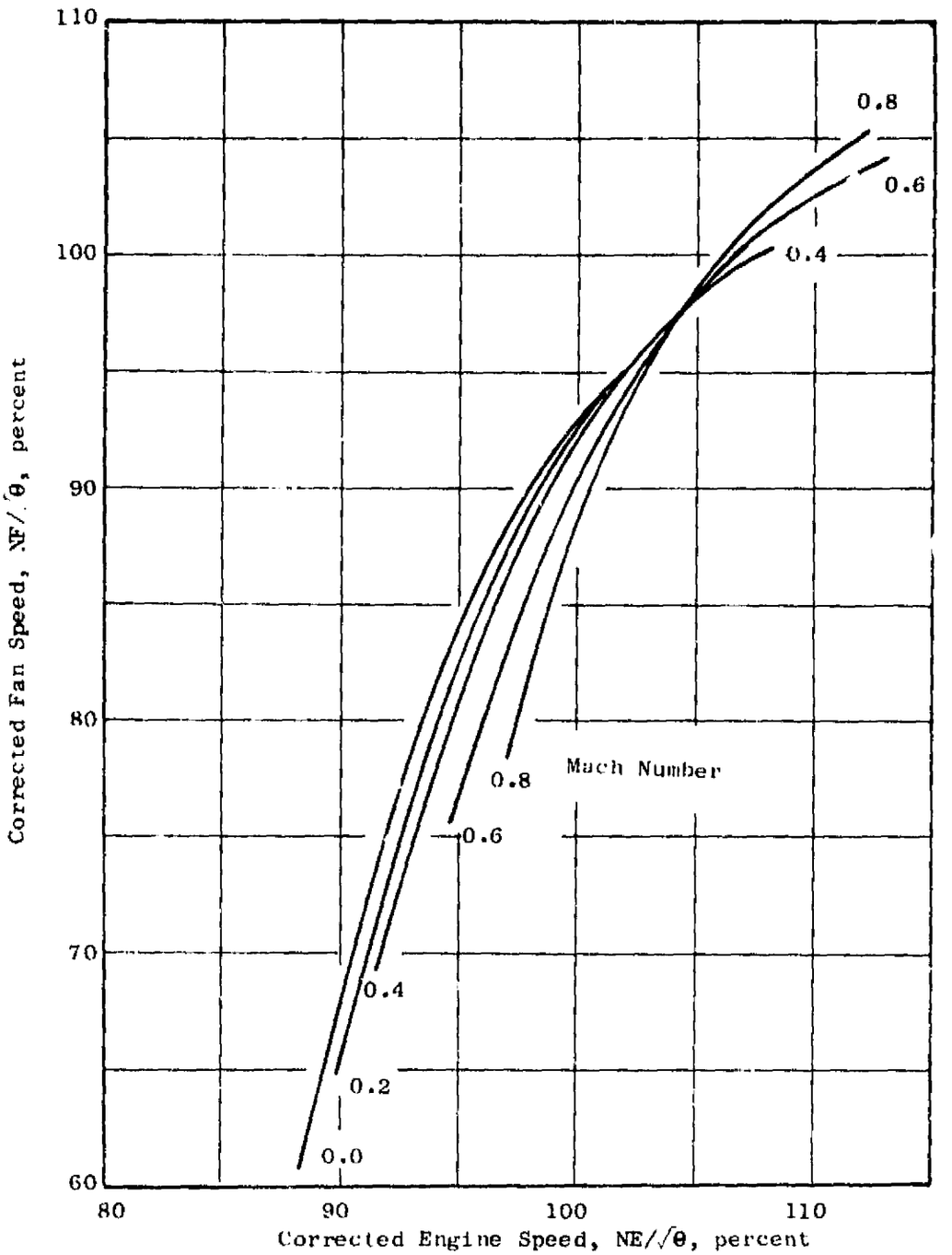

Figure 102. Cruise Performance; Fan Speed.

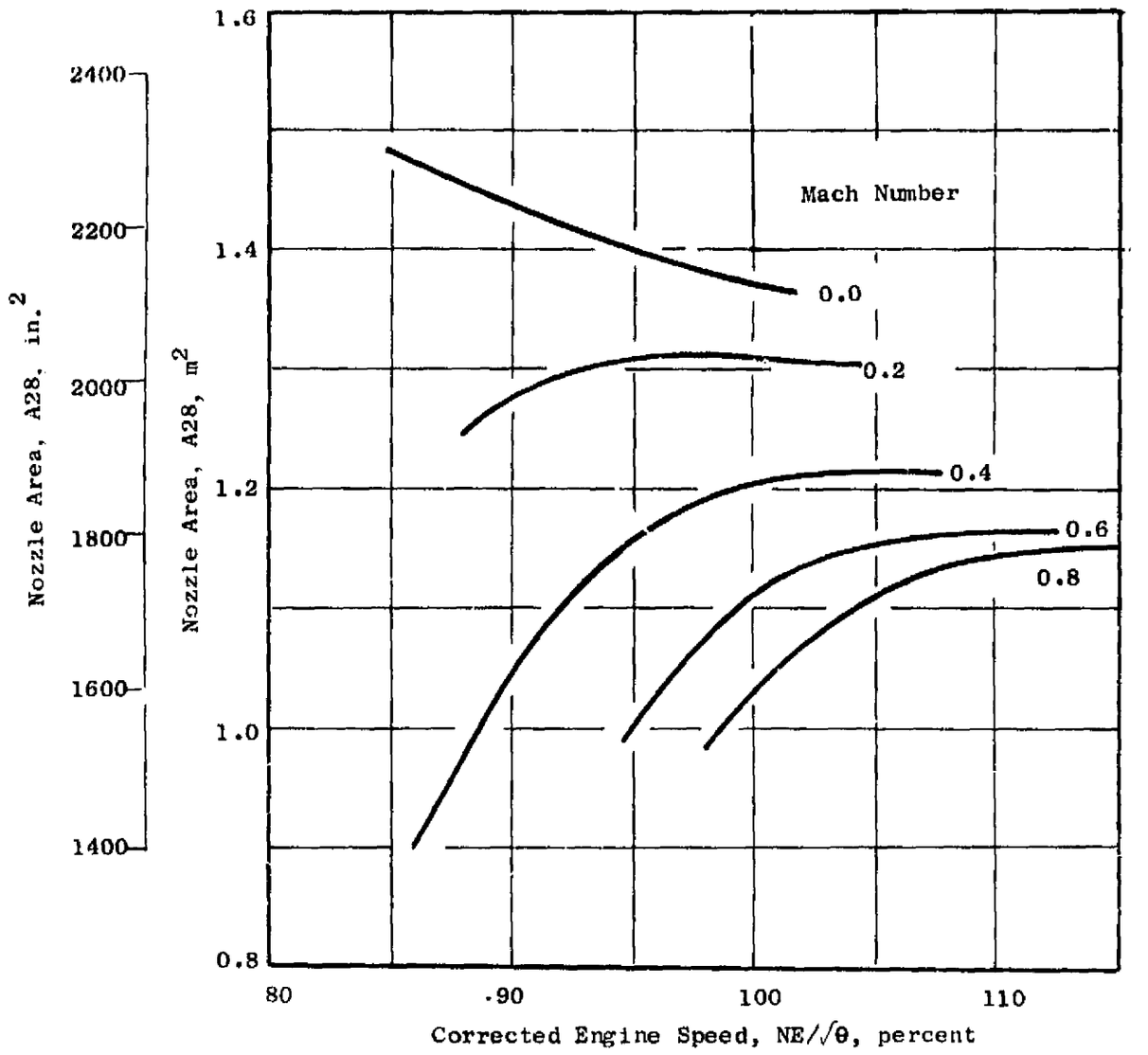

Figure 103. Cruise Performance; Nozzle Area.

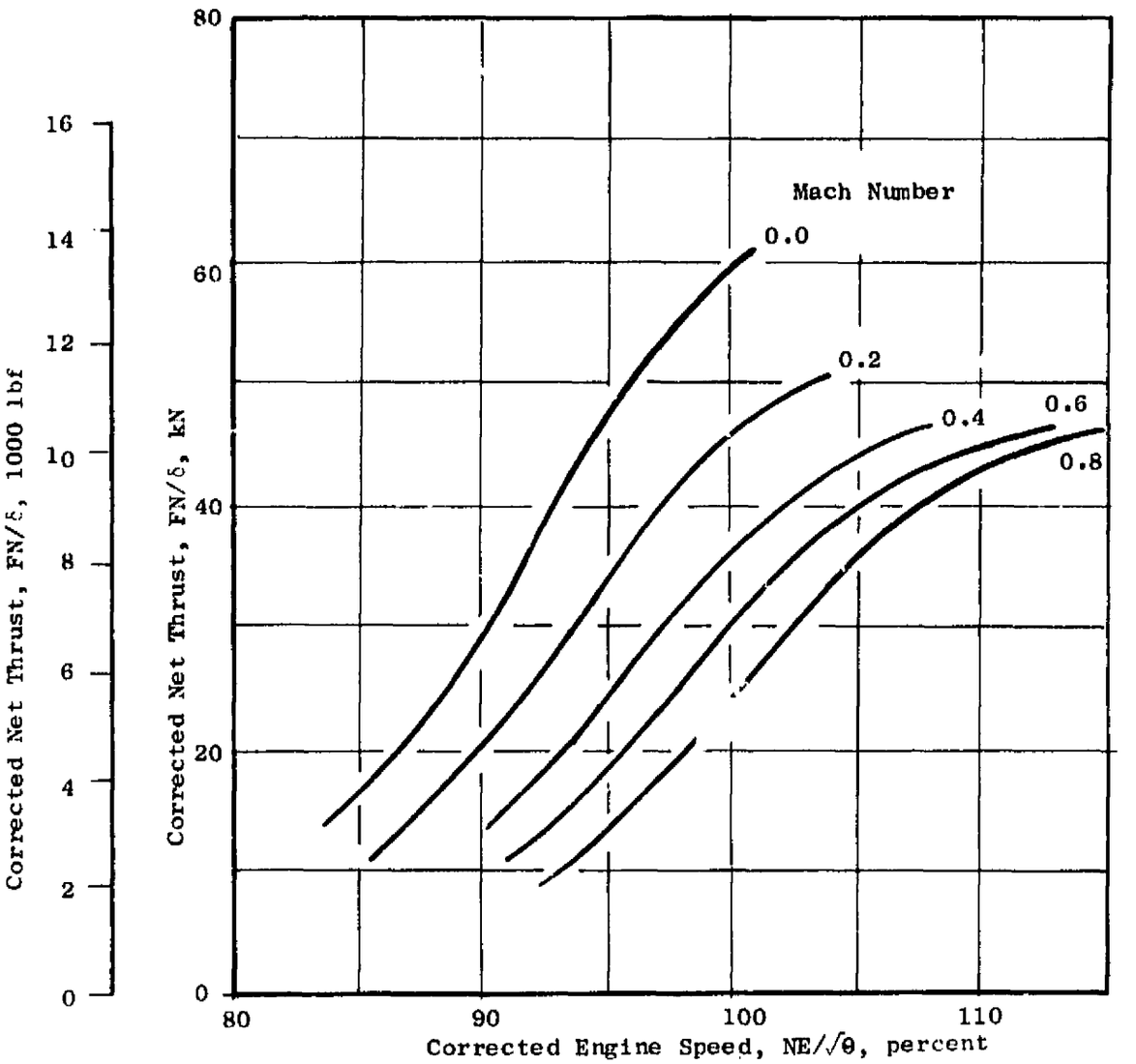

Figure 104. Cruise Performance; Net Thrust.

8.0 COMPATIBILITY AND DISTORTION

The LF459 fan design has been investigated from the point of inlet and exhaust system compatibility. This work has followed a process wherein established distortion requirements and applicable data were reviewed to define anticipated inlet total pressure, inlet total temperature, and exit static pressure distortions. These data identified the altitude, Mach number, and power settings that yield the highest distortions or combinations of distortions. The sensitivity of the fan designs to distortion was assessed by comparisons of the LF459 aerodynamic design with other existing designs that had been built and and tested for distortion sensitivity.

The fan sensitivity and distortion levels were then used to define those altitude, Mach number, and power settings where fan surge margin is a minimum. These conditions are called stability tracking points. The excess surge margin at each tracking point was then defined.

8.1 INLET AND NOZZLE DISTORTIONS

The design requirements establish the LF459 fan design point minimum surge margin at 18 percent. Further, the fan is to be capable of operation with the following distortions:

- $(\Delta P_T/P_T)_{Max} = 0.15$, inlet total pressure distortion.
- $(\Delta P_S/P_S)_{Max} = 0.15$, exit static pressure distortion.
- 50% of inlet face at least 27.8° C (50° F) above ambient. (At sea level static conditions, this becomes $(\Delta_T/T_T)_{Max} = 0.092$).

It was assumed here that these may act in any combination.

Inlet data were evaluated against the requirements to further determine the maximum distortion conditions for the fan. The data chosen for this work are contained in References 11 and 12 and are from a lift-fan installation test. A typical angle of attack versus yaw plot is shown in Figure 105; lines of constant $(\Delta P_T/P_T)_{Max}$ are shown. The distortion, even at high angles of attack and yaw, is quite low; about 0.06 is the highest value shown. In fact, the highest value of $(\Delta P_T/P_T)_{Max}$ seen in this data set is 0.10. However, one comment on these data is appropriate; they are steady-state measurements. The unsteady, time-variant distortion can be higher. Experience with subsonic inlets shows that a value of approximately 1.5 typifies the ratio between unsteady and steady-state distortion. The predicted worst unsteady distortion from this data set is then about 0.15, the same as the requirements.

Similarly, fan exit static pressure distortion data from Reference 15 were investigated. The data show a $(\Delta P_S/P_S)_{Max}$ of about 0.05. This is a

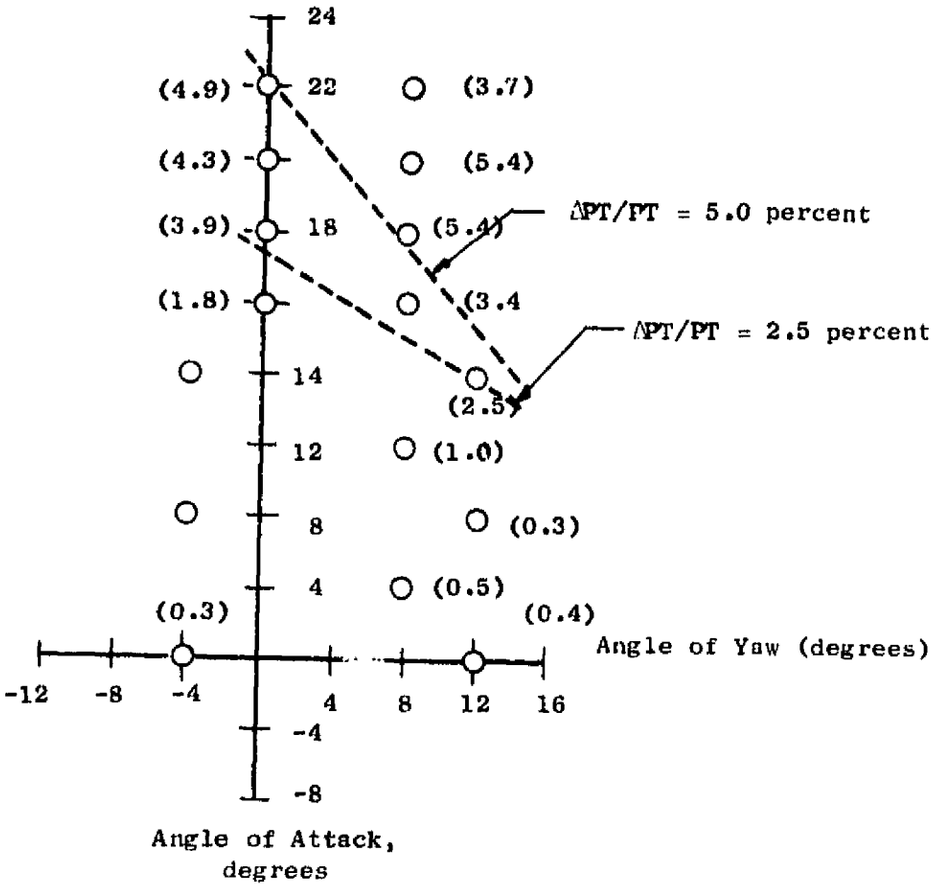

Vo = 53 m/sec (0.03 knots)
Mass Flow Ratio = 1.0
Numbers in ( ) are $(\Delta PT/PT)_{Max}$ in percent

Figure 105. Lift/Cruise Fan Inlet Distortion.

small data set and the values obtained are steady state. Further, nozzle exit crossflow can increase the static pressure distortion level. The requirement of 0.15 is not unreasonable and was used for the fan exit distortion limit.

Inlet temperature distortion is a strong function of the particular installation when the source is reingested exhaust gases. The data in References 11 and 12 were used to assess anticipated levels of temperature distortion for the lift fan. These data indicate that temperatures up to 39° C (70° F) above ambient were observed. Using this as a limit at standard day conditions, the temperature distortion can be described as an equivalent one-point pressure distortion. The 39° C (70° F) condition results in a $(\Delta T/T)_{Max}$ of 0.13, or 0.03 in equivalent $(\Delta P_T/P_T)_{Max}$.

The above approach was used to modify the inlet total pressure distortion by computing values of equivalent local pressure levels for an assumed one-per-revolution, square, wave pattern of temperature distortion. The high temperature region overlaid the low pressure region; this tended to increase the resulting equivalent pressure distortion.

8.2 FAN DESIGN DISTORTION SENSITIVITY

Distortion sensitivity is defined as the amount of surge pressure ratio lost per unit of distortion. In turn, surge pressure ratio loss can be related to surge margin. These are shown in Figure 106; the equations are defined at constant airflow and at constant corrected speed. It should be noted that the requirement of 18-percent stall margin is based on a constant corrected speed definition of surge margin. However, at this point in the design, it is not possible to predict with sufficient accuracy the airflow rollback and speed line shapes for distorted inflow conditions. Because of this inability to define speed line shapes prior to test, use of constant corrected speed definitions of surge margin and surge pressure ratio loss at this point in the design can lead to significant errors in the stability analysis. The use of constant corrected speed or constant corrected airflow definitions is discussed in detail in Reference 16.

The work shown here uses constant corrected airflow definitions. The aerodynamic design of the LF459 fan was compared to previously tested designs. These comparisons led to the estimate of distortion sensitivity shown in Figure 107.

Sensitivity to exit static pressure distortions has been reviewed. Data from large bypass turbofan engines, where exit static pressure distortions are generated by the engine service pylon, were used to develop a sensitivity curve shown in Figure 108. These data indicate that static pressure distortion sensitivity is a strong function of airflow, with sensitivity decreasing with increasing airflow. However, at reduced airflows, the level of distortion is reduced such that loss of surge margin is not excessive at any airflow, where loss of surge margin is defined at constant corrected airflow.

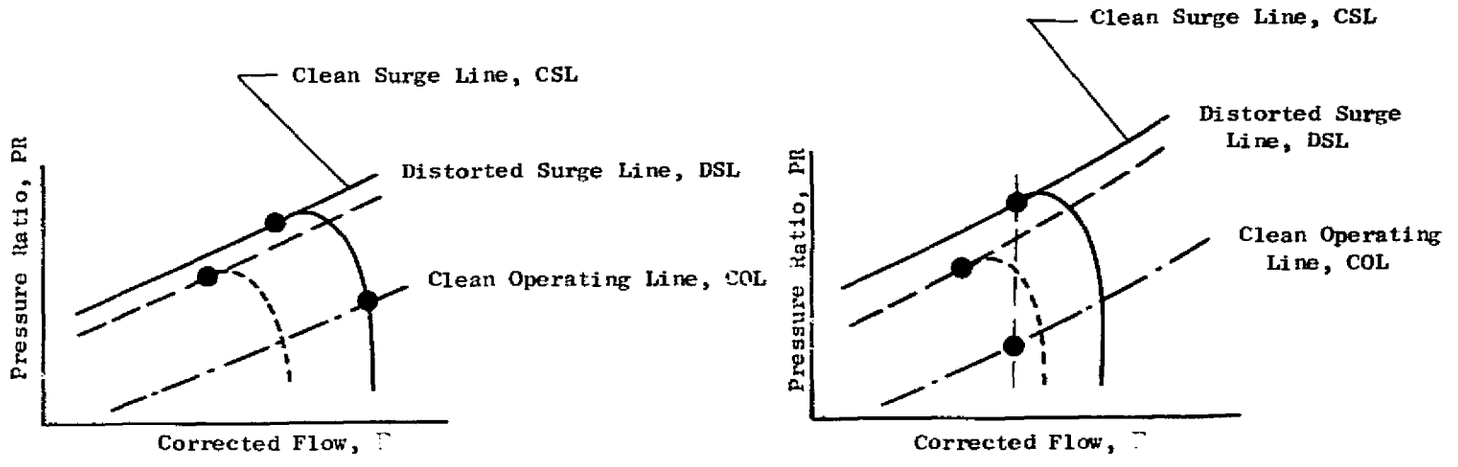

SM = Stall Margin
ΔPRS = Change of Stall Pressure Ratio

Corrected Speed = Constant

$$SM = \frac{(PR/W)_{CSL} - (PR/W)_{COL}}{(PR/W)_{COL}}$$

$$\Delta PRS = \frac{(PR/W)_{CSL} - (PR/W)_{DSL}}{(PR/W)_{CLS}}$$

Corrected Flow = Constant

$$SM = \frac{(PR)_{CSL} - (PR)_{COL}}{(PR)_{COL}}$$

$$\Delta PRS = \frac{(PR)_{CLS} - (PR)_{DSL}}{(PR)_{CLS}}$$

Figure 106. Fan Stability Definitions.

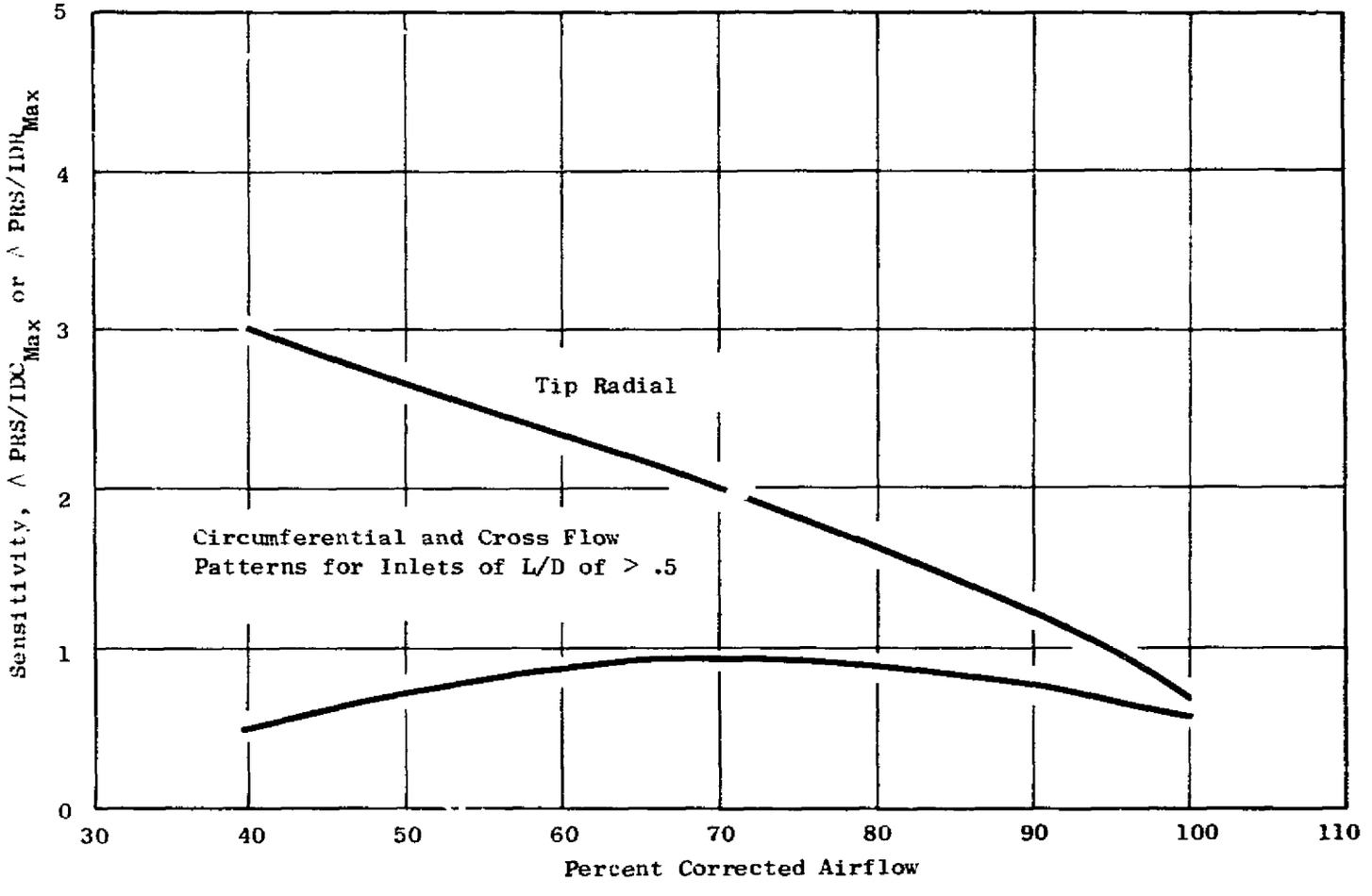

Figure 107. Total Pressure Distortion Sensitivity.

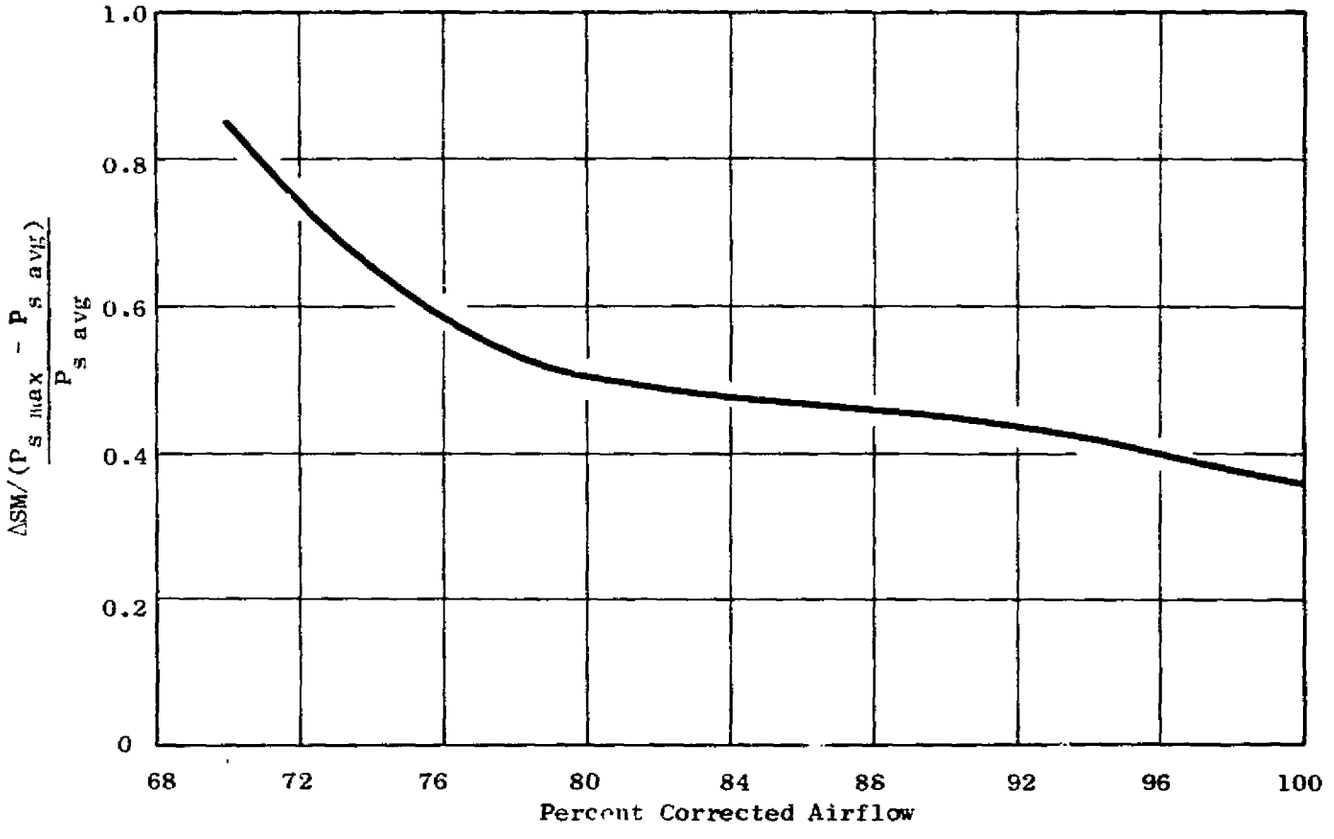

Figure 108. Static Pressure Distortion Sensitivity.

8.3 STABILITY TRACKING POINTS

The work done to date shows that the distortion requirements represent the worst case for the fan stability assessments. Since temperature distortion will only occur in the vertical lift mode in ground effect, sea level static conditions are the place where the fan stability assessment was performed. Further, fan operation would be at or very near to design corrected speed power conditions.

The stability stack for the fan is shown in Figure 109. Since only one condition has been identified, estimates of the stability margin both for constant corrected speed and for constant corrected airflow are shown. The constant corrected speed case assumes that the speed line is invariant with distortion. In both cases, excess margin is demonstrated so that no stability problems are foreseen for the LF459 fan operating with 18-percent surge margin, the defined pressure distortion requirements, and an inlet temperature distortion due to 39° C (70° F) above-ambient temperatures. It should be noted that the distortions were assumed to act in the worst combination: low pressure and high temperature overlaid with inlet and exit distortions independently affecting loss in surge pressure ratio. The stability stack provides for internal and transient destabilizations consistent with experience for other large fan designs.

8.4 SUMMARY

The Statement of Work distortion requirements have been assessed with respect to distortion data from a typical lift-fan installation. The inlet total pressure and exit static pressure distortion requirements appear to be consistent with measured data. The temperature distortion requirement of 28° C (50° F) above ambient over 50 percent of the engine face may be low. Data show that inlet temperatures can reach 39° C (70° F) above ambient. This level was used in the evaluation of fan surge margin.

The highest distortion condition is where all three distortions interact. A fan stability stack at this condition shows adequate remaining surge margin.

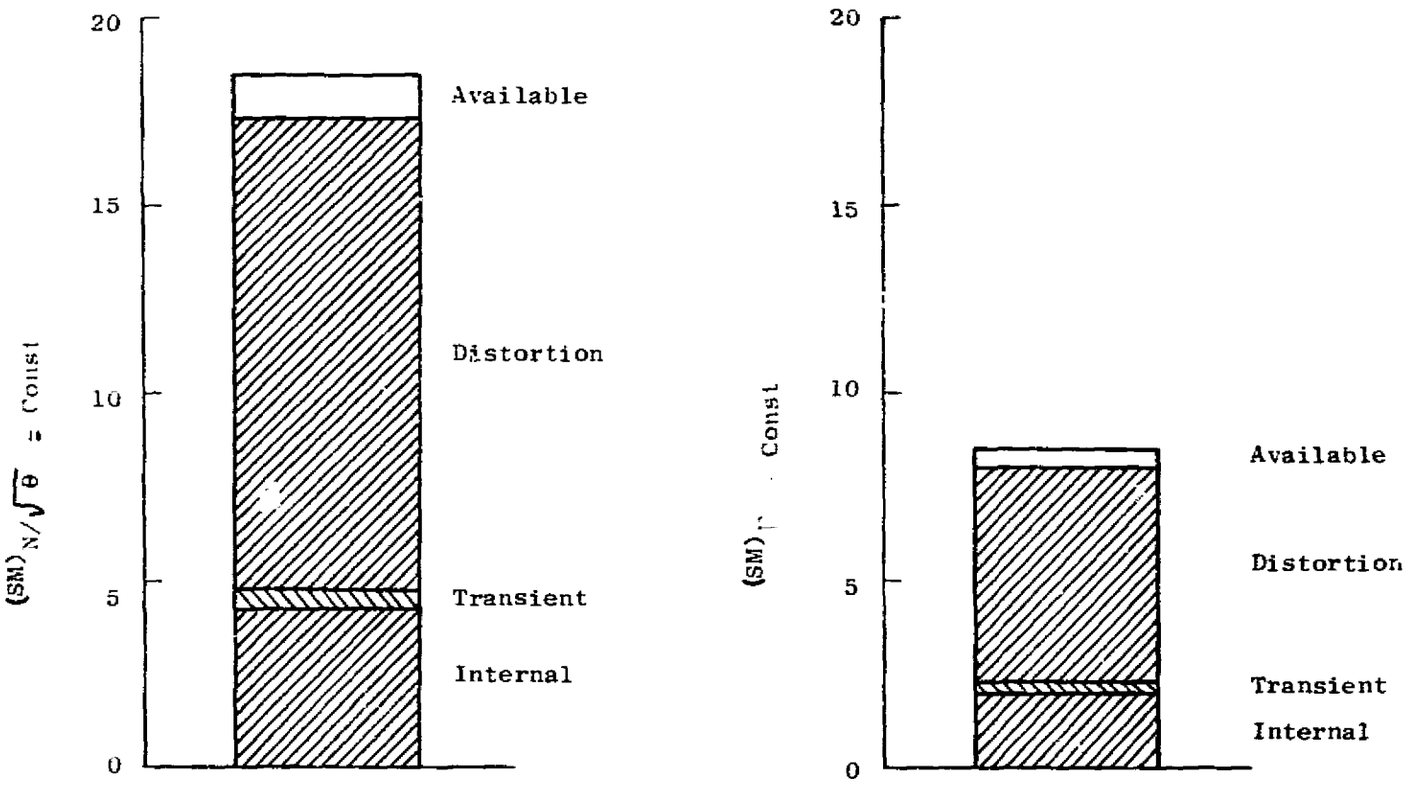

- SLS is Worst Case for Distortion - P_T, T_T, P_S
- Assumed - High Temperature Overlays Low Total Pressure
  - 180° Square Wave of P_T and T_T
  - Worst Combination Used

Figure 109. Sea Level Static Stability Stack.

9.0 INSTALLATION

9.1 FAN

The LCF459 propulsion system contains both turbotip fans and YJ97-GE-100 gas generators. Because of the unique features of this system, the aircraft-furnished components will include the interconnect ducting, the fan exhaust systems, and inlets for the gas generator and fans. The installation features and requirements are defined for this system of both propulsion and aircraft-furnished components.

9.1.1 Installation Envelopes

The installation drawings of the LCF459 fan are shown in Figure 110 and 111. Figure 110 shows an installation with the scroll inlet flange facing forward, typical of a lift/cruise fan installation. Figure 111 shows a rearward scroll inlet, typical of a nose or pod-type installation. These are only two scroll inlet configurations. The orientation of the scroll inlet can be selected to meet the particular installation arrangement.

9.1.2 Inlet and Exhaust Attachments

The flow-path attachments as identified on the installation drawing are:

- Scroll inlet, a 44.45-cm (17.5 in.) inside-diameter, bolted-flange connection
- Fan inlet outer flow path, a 151.2-cm (59.52 in.), sliding attachment on the forward air-seal support structure
- Fan exit outer flow path, a bolted-flange attachment with a 172.7-cm (68.00 in.) diameter, bolt circle
- Fan exit inner flow path, a 71.12-cm (28.00 in.) diameter attachment for the fan exit tail cone. This tail-cone fairing must include an access panel for sump servicing. A vent area of 64.5 cm^2 (10.0 $in.^2$) must be provided for cooling air for the air/oil heat exchanger.

The contours and restraints of the inlet and exhaust attachments have been discussed in Section 4.2, Aerodynamic Design.

The flange attachments provided on the fan are not sized for large load transmission. Table XXXV gives the maximum allowable shear and moments that may be transferred to each of the inlet and exhaust attachments.

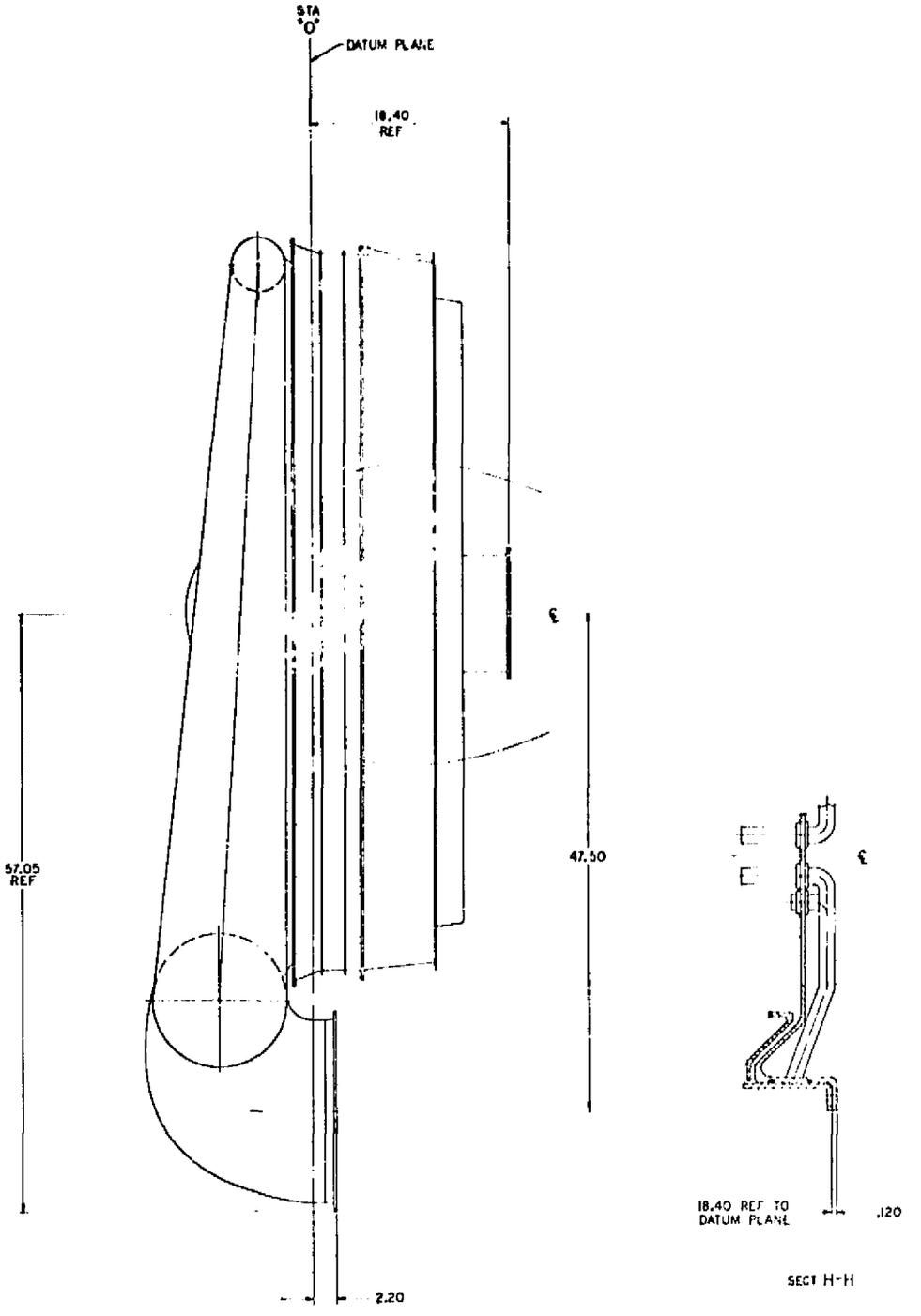

Figure 110. Fan Installation; Lift/Cruise.

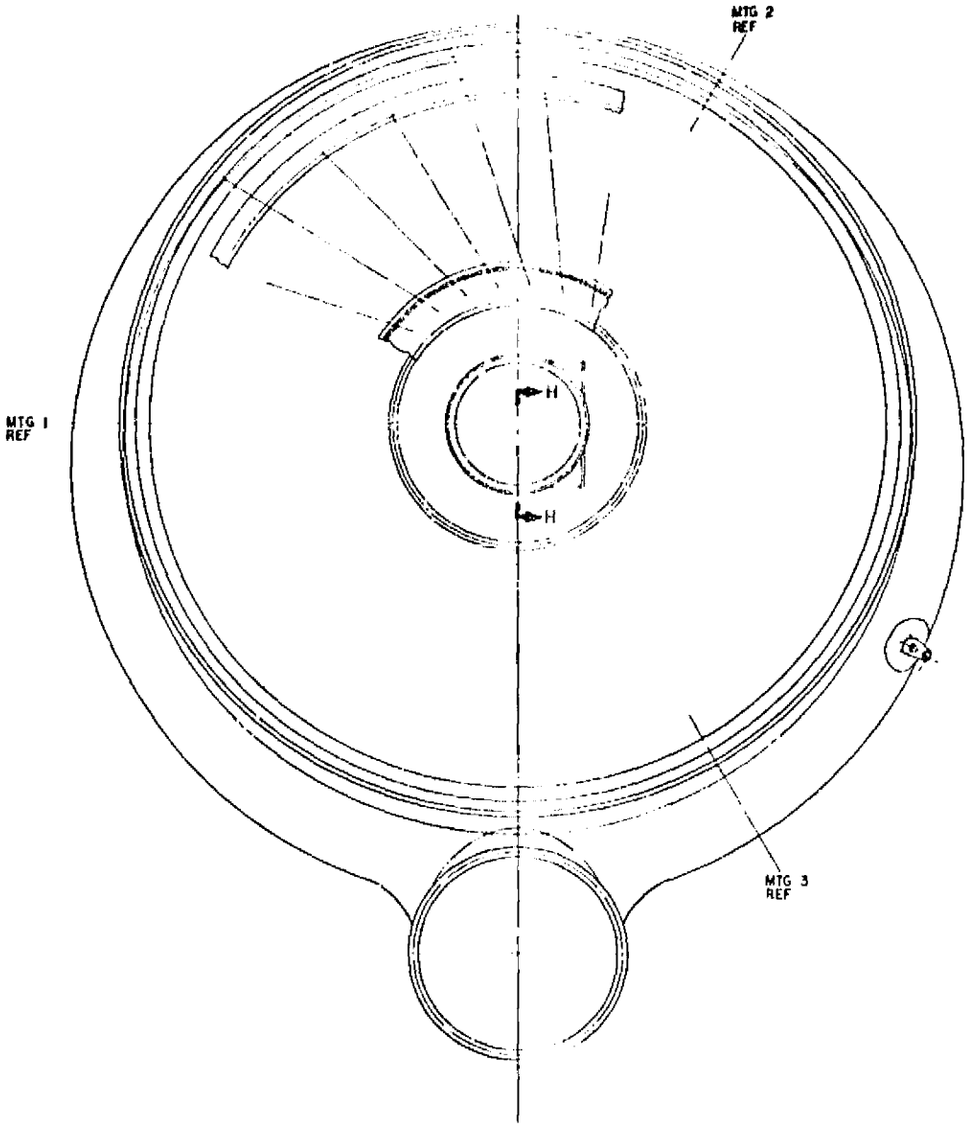

Figure 110. Fan Installation; Lift/Cruise (Concluded).

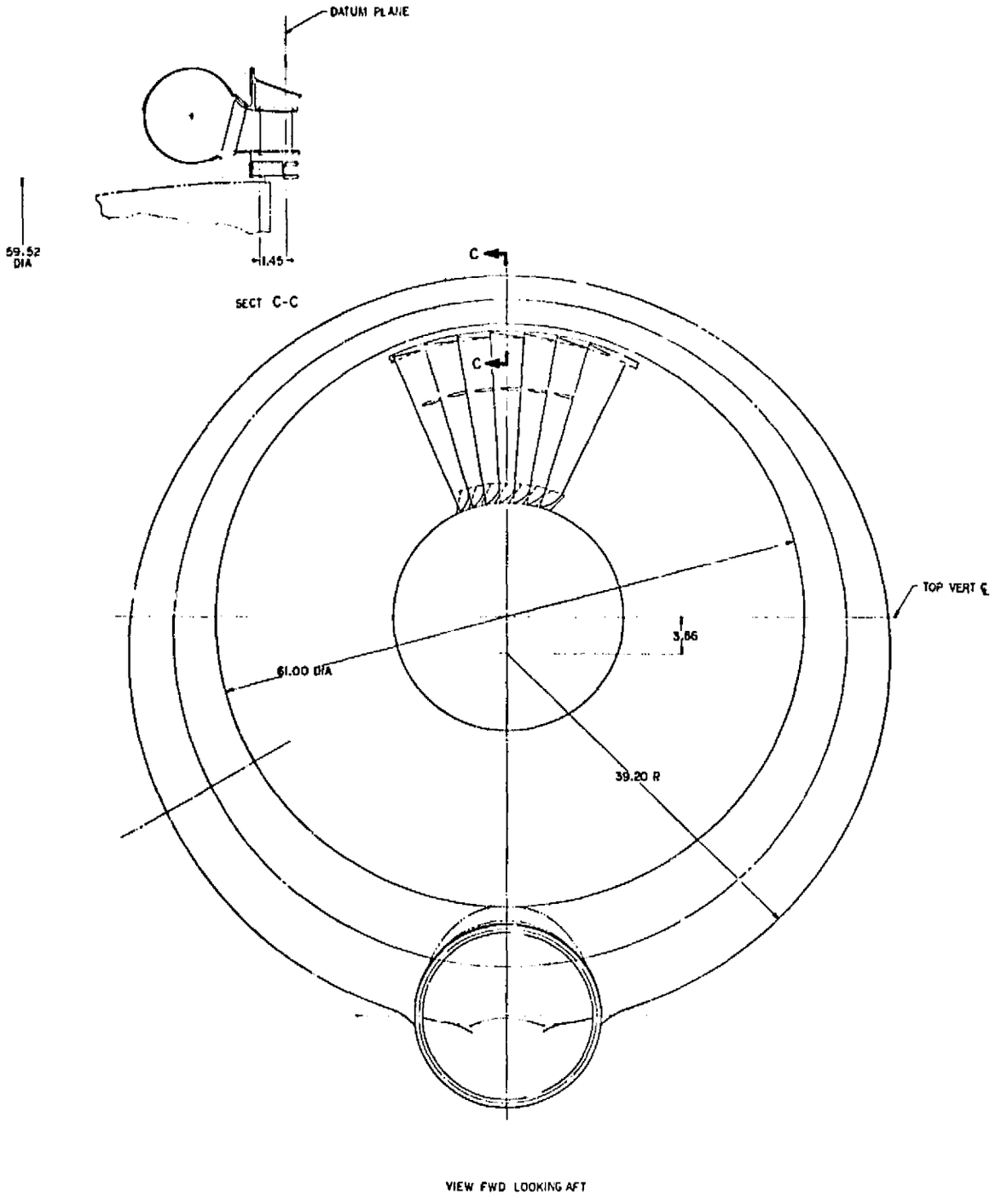

Figure 111. Fan Installation; Nose.

FOLDOUT FRAME 1

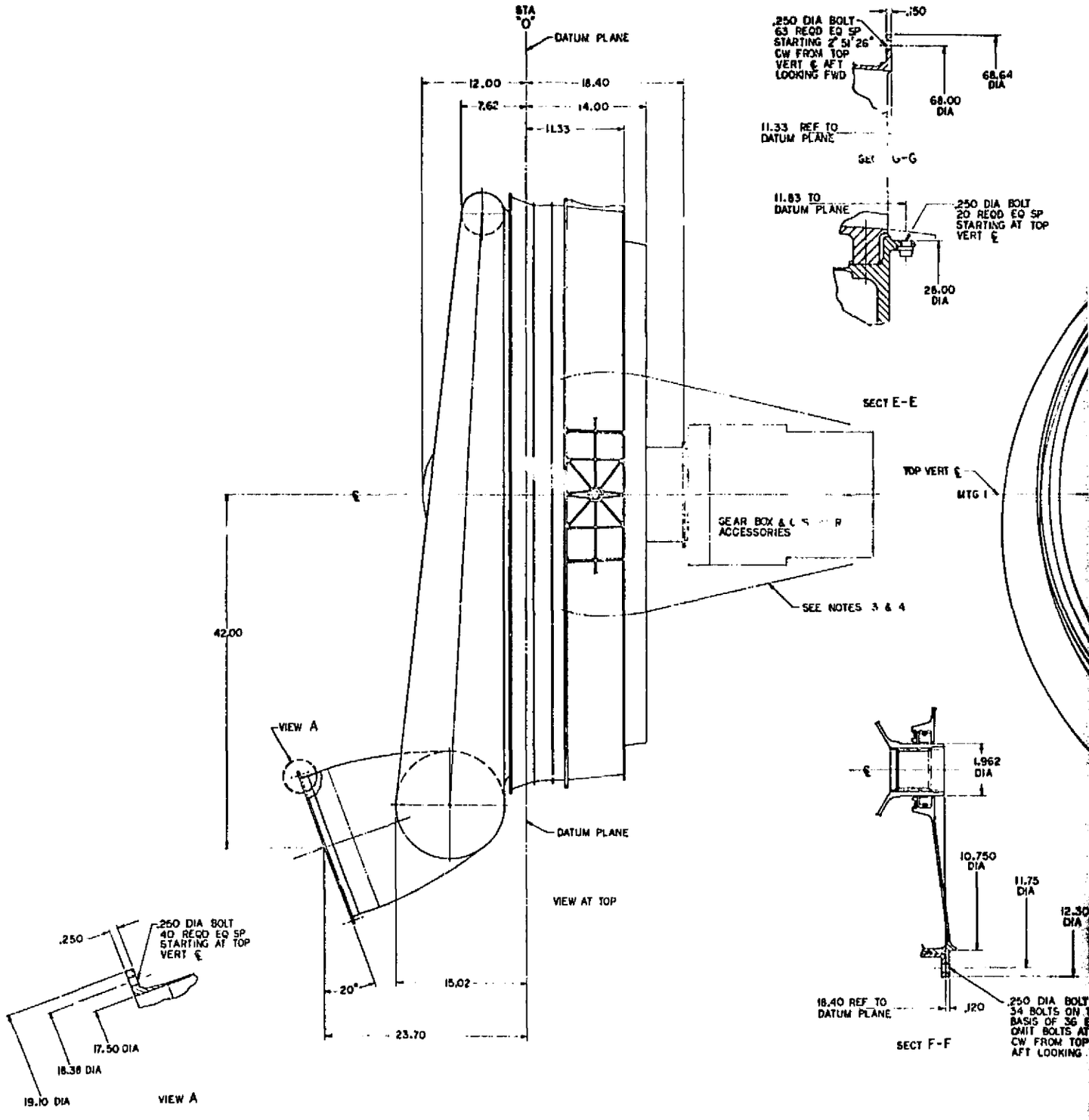

Figure 111. Fan Installation

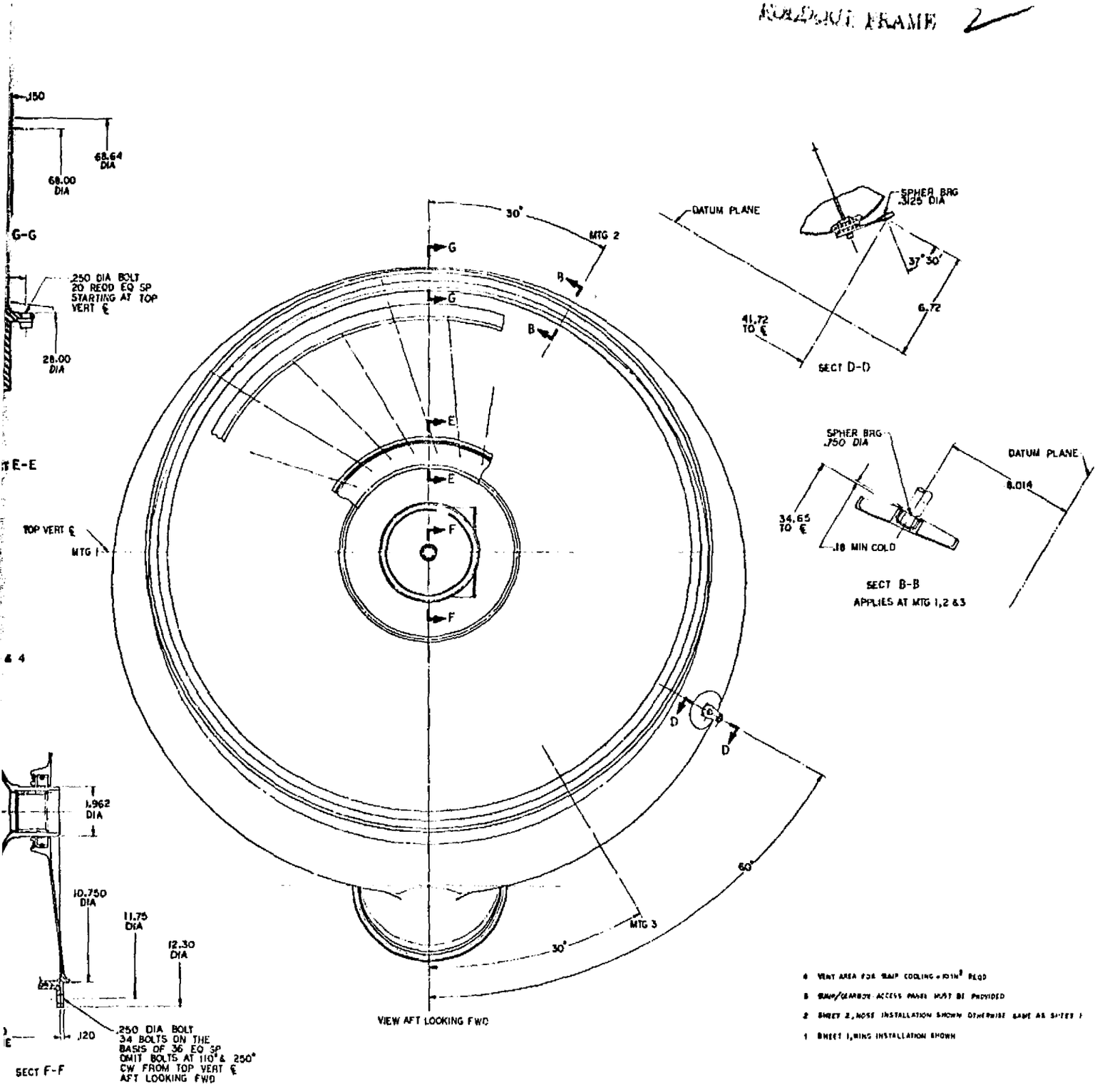

Fan Installation; Nose (Concluded).

9.1.3 Mounting System

The fan contains three mount points, equally spaced around the periphery of the fan frame. The relative angular position of these mounts can be selected to meet the particular installation simply by indexing the frame-to-scroll flange attachment. The direction of restraint at each mount point is both axial and tangential as shown in Figure 112. This mounting system is redundant in one axis as required for transmission of blade-out forces. The forces due to typical loading conditions are given in the figure.

9.1.4 Controls and Accessories

The fan system is an integral propulsion unit except for the hot gas attachment at the scroll. Controls and accessory attachments to the fan include:

- Two electromagnetic fan speed sensors - a fan speed indicator and overspeed-control system must be provided as in the aircraft system.
- Lubrication pressure and temperature sensors - sensors are provided in the fan for cockpit display and monitoring.
- Fan hub vibration - two vibration pickups will be provided for fan vibration monitoring.
- Scroll shutoff valve - a shaft attachment is provided for shutoff of one-third of the scroll arc in the event of one-engine failure. The aircraft system must provide the actuation, sensing, and control for this valve system.
- Power takeoff - a spline attachment and mounting flange is included in the fan for delivering power from the fan shaft to drive aircraft electrical and hydraulic systems. The design characteristics for this attachment are given in Table XXXVI. The power-takeoff option is available on fans mounted with the thrust axis horizontal. Vertical-mounted fans presently are not designed with this option.
- Research and performance instrumentation will be provided in the fan system to meet the requirements of the flight research program.

9.1.5 Weights and Inertias

The weights and inertias of the LCF459 fan are given in Table XXXVII.

Table XXXV. Fan Attachment Load Limits.

	Shear		Axial Force		Moment	
	kN	lbf	kN	lbf	N-m	lbf-in.
Scroll Inlet	445	100	445	100	1356	1000
Fan Inlet Tip	222	50	222	50	678	500
Fan Exit Tip	1334	300	1334	300	4067	3000
Fan Exit Hub	667	150	667	150*	2034	1500

* In addition to normal airloads on fan hub fairing.

Table XXXVI. Fan Power Takeoff Ratings.

Pad Drive Speed	1350 to 4500 rpm
Maximum Continuous Torque, N-m (lbf-in.)	452 (4000)
Static Overhung Moment, N-m (lbf-in.)	283 (2500)
Static Shear Force, N(lbf)	756 (170)

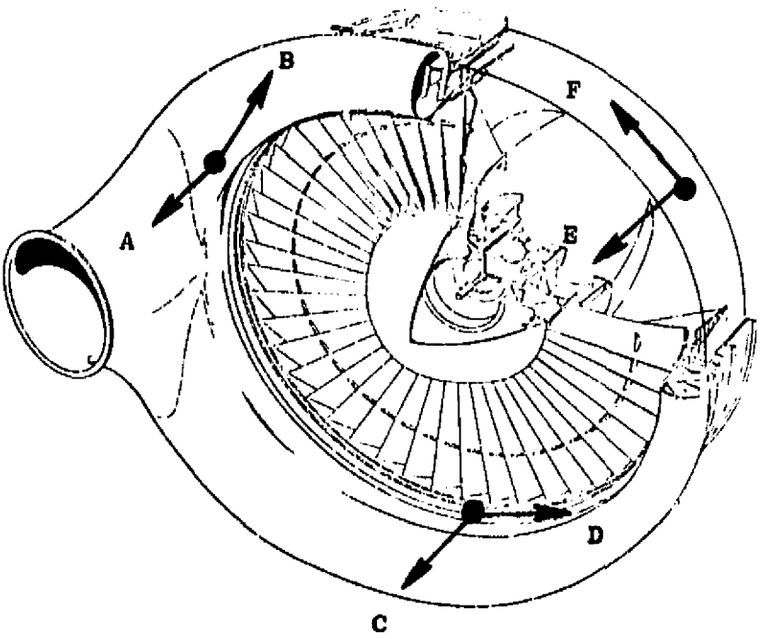

Maneuver	A	B	C	D	E	F
1-g Down	0	582	0	-52	0	477
1-g Forward	351	0	306	0	260	0
1-g Side	0	458	0	458	0	-458
1 rad/sec pitch	-2138	0	4276	0	-2138	0
1 rad/sec yaw	4940	0	0	0	-4940	0

Figure 112. Fan Mounting System.

9.2 YJ97 ENGINE

9.2.1 Installation

The installation of the YJ97-GE-100 engine in a configuration adapted for the turbotip fan is shown in Figure 113. The engine is the basic YJ97-GE-100 as defined in the model specification, Reference 17. The configuration has been modified for attachment of the exhaust ducting system in place of the normal turbojet jet exhaust nozzle.

9.2.2 Inlet and Exhaust Attachments

The flow-path attachments to the engine include the inlet and exhaust system ducting. The inlet attachment is a bolted flange with a flow-path diameter of 51.18 cm (20.15 in.). Details of the engine inlet hub geometry are defined on the installation drawing for attachment of an aircraft-furnished, bullet-nose configuration.

The exhaust attachment uses a bolted flange joint which also includes the tip seal of the engine second-stage turbine. The geometry of this flange attachment is defined on the installation drawing. The exhaust ducting system must also include the engine exhaust cone and deswirl vanes. The geometry of the tail cone forward face is very critical and must be retained to assure proper cooling of the second-stage disk rim. The vanes which support the tail cone must be designed to remove residual swirl that exists in the turbine discharge flow. The average swirl angle is about 8 to 9 degrees at the turbine discharge plane.

The allowable forces and moments that may be transmitted to the engine through the inlet and exhaust attachments are defined in Table XXXVIII.

9.2.3 Mounting System

The engine includes an independent mounting system as shown in the installation drawing. Two thrust mounts are located on opposite sides of the engine near the compressor-to-combustor-casing flange joint. A forward, vertical mount is located on the top of the front frame. A side-force, or drag, link mount is provided on the top of the engine. As required for the aircraft installation, this mount may be either top or bottom and oriented for either right- or left-hand installations.

Mounting system reactions for typical unit maneuver loadings are given in Figure 114.

9.2.4 Controls and Accessories

The engine has a standard, hydromechanical, fuel control with variable stator control. The fuel control has the following functions:

Table XXXVII. Fan Weights and Inertias.

Fan Weight, kg (lbm)	415 (915)
Rotor Moment of Inertia, N-m-sec^2 (lbf-ft-sec^2)	35.5 (26.2)
Fan Moment of Inertias, N-m-sec^2 (lbf-ft-sec^2)	
• About Axis through Scroll Inlet	117 (86)
• About Axis Normal to Scroll Inlet	129 (95)
• About Axis of Rotation	203 (150)

Table XXXVIII. YJ97 Attachment Load Limits.

Inlet Attachment	
Axial Force, kN (lbf)	334 (75)
Shear Force, kN (lbf)	89 (20)
Moments, N-m (lbf-in.)	271 (200)
Exhaust Attachment	
Axial Force, kN (lbf)	2224 (500)
Shear Force, kN (lbf)	890 (200)
Moments, N-m (lbf-in.)	2712 (2000)

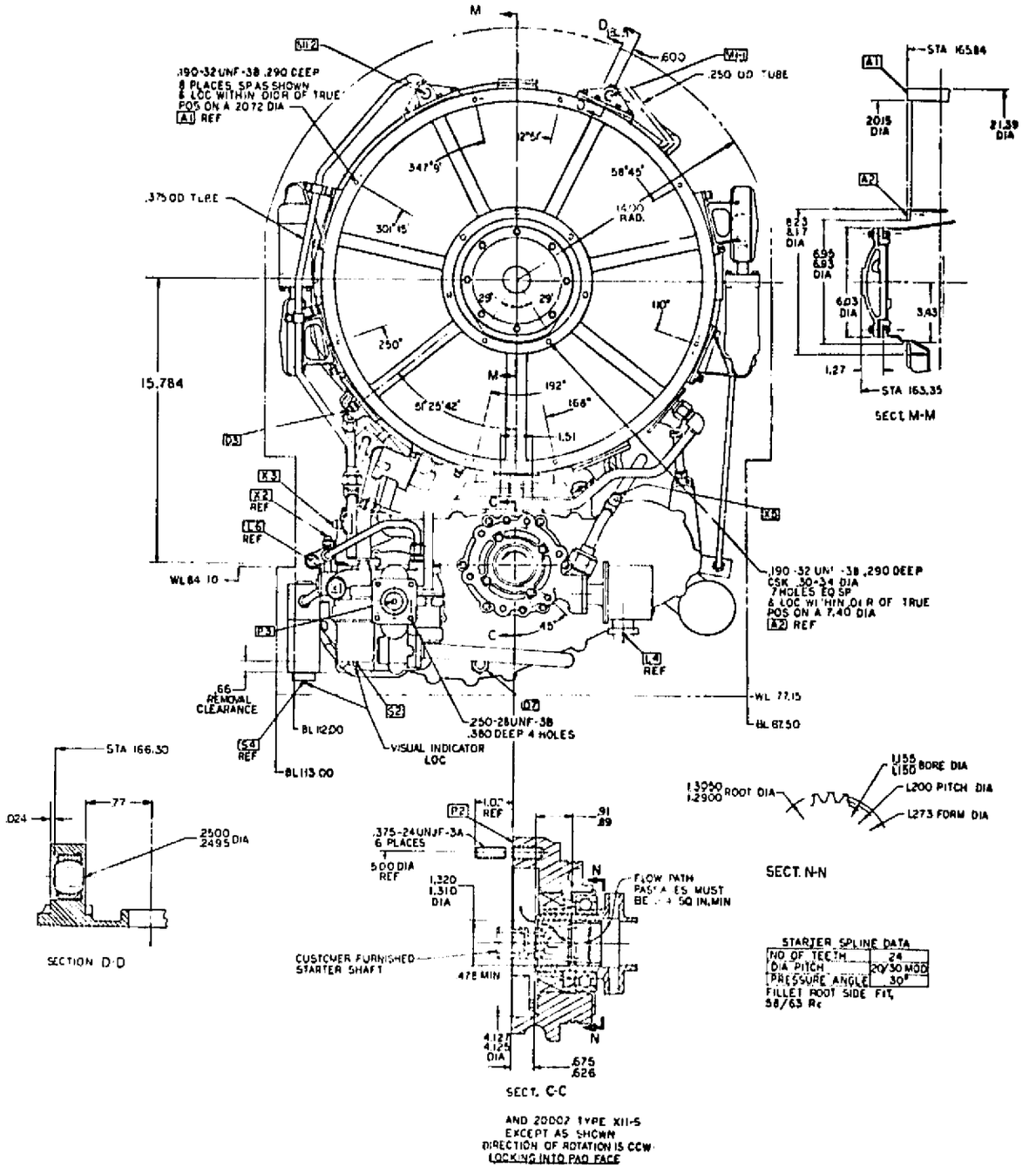

Figure 113. YJ97-GE-100 Installation.

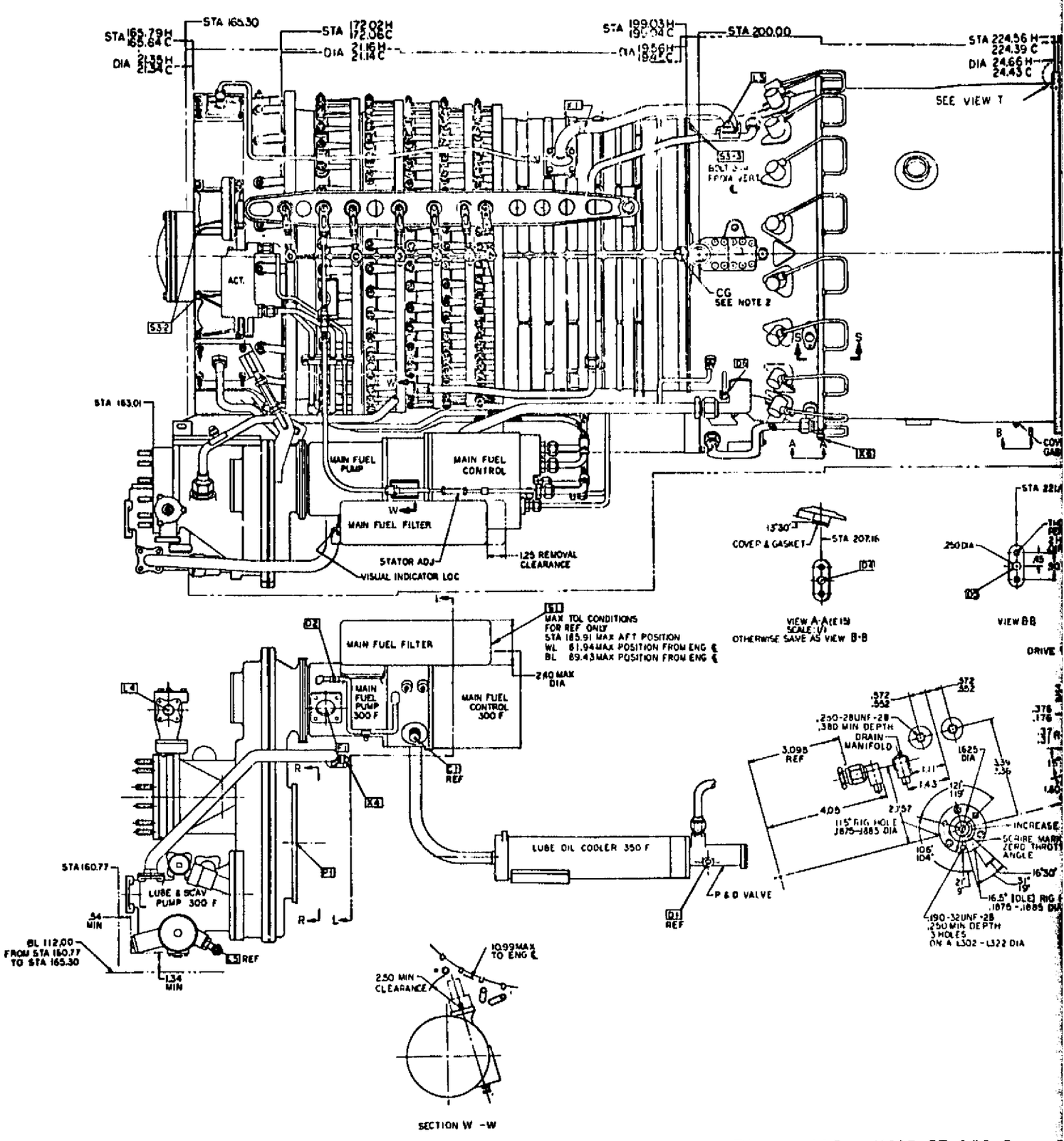

Figure 113. YJ97-GE-100 Instal

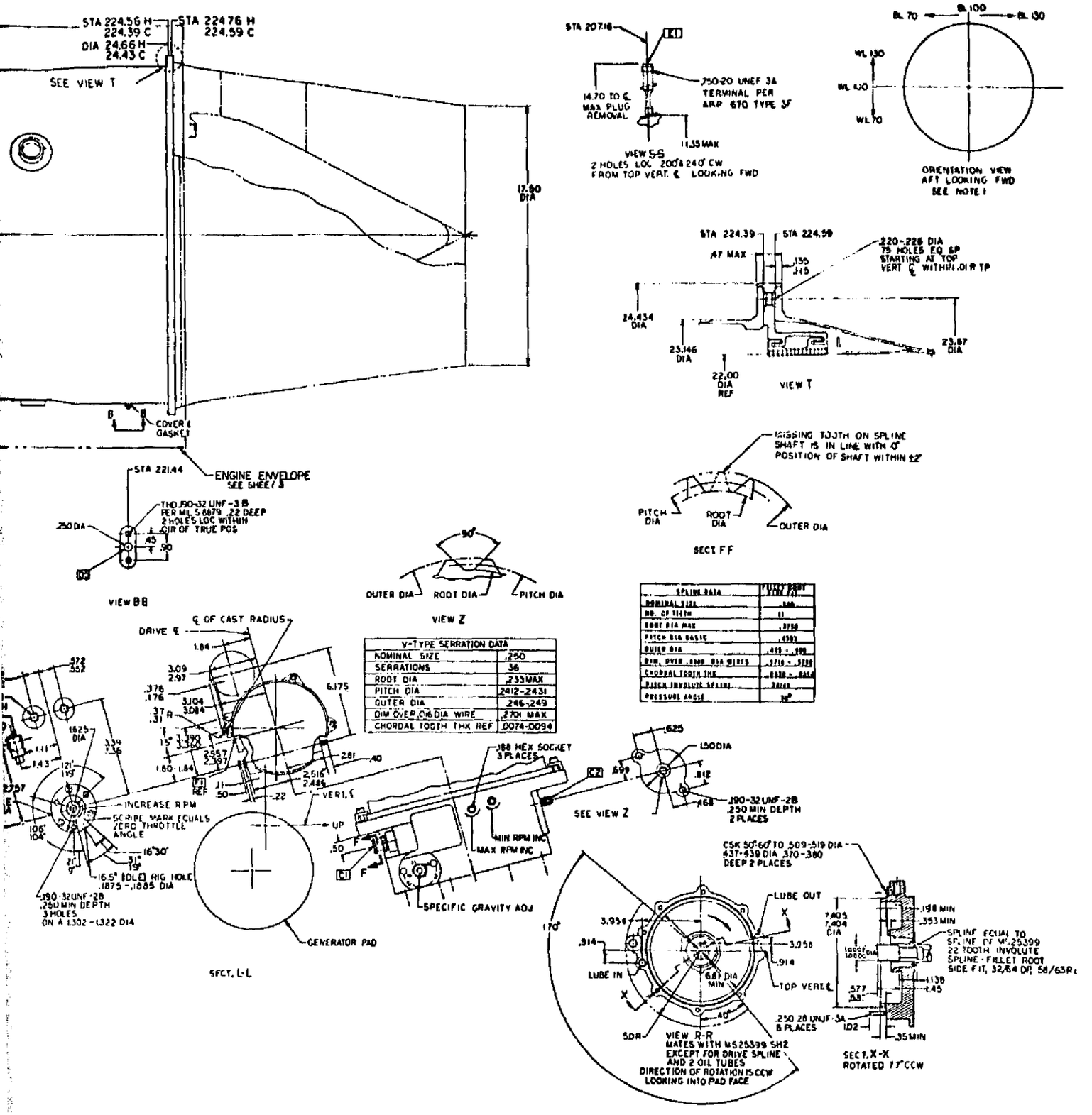

97-GE-100 Installation (Continued).

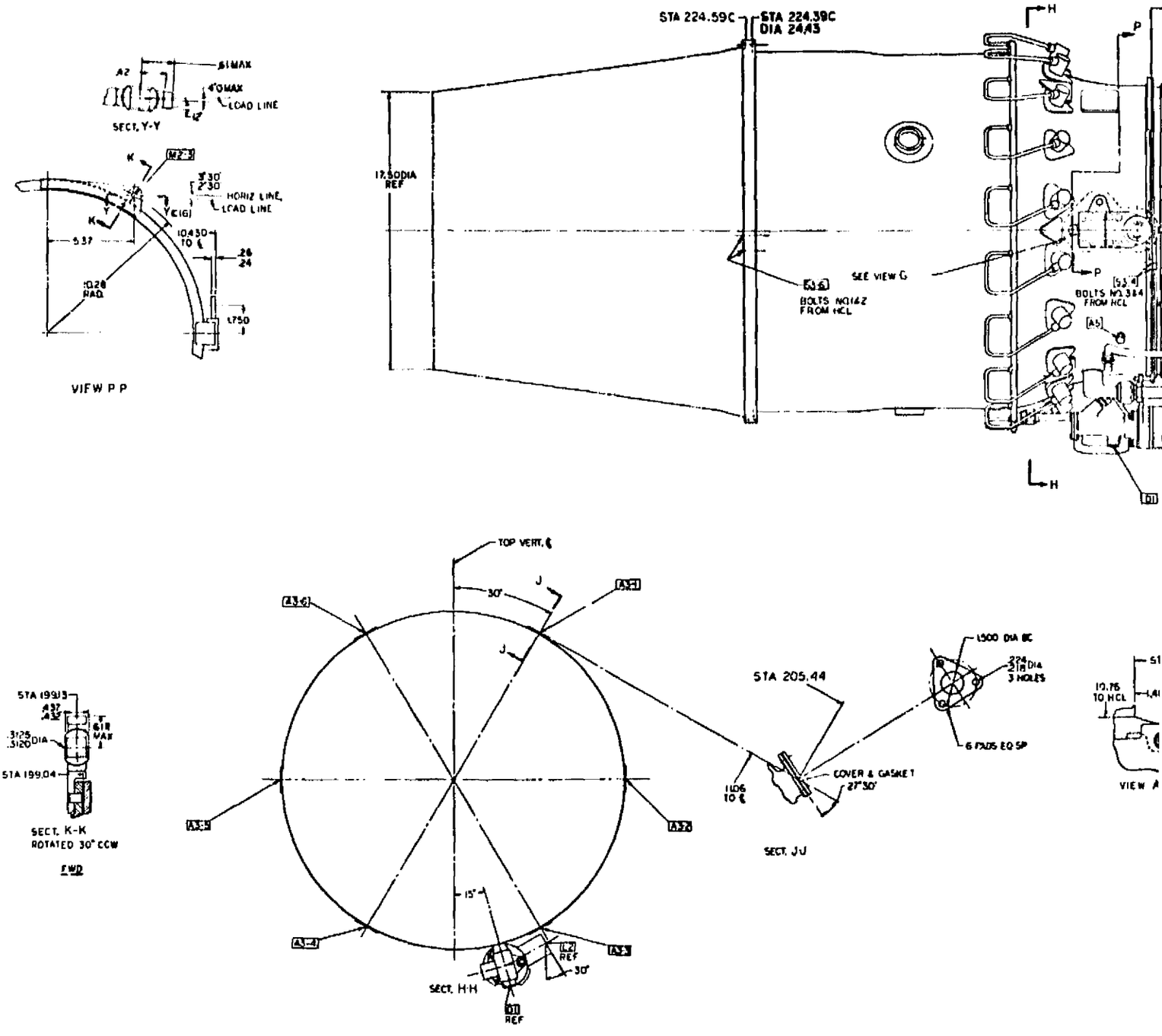

Figure 113. YJ97-GE-100 Installatio

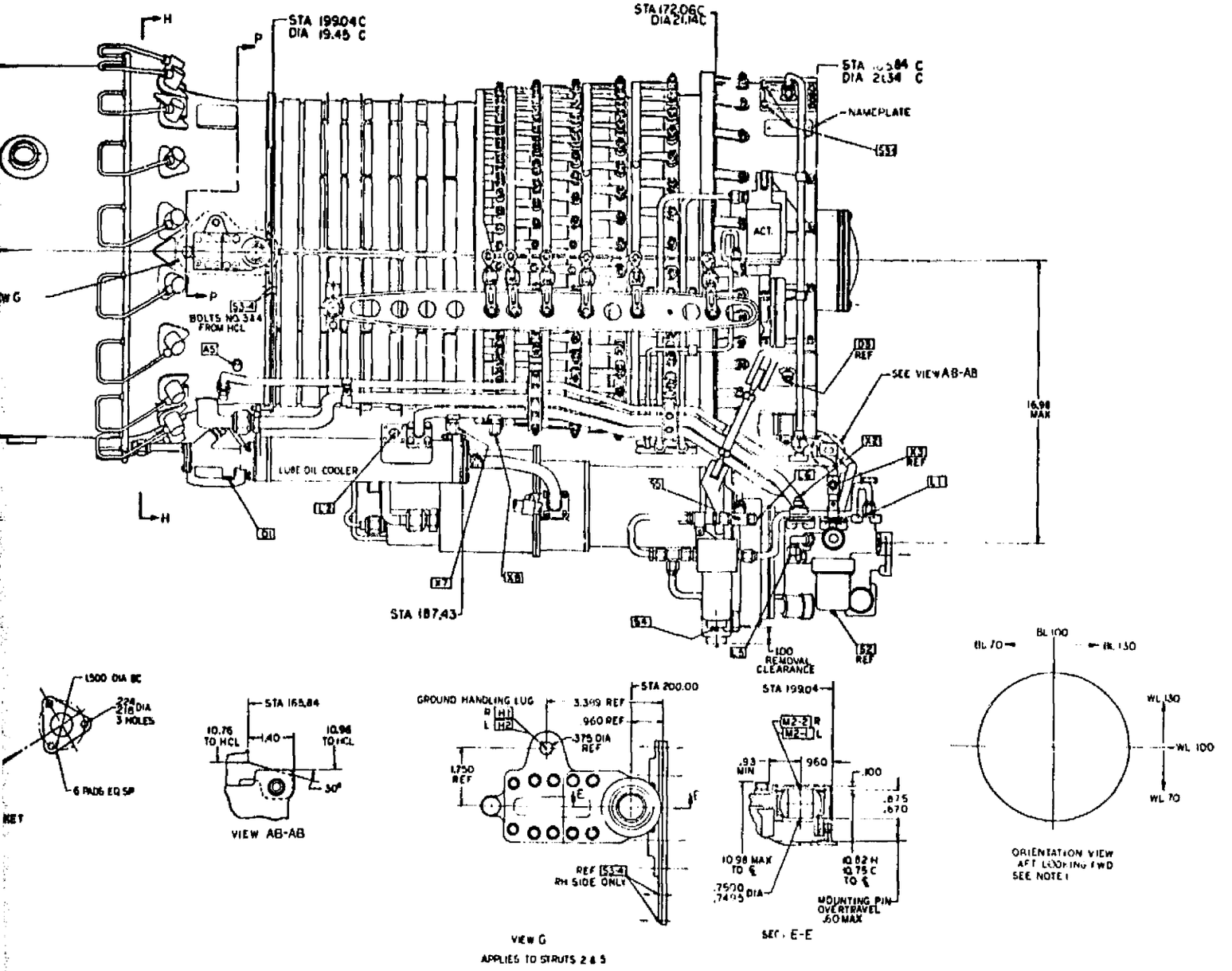

J97-GE-100 Installation (Continued).

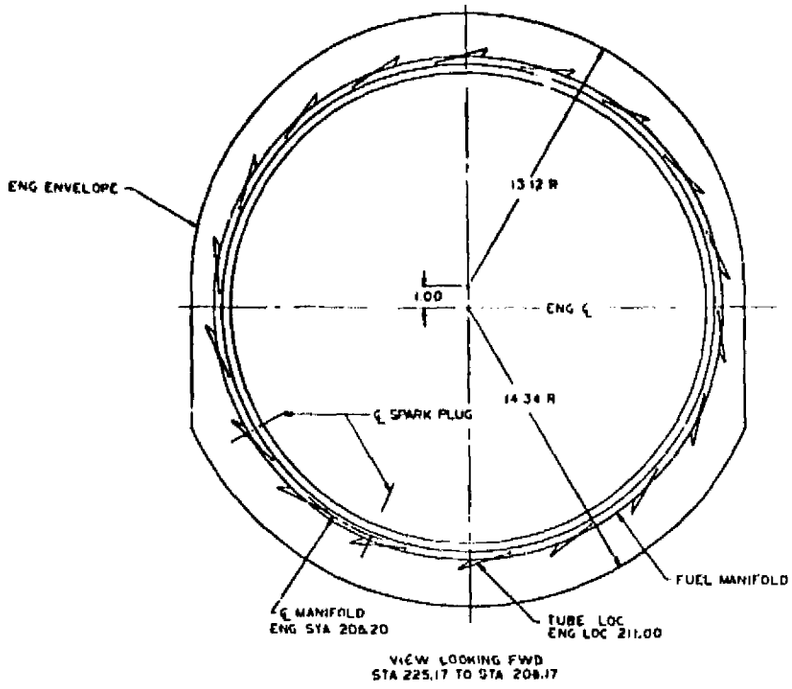

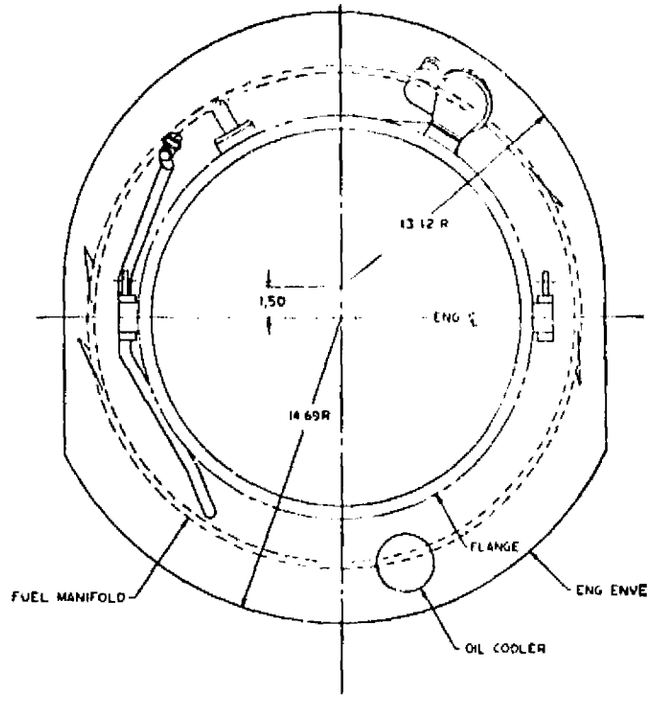

Figure 113. YJ97-GE-100 Installat

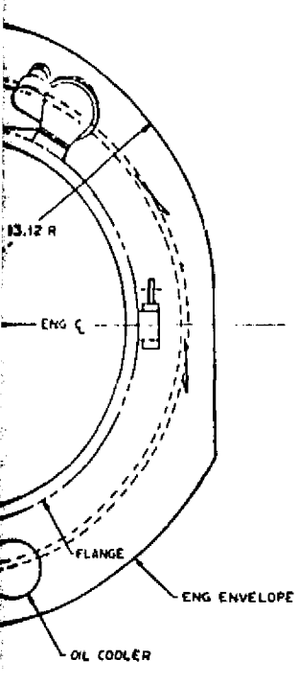

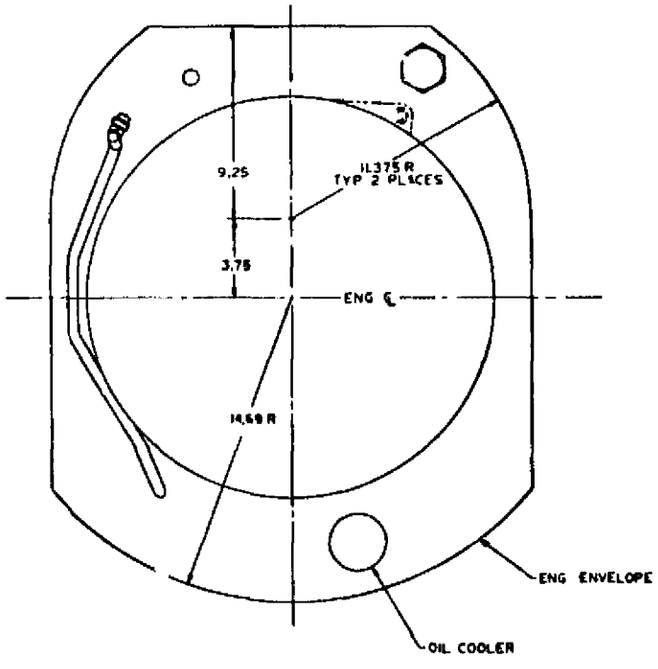

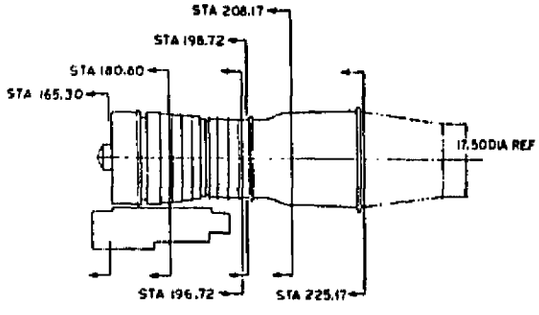

BASIC VIEW OF ENGINE

VIEW LOOKING FWD
STA 198.72 TO STA 196.72

7-GE-100 Installation (Continued).

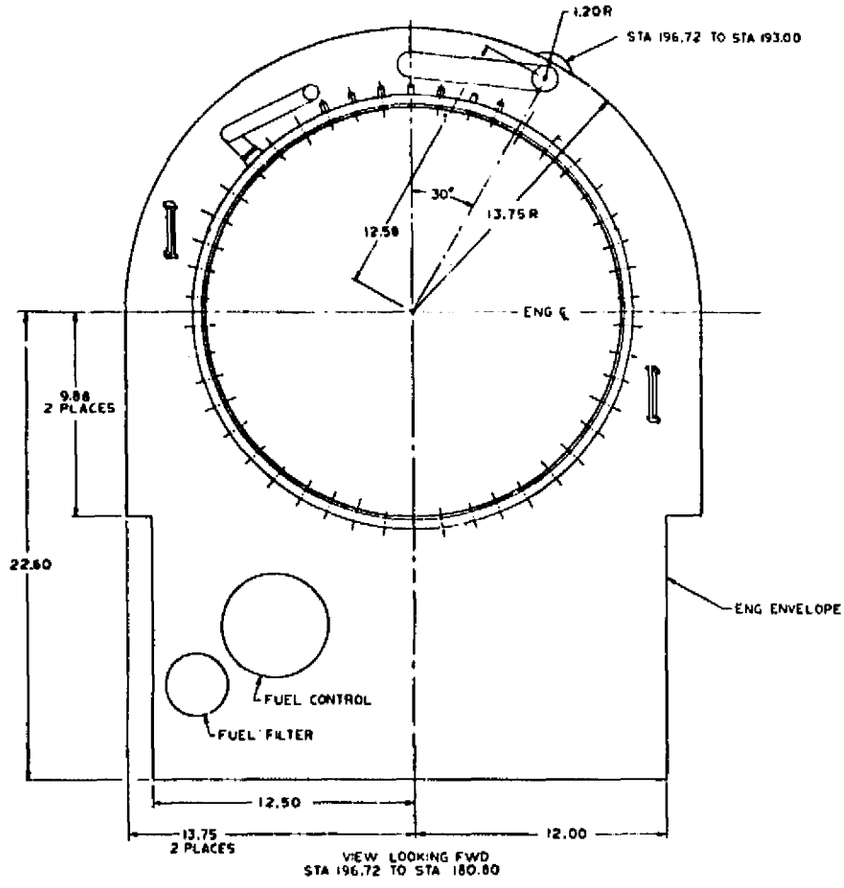

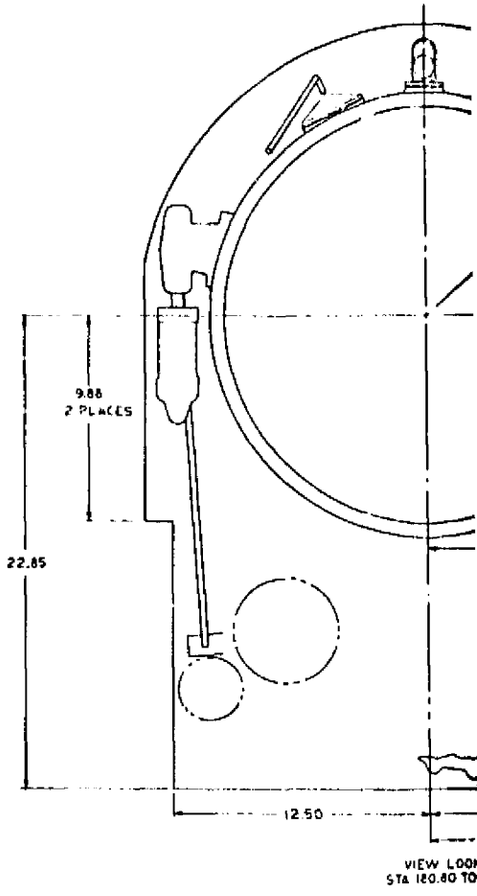

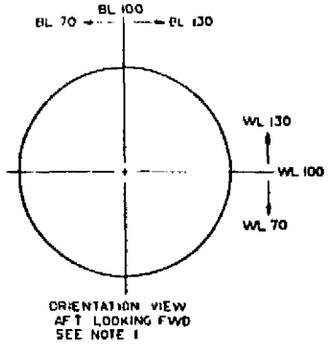

Figure 113. YJ97-GE-100 Installat

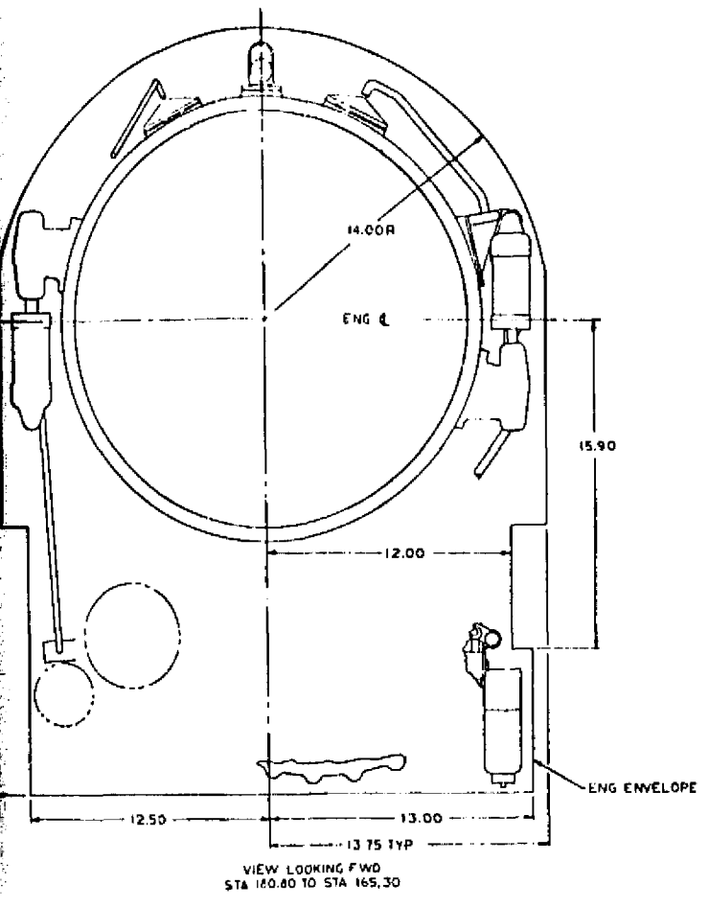

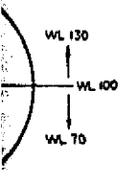

INSTALLATION CONNECTIONS

IDENT	NAME	DESCRIPTION	STA	WL	BL
	ATTACHMENTS				
A1	ENG AIR INLET FLANGE	SECTION M - M	159.84		
A2	NOSE FAIRING	SECTION M - M	159.84		
A3	AIR LOAD REACTION PADS	SECTION H - H			
	-1		165.44	109.50	105.58
	-2			108.80	141.86
	-3			98.42	105.59
	-4			98.42	94.47
	-5			100.90	66.96
	-6			109.50	94.47
A4	P&S TAP (PLUG, TO MAX DEPT)	.0175 -20 UNJF-3B	159.60	93.50	107.81
	CONTROLS				
C1	POWER LEVER	SECTION F - F	159.46	82.50	99.87
C2	POWER LEVER EXTENSION	VIEW Z	159.46	89.50	94.76
	DRAINS				
D1	DRAIN P & D LEVEL OVERBOARD FUEL	AND 10010-4	201.46	87.86	103.47
D2	MANIFOLD OVERBOARD FUEL	GE B6A6P04 STYLE A	175.22	80.67	91.76
D3	PORT NO. 1 SUMP SEAL LUBE	GE B6A6P06 STYLE A	167.62	97.86	109.21
D4	FWD - COMBUSTOR FUEL	VIEW A - A	207.16	88.74	100.00
D5	REAR COMBUSTOR FUEL	VIEW B - B	221.88	86.25	100.00
D6	NO. 2 SUMP SEAL LUBE	MATES WITH MS27656-4	201.82	90.69	94.81
D7	MAGNETIC PLUG LUBE	.812 HEX HEAD	169.39	76.92	101.82
	ELECTRICAL				
E1	SHIELD PLUG (2)	VIEW S - S	207.46		
	FUEL				
F1	MAIN FUEL INLET	MS 33656-20	176.76	81.91	96.45
	HANDLING				
H1	GROUND HANDLING LUG RH	VIEW G	202.49	101.75	118.63
H2	GROUND HANDLING LUG LH	VIEW G	202.49	101.75	89.97
	LUBE				
L1	LUBE SUPPLY PORT FROM TANK	MS33656-12	182.85	66.72	108.29
L2	SCAVENGE RETURN TO TANK	MS33720-10	192.33	69.09	108.96
L3	VENT FOR TANK	GE B6A6P08 STYLE A	201.74	108.83	92.49
L4	SUMP VALVE OVERBOARD	MS33720-17	169.93	88.96	94.96
L5	LUBE PRESSURE PORT	MATES WITH MS33656-4	167.83	82.89	110.15
L6	ALTERNATOR LUBE SCAVENGE	GE B6A6P08 STYLE A	169.53	84.65	111.17
	MOUNTING				
M1	MOUNTING, FRONT FRAME	SECTION D - D			
	-1 LEFT SIDE		159.30	118.31	93.84
	-2 RIGHT SIDE		159.30	118.31	104.96
M2	MOUNTING, AFT				
	-1 LEFT SIDE	SECTION E - E	208.80	100.00	99.23
	-2 RIGHT SIDE	SECTION E - E	238.80	100.00	118.25
	-3 TOP	VIEW F - F	209.11	108.77	109.37
	DRIVE PADS				
P1	AC/DC GENERATOR	VIEW R-R	172.76	85.35	105.15
P2	STARTER	SECTION C-C	165.81	84.22	100.00
P3	TACH GENERATOR	AND 7006 TYPE	164.27	83.10	100.00
		AV -8 EXCEPT AS SHOWN			
	SERVICE				
S1	MAIN FUEL FILTER		165.85	82.82	84.61
S2	LUBE & SCAVENGE FILTER		164.65	78.89	108.95
S3	VIBRATION PICKUP				
	-1 FRONT FRAME	VERTICAL	160.98		
	-2 FRONT FRAME	HORIZONTAL	160.84		
	-3 COMPR FRAME	FWD VERTICAL	199.18		
	-4 COMPR FRAME	FWD HORIZONTAL	199.18		
	-4 NOZZLE ASSY	FWD HORIZONTAL	220.71		
S4	ALTERNATOR LUBE FILTER		171.68	79.89	111.48
S5	ALTERNATOR LUBE FILTER	SCREEN	170.99	84.78	111.12
	INSTRUMENTATION				
I1	SUMP SCA. PRESSURE - AFT SUMP	GE B6A6P08 STYLE A	192.60	107.69	89.38
I2	LUBE SUPPLY - GENERATOR	SEE NOTE 11	168.93	88.81	108.25
I3	LUBE SUPPLY - ENGINE		164.65	86.81	104.95
I4	LUBE SCAVENGE - AFT SUMP		176.25	90.89	92.38
I5	SUMP VENT PRESSURE		168.79	87.72	94.96
I6	FUEL MANIFOLD PRESSURE		208.84	81.10	104.85
I7	LUBE SCAVENGE TEMPERATURE		187.90	89.87	107.88
I8	LUBE SCAVENGE PRESSURE		185.56	89.87	107.88

D CUSTOMER TO PROVIDE OIL TANK AND IGNITION EXCITATION, WHICH MUST BE COORDINATED WITH THE MANUFACTURER

12 CUSTOMER TO PROVIDE 75 HARNESS IN EXHAUST DUCTING, AND MUST BE COORDINATED WITH THE MANUFACTURER

11 THESE FITTINGS ARE CAPPED WITH HARDWARE SUITABLE FOR ENGINE OPERATION WHEN THE ENGINE IS SHIPPED

10 ALL CUSTOMER CONNECTION LOCATIONS ARE DIMENSIONED TO THE CENTER OF A PLANE COINCIDENT WITH THE END OF FITTINGS, SHAFTS, PLUGS, ECT AND THE FACES OF FLANGES, PADS ETC UNLESS OTHERWISE SPECIFIED

9 TOLERANCES OF STA, BL, AND WL DIMENSIONS ARE ± .03 UNLESS OTHERWISE SPECIFIED

8 GE B6A6 TYPE FITTINGS ARE EQUIV TO CORRESPONDING SIZE OF MS 33656 TYPE FITTINGS EXCEPT SEALING SURF. ARE SPHERICAL RATHER THAN CONICAL

7 ANY DEVIATION FROM MOUNTING ARRANGEMENT GIVEN IN NOTES 4, 5, AND 6 MUST BE COORDINATED WITH THE MANUFACTURER

6 THE TANGENTIAL LINK M2-3 IS DESIGNED TO ACCEPT THE ANGULAR LIMITS SHOWN

5 THE SIDE (THRUST) MOUNTS M2-1 AND M2-2 ARE DESIGNED TO ACCEPT THRUST AND MANEUVER LOADS IN FORWARD, AFT, AND VERTICAL DIRECTIONS BUT NOT SIDE LOADS

4 THE FRONT MOUNTS M1-1 AND M1-2 ARE DESIGNED TO ACCEPT VERTICAL LOADS ONLY

3 ALL GASKETS AT CUSTOMER INTERFACES ARE TO BE PROVIDED BY THE CUSTOMER

2 CG AT STA 196.76 PLUS OR MINUS 3.00

1 ALL DIM. ARE HOT & COLD UNLESS OTHERWISE SPECIFIED
A1 ALL STATIONS (STA) ARE AXIAL. S MEASURED FWD (MINUS) & AFT (PLUS) FROM STA 200.00
B1 ALL BUTTOCK LINE (BL) & WATER LINE (WL) DIM ARE MEASURED HORIZ & VERT FROM ENGINE AXIS PER DIAGRAM (D1)
C1 'H' AND 'C' FOLLOWING A DIM. SPECIFY HOT & COLD

YJ97-GE-100 Installation (Concluded).

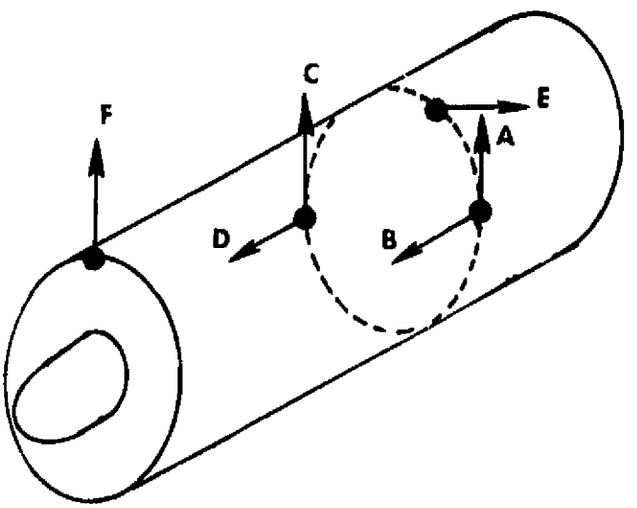

Maneuver	A	B	C	D	E	F
1-g Down	343	0	343	0	0	28
1-g Forward	0	-358	0	-358	0	0
1-g Right	292	- 13	-292	13	716	0
1 rad per pitch	-447	0	-447	0	0	893
1 rad per yaw	0	1400	0	-1400	0	0

Figure 114. YJ97 Mounting System.

- Isochronous speed governing
- Acceleration fuel limiting
- Deceleration fuel limiting
- Stator vane control
- Minimum 90.7 kg/hr (200 lbm/hr) fuel flow
- Corrected speed, 14,890 rpm, limit

This engine control system has been shown, through testing, to be adequate for the interconnect control system using gas power transfer. References 7 and 8 describe these test programs. The method of control requires a rotor speed change to initiate the fuel flow changes during gas transfer. The reaction time is dependent on the inertia effects of the engine rotor system; thus, there is a time delay prior to initiation of the fuel flow changes. Improvements in engine response can be obtained through the use of some method of fuel flow anticipation coupled with commands for flow transfer. Such a modification of the engine control system can be achieved while retaining the present hydromechanical control. This engine control system is presently not being considered, but it is a method of improving system response if required for an aircraft with desirable control characteristics.

The engine user must also provide the following installation items as required for operation of the engine:

- A starter, transfer-gearbox mounted
- An inlet-nose fairing
- Engine-to-aircraft fittings on lines

    1. Fuel and lube supply
    2. Blank-off plates
    3. Pressurization and drain valve overboard and fuel drains
    4. Oil drains
    5. Oil return lines
    6. Combustor drain

- Engine rotor speed sensor and indicator
- Engine oil pressure sensor and indicator
- Engine exhaust gas temperature indicator
- Main fuel control power lever actuation
- Engine to aircraft electrical wiring

- Oil tank
- Ignition excitation

Power extraction is provided in the engine through compressor discharge bleed and accessory gearbox power extraction. The existing engine design limits are:

- 4 percent compressor bleed
- 18.6 kW (25 horsepower) at a speed of 7990 rpm with the engine at design speed of 13,650 rpm.

This level of shaft horsepower is not capable of meeting the requirements for most V/STOL applications. A much larger power extraction allowance has been provided at the fan shaft power takeoff. The penalities for power extraction from the low pressure system are also much smaller than from the high pressure or engine system.

9.2.5 Weights and Inertias

The weights and inertias of the JY97-GE-100 engine are given in Table XXXIX.

Table XXXIX. YJ97 Weights and Inertias.

Total Engine Weight, kg(lbm) ---------- 326 (715)

Rotor Moment of Inertia, N-m-sec^2 (lbf-ft-sec^2) ---------- 2.34 (1.73)

Center of Geometry Location - See Figure 113

System Moment of Inertias, N-m-sec^2 (lbf-ft-sec^2)

- About Axis of Rotation ---------- 8.0 (5.9)
- Vertical through Center of Gravity ---------- 31.6 (23.3)
- Horizontal through Center of Gravity ---------- 32.8 (24.2)

10.0 CONCLUSIONS

The initial phase of the detail design of the LCF459, a 1.5-m (59 in.) diameter fan, has been completed. The fan system was designed for application in the NASA/Navy Research and Technology Aircraft which uses the available YJ97 engine as the gas source. Typical aircraft systems use three fans and three engines with gas interconnect and flow transfer for thrust modulation.

The LCF459, as established, was defined for minimum cost and low risk, and includes the following mechanical features:

- A 52-bladed, titanium rotor with midspan and tip shrouds.
- A cast turbine carrier with one carrier per fan blade.
- A structural rear frame for supporting the rotor. The frame also serves as the stage outlet guide vane row.
- A self-contained lubrication system integrated in the bearing sump housing.
- A single-bubble, H5188 scroll with a shutoff valve utilized during one-engine-inoperative conditions.
- A pumping system incorporated in the cast carrier to supply air for fan inlet seal pressurization.
- An impingement-cooled outer frame case for seal clearance control.
- A fan shaft power takeoff for aircraft accessories.
- Capability of operating with the thrust angle either horizontal or vertical.

The total fan assembly weighs 415 kg (915 lbm) as compared to the preliminary design weight estimate of 386 kg (850 lbm). This eight-percent weight increase is the price for a 25-percent reduction in estimated fan manufacturing cost. Design and manufacturing risks have also been reduced through the use of less exotic materials and fabrication methods.

The estimated, uninstalled, design-point thrust of the fan is 70.28 kN (15,800 lbf) on a 32° C (90° F) day, which is a thrust-to-weight ratio of 17.2. This design-point thrust can only be achieved with gas power transfer between interconnected YJ97-GE-100 engines. The installed V/STOL thrust of one fan and one engine is 57.96 kN (13,030 lbf) at sea level static on a 32° C (90° F) day. This condition gives a thrust-to-weight ratio of 14.2 for the fan only and 8.0 for the combined engine and fan system.

11.0 NOMENCLATURE

A28	Fan nozzle area, m^2 ($in.^2$)
COL	Clean operating line
CSL	Clean stall line
CZ1	Turbine nozzle exit velocity, m/sec (ft/sec)
CZ2	Turbine exit axial velocity, m/sec (ft/sec)
DSL	Distorted operating line
F	Force, N (lbf)
FN	Net thrust, N (lbf)
h	Energy, J/g (Btu/lbm)
IDC	Circumferential distortion index
IDR	Radial distortion index
MR	Relative Mach number
MZ	Axial Mach number
NE	Gas generator speed, percent
NF	Fan speed, percent
PR	Pressure ratio
PRS	Stall pressure ratio
PS	Static pressure, kN/m^2 ($lbf/in.^2$)
PT	Total pressure, kN/m^2 ($lbf/in.^2$)
R1	Turbine blade inlet relative velocity, m/sec (ft/sec)
R2	Turbine blade exit relative velocity, m/sec (ft/sec)
SM	Stall margin
u	Turbine rotor tangential speed, m/sec (ft/sec)
V1	Turbine nozzle exit velocity, m/sec (ft/sec)
V2	Turbine exit absolute velocity, m/sec (ft/sec)
W1	Fan inlet outer seal leakage, kg/sec (lbm/sec)
W2	Fan inlet inner seal leakage, kg/sec (lbm/sec) or gas generator inlet airflow, kg/sec (lbm/sec)
W3	Fan exit inner seal leakage, kg/sec (lbm/sec)
W4	Fan exit outer seal leakage, kg/sec (lbm/sec)
W5	Turbine tip seal leakage, kg/sec (lbm/sec)
W22	Fan inlet airflow, kg/sec (lbm/sec)
WF	Fuel flow, kg/hr (lbm/hr)

$\alpha 1$		Turbine nozzle exit air angle, degrees
$\beta 1$		Turbine rotor inlet ralative air angle, degrees
$\beta 2$		Turbine rotor exit relative air angle, degrees
Γ		Turbine exit swirl angle, degrees
	or	Corrected airflow, kg/sec (lbm/sec)
δ		Correction to standard pressure
Δ		Incremental change or difference
η		Efficiency, percent
θ		Correction to standard temperature
	or	Aircraft bank angle, radians (degrees)
ψ		Aircraft pitch angle, radians (degrees)
	or	Stream function

12.0 REFERENCES

1. General Electric Company, Aircraft Engine Group, Cincinnati, Ohio; "NASA/Navy Lift/Cruise Fan Preliminary Design Report," NASA Contractor Report CR-134837, July 1975.

2. General Electric Company, Aircraft Engine Group, Cincinnati, Ohio; "Additional Design Studies of the NASA/Navy Lift/Cruise Fan," NASA Contractor Report CR-134928, January 1976.

3. General Electric Company, Aircraft Engine Group, Cincinnati, Ohio; "Cost Reduction Studies of the NASA/Navy Lift/Cruise Fan," NASA Contractor Report CR-135155, April 1977.

4. Military Specification; "General Specifications for Turbojet and Turbofan Aircraft Engines," MIL-E-5007D, October 1973.

5. McDonnel Aircraft Company, St. Louis, Missouri; "Design Definition Study on a Lift/Cruise Fan Technology Aircraft, Volume I, Navy Operational Aircraft," NASA Contractor Report CR-137678, June 1975.

6. McDonnel Aircraft Company, St. Louis, Missouri; "Design Definition Study on a Lift/Cruise Fan Technology Aircraft, Volume II, Technology Aircraft," NASA Contractor Report CR-137698, June 1975.

7. McDonnell Aircraft Company, St. Louis, Missouri; "A Full Scale Test of a New V/STOL Control System, Energy Transfer Control (ETC)," Report MDCA 1588, June 1972.

8. McDonnell Aircraft Company, St. Louis, Missouri; "A Full Scale Test of a New V/STOL Control System, Energy Transfer Control (ETC), Phase II - Engine-Out Operation," Report MDCA 1588, Supplement I, April 1973.

9. Rockwell International Corporation, Los Angeles, California; "Design Definition Study of NASA/Navy Lift/Cruise Fan V/STOL Aircraft, Volume I - Summary Report of Navy Multimission Aircraft," NASA Contractor Report CR-137695, July 1975.

10. Rockwell International Corporation, Los Angeles, California; "Design Definition Study of NASA/Navy Lift/Cruise Fan V/STOL Aircraft, Volume II - Summary Report of Technology Aircraft," NASA Contractor Report CF-137696, June 1975.

11. McDonnell Aircraft Company, St. Louis, Missouri; "Wind Tunnel and Ground Static Investigation of a Large Scale Model of a Lift/Cruise Fan V/STOL Aircraft," NASA Contractor Report CR-137916, August 1976.

12. McDonnel Aircraft Company, St. Louis, Missouri; "Wind Tunnel and Ground Static Investigation of a Large Scale Model of a Lift/Cruise Fan V/STOL Aircraft - Wind Tunnel Investigations of Fan Nacelle Length Effects," NASA Contractor Report CR-137916 (Addendum 1), October 1976.

13. General Electric Company, Aircraft Engine Group; "YJ97-GE-100 60-Hour Official Endurance Test," General Electric Report 1269AEG53, 1969.

14. Military Specification; "Requirements for System Safety Program for Systems and Associated Sub-systems and Equipment," MIL STD 882, July 15, 1969.

15. McDonnell Aircraft Company; "Design of a Thrust Vectoring Nozzle for V/STOL Transport Lift Cruise Fans," Report MDCA 2738, March 1, 1974.

16. General Electric Company; "Analysis of Pressure Distortion Testing," NASA Customer Report CR-2766, November 1976.

17. General Electric Company; "Engine, Aircraft, Turbojet YJ97-GE-100," Model Specification E-1155, October 15, 1969.